UNIVERSITÉ DE MONTRÉAL

SEISMIC EVALUATION AND RETROFIT OF EXISTING CONCENTRICALLY BRACED STEEL FRAMES IN CANADA

YASAMAN BALAZADEH MINOUEI

DÉPARTEMENT DES GÉNIES CIVIL, GÉOLOGIQUE ET DES MINES

ÉCOLE POLYTECHNIQUE DE MONTRÉAL

THÈSE PRÉSENTÉE EN VUE DE L'OBTENTION

DU DIPLÔME DE PHILOSOPIAE DOCTOR

(GÉNIE CIVIL)

AOÛT 2017

UNIVERSITÉ DE MONTRÉAL

ÉCOLE POLYTECHNIQUE DE MONTRÉAL

Cette thèse intitulée :

SEISMIC EVALUATION AND RETROFIT OF EXISTING CONCENTRICALLY BRACED STEEL FRAMES IN CANADA

présentée par : BALAZADEH MINOUEI Yasaman

en vue de l'obtention du diplôme de : Philosophiae Doctor

a été dûment acceptée par le jury d'examen constitué de :

M. LÉGER Pierre, Ph. D., président

Mme KOBOEVIC Sanda, Ph. D., membre et directrice de recherche

M. TREMBLAY Robert, Ph. D., membre et codirecteur de recherche

M. GOULET James-A., D.Sc., membre

M. BHOWMICK Anjan Kanti, Ph. D., membre externe

DEDICATION

Dedicated to my parents,

Maryam Taghizadeh-Milani and Alireza Balazadeh-Minouei

and my husband,

Ali Imanpour

ACKNOWLEDGEMENTS

I would also like to show my gratitude to Professor Sanda Koboevic. Her support and financial assistance through the Natural Sciences and Engineering Research Council of Canada grant is greatly appreciated.

I would like to express my deepest appreciation and gratitude to Professor Robert Tremblay for his valuable advice, continuous support and endless encouragement through my Ph. D. study. It is an honor for me to have worked with him, as I have learned so many things from him in the research area and my life. His nice and inspiring attitude during my work is greatly appreciated.

I wish to express my sincere appreciation to Professor Ali Davaran for his valuable guidance throughout my work. I am grateful to Martin Leclerc and Romain Siguier at the Structural Engineering Laboratory of Polytechnique Montréal for their patience and assistance during the experimental tests. The help of the undergraduate students working at the laboratory is acknowledged.

I wish to specially thank Karl Auger and Guillaume Toutant for their collaboration during the experimental program. Also, I would like to acknowledge Yan Jiang and Morteza Dehghani for their guidance to develop numerical models. I am grateful to Clélia, helping me to prepare the French version of the abstract.

I wish to thank the external jury: Professor Anjan Bhowmick, Professor Pierre Léger and Professor James Goulet to have read and evaluated this Ph. D. dissertation.

My special gratitude is extended to my parents: Maryam and Alireza and my brother, Mani for their endless support and encouragement. They always motivate me at difficult situations.

My deepest and heartfelt appreciation and gratitude goes to my beloved husband, Ali, who is always besides me and helps me reaching my goals. He was a great advisor and supporter at each stage of my Ph. D. study. I am truly blessed to have him by my side.

RÉSUMÉ

Les nouveaux bâtiments en acier conçus selon les dispositions sismiques du Code national du bâtiment du Canada (CNB) (CRNC 2010) et les règles de calcul des charpentes en acier CSA S16 (CSA 2009) doivent résister en toute sécurité aux charges sismiques et développer une ductilité suffisante tout en maintenant une résistance et une rigidité adéquates. La conception parasismique avec les détails de conception spécifiques aux structures en acier a été introduite dans l'édition 1989 de la norme CSA. Ainsi, les structures conçues avant les années 1990 pourraient ne pas développer la réponse sismique ductile souhaitée. À ce jour, les recherches consacrées à l'évaluation sismique des cadres à contreventements concentriques existants conçus conformément aux codes des années 1980 sont très limitées au Canada.

Le premier objectif de cette recherche est d'évaluer la réponse sismique de cadres contreventés en acier conçus conformément à la norme de conception d'acier CNB et CSA-S16.1-M78 de 1980. Cela a été fait sur un cadre de 10 étages avec contreventement en X en traction seulement et un cadre de 10 et 3 étages avec contreventement en chevron en traction-compression. Les bâtiments sélectionnés étaient situés sur la côte ouest du Canada, et n'incluaient pas de considérations particulières de ductilité sismique pour les contreventements, leurs connexions et les poutres. L'impact de l'utilisation de différentes méthodes sur l'évaluation des cadres contreventés en traction seulement et en chevron a été étudié. Le deuxième objectif de cette recherche est de proposer des stratégies de réhabilitation qui répondent aux critères d'acceptation de l'ASCE 41-13 pour améliorer la réponse sismique du cadre existant de 10 étages avec contreventement en chevron. Les critères d'acceptation spécifiés dans l'ASCE 41 pour les colonnes en acier ont également été étudiés par simulation numérique. La ductilité des colonnes en acier dans des cadres à contreventements concentriques en acier a été évaluée à l'aide d'un chargement monotone et d'un chargement sismique basé sur des résultats d'analyse dynamique.

L'évaluation sismique des contreventements concentriques a été effectuée selon les recommandations du Guide de l'utilisateur du CNB 2010 en utilisant l'analyse spectrale ont été considérées pour l'évaluation sismique des cadres. On a ensuite procédé à une évaluation systématique de niveau 3 selon ASCE 41-13 en utilisant la procédure dynamique linéaire (LDP) et la procédure dynamique non linéaire (NDP). L'évaluation selon ASCE 41-13 a été effectuée car il n'existe pas de dispositions spécifiques pour l'évaluation sismique et la réhabilitation des

bâtiments existants dans les codes canadiens. Pour l'évaluation selon ASCE 41-13, on a adopté, les mêmes objectifs de performance que ceux qui sont spécifiés de manière implicite dans le CNB 2010, soit la prévention de l'effondrement sous une sollicitation sismique établie pour une probabilité de dépassement de 2% sur 50 ans. Des analyses spectrales et des analyses dynamiques temporelles non linéaires (NLTHA) ont été menées pour l'évaluation selon ASCE 41-13. Dans le second cas, deux types de modèles numériques ont été employés: des modèles reproduisant le comportement non linéaire des diagonales de contreventement pour des actions contrôlées en déformation et des modèles tenant compte du comportement non linéaire des composantes primaires pour des actions contrôlées en déformation et des actions contrôlées en force. Dans tous les cas, les comportements non-linéaires ont été simulés à l'aide d'éléments fibres dans le logiciel OpenSees. Ces modèles ont été utilisés pour vérifier l'impact de la réponse non linéaire de différentes composantes sur la réponse sismique.

L'évaluation sismique du cadre de 10 étages avec contreventements en X en traction seulement a montré que l'approche LDP de l'ASCE 41 aboutit à des résultats d'évaluation moins pénalisants comparés à ceux de l'approche CNB 2010. Pour la procédure NDP de l'ASCE 41, les résultats moyens provenant de dix enregistrements du mouvement au sol se sont avérés être moins sévères que le résultat maximum obtenu de trois enregistrements. Les résultats de l'analyse dynamique non linéaire pour le cadre de 10 étages avec contreventements en X en traction seulement ont révélé une concentration de déformation inélastique importante dans les contreventements le long de la hauteur du cadre. Cette réponse insatisfaisante a induit des moments de flexion considérables dans les colonnes, qui ne pouvaient pas être identifiées par une analyse dynamique linéaire. Une analyse éléments finis 3D complémentaire a été effectuée sur les colonnes du cadre de 10 étages avec contreventements en X en traction seulement pour évaluer leur ductilité sismique et valider la réponse sismique obtenues avec les modèles OpenSees. Les résultats des deux études ont indiqué que les colonnes en acier de ce cadre peuvent offrir une ductilité plus élevée que les limites de ductilité spécifiées dans ASCE 41.

L'évaluation selon le CNB 2010 des cadres de 10 et 3 étages existants avec contreventements en chevron a révélé que toutes les diagonales des deux cadres soient renforcées, alors que toutes ces étaient jugées acceptables selon l'approche ASCE 41 LDP. Cependant, ASCE 41 NDP a montré des comportements inélastiques importants dans les niveaux inférieur et supérieur du cadre contreventé de 10 étages, avec des déformations plastiques dans les diagonales excédant les

capacités spécifiées dans ASCE 41. ASCE 41 NDP a aussi prédit que la rupture par flambement des poutres selon leur axe fort se produirait avant le flambement des diagonales. Ce comportement a été confirmé par une analyse 3D détaillée par éléments finis d'une partie de deux étages de la structure. Une plastification ductile en flexion des poutres a également été observée par NDP ASCE 41 et le flambement et la plastification des poutres ont conduit à un effondrement du cadre. Dans les analyses, la plastification en traction des diagonales n'a pu se développer en raison de la flexibilité de la poutre. Cette déficience n'a pu être identifiée en utilisant les critères d'acceptation de l'ASCE 41 pour les poutres de cadres avec contreventements en chevron. L'évaluation ASCE 41 LDP a indiqué que les colonnes avaient une capacité insuffisante. Comme le flambement des poutres s'est produit en premier dans ASCE 41 NDP et provoquait l'effondrement du cadre, cette approche n'as pas permis d'évaluer les colonnes. Les poutres du cadre de 10 étages avec contreventements en chevron ont été réhabilitées pour évaluer la réponse sismique des colonnes et des diagonales. L'approche NPD de ce cadre renforcé a alors montré un flambement des colonnes. L'évaluation sismique des cadres avec contreventements en chevron ont confirmé la nécessité de réhabiliter ces cadres. Pour le cadre de 10 étages, plusieurs scénarios de réhabilitation ont été proposés. Les poutres ont d'abord été modifiées pour respecter le critère de l'ASCE 41 pour les poutres des contreventements en chevron. L'évaluation subséquente a montré que cette correction à elle seule n'était pas suffisante et qu'il était nécessaire de réparer les colonnes ainsi que les fondations. Des hypothèses de modélisation plus réalistes pour la rigidité du système telles que la présence de colonnes de gravité, la fixation de la base des colonnes et la continuité des colonnes en flexion ont alors été considérées dans les modèles. Les cornières dos-à-dos utilisées pour les diagonales ont été remplacées par des profilés tubulaires circulaires qui offrent une meilleure ductilité et capacité de dissiper l'énergie, permettent de plus grandes déformations plastiques et imposent des efforts de tension relativement moindres en régime inélastique. Plusieurs options ont été envisagées pour concevoir les diagonales, y compris l'application du facteur m spécifié dans ASCE 41 LDP, en utilisant la résistance au flambement attendue des diagonales, P_{CE}, et en considérant la résistance attendue en traction et la résistance post-flambement des diagonales, T_{CE} et 0.3 P_{CE}. Le dernier scénario étudié est celui où les diagonales ont été choisies en fonction de leur résistance attendue en traction et leur résistance post-flambement attendue en compression tout en maintenant la sollicitation imposée à la fondation en deçà de sa capacité. Parmi les schémas examinés, le scénario utilisant les plus

grandes sections pour les diagonales pour augmenter la résistance latérale du cadre sans dépasser la capacité de la fondation a donné lieu au nombre minimum d'effondrements. Les poutres de ce cadre ont été ajustées pour rencontrer les critères de l'ASCE 41 pour les diagonales retenues. Les colonnes ont été conservées sans renforcement. Malgré que ce cadre réhabilité fût inacceptable en raison des cas d'effondrement observés, il a été conservé comme élément de la solution finale qui consistait en un système structural mixte. Deux types de systèmes mixtes ont été proposés comme stratégie de réhabilitation pour obtenir une réponse sismique respectant les critères de ASCE 41 NDP. Ces systèmes comprenaient respectivement un cadre de moment en acier à faible ductilité et une ferme rigide en acier, chacun travaillant avec le cadre en chevron réhabilité. Deux configurations ont aussi été considérées pour la ferme rigide: 1) une ferme continue sur la hauteur du bâtiment; et 2) une ferme avec une rotule à la mi-hauteur du bâtiment. Il a été constaté que le choix le plus économique en termes de quantité d'acier était la ferme avec une rotule à mi-hauteur. L'application de ce schéma de réhabilitation a permis d'éliminer les cas d'effondrement du cadre et de satisfaire toutes les exigences de l'ASCE 41 NDP, cela sans renforcement des colonnes.

Compte tenu de la bonne performance obtenue avec le système mixte avec ferme articulée à mi-hauteur, le même concept a été appliqué au contreventement original avec diagonales faites de cornières doubles. Le système a permis d'éliminer les cas d'effondrement. Cependant, les poutres ont subi un flambement limité et un renforcement est nécessaire pour les colonnes et les fondations, ce qui rend cette solution moins intéressante.

ABSTRACT

New steel buildings designed according to the seismic provisions of the National Building Code of Canada (NBCC) (NRCC 2010) and the steel structures design standard CSA S16 (CSA 2009) are conceived to safely resist seismic loads and develop sufficient ductility while maintaining adequate strength and stiffness. The special seismic design and detailing requirements for steel structures were introduced in the 1989 edition of the CSA standard. Thus, the structures designed prior to 1990's may not develop the ductile seismic response. To date, very limited research in Canada has been devoted into the seismic evaluation of existing concentrically braced frames designed in accordance with the 1980's codes.

The first objective of this research is the evaluation of the seismic response of steel braced frames designed in accordance with the 1980 NBCC and CSA-S16.1-M78 steel design standard. This was done on prototype 10-storey tension-only X-braced frame and 10- and 3-storey tension-compression chevron braced frames. The selected buildings were located on the west coast of Canada, and they did not include any specific seismic ductility considerations for braces, brace connections and beams. The impact of the application of various methods on the evaluation of tension-only and chevron braced frames was investigated. The second objective of this research was to develop retrofit strategies to improve the seismic response of the 10-storey existing chevron braced frame in accordance with the ASCE 41-13 guidelines. The acceptance criteria specified in ASCE 41-13 for steel columns were also investigated through numerical simulations. The ductility of steel columns in concentrically steel braced frames was evaluated using monotonic loading and seismic loading based on dynamic analysis results.

The seismic assessment of the existing concentrically braced frames was first conducted in accordance with the recommendations of the User's Guide to NBCC 2010 using response spectrum analysis. Subsequently, a tier-3 systematic evaluation according to ASCE 41-13 was carried out using Linear Dynamic Procedure (LDP) and Nonlinear Dynamic Procedure (NDP). This second evaluation was performed as there are no specific provisions for seismic evaluation and retrofit of existing buildings in current Canadian codes. The performance objectives were set same as those implied in NBCC 2010, i.e. collapse prevention under ground motion level established for a probability of exceedance of 2% in 50 years. Response spectrum analysis and nonlinear time-history analysis (NLTHA) methods were conducted to use ASCE 41-13. For

NLTHA, two different types of numerical models were considered: models reproducing nonlinear responses associated to deformation-controlled actions in the bracing members and models accounting for nonlinear response for both deformation- and force-controlled actions in primary components. In all cases, nonlinear responses were simulated using fiber elements in the OpenSees program. These models were used to verify the impact of the nonlinear response of different components on seismic response.

The seismic evaluation of the 10-storey tension-only X-braced frame showed that the ASCE 41 approach results in less stringent assessment results compared to the NBCC 2010 approach. In the ASCE 41 NDP evaluation, the mean results from ten ground motion records are less severe than the maximum of three records. The results from the nonlinear dynamic analysis for the 10-storey tension-only X-braced frame revealed a significant concentration of inelastic deformation demands on the braces along the frame height. This unsatisfactory response induced considerable bending moment demands on the columns, which could not be identified by linear dynamic analysis. A complementary detailed 3D finite element analysis was performed on the columns to evaluate their seismic ductility and validate the seismic response of the braced frame columns modelled in OpenSees. The finding of both studies indicated that steel columns of this frame can exhibit higher ductility compared to the ductility limits specified in ASCE 41.

The NBCC evaluation of the existing 10- and 3-storey chevron braced frames revealed that all the braces in both frames required to be strengthened, whereas all bracing members were found to be acceptable in accordance with the ASCE 41 LDP. However, ASCE 41 NDP showed high inelastic deformation demands in the lower and upper levels of the 10-storey braced frame, in excess of the brace deformation capacities specified in ASCE 41. From ASCE 41 NDP, beams of the chevron braced frames are expected to fail by strong axis buckling prior to brace buckling. This response was confirmed by a detailed 3D finite element analysis of a two-storey sub-assemblage. Beam ductile flexural yielding was also observed in ASCE 41 NDP and both beam buckling and yielding led to frame collapse. In the analyses, brace tension yielding could not develop because of the beam flexibility. This deficiency could not be identified using the ASCE 41 acceptance criteria for beams of chevron braced frames. ASCE 41 LDP evaluation results indicated that columns have insufficient capacities. As beam buckling occurred first when the NLTHA was applied, columns could not be assessed using ASCE 41 NDP, because beam buckling caused the frame collapse. The beams of the 10-storey chevron braced frame were

retrofitted to evaluate the seismic response of columns and braces. NDP of this frame showed column buckling.

Seismic assessment of the studied chevron braced frames confirmed the need to retrofit the frames. For the 10-storey frame, several retrofit schemes were proposed. The beams were retrofitted first, in accordance with the requirements prescribed in ASCE 41. The subsequent evaluation showed that this solution by itself was not sufficient and it was required to also repair the existing columns as well as the foundations. More realistic modeling assumptions for the system stiffness such as the presence of gravity columns, the fixity of the column bases and the flexural continuity of columns at the splices were introduced in the models. The existing double angle braces were replaced by more effective circular tubing members that display higher ductility and larger plastic deformation and energy dissipation capacity while imposing relatively lower forces upon yielding. Several options were considered to design the braces including the application of the m-factor specified in ASCE 41 LDP, using the expected buckling strength of braces, P_{CE} and considering yielding and post-buckling strength of braces, T_{CE} and 0.3 P_{CE}. The last scenario was the application of yielding and post-buckling strength of braces, while limiting the brace sizes such that the imposed demand on the foundations remained within its capacity. Among the schemes examined, the scenario that used larger brace sizes to increase the frame lateral resistance without exceeding the capacity of the foundation was found to have the minimum number of collapse occurrences. New beams were selected to meet ASCE 41 criteria for chevron braced frame beams. Although unacceptable because of global occurrence, this retrofitted chevron braced frame was kept as part of the final solution that consisted in a dual framing system. Two types of dual systems were proposed as the retrofit strategy to satisfy the ASCE 41 NDP acceptance criteria. The two proposed systems included respectively a low-ductility steel moment frame and a stiff elastic truss acting in combination with the retrofitted braced chevron braced frame. Two configurations were considered for the stiff elastic truss: 1) a continuous truss over the full building height; and 2) a truss with a hinge at the building mid-height. It was found that the most economical choice in terms of steel tonnage was the truss with a hinge at mid-height. The application of this retrofit scheme could satisfy all ASCE 41 NDP without frame collapse. The retrofit did not require reinforcement of the existing columns and foundations, which has value from a constructability point of view.

Finally, in view of the good performance obtained with the hinged elastic truss dual system, the concept was also applied to the existing chevron braced frame with the original beams and double angle braces. Satisfactory overall response could be achieved, without collapse. However, limited beam buckling was observed, which can be a matter of concern, the existing columns had to be reinforced ad the foundations would require strengthening, which makes this last solution less attractive.

TABLE OF CONTENTS

LIST OF TABLES

LIST OF FIGURES

LIST OF SYMBOLS AND ABBREVIATIONS

Symbols

A	Design acceleration ratio, cross-section area
A_g	Gross area
A_{gv}	Gross area in shear for block failure
A_n	Critical net area
A_{nv}	Effective net area reduced for shear lag
C_r	Factored compressive resistance of a member
C_1	Modification factor to relate expected maximum inelastic displacements to displacements calculated for linear elastic response
C_2	Modification factor to represent the effects of pinched hysteresis shape, cyclic stiffness degradation and strength deterioration on the maximum displacement response
C_r	Factored compressive resistance of a member
D	Dimension of the building in a direction parallel to the applied forces, Dead load
E	Earthquake load, Young's modulus of elasticity
F	Foundation factor
F_a	Acceleration-based site coefficient
F_t	Portion of V to be concentrated at the top of the structure
F_u	Specified minimum tensile strength
F_{ue}	Expected tensile strength
F_v	Velocity-based site coefficient
F_y	Specified minimum yield stress
F_{ye}	Expected yield strength
I	Importance factor, moment of inertia

I_E	Earthquake importance factor of the structure
J	Force-delivery reduction factor
J_{Base}	Numerical reduction coefficient for base overturning moment
K	Coefficient that reflects the material and type of construction, effective length factor
L	Live load, length
M_{CEx}	Expected bending strength of a member about the x-axis
M_{CEy}	Expected bending strength of a member about the y-axis
M_{CLx}	Lower-bound flexural strength of the member about the x-axis
M_{CLy}	Lower-bound flexural strength of the member about the y-axis
M_r	Factored moment resistance of a member
M_{UFx}	Bending moment in the member about the x-axis
M_{UFy}	Bending moment in the member about the y-axis
M_v	Factor to account for higher mode effect on base shear
M_x	Bending moment in a member for the x-axis
M_y	Bending moment in a member for the y-axis
P_{CE}	Expected compressive strength of the brace
P_{CL}	Lower-bound axial strength of a column
P_e	Euler buckling strength
P_{Gi}	Axial load in the column at level *i* due to gravity loading
P_{UF}	Design axial force in a member
P_y	Axial load causing yield over the whole section
P_{ye}	Member expected yield axial strength
P_{yn}	Nominal axial yield strength

Q_{CE}	Expected strength of a deformation controlled action of an element at the deformation level under consideration
Q_{CL}	Lower-bound estimate of the strength of a force-controlled action of an element at the deformation level under consideration
Q_E	Action caused by the response to selected Seismic Hazard Level
Q_G	Action caused by gravity loads
Q_{UD}	Deformation-controlled action caused by gravity loads and earthquake forces
Q_{UF}	Force-controlled action caused by gravity loads and earthquake forces
R	Force modification factor
R_d	Ductility-related force modification factor
R_o	Overstrength-related force modification factor
S	Seismic response factor
$S(T_a)$	Design spectral response acceleration for a period of T_a
$S_a(0.2)$	5% damped spectral response acceleration, expressed as a ratio to gravitational acceleration, for a period of 0.2 seconds
$S_a(1.0)$	5% damped spectral response acceleration, expressed as a ratio to gravitational acceleration, for a period of 1.0 second
$S/S_{a,gm}$	Ratio between the NBCC and ground motion spectra
T	Fundamental period of the structure
T_a	Fundamental lateral period of the structure in the direction under consideration
T_{CE}	Expected tensile strength of the brace
T_r	Factored tensile resistance of a member
T_1	Computed period from dynamic analysis
U_t	Factor to account for efficiency of the tensile area

U_1	Factor to account for moment gradient and for second-order effects of axial force acting on the deformed member
V	Minimum lateral seismic force at the base of the structure, Lateral earthquake design force at the base of the structure
V_p	Plastic shear resistance of the beam
W	Seismic weight
Z	Plastic section modulus
b	Flange width
h	Web width
h_n	Building height
m	Component demand modification factor to account for expected ductility associated with this action at the selected Structural Performance Level
m_x	Value of m for bending about the x-axis of a member
m_y	Value of m for bending about the y-axis of a member
r_y	Radius of gyration of a member about its weak axis
t	Flange thickness
t_{kp}	Thickness of the knife plate
t_p	Thickness of the gusset plate
t_w	Web thickness
w	Web thickness
β	Coefficient for weak axis bending in beam-columns
Δ_t	Axial deformation at expected tensile yield strength
δ_{avg}	The average of displacements at the extreme points of the diaphragm at level x
δ_{max}	The maximum displacement at any point of the diaphragm at level x
κ	Knowledge factor

ϕ	Resistance factor
ω_1	Coefficient to determine equivalent uniform bending effect in beam-columns
θ_p	Plastic rotation
θ_y	Yield rotation

Abbreviations

ASCE	American society of civil engineers
BRB	Buckling-restrained brace
BS	Block shear
BSE-1E	Basic safety earthquake-1 for use with the basic performance objective for existing buildings
BSE-2E	Basic safety earthquake-2 for use with the basic performance objective for existing buildings
CBF	Concentrically braced frame
CC	Conventional construction
CSS	Cross-section strength
DBF	Ductile braced frame
DCR	Demand-capacity ratio
EBF	Eccentrically braced frame
ESFP	Equivalent static force procedure
IP	In-plane
HSS	Hollow structural sections
LDP	Linear dynamic procedure
LSP	Linear static procedure
LTB	Lateral torsional buckling

NBCC	National Building Code of Canada
NCBF	Non-seismic concentrically braced frame
NDBF	Nominal ductility braced frame
NDP	Nonlinear dynamic procedure
NS	Net section
NSP	Nonlinear static procedure
OMS	Overall member strength
OOP	Out-of-plane
OpenSees	Open system for earthquake engineering simulation
RBS	Reduced beam sections
RSA	Response spectrum analysis
SCBF	Special concentrically braced frame
SD	Standard deviation
SF	Scale factor
UFM	Uniform force method
UHS	Uniform hazard spectral
YGS	Yielding on gross section

LIST OF APPENDICES

CHAPTER 1 INTRODUCTION

1.1 Background

New steel buildings designed in accordance with the seismic provisions of the National Building Code of Canada (NBCC) (NRCC 2010) and the steel structures design standard CSA S16 (CSA 2009) are conceived to safely resist seismic loads and develop sufficient ductility while maintaining adequate strength and stiffness. However, it was only in 1989 that the special seismic design and detailing requirements for steel structures were introduced in the CSA S16 standard (Redwood and Channagiri 1991, Mitchell et al. 2010). Thus, it is likely that the buildings designed prior to 1990's do not develop the desired ductile response under seismic loads. In the 1980's, concentrically braced frames with tension-only X-bracing and chevron bracing were commonly used to resist lateral loads in steel buildings in Canada. Back-to-back double angles were used for braces, whereas W sections were usually selected for beams and columns. Braces were connected to gusset plates by bolts, often arranged in a single bolt line or in double row bolt configurations, if angles with wider legs were used. Chevron-type brace frames have been particularly popular, both in Canada and in U.S. because of their structural efficiency and architectural flexibility. Aging buildings with concentrically braced frames represent a large percentage of existing steel building stock in Canada and U.S., and have potential to increase significantly the seismic risk in large cities. It is therefore essential to properly asses the seismic behaviour of such buildings and put forward cost-efficient retrofit solutions if deemed necessary.

Several experimental and numerical studies have been carried out in U.S. to investigate the seismic behaviour of existing concentrically braced frames with limited ductility named non-ductile concentrically braced frames (NCBF) (Goel 1992, Johnson et al. 2014, Sloat 2014, Hsiao 2014, Sen et al. 2016a). These studies confirmed the likelihood of seismic deficiencies associated with non-compact brace sections, excessive brace slenderness and non-ductile failure modes in connections. Typical brace fracture observed in the experiments conducted on NCBFs is shown in Figure 1.1. Khatib et al. (1998) studied the seismic response of chevron-type NCBFs and concluded that, in addition to potential braces and brace connections problems, beams may be prone to develop plastic hinging because of the insufficient resistance caused by a substantial

difference between the new and old seismic design procedures. This behaviour can lead to soft-story response and compromise the system gravity load resisting capacity.

The principal document for seismic evaluation and the retrofit of existing building in U.S. is the ASCE 41-13 standard (ASCE 2013). It is the combination of former U.S. national standards for seismic evaluation (ASCE 31-03) and seismic retrofit (ASCE 41-06). The evaluation and retrofit process begins with the selection of the appropriate performance objectives to maximize benefits (e.g. improved safety or reduction of damage and downtime periods) while considering the cost and feasibility. Performance objective defines the desired structural and non-structural performances and the specific levels of seismic hazard. A three-tiered evaluation procedure is proposed including Tier 1: screening, Tier 2: deficiency-based evaluation, and Tier 3: systematic evaluation. In Tier 3, seismic demand is evaluated from structural analysis and the evaluation is performed at the components level by verifying acceptance criteria reflecting the expected capacity of the components.

Unlike the U.S., where the state-of-the-art documents for the evaluation and retrofit of the existing structures are available, in Canada the sources are rather limited. NBCC 2010 defines the seismic load to be used for the initial assessment: 60% of earthquake loads prescribed for new buildings that are established for a probability of exceedance of 2% in 50 years. If the deficiencies are identified for this load level, the retrofit is required and should be designed for higher seismic forces, preferably meeting the performance objective for new buildings, i.e. collapse prevention for a seismic hazard with probability of exceedance of 2% in 50 years. Future building use, control of seismic damage and the differential in upgrading costs with force levels can justify the use of lower seismic loads (Allen et al. 1992). The Code de construction du Québec (Code de construction 2015), addresses specifically the existing buildings designed in accordance with the 1990 or earlier edition of the NBCC. It is specified in this document that if the building's seismic force resisting system is modified, the seismic weight is increased by more than 5% or the intervention affects more than 25% of the total floor area for post-disaster buildings, the seismic lateral resistance should be increased to a minimum of 60% of the level prescribed in NBCC 2005 (NRCC 2005). More information about the levels of seismic loads, analysis procedures and acceptance criteria for seismic evaluations is provided in NRC Guidelines for the seismic evaluation of existing buildings (Allen et al. 1992). Information is also available for retrofit of existing buildings (Allen et al. 1995) and rapid screening techniques

(NRC 1993). However, all documents are based on old U.S. guidelines (ATC-14 1987, ATC-22 1989, FEMA 1992a, FEMA 1992b) and 1990 edition of NBCC and are no longer up-to-date. In 2013, a procedure for rapid screening of existing buildings has been updated to reflect NBCC2010 provisions but other documents remained unchanged (Saatcioglu et al. 2013).

In the absence of comprehensive Canadian guidelines for seismic evaluation of existing buildings, the application of the Tier 3 ASCE 41 procedure can be used to explore the potential for savings using specific provisions for seismic assessment and retrofit of existing buildings. In such case, the procedures and the acceptance criteria need to be adapted to Canadian normative context. Certain assumptions, which are currently in use in ASCE 41 seem conservative and need a critical review. For example, presently it is required that the beams of chevron braced frames be evaluated as force-controlled (non-ductile) components. In more recent experimental studies, Sen et al. (2016) argued that the flexural yielding of the beams can, in fact, provide additional energy dissipation mechanism, and eventually reduce retrofit costs. Accepting ductility which can develop through beam flexural yielding would have a favorable impact on the extent of required retrofit in such structures and thereby reduce its cost. However, before this concept can be widely applied, further studies are needed to investigate the impact of such behaviour on system response. The past studies did not address behaviour of frames with beams that have small tributary gravity loading. Such light beams may fail by instability prior to developing ductile flexural yielding, with detrimental consequences on frame response. Therefore, it is necessary to investigate this more critical failure mode to establish the limits on acceptable beam demand-to-capacity ratios. Similarly, establishing more precisely the relationship between the flexural ductility that can develop in columns and their axial load would increase the instances when the flexural action could be considered as deformation-controlled, and this in turn would have a beneficial impact on assessment results. Present ASCE 41-13 requirements for steel columns are rather conservative compared to the experimental evidences and could be relaxed. The study conducted by Bech et al. (2015) confirmed the potential that columns develop flexural ductility for levels of axial load higher than the ones presently considered. However, further numerical and experimental studies are required before such modifications could be safely incorporated into codified assessment procedures.

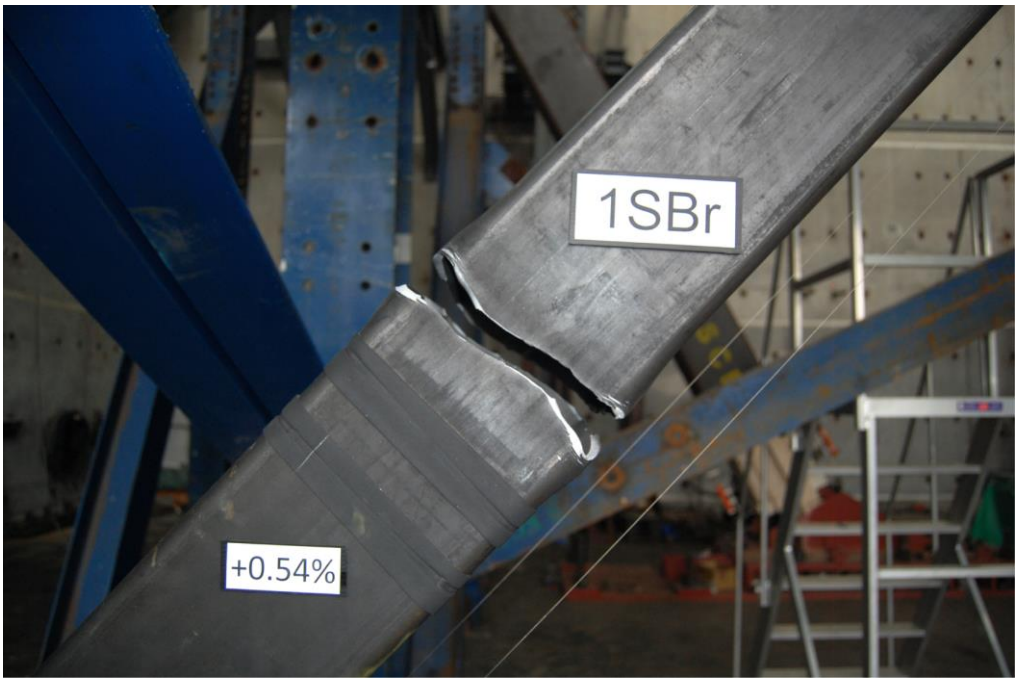

Figure 1.1: Brace fracture of NCFB specimen (Sen et al. 2016a).

1.2 Objectives

The general objectives of this Ph. D. thesis are:

- Evaluate the seismic performance of multi-storey concentrically braced frames with focus on tension-only and chevron braced frames to identify the deficiencies of these systems and compare the assessment results obtained from NBCC 2010 and ASCE 41-13 evaluation methods. The evaluation should include an explicit verification of yielding and buckling limit states for the main structural components (braces, beams and columns) and examine the global stability performance of braced frames.
- Examine the possibility of allowing flexural yielding in beams of chevron braced frames with consideration of the anticipated high compression force demand.
- Assess the appropriateness of current ASCE 41 acceptance criteria for braced frame columns subjected the high axial compression combined with drift induced flexural demand and/or plastic rotations.
- Propose retrofit solutions using ASCE 41-13 procedures to improve the seismic response of a seismically deficient multi-storey chevron braced frame.

1.3 Research methodology

The research methodology that was adopted can be summarized as follows:

– A literature review was carried out on the evaluation and retrofit of existing concentrically braced frames (CBFs), including the documents currently used in Canada and the U.S. for the seismic evaluation of buildings. The provisions of the 1980 NBCC (NRCC 1980) and CSA-S16.1-M78 (CSA 1978) steel design standard to be used for the design of prototype structures were also studied.

– The following tasks were performed to achieve the first objective:

  • A prototype 10-storey building with tension-only X-braced frames in one direction and tension-compression chevron braced frames in other direction was designed in accordance with the provisions of the 1980 NBCC and CSA-S16.1-M78 steel design standard. The same building with only three storeys and chevron braced frames was also examined. Both buildings were assumed to be located on a site class C in Vancouver, British Columbia. Seismic conditions in Vancouver are similar to those that prevail in north western U.S. and the site was chosen so that the results could also apply to this region.

  • Seismic evaluation of the structures was carried out using the approach proposed in the 2010 NBCC and the ASCE 41-13. For the former, the evaluation was performed using linear analysis under 60% and 100% of the NBCC 2010 seismic loads. Seismic loads in the NBCC are specified for a probability of exceedance of 2% in 50 years and the target performance is collapse prevention. Seismic evaluation results under 60% NBCC seismic loads are used to determine if the retrofit is needed. For ASCE 41, a Tier 3 evaluation using linear and nonlinear dynamic analysis procedures (LDP and NDP) was performed to verify collapse prevention performance under a seismic hazard corresponding to a probability of exceedance of 2% in 50 years, i.e. same as in the NBCC to allow a direct comparison.

  • For the ASCE 41 assessment, the influence of the seismic hazard level was investigated by also considering probabilities of exceedance 5% in 50 years and 10% in 50 years for the evaluation of both chevron braced frames using the nonlinear dynamic procedure.

  • The ASCE 41 linear and nonlinear procedures had to be adapted for Canadian application.

- Linear analysis was performed using commercially available structural analysis programs. For nonlinear dynamic analysis, the concentrically braced steel frames were modelled in *OpenSees* finite element structural analysis platform (McKenna and Fenves, 2004). Different models were employed to examine the effect of nonlinearity on structural members. A set of 10 ground motion records was used to evaluate the seismic performance of the concentrically braced frames. Attention was paid in the model to properly simulate instability limit states at the local (member) and global (frame) levels.
- Column axial forces for ASCE 41 LDP assessment were determined using two scenarios including the application of the force-delivery reduction factor and limit-state analysis both specified in ASCE 41. This comparison was used to determine the appropriateness of the force-delivery reduction factor to predict the loads in force-controlled members.

– For the second objective, the following tasks were performed:

- A comprehensive study of the beam flexural and stability response in the 10-storey chevron braced frame was conducted using five different types of modelling in the OpenSees program.
- The results from OpenSees simulations were validated by means of a detailed 3D finite element analysis of the beam and braces of the first two levels using the ABAQUS software (Dassault 2012). The FE model accounted for inelastic response of the braces and beams. For the beams, flexural yielding as well as in-plane and out-of-plane buckling could be predicted, including the restraint offered by the floor slabs.

– For the third objective, the following tasks were performed:

- Comprehensive 3D finite element analysis in ABAQUS was performed for individual columns of the 10-storey tension-only braced frame. This analysis technique was used because the OpenSees program can not predict local buckling effects on the column flexural strength and ductility and the flexural-torsional buckling limit states. In the analyses, the columns were initially subjected to different levels of axial loads varying from 0.1 to 0.9 times their lower-bound axial compressive strength, and the storey drift was monotonically increased until stability failure of the columns occurred. The results obtained from both OpenSees and ABAQUS programs were compared, and the effect of local buckling on the

column flexural strength was examined. The results were used to evaluate the appropriateness of the current ASCE 41 limits for steel columns subjected to axial compression and flexure.

- An extensive experimental program was performed on four full-scale W-shaped columns using the Multi-Directional Hybrid Testing System (MDHTS) of the Structural Engineering Laboratory at Polytechnique Montréal. The tests aimed at investigating the plastic rotation capacity of the columns and their buckling response. The test results were used to validate the analysis results from the OpenSees and ABAQUS numerical simulations. The results were also considered to assess the ASCE 41 limits for steel columns subjected to axial compression and flexure.

– For the fourth objective, the following tasks were performed:

- Different retrofit solutions were examined for the 10-storey chevron braced frame. Various approaches were investigated to replace the braces with the main objectives of minimizing the force demand on beams, columns, and foundations while achieving uniform demand to capacity ratios along the frame height to avoid soft-story response.
- Two dual frame options were considered, one by adding back-up steel moment frames and one by adding stiff vertical elastic trusses acting as vertical spines. Both additional systems were placed on the perimeter of the building and acted in parallel with the retrofitted chevron braced frames with retrofitted beams and braces. Two configurations were considered for the stiff vertical elastic trusses: continuous trusses over the full building height and trusses with a hinge at the mid-height. The latter was also used in combination with the existing chevron braced frames with reinforced columns only.
- The effectiveness of all retrofit scenarios was assessed by comparing the required steel tonnage and anticipated base reactions to those obtained with new reference chevron braced frames designed in accordance with current Canadian seismic design provisions.

1.4 Organization

This dissertation consists of 8 chapters and three appendices. In Chapter 1 the motivation for the study is discussed, the main objectives of the research are defined and the applied methodology is

described. Chapter 2 presents the literature review on the seismic evaluation and retrofit of existing concentrically braced frames and seismic behaviour of steel columns. A detailed description of the methodology applied in this research is described in Chapter 3. Chapters 4 to 6 describe 3 articles that present the main tasks performed in this research and the main findings of the research. The three articles, which have been submitted for publication in scientific journals, are:

1) Balazadeh-Minouei, Y., Koboevic, S., and Tremblay, R. 2017. Seismic Evaluation of a Steel Braced Frame using NBCC and ASCE 41. *Journal of Constructional Steel Research*. http://dx.doi.org/10.1016/j.jcsr.2017.03.017.

2) Balazadeh-Minouei, Y., Koboevic, S., and Tremblay, R. 2017. Seismic Assessment of Existing Steel Chevron Braced Frames. Submitted to the *Journal of Structural Engineering, ASCE* on February 6, 2017 (initial version) and June 12, 2017 (revised version).

3) Balazadeh-Minouei, Y., Tremblay, R., and Koboevic, S. 2017. Seismic Retrofit of an Existing 10-Story Chevron Braced Steel Frame. Submitted to the *Journal of Structural Engineering, ASCE* on July 14, 2017.

Chapter 7 presents a general discussion of results, while the summary of the project, the main conclusions as well as the recommendations for future studies is described in Chapter 8. In Appendix A, the experimental study of steel columns is explained. Appendix B presents the details of modelling using OpenSees and ABAQUS. Appendix C describes the updating of a cross section modelled in OpenSees.

CHAPTER 2 LITERATURE REVIEW

This chapter summarizes a literature review that is divided into four parts:

In the first part, the seismic design requirements of NBCC 1980 (NRCC 1980) and CSA 1978 (CSA 1978) are presented. In addition, the requirements of current Canadian steel design standard (CSA 2009) prescribed for conventional constructions are outlined to provide a comparison between the requirements of the previous and current editions of the standard.

The second part of this chapter discusses current guidelines for seismic evaluation and retrofit of the structures in Canada and the U.S. The recommendations for the evaluation of existing structures specified in Commentary L of NBCC and Code de construction du Québec are first presented. Other available Canadian documents on seismic evaluation and retrofit are also reviewed. Then, the provisions of the ASCE 41 standard are outlined to provide an insight for the reader on the state-of-the-art U.S. document on evaluation and retrofit of existing buildings.

In the third part of this chapter, past numerical and experimental studies examining the seismic response of concentrically braced frames are described. Different retrofit solutions proposed in the literature review to improve the seismic behaviour of such structures are presented. As the bracing members of studied frames (CBFs) were double angle sections, a review of modelling techniques available for such sections is also provided.

In the last part of this chapter, the numerical and experimental studies on the response of steel columns are summarized.

2.1 Seismic design requirements of NBCC 1980, CSA 1978 and CSA 2009

2.1.1 NBCC 1980

According to National Building Code of Canada (NBCC) (NRCC 1980), the minimum earthquake lateral design load, V, is calculated by Equation 1:

(1) $V = ASKIFW$

In this equation, A is the design acceleration ratio, S is the seismic response factor, K is a ductility coefficient that depends on the type of construction, F is the foundation factor, I is the importance factor, and W is the seismic weight. The design acceleration ratio, A, varies between 0 and 0.08.

The seismic response factor, *S*, equal to $0.5/\sqrt{T}$, need not exceed 1. The fundamental period of the structure, *T*, is taken equal to $0.09h_n/\sqrt{D}$; where, h_n is the building height and *D* is the dimension of the building in a direction parallel to the applied forces. Alternatively, the natural period of the fundamental mode can be determined using the Rayleigh method. Note that in 1980s, contrary to the current NBC edition, no limitation on the period of vibration was imposed if other methods of mechanics were used to determine its value. In Equation 1, the *K* factor is equal to 1.3 and 1.0 for tension-only X-bracing and tension-compression chevron bracing, respectively.

The equivalent static force procedure can be used to determine seismic forces for regular structures. The minimum in-plane torsional moments are calculated using accidental eccentricity equal to 0.05 times the building dimension perpendicular to the direction of loads. Different load combinations compared to the NBCC 2010 (NRCC 2010) were specified in NBCC 1980 including: 1.25D + 1.5L, 1.25D + 1.5E, and 1.25D + 0.7 (1.5L + 1.5E); where D, L and E are the specified dead, live (including snow) and earthquake loads, respectively. It is required to consider the P-delta effects in the analysis. The inter-story drift due to seismic loads is limited to 0.005 times the storey height.

2.1.2 CSA-S16.1-M78

The 1978 edition of CSA S16 did not include any special provisions for ductile seismic response; thus, the same design requirements are used for earthquake and wind loads.

The brace design procedure has been modified in CSA S16 since the 1978 edition. In CSA-S16.1-M78 (CSA 1978), the block shear failure modes and shear lag effects have not been considered in the design procedure for braces in tension. The factored tension resistance of bolted connected elements, T_r, in CSA-S16.1-M78 is determined from Equation 2:

(2) $T_r = \varphi A_n F_y$ if $A_n F_u \geq A_g F_y$

$T_r = \varphi A_n F_u \left(\frac{A_n}{A_g} \right)$ if $A_n F_u < A_g F_y$

$T_r \leq \varphi 0.85 A_n F_u$

where, A_g is the gross cross-section area, A_n is the critical net cross-section area which should be less than $0.85A_g$, F_y and F_u are the specified minimum yield stress and the specified minimum tensile strength, respectively and ϕ is the resistance factor. When the yielding of gross cross-section occurs before the fracture of net area, $A_nF_u \geq A_gF_y$, the resistance of the connection should be defined by the yielding of net section. If the net section fracture is the governing failure mode, the resistance of connection should be reduced by the ratio A_n/A_g, to account for the limited ductility of the connection. Also, the T_r value is limited to $\phi\ 0.85A_n\ F_u$. The factor 0.85 is applied to increase the reliability index for such brittle failure mode. In these equations, the specified minimum yield stress and tensile strength of the steel material, F_y and F_u, are taken as 300 MPa and 450 MPa, respectively, as specified in CSA-G40.21-300W. Based on this code, the brace connection should be designed for not less than 50% of the factored tension, T_r, or compression member resistance, C_r, depending on the governing failure mode in the design. This requirement has been removed from CSA S16 since 2001.The requirement has been withdrawn as it was often misapplied resulting in grossly oversized connection (CSA S16-04).

2.1.3 Conventional construction in CSA S16-09

Canadian steel standard does not provide any specific acceptance criteria for the evaluation of structural members of existing concentrically braced frames. However, section 27.11 in Chapter 27 of CSA S16, specifies design requirements for conventional construction (CC) systems which rely on the intrinsic ductility to provide limited ductile structural response. In view of their limited ductility, the existing steel frames, designed before the introduction of ductile detailing requirements into S16.1, could be classified as conventional construction systems, and thus the design provisions given for these systems could be used in seismic assessment.

Provisions for the structures with R_d = 1.5 were included for the first time in the eight edition of CAN/CSA-S16-01 (CSA 2001) in recognition that many of such structures are built in the areas of considerable seismic risk and that most frequent failures of steel structures in earthquakes are associated with brittle behaviour of connections. Specific requirements prescribed in CAN/ CSA S16-09 (CSA 2009) for CC systems are outlined below:

- If the specified short-period spectral acceleration ratio ($I_EF_aS_a(0.2)$) is greater than or equal to 0.35, the height of seismic force resisting systems may exceed 15 m provided that all factored seismic forces for ultimate limit states are augmented linearly by 2% per metre of height above

15 m. The final forces should remain below the elastic forces corresponding to R_dR_o = 1.3. If the specified short-period spectral acceleration ratio ($I_EF_aS_a(0.2)$) is greater than 0.75, or the specified one-second spectral acceleration ratio ($I_EF_vS_a(1.0)$) is greater than 0.3, the height of seismic force resisting systems can not exceed 40 m. Finally, the height of structure should not exceed 60 m, if the specified short-period spectral acceleration ratio is greater than or equal to 0.35 but less than or equal to 0.75 ($0.35 \leq I_EF_aS_a(0.2) \leq 0.75$).

- The dynamic analysis procedure should be used to determine the seismic forces and deformations of conventional constructions.

- The ductility-related and over-strength force modification factors, R_d and R_o, should be equal to 1.5 and 1.3, respectively.

- Columns, beams and braces with I-shaped or HSS sections should satisfy limits for Class 1 or 2 section.

- The seismic design requirements including seismic load path, members and connections supporting gravity loads, material requirement, bolted connections, probable yield stress and stability effects (Clause 27.1.3 to Clause 27.1.8) given in chapter 27 of CSA S16 should be satisfied.

- The width-to-thickness ratios should be less than $170/\sqrt{F_y}$ for the legs of angles and flanges of channels and $670/\sqrt{F_y}$ for the webs of channels, when the slenderness of bracing members equal to or less than 200.

- Connections should be designed so that the expected governing failure mode is ductile. Otherwise, they should be proportioned to resist gravity loads combined with 1.3 times the member factored seismic forces. The connection design load should not exceed the member gross section strength.

- If the column is part of two or more intersecting seismic-force-resisting system, and the seismic induced axial load of column is determined from analysis of the building in any two orthogonal directions for 100% of the seismic loads applied in one direction and 30% of the earthquake loads applied in the perpendicular direction, the column should be designed to resist the gravity load combined with 1.3 times of the member factored seismic force.

- The factored seismic forces of diaphragms should be determined for the forces corresponding to $R_d R_o = 1.3$.

- An additional out-of-plane transverse force should be considered for the compression members of seismic force resisting system that are intersected by bracing members. This force should be equal to 10% of the axial load carried by the compression members at the intersection point.

2.2 Canadian and U.S. guidelines for seismic evaluation and retrofit of the structures

2.2.1 Commentary L of NBCC 2010 and Code de construction du Québec

In Canada, there are very limited guidelines for the seismic assessment of existing buildings. In NBCC 2010, the information for the evaluation and rehabilitation of existing structures are provided in Commentary L. For seismic loads, Commentary L refers to the Guidelines for seismic evaluation of existing buildings (NRCC 1993). Also, ASCE 11 (ASCE 1991) and Allen et al. (1995) were considered in this commentary for the assessment and retrofit of existing buildings. The documents are based on old U.S. guidelines (ATC-14 1987, ATC-22 1989, FEMA 1992a, FEMA 1992b) and 1990 edition of NBCC and are no longer up-to-date. The guidelines for seismic evaluation of existing buildings specifies that for the seismic assessment of the structure, a load factor of 0.6 should be applied to seismic loads to establish if seismic retrofit will be required. The guidelines also provide system-specific checks based on experience gained from past earthquakes and anticipated deficiencies due to the code changes. When retrofit is required, retrofit must be designed based on a more detailed investigation and using higher seismic loads, preferably those prescribed for new buildings, considering the future use of the building, control of seismic damage, and the differential in upgrading costs with force level (Allen et al. 1992). In this document, the information regarding the levels of the seismic loads, analysis procedures and acceptance criteria for seismic evaluations is provided. Guidelines for seismic retrofit of existing buildings are available in Allen et al. (1995). A procedure for rapid screening of existing buildings is provided that considers several parameters including seismicity, soil conditions, type of structure, building irregularities, building importance and non-structural hazards (Saatcioglu et al. 2013).

The Code de construction du Québec (Code de construction 2015), addresses specifically the existing buildings designed in accordance with the 1990 or earlier edition of the NBCC. It is specified in this document that if the building's seismic force resisting system is modified, the seismic weight is increased by more than 5% or the intervention affects more than 25% of the total floor area for post-disaster buildings, the seismic lateral resistance should be increased to a minimum of 60% of the level prescribed in NBCC 2005 (NRCC 2005).

2.2.2 ASCE 41-13 evaluation procedure

The ASCE 41-13 standard (ASCE 2013) is the state-of-the-art reference for the seismic evaluation and retrofit of building structures in the United States. To initiate the evaluation process, it is necessary to establish the performance objectives by selecting a performance level for a given level of seismic hazard. Several target building performance levels are defined for structural and non-structural components including operational, immediate occupancy, life safety and collapse prevention performance level. The earthquake hazard level varies from 50% probability of exceedance in 50 years to risk-targeted maximum considered earthquake (MCER) that is 2% probability of exceedance in 50 years. To meet the basic performance objective, the existing building must exhibit the life safety performance for 20% in 50 years seismic hazard (BSE-1E) and the collapse prevention performance for 5% in 50 years hazard (BSE-2E). These objectives are less severe than the performance objective envisioned for new buildings in NBCC 2010: collapse prevention for 2% in 50 years seismic hazard.

To validate if the performance objectives are achieved, a three-tiered evaluation procedure is proposed ranging from screening (Tier 1), deficiency-based evaluation (Tier 2) to systematic evaluation (Tier 3). In Tier 1 evaluation, the potential deficiencies of the building are identified on the basis of the performance of similar structural systems in past seismic events. According to Tier 2 deficiency-based evaluation, the deficiencies identified in Tier 1 are further evaluated to determine if they represent actual deficiencies that should be corrected. In Tier 3 systematic evaluation, a comprehensive evaluation of the existing building should be performed to account for the nonlinear response of the structure. In Tiers 2 and 3, the seismic demand of the structure is evaluated using static and dynamic analysis procedures, linear or nonlinear, as required, and the demand imposed to each component is assessed using prescribed acceptance criteria. Linear analysis is usually performed to carry out a preliminary assessment. For the evaluation of existing

buildings with severe deficiencies, it is expected that selecting appropriate performance objectives, using a Tier 3 systematic evaluation with advanced nonlinear analysis and applying realistic acceptance criteria for structural components can provide more efficient retrofit solutions compared to simply applying seismic design provisions for new buildings.

ASCE 41-13 requires that structural components be classified as either primary or secondary components. A primary component should resist seismic forces and accommodate imposed seismic deformations to provide the selected performance level for the structure. If a structural component accommodates seismic deformations, but is not required to resist the seismic forces, it should be categorized as a secondary component. The structural elements are categorized as either deformation-controlled (ductile) or force-controlled (non-ductile) components. For the same structural component, the same actions may be classified in different categories. For instance, the flexural behaviour of the beams and columns can be considered deformation-controlled or force-controlled depending on the amplitude of the axial loads. However, the following actions in concentrically braced frames remain constant in their classifications as the force- or deformation-controlled elements:

- Axial tension and compression of braces should be evaluated as deformation-controlled;

- Actions on brace connections including tension, compression, shear and bending actions should be considered force-controlled; unless, the connections are modeled and experimental results indicate that stable and desirable ductility can be obtained in a specific connection element.

The deformation-controlled elements are evaluated using expected strength, Q_{CE}; while, lower-bound strength, Q_{CL}, should be determined for the assessment of force-controlled components. The expected yield strength is defined as the mean value of resistance of a component at the deformation level for a group of similar components that considers the variability in material strength including strain hardening and plastic section development. The lower-bound strength is determined from the lower bound yield strength which is equal to the mean minus one standard deviation of the yield strengths for a population of similar components. The expected strength is calculated using expected material properties, while the lower-bound strength is defined using lower-bound material properties.

The acceptability of deformation- and force-controlled actions should be evaluated for each element. In the linear procedures, the acceptance criteria for deformation –controlled actions in primary and secondary components are determined by Equation 3:

(3) $m\kappa Q_{CE} \geq Q_{UD}$

where, Q_{CE} is the expected strength of a component at the deformation level under consideration, Q_{UD} is the deformation-controlled design action due to gravity loads and earthquake loads, which equals to $Q_G \pm Q_E$, m is the component demand modification factor to account for expected ductility related to this action at the selected structural performance level, and κ is the knowledge factor.

The acceptance criteria for force controlled actions in primary and secondary components are defined by Equation 4:

(4) $\kappa Q_{CL} \geq Q_{UF}$

where, Q_{CL} is the lower-bound strength of a component at the deformation level under consideration, and Q_{UF} is the force-controlled design action that is determined by the following equation:

(5) $$Q_{UF} = Q_G \pm \frac{Q_E}{C_1 C_2 J}$$

In Equation 5, C_1 is the modification factor that relates expected maximum inelastic displacements to displacements calculated for linear elastic response, C_2 is the modification factor to consider the effect of pinched hysteresis shape, cyclic stiffness degradation, and strength deterioration on the maximum displacement response, and J is the force delivery reduction factor, calculated as the smallest demand capacity ratio (*DCR*) of components in the load path delivering force to the component. To calculate the demand capacity ratio, *DCR*, the value of Q_{UD} should be divided by Q_{CE}.

The columns of concentrically braced steel frames should be evaluated as the columns of fully restrained moment frames. If the column axial load exceeds 50% of the lower-bound axial compressive strength, P_{CL}, the column should be considered force-controlled for both axial loads and flexure, and when the column axial load is less than 50% of the lower-bound axial column strength, the column should be considered deformation-controlled for flexure and force-

controlled for axial compression. The equations 6 to 8 are employed to evaluate steel columns with compressive axial force and flexural demand:

For $\frac{P_{UF}}{P_{CL}} < 0.2$:

$$(6)\ \frac{P_{UF}}{2P_{CL}} + \frac{M_x}{m_x M_{CEx}} + \frac{M_y}{m_y M_{CEy}} \le 1.0$$

For $0.2 \le \frac{P_{UF}}{P_{CL}} \le 0.5$:

$$(7)\ \frac{P_{UF}}{P_{CL}} + \frac{8}{9}\left[\frac{M_x}{m_x M_{CEx}} + \frac{M_y}{m_y M_{CEy}}\right] \le 1.0$$

For $\frac{P_{UF}}{P_{CL}} > 0.5$:

$$(8)\ \frac{P_{UF}}{P_{CL}} + \frac{M_{UFx}}{M_{CLx}} + \frac{M_{UFy}}{M_{CLy}} \le 1.0$$

In these equations, P_{UF} is axial force in the member and P_{CL} is lower-bound compression strength of the column. In Equations 6 and 7, M_x, M_y, M_{CEx} and M_{CEy} are bending moments in the member and expected bending strengths of the column for the x-axis and y-axis, respectively; and m_x and m_y are values of m for the column bending about the x-axis and y-axis. In Equation 8, M_{UFx}, M_{UFy}, M_{CLx} and M_{CLy} are bending moments in the member and lower-bound flexural strengths of the member about the x-axis and y-axis, respectively. For the member with the axial load that varies between 10% and 50% of the lower bound axial strength, the *m*–factors should be determined with respect to the ratio of P_{UF}/P_{CL}, flange slenderness and web slenderness.

The ASCE 41-13 approach for the evaluation of beams and columns depends on the ratio of the axial load to the axial strength of the member (P_{UF}/P_{CL}). If the strength of beams with axial loads exceeds 10% of the members' axial strength, the evaluation should follow the procedure prescribed for columns.

2.3 Numerical and experimental studies on seismic behaviour of existing CBFs

Several experimental and numerical studies addressed the behaviour of existing concentrically braced frames, and examined different retrofit strategies. The experimental studies mentioned in this section were carried out at University of Washington.

2.3.1 Experimental studies

Johnson et al. (2014) selected fourteen existing concentrically braced frames designed as per standards before 1988 in high seismic zones of the U.S. In these systems, the most common type of brace cross section was hollow structural sections (HSS); however, other brace cross sections including wide flanges, angles and pipes were also used. The most common type of lateral load resisting system in buildings less than 5-storey height was chevron braced frame, and this system was found popular in 70% of the surveyed buildings. The demand-capacity ratio specified in ASCE 41 was used for the evaluation of structural members. The assessment results showed that 75% of chevron braced frames had inadequate resistance of beams. Insufficient flexural strength of the beams was a consequence of the design approach in 1980's codes which did not consider the unbalanced load effects in the beam design. The columns also had insufficient strength, because they were not designed to develop the capacity of braces. Brace net section fracture was identified as a common deficiency of brace connections. The full-scale quasi-static cyclic tests were performed on a single bay, single diagonal brace configuration to evaluate connections designed in accordance with current and older detailing practices which are used in special concentrically braced frames (SCBFs) and non-seismic concentrically braced frames (NCBFs). The performance of non-seismic concentrically braced frames was studied on the first test specimen (NCBF 0). A pair of double angles was used to connect the beam web and the gusset plate to the column flange, and the connections were designed based on the 1988 UBC (ICBO 1988). In this test specimen, the fracture of welds occurred at 0.52% storey drift, which revealed that the connection had a non-ductile behaviour. The second specimen (NCBF 1) consisted of an HSS 7x7x1/4 brace cross section with high width-thickness ratio, connected by means of a thin gusset plate and short spliced length. A plastic hinge formed in the brace at 0.51% drift in compression with minimal damage in the connection. This test shows the concern regarding the brace compactness that can be an important issue for the evaluation and retrofit of NCBF systems

compared to the connection capacity. Figure 2.1 shows the fracture of connection in the specimen NCBF 0 and brace hinge formation in the NCBF1 test.

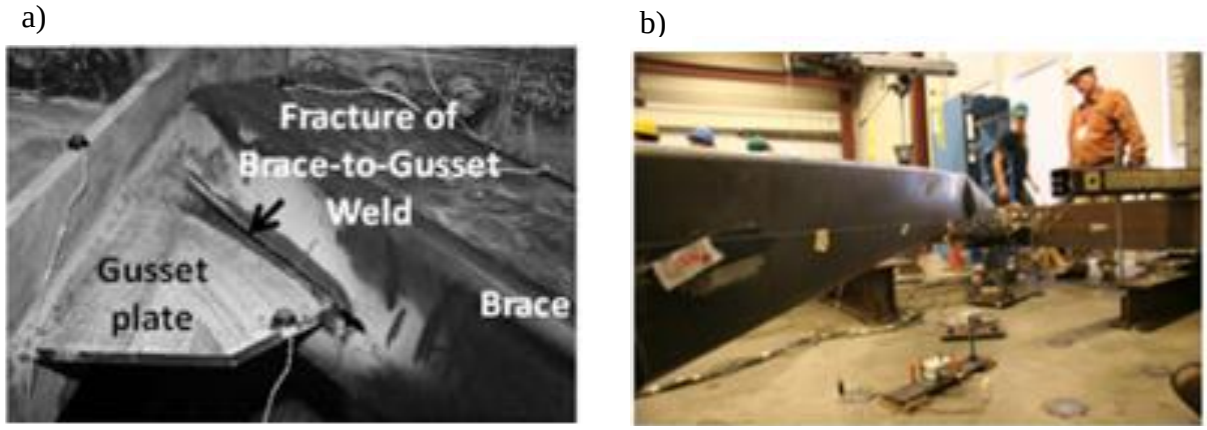

Figure 2.1: a) Connection fracture in NCBF 0; and b) Brace hinge formation in NCBF 1 (Johnson et al. 2014).

In the third test, NCBF 2, a more compact brace cross section, HSS5x5x3/8 was used. No plastic hinge was formed in the braces; therefore, the axial and rotational demands increased on the connection, and weld tearing occurred at the end of the gusset plate-to-beam welds which led to the brace connection fracture. The detailing connection of NCBF 3 is the same as NCBF 2; however, there was no minimum toughness requirement for the welds, which were designed according to AWS E71T-11. In this test, the specimen reached the maximum drift of 3.3% but the failure mechanism was non-ductile. Figure 2.2 shows the fracture of the connection at the end of tests for specimens NCBF 2 and NCBF 3.

a) b)

Figure 2.2: a) Connection fracture in NCBF 2; and b) Weld fracture in NCBF 3 (Johnson et al. 2014).

The first SCBF test, SCBF 1, was a bolted connection designed according to the current AISC Seismic Provisions (ANSI/AISC 341-10). The brace fractured at 2.78% drift and no damage occurred for the elements of brace connections. The NCBF 4 test was a common bolted connection used in existing braced frames. The details of this connection were similar to the NCBF 3 specimen; however, a deficient bolted joint was used in NCBF 4. This connection had a ductile behaviour, and its performance was similar to the SCBF connection. Figure 2.3 shows the brace fracture in the SCBF 1 specimen, and the bolt hole elongation in the web of the beam of the NCBF 4 specimen.

a) b)

Figure 2.3: a) Brace fracture in SCBF 1; and b) Bolt hole elongation in the web of the beam of NCBF 4 (Johnson et al. 2014).

It was shown that the ductility of some NCBF systems is higher than expected; nevertheless, such systems may result in undesirable failure modes. Also, the replacement of the non-seismically compact brace by a seismically compact section can be an efficient retrofit approach to prevent brace fracture at small inelastic deformations.

Sloat (2014) has evaluated the response of the braces and connections in existing non-ductile concentrically braced frames, and he proposed several retrofit solutions to improve their seismic performance. It was concluded in this study that the severe local brace slenderness can be retrofitted by replacing the brace with a compact section or by filling the brace with concrete. Additionally, the gusset plate to the beam weld is vulnerable due to the lack of brace end clearance on the gusset plate. This weld can be protected by the application of an in-plane buckling brace with a knife plate retrofit. Also, the bolt reinforcement can be used to improve the deficient gusset plate/beam to shear tab weld.

Sen et al. (2014) studied the response of three full-scale two-storey chevron braced frame with weak beams. The first NCBF specimen, Specimen 1, was considered as a pilot test with the details of actual NCBF system. A non-seismically compact brace cross section, HSS7x7x1/4, was used for both storeys, as the compactness requirements were usually not satisfied in NCBF systems. In Specimen 1, a beam cross-section with a low flexural strength, not capable to resist the unbalanced load demands induced by the expected brace capacities, was selected for the bottom level (W16x45). A larger W24x94 section was used for the beam at the top level, as the purpose of this test was the evaluation of the beam at the bottom level. Specimen 2 and Specimen 3 were considered as the retrofit solutions for the pilot specimen. The seismically compact brace cross sections, HSS5x5x3/8, were used at the bottom level of Specimen 2. In-plane buckling of the braces was induced by designing knife plate connections with the clearance of $3.25t_{kp}$, where t_{kp} is the thickness of the knife plate. The net section reinforcement was added for the braces at the second level. The gusset plate connections at the first storey were designed using the balanced design procedure. The same beam cross sections used for Specimen 1 were considered for the second test. The third specimen was retrofitted using wide flange bracing members, H175x175x7.5x11 at the first storey. These braces were designed for out-of-plane buckling. Also, the brace connections were designed in accordance with the balanced design procedure. Another full-scale two-storey chevron braced frame was added to this program, named Specimen 4 (Sen et

al. 2016a). Specimen 4 with ductile braces and connections was intended to evaluate the response of a yielding-beam chevron braced frame. In this specimen, the braces at both levels were replaced by HSS5x5x3/8. The braces were connected to the 12-mm gusset plates. A new W16x45 beam was applied at the first storey and a single row of 19-mm-diameter shear studs at the distance of 115 mm was installed to increase the composite action. In Specimen 4, the first-storey beam was laterally braced at the mid-span. Also, the fully restrained welded web-welded flange beam-to-column connections were considered at this level. The rotation was permitted at the ends of the braces of the second storey.

For Specimen 1, the brace fracture at the first storey of the NCBF system occurred at much smaller deformations compared to SCBFs. However, the brace at that level did not buckle; because the flexural capacity of the beam at the first storey was much less than the brace axial capacity; thus, the beam acted similarly to a link beam in the eccentrically braced frame (EBF) system. Later in the test, the partial fracture happened at the brace-beam connection. Note that the brace fracture occurred in Specimen 1 as a result of high brace local slenderness. The study of Goel (1992) showed that severe local buckling is common in non-compact braces, which can cause an earlier brace fracture. Figure 2.4 shows the brace fracture and partial fracture of brace-beam gusset plate connection at the first level. This specimen exhibited a highly non-ductile performance.

a) b)

Figure 2.4: a) Brace fracture of first storey brace; and b) Partial fracture of first storey brace-beam gusset plate (Sen et al. 2016a).

In Specimen 2, the out-of-plane buckling of the braces occurred at the first level, though these braces were designed for in-plane buckling. The system showed a significant ductility, which could be as a result of the weak beam. Several factors including torsional rotation of the beam, ductile tearing of the gusset plate interface welds, lack of lateral support at the brace intersection, and the gusset plate flexural stiffness compared to the knife plate may have contributed to the out-of-plane buckling of braces. Out-of-plane displacement of the brace at the first level and yielding of bottom beam flange and gusset plate are illustrated in Figure 2.5.

a)

b)

Figure 2.5: a) Out-of-plane deformation of brace; and b) Bottom beam flange yielding and gusset plate elliptical yielding (Sen et al. 2014).

The brace-beam-column gusset plate connections failed at the second storey of Specimen 3, which was the combination of net section, brace base metal and splice weld rupture. Figure 2.6 shows the out-of-plane displacement of the wide flange brace and the brace connection failure at the second storey.

a) b)

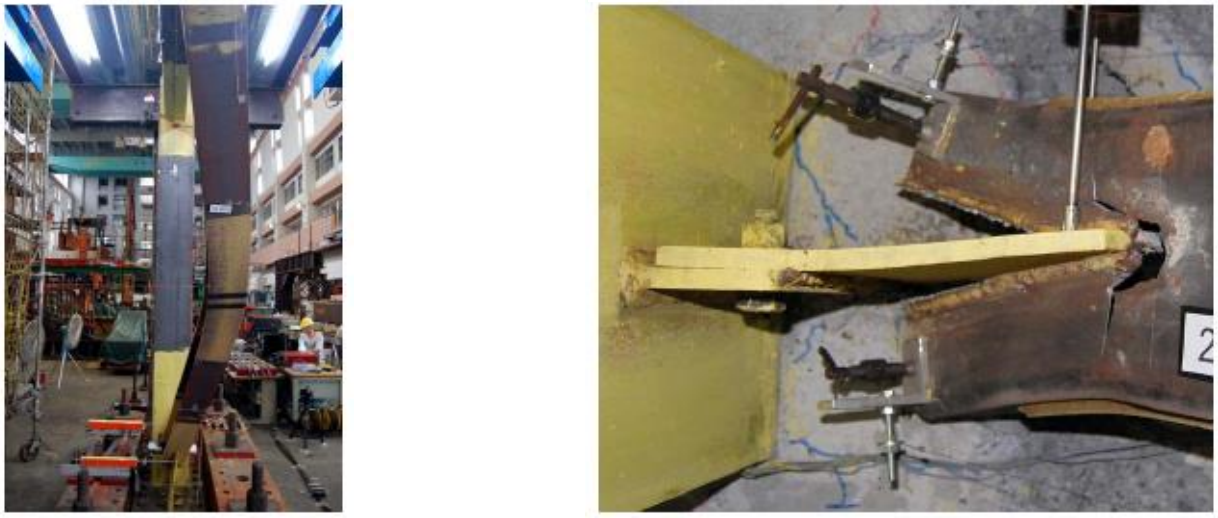

Figure 2.6: a) Out-of-plane deformation of wide flange brace; and b) Brace connection fracture at the second level (Sen et al. 2014).

In Specimen 4, all braces buckled, which caused the inelastic deformations at storeys 1 and 2. The tensile force in the brace was limited by the yielding-beam mechanism; however, there was no degradation in the lateral resistance of the frame as a result of frame action. In this test, the frame performed well and the beam at the first level had limited damage.

The test results demonstrated that the most vulnerable elements in concentrically braced frames are HSS braces that are noncompliant with SCBF seismic slenderness limits. If the braced frame has ductile braces with deficient connections, the retrofit strategy should be employed for the connections. The results of the experimental study confirmed that the beams of the chevron braced frame with axial-flexural demand to capacity ratios (DCRs) of 2.5 or less are of least priority for seismic retrofit.

Sen et al. (2015) evaluated the behaviour of connections in non-ductile concentrically braced frames, and examined retrofit strategies to improve their seismic performance. For the braces with bolted end plate connections, the replacement of the brace member was the proposed retrofit scheme. Three options were suggested including an out-of-plane (OOP) buckling brace, in-plane (IP) brace buckling and buckling-restrained brace (BRB), which improved the performance to various extents, but in all cases an increased deformation capacity was achieved compared to the existing braced frame.

Eight full-scale specimens were tested to define the impact of different connection deficiencies on the seismic behaviour of non-ductile concentrically braced frames (Sen et al. 2016b). In the tests, several connection details including split double angle, continuous shear plate, end plate, split shear plate and integrated gusset-shear plate connections using HSS braces with different local slenderness ratios were examined. The study showed that the HSS braces with high local slenderness limit the deformation capacity of the frame due to the onset of local buckling at small brace deformations followed by global brace buckling. Gusset plate-to-beam and shear plate-to-gusset and -beam welds sized sufficiently for the uniform force method (*UFM*) are found to be susceptible to fracture. It was concluded that the high retrofit priorities are the braced frames with HSS braces with local slenderness ratios greater than 1.5 times the limit defined for the special concentrically braced frames or with brace-to-gusset weld demand to capacity ratios (*DCR*s) exceeding 1.5. Gusset plate-to-beam, gusset plate-to-end plate, shear plate-to-gusset and -beam welds, which have the elliptical clearance less than two times of gusset plate thickness ($2t_p$), are also identified as higher retrofit priorities.

Astaneh-Asl et al. (1985) evaluated the cyclic behaviour of nine full-scale double angle bracing members composed of angles with unequal long leg placed back-to-back. Angles were connected by stitches, and the gusset plates were placed at the end of braces. The braces buckled out-of-plane. In all of specimens, two plastic hinges formed at the gusset plates and one at the midspan. It was found that the ductility of the out-of-plane buckling double-angle braces depended on the performance of end gusset plates and stitches. Astaneh-Asl et al. (1984) also tested eight full-scale double angle bracing members with short legs placed back-to-back. The double angle braces buckled in-plane, and three plastic hinges formed in the member. The deformed shape of specimens was close to the deformed shape of an axially loaded column with a fixed-fixed boundary condition.

The experimental study on the non-seismic concentrically braced frames (NCBFs) showed the deficiency of braces and brace connections are the primary concern for these systems. Even though the weak beams in chevron-braced frames seem to be problematic components, the studies indicated that braces and brace connections are still the priority for the retrofit of existing braced frames as beams could develop certain flexural ductility. No experimental study addressed the seismic evaluation of existing chevron braced frames with light beams carrying small tributary gravity loading.

2.3.2 Numerical studies

The undesirable nonlinear response of chevron bracing systems for high seismic demands was evaluated by several researchers (Anderson 1975; SEAONC 1982; Shibata and Wakabayashi 1983a, 1983b; Uang and Bertero 1986; Khatib et al. 1988; Nakashima and Wakabayashi 1992; Tremblay and Robert 2000, 2001; Tremblay 2001; Kim and Choi 2004). Because these systems have numerous architectural and structural advantages, the evaluation of their response in moderate seismic regions gained interest. In the study by Hines et al. (2009), the performance of low-ductility 3-, 6-, 9- and 12-storey chevron braced frames was assessed at collapse performance level. The frames located on Site Class D in Boston, Massachusetts, were designed using the response modification factor of 3 under 2% in 50-year seismic loads determined from IBC 2006 (ICC 2006). The objective was to investigate the reserve capacity provided by gravity load carrying system and gusset plate connections. They concluded that the improvement in details for gusset plate connections can allow that the connections are considered as a reserve component in the system.

Tremblay and Robert (2000) investigated two design approaches for multi-storey chevron braced frames including 2, 4, 8, and 12 storeys. The structure was first designed in accordance with the requirements of CSA-S16.1 (CSA 1994) for the nominal ductility (NDBF) category, using the force modification factor R = 2.0. Following this approach, the beam sections should provide sufficient strength to initiate brace buckling. However, no minimum flexural capacity was required for the beams to reduce the degradation in storey shear stiffness and strength. In the second design approach, the beams were designed to carry the combination of their tributary gravity loads and the loads induced in the braces after buckling. The vertical support provided by the braces was neglected, and the R factor equal to 3 was used. It was proposed that these systems be categorized as a ductile braced frame (DBF) in CSA-S16.1 with seismic loads equal to the two-thirds of the loads specified for nominal ductility braced frame (NDBF) systems. Several fractions of the brace tension yield load were studied to examine the required beam capacity. The structure designed by 100% of brace tension yield load exhibited much higher storey shear capacity after buckling of braces compared to NDBF systems. However, additional weight of steel material is required for the beams. The increase in steel tonnage is less noticeable in taller buildings or when the structure is designed for a lesser level of brace tension yield load.

Tremblay and Robert (2001) evaluated the performance of the designed chevron braced frames, using nonlinear time history analyses. The analyses results were used to define the allowable height of chevron braced frames with beams capable of resisting various levels of loads induced after brace buckling. The allowable height of a system with 60% of brace tension yield load (DBF-60) is a 4-storey chevron braced frame. This conclusion considered as a provision in the steel structures design standard CAN/ CSA S16-09. The height of the NDBF system and a system with 100% of brace tension yield load (DBF-100) were also limited to 2-storey and 8-storey, respectively. If small gravity loads applied to the beams of the chevron braced frame, the height of DBF-100 system can be increased to 12-storey. The flexibility of beams required to develop the maximum tension forces in the braces of DBF-60 system were 10% to 25% lesser than the value assumed in the design. For the design of the beam end connection, the maximum tension load that develops in the beams of ductile braced frames should be considered up to 1.25 times the values assumed in the design procedure. The columns of inverted-V bracing systems should be designed for a compressive force, while all compression braces reached to their buckling strength, simultaneously.

Jiang et al. (2012a) evaluated the seismic performance of 4- and 10-storey concentrically braced steel frames, located in Montreal, Quebec and Vancouver, British Columbia. The frames were designed in accordance with the provisions of the 1980 NBCC and the CSA-S16.1-M78 standard. The lateral resistance in two orthogonal directions was provided by tension-only braced frame and chevron braced frame with back-to-back double angle braces. The structures were evaluated based on the requirements of NBCC 2010 and CSA S16-09 design standard. The study showed that the seismic design loads of the 10-storey building have increased significantly since 1980, because of the new seismic hazard data, the upper limits imposed on periods of structures designed in accordance with NBCC 2010 and the amplification of seismic load required for conventional construction with the height of more than 15 m. It was found that most of the braces and all of brace connections in 4- and 10-storey buildings did not satisfy axial strength requirements. In the 10-storey building, all beams of the braced frames located in Vancouver and all beams of chevron braced frame in Montreal had inadequate resistance. Additionally, all columns and their anchorage to foundations of the 10-storey braced frames in Vancouver did not have sufficient axial capacity.

Harris and Speicher (2015) evaluated 4-, 8- and 16- storey steel special concentrically braced frames (SCBF) located in a high seismic zone using the ASCE 41 standard. Different analysis procedures such as linear static procedure (LSP), linear dynamic procedure (LDP), nonlinear static procedure (NSP) and nonlinear dynamic procedure (NDP) were used for the assessment. It was found that the LSP yields more conservative results compared to the LDP; mainly because of the differences in the distribution of seismic demands and the limitation of using only the fundamental mode in the LSP. However, the NSP results are less conservative in comparison to the NDP, as a result of the differences in the distribution of seismic demands and the limitations associated with the modal analysis in the NSP. It was concluded that the nonlinear procedures provide more rigorous evaluation approach and less conservative assessment results compared to the linear procedures. The evaluation results showed the inherent conservatism of the linear procedures; however, this conservatism required less analytical resources and proficiency of the analyst. In this study, the assessment results of brace members, obtained by linear and nonlinear procedures, were not always consistent. The evaluation results indicated that columns with high axial and flexural demands and bracing members are likely to be deficient in view of the acceptance criteria given in ASCE 41. They concluded that the refinement of interaction equations for specific failure mechanisms can lead to consider the column as a deformation-controlled component instead of a force-controlled member. It was suggested that stability of a beam-column should be considered in ASCE 41 in addition to capturing flexural plasticity, when $P/P_{CL} \leq 0.5$ for nonlinear procedures.

The seismic response of a 2-storey braced frame designed in accordance with the 1980's codes and located in California was evaluated using nonlinear static analysis proposed in ASCE 41-06 (ASCE 41-06) by Callister and Pekelnicky (2011). The results of the seismic assessment of the structures revealed that the brace connections were prone to fracture. The structure became more flexible after the fracture of brace connections; however, the gravity frames had adequate flexibility to accommodate the drifts, and the structure was stable during the seismic event. The studied building showed satisfactory performance for the life safety level.

Hsiao et al. (2014) used a practical nonlinear model for concentrically braced frames that was calibrated against experimental results. The numerical models were developed in *OpenSees* (Mazzoni et al. 2009) to evaluate the seismic performance of concentrically braced frames. In

these models, force-based beam-column elements were used to model braces, beams and columns. Also, a multicomponent connection model was developed to simulate the gusset plate connections. The *OpenSees* model was verified using the experimental results from the special concentrically braced frame tests (Hsiao et al. 2012). In this study, the numerical and experimental methods were used for the seismic evaluation of an NCBF system. It was concluded that the deficiency in braces or brace connections for the NCBFs is expected during the moderate seismic event. Also, the collapse of NCBFs is predictable under the maximum considered earthquake (MCE).

Aguero et al. (2006) performed a study to investigate the possibility of modelling the seismic inelastic cyclic response of steel bracing members using the *OpenSees* computer program. In this study, two types of cross sections were considered for braces including rectangular and square steel tubes. The efficiency and accuracy that obtained by the application of the force (FBE) and displacement (DBE) based elements were compared. FBE and DBE models were evaluated for several combinations of number of elements along the brace length, number of integration points along the element length, number of fibers used to define the cross section and amplitude and number of displacement increments. The numerical predictions were compared to individual brace and full-scale frame test results. Also, the influence of time step and brace discretization on the dynamic seismic response was investigated for a typical braced steel frame.

Jiang et al. (2012b) developed a model for the back-to-back double angle bracing member in the *OpenSees* finite element structural analysis platform (McKenna and Fenves 2004). Centres of gravity of each angle were connected by high stiffness elastic beam column elements. *Zerolength* elements were used to model the brace connections. In this study, several material properties were assigned to the *zerolength* elements. The *pinching4* material was used to reproduce the nonlinear axial load-deformation response caused by local yielding of the brace member and brace connection, bearing of bolts, shear deformation and slippage of bolts, uniaxial *Giuffré-Menegotto-Pinto* steel material with isotropic hardening (Steel 02) was assigned to the elements to simulate the nonlinear behaviour of braces, and elastic properties were applied for torsional response. The stiff elastic beam-column elements were considered to connect the brace-to-gusset connection to the structural members such as beams or columns. The contact behaviour between the two angles of braces was simulated using stiff elastic beam column elements and *zerolength* elements with elastic-perfectly plastic gap material that were used at each pair of nodes. Also,

one stitch was used at the middle of bracing member to connect the double angles. The stitch was modelled using a stiff elastic beam column element.

Sen et al. (2014) evaluated chevron braced frames with weak beam using numerical and experimental study. Numerical models were developed in ABAQUS (Dassault 2013) using shell elements for the steel members and solid elements for the concrete slab. The initial out-of-plane geometrical imperfections in the braces were not exceeded L/500, where L was the brace length. The steel material properties used in the numerical models were derived from coupon tests. In both numerical and experimental studies, the frame was subjected to the same increasing amplitude cyclic loading protocol applied at the top slab. The experimental response of the specimens mentioned in section 2.3.1 was compared with the behaviour of the numerical model. Figure 2.8 shows that the global responses of the experiments and the finite element analyses were match reasonably well. Some test events such as brace and connection fracture were manually initiated in the numerical model to provide the reasonable similarity between both experimental and numerical results.

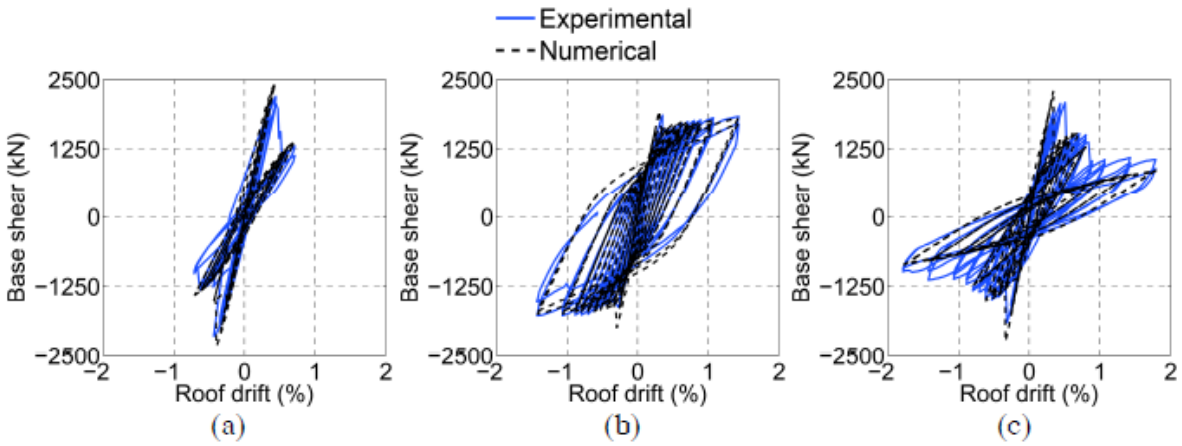

Figure 2.7: Roof drift-base shear hystereses for a) Specimen 1; b) Specimen 2; and c) Specimen 3 (Sen et al. 2014).

In the past studies, the seismic response of the concentrically braced frames with different heights was evaluated. Also, the ASCE 41 procedures were considered for the assessment of special concentrically braced frames. In this research study, the seismic response of existing concentrically braced frames including tension-only and chevron braced frames was evaluated to

identify the deficiencies of these systems. The evaluation results were compared to determine the impact of the application of different procedures on the assessment results.

2.4 Seismic behaviour of steel columns

In section 2.3.2, the acceptance criteria of ASCE 41 for steel columns are specified. No ductility is considered for columns when the P_{UF}/P_{CL} ratio equals 0.5. This section describes the experimental studies that were performed on steel columns to evaluate the seismic response and ductility of these members and thereby evaluate the appropriateness of the ASCE 41 criteria.

Newell and Uang (2008) performed a study to provide the information regarding the performance assessment of steel columns under combined axial load and drift demands. The cyclic test was conducted on nine full-scale wide-flange (W14) column specimens subjected to different levels of axial load demands including 35, 55 and 75% of nominal axial yield strength P_{yn} at large drifts (e.g. 10%) in the strong axis direction. The specimens were representative of the column sections at bottom stories of multi-storey braced frames. The loading began with the application of gravity load to the specimen; then, the loading sequence continued as the combination of target column compressive axial load and storey drift ratio, which was applied in-phase. According to the test results, flange local buckling was the dominant buckling mode observed for all specimens except one. The reason is attributed to the stocky web that delays the onset of flange local buckling, which provides large deformation capacity for the specimens. The global buckling was not observed during the tests. The authors concluded that the plastic rotation capacities defined in ASCE 41 are extremely conservative; while ASCE 41 does not admit any plastic rotation capacity at axial load ratios greater than 0.5, the specimens showed considerable rotation capacity for that axial load level. Figure 2.8 shows the deformed shape of the specimen W14x132 subjected to 75% of nominal axial yield strength at 4% and 10% storey drift.

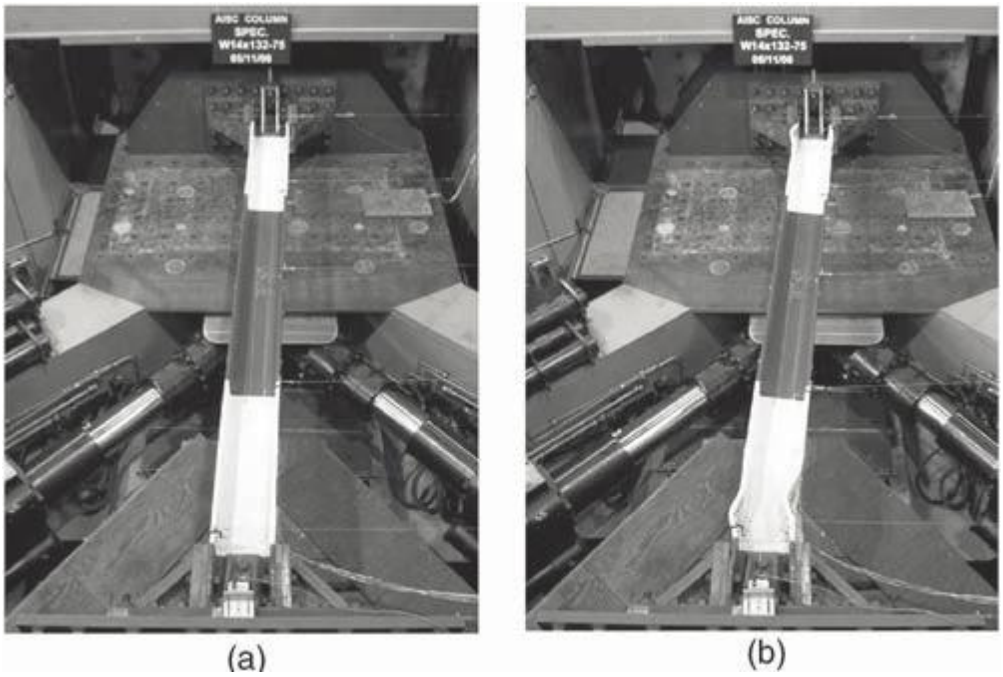

Figure 2.8: Overall deformed shape of specimen W14x132-75 at a) 4% drift; and b) 10% drift (Newell and Uang 2008).

MacRae et al. (1989) tested eight 250 UC 73 (Universal column with the height of 250 mm and the weight of 73 kg/m similar to W25) I-shaped column sections that were subjected to different levels of axial loads including 0.0, 0.3, 0.4, 0.5, 0.6, 0.7 and 0.8 of P_y and cyclic strong axis bending. The results confirmed that the governed failure mechanism of column specimens was flange local buckling.

The buckling and post-buckling responses of columns in the multi-storey braced frames were evaluated by Lamarche and Tremblay (2011). Four full-scale W-shaped, W310x129, column specimens were examined for several loading protocols including monotonic and cyclic loadings. The axial load was applied eccentrically to one of the specimen; while, concentric axial load was applied to the others. Three tests were performed under quasi-static cyclic loading, and dynamic cyclic loading was considered for one test. The cyclic test was performed in two steps: at first, a static axial load corresponding to 60% of the column nominal compressive resistance was applied to reproduce the gravity induced axial load, the loading followed by cyclic axial displacements imposed to simulate the seismic demands expected in the columns of braced frames. The weak axis buckling occurred for all of column specimens followed by the formation of a flexural plastic hinge at the mid-height of the specimen. According to the experimental results, the

specimens subjected to monotonic and quasi-static cyclic axial displacements can carry the gravity loads with the axial deformations corresponding to 0.53% of the column height; while, the out-of-plane displacements are equal to 0.037 of the column height at the mid-height of specimen. In the cyclic tests, local flange buckling occurred before global buckling for the eccentric loading case; however, in the centrally loaded cyclic tests, local flange buckling developed in the post-buckling range. Furthermore, the comparison of quasi-static and dynamic cyclic tests shows that high strain rates could increase the column buckling and post-buckling compressive strength. Figure 2.9 showed the buckling of column in the quasi-static cyclic test, where the concentric axial load was applied to the column.

Figure 2.9: Column specimen at the end of test (Lamarche and Tremblay 2011).

To validate experimental results, the *OpenSees* model of the column was developed using nonlinear beam-column elements. The residual effects were considered. It was found that the *OpenSees* model could reproduce the buckling and post-buckling response of columns both in monotonic and cyclic loadings. Figure 2.10 shows the comparison of experimental result and numerical prediction with and without inclusion of residual stresses. Residual stresses have a significant impact on the buckling load, which reduces in the post-buckling range.

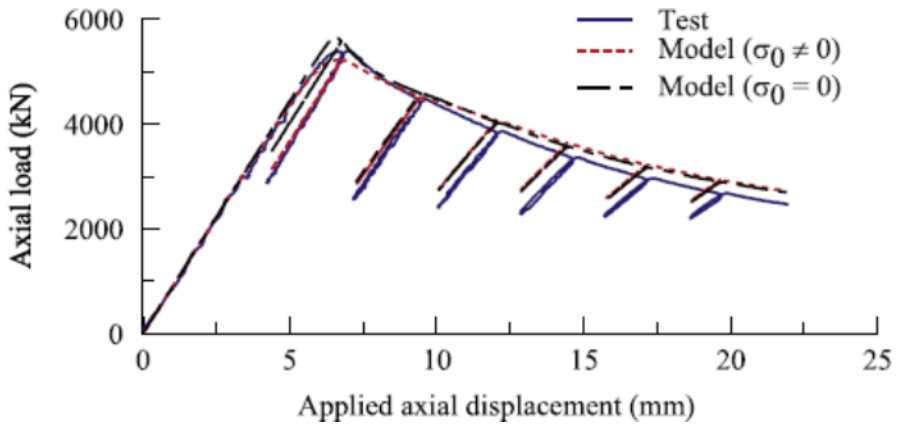

Figure 2.10: Axial load-axial displacement response of the W-shaped column (Lamarche and Tremblay 2011).

Cheng et al. (2013) performed an experimental study in which six H-section steel beam-columns with large width-to-thickness ratios were subjected to combined constant axial load and cyclic rotation in the strong axis direction. The effect of axial load ratio was investigated by considering two levels of axial load ratios including 0.2 and 0.4 times nominal yield axial load of the member. The effect of the width-to-thickness ratios of flange and web was also evaluated. In the first step of the test, the axial load was applied to the specimen. Then, cyclic rotation was applied to the column while the axial load level was unchanged. When the cyclic lateral displacement reached the rotation of 0.02 radians, the monotonic lateral displacement was applied to the specimen until the failure occurred. It was found that local buckling was the governed failure mode of all specimens, and the inelastic behaviour of columns was influenced by the combinative mode of flange and web slenderness. It was also concluded that such sections offer limited strength, while providing certain level of ductility as well as dissipating limited amount of energy during the tests. Figure 2.11 shows the local buckling of both flanges and web concentrated near the bottom of specimen.

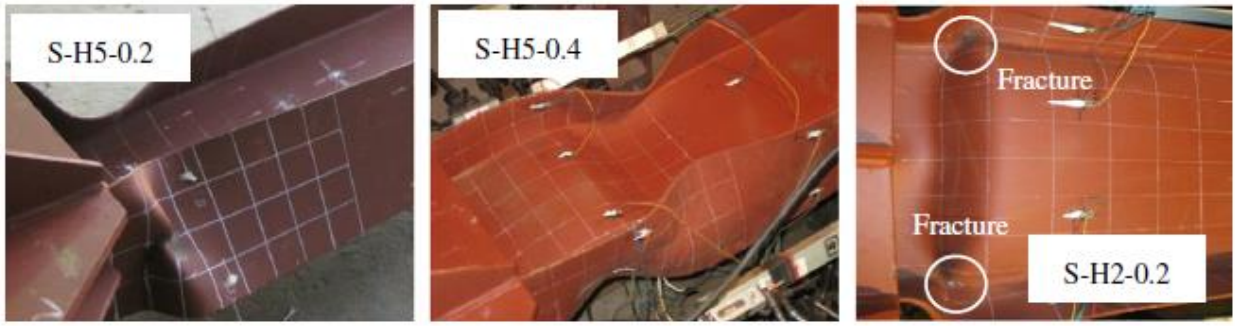

Figure 2.11: Failure modes of specimens (Cheng et al. 2013).

Zargar et al. (2014) tested a 1:8 scale W36x652 section subjected to high axial loads and large lateral displacement. The governing failure modes of specimens under different cyclic and monotonic loading protocols were lateral torsional buckling and web buckling. The test results confirmed that the plastic rotation capacity of the W36x652 section calculated by ASCE41 was considerably conservative compared to the test results. The lateral torsional buckling mode of one of the specimens is shown in Figure 2.12.

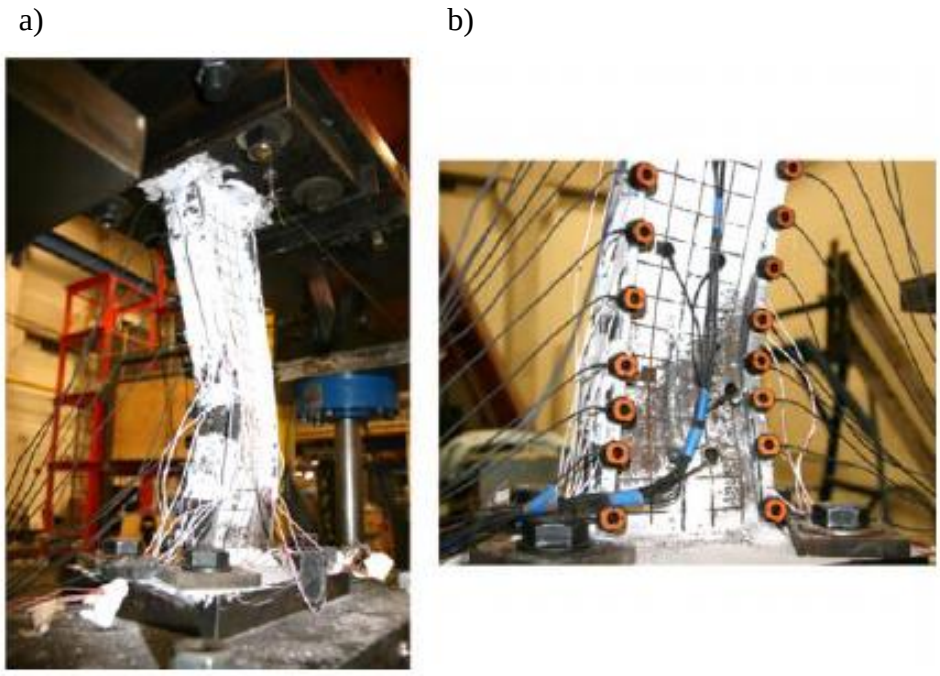

Figure 2.12: Lateral torsional buckling a) south flange view; and b) east view (Zargar et al. 2014).

The New Zealand Steel Structures Standard (NZS 3404) limits the plastic hinge rotation for the members of several seismic-resisting systems. The limiting hinge plastic rotation is defined based on the level of axial load in the member. For instance, the column with 80% of nominal section capacity can offer a plastic hinge rotation capacity of 0.008 radians. This limitation varies from 0.04 radians to 0.013 radians for the column loaded with 0.15 of nominal compression strength to the moderately axially loaded members with 50% of nominal compressive strength, respectively.

Bech et al. (2015) evaluated three high rise steel moment frames typical of the Pre-Northridge structures using ASCE 41 standard. The evaluation results indicated that steel columns should be classified as deformation controlled elements; though, the columns with high un-factored gravity load demands should be evaluated as force controlled members to prevent overloading the columns under combined gravity and seismic loads.

The performance of steel wide-flanged beam-columns under a combined axial and cyclic lateral loading scheme was evaluated by Fogarty and El-Tawil (2015). The numerical results showed that the strength of the columns with sections classified as highly ductile members in accordance with the current AISC Seismic Provisions (ANSI/AISC 341-10), reduce increasingly as a result of local buckling and lateral torsional buckling. The strength reduction occurred at drift level lower than 4%. Also, the slenderness ratio of web, h/t_w, has a significant effect on the strength of column compared to the flange slenderness ratio, b/t, for the sections that satisfy the current AISC Seismic Provisions' flange width-to-thickness ratio limit for highly ductile member. The results indicated that the dominant buckling mode of column changes from local buckling to lateral torsional buckling as the unbraced length increases, which shows the important role of L/r_y ratio. According to this study, the provisions of current AISC seismic design guidelines are potentially unconservative.

In the recent studies, twenty-five deep, slender column specimens were subjected to strong-axis inelastic cyclic loading with several levels of constant axial load (Uang et al., 2015). The results confirmed that the slenderness ratio had a significant effect on the failure mode. Also, the presence of an axial load produced significant local buckling and axial shortening in the specimens. Most of the column specimens tested in this study could not develop a plastic rotation of 0.03 radians, as the level of axial load affects the plastic rotation capacity of the column.

The review of experimental results showed that the acceptance criteria specified in ASCE 41 are conservative and that there is a potential for their relaxation. In this research study, both numerical and experimental studies were performed to assess further the appropriateness of the ASCE 41 acceptance criteria.

CHAPTER 3 METHODOLOGY AND RESEARCH ACTIVITIES

In this chapter, the key accomplishments of the research to achieve the specific objectives are presented. The research methodology is explained in the first part; while, the main activities of this study are discussed in the second part of this chapter.

3.1 Methodology

3.1.1 Seismic evaluation of existing concentrically braced frames

As the special seismic design provisions for steel structures were introduced in the 1989 edition of CSA S16, it is possible that the structures designed in accordance with the previous editions of the standard do not develop the ductile seismic behaviour. Thus, it is required to evaluate the seismic response of existing structures to identify the potential deficiencies. To achieve this objective, a 10 storey tension-only X-braced frame and 10- and 3-storey tension-compression chevron steel braced frames were designed in accordance with the 1980 NBCC (NRCC 1980) and CSA-S16.1-M78 (CSA 1978) steel design standard and their seismic response was assessed. The studied 10-storey building has a regular structural arrangement in plan with five 9.144 m wide bays in each orthogonal direction. The story heights are 4.572 m at the first floor and 3.962 m at the other nine levels. The specification of the plan and the storey height of the 3-storey building is the same as the 10-storey building. The lateral resistance of these buildings was provided by tension-only braced frames with back-to-back double angle members in the X configuration in one direction and the chevron braced frames in the other. The chevron braced frames included light beams supporting limited gravity loads. In 1980's, the beams of the chevron braced frames were not designed for the unbalanced vertical load induced by tensile and compressive forces in the tension and compression bracing members in combination with gravity loads. It should be noted that different heights were considered for the chevron braced frames to determine their effects on the seismic response of the structure. The studied buildings were located in Vancouver, British Columbia on class C site. The calculation of the factored compressive resistance of double angle braces and the block shear failure mode in brace connections are explained in APPENDIX B.

The seismic evaluation of the tension-only X-braced frame and tension-compression chevron braced frame was performed using different procedures including the procedures of NBCC 2010

(NRCC 2010) and ASCE 41-13 standard (ASCE 2013) to determine the impact of the application of different procedures on the seismic evaluation of existing braced frames. Initial assessment of the structures was carried out in compliance with NBCC 2010 requirements under 60% of seismic loads for a probability of exceedance of 2% in 50 years. As the retrofit of existing buildings should be performed for higher force levels, preferably meeting the performance objective for new buildings in accordance with NBCC 2010, the seismic evaluation was redone under 100% of the NBCC 2010 seismic loads. Also, the ASCE 41 standard was considered for the assessment of existing braced frames, as this standard is the state-of-the-art reference for the seismic evaluation and retrofit of building structures in the U.S, and it provides the acceptance criteria for structural members, while there is no acceptance criterion in the Canadian codes. Thus, the Tier 3 ASCE 41 procedure was used under 100% NBCC seismic loads to identify the potential deficiencies of the concentrically braced frames. Four analysis procedures are considered in ASCE 41 including linear static, nonlinear static, linear dynamic and nonlinear dynamic procedures. Although static procedures would be permitted for the regular structure studied, linear dynamic procedure (LDP) and nonlinear dynamic procedure (NDP) were used to obtain more realistic estimates of the seismic demand including dynamic effects. Also, nonlinear dynamic procedure (NDP) could provide a better understanding of the frame response and identify more precisely possible failure mechanisms.

The procedures of NBCC 2010 and ASCE 41 LDP were considered to evaluate the seismic response of existing concentrically braced frames using the response spectrum analysis (RSA). For this analysis, a three-dimensional model of the entire structure was employed in ETABS (CSI 2008) to account for accidental torsion. The model included the braces, beams and columns of the frames and all components were represented using elastic frame elements. Rigid diaphragms were considered at every level. In the tension-only X-braced frame, one of the two intersecting braces at every level was removed to simulate tension-only response. In this model, rigid column base was assumed. The response spectrum analysis was performed using the NBCC 2010 design spectrum for the site.

In the ASCE 41 NDP, several models were created for the studied structures in the OpenSees finite element structural analysis platform (McKenna and Fenves, 2004). Models B to D were developed, which were two-dimensional models and they were considered to verify the impact of the nonlinear response of different components on the seismic response of braced frames. The

details of models in OpenSees are mentioned in APPENDIX B. In Model B of both tension-only X-braced frame and chevron braced frame, only inelastic brace behaviour was represented, while all the other elements were modeled for elastic response. The specification of Model C was different in the studied braced frames as the deficient element was added to the model for each case. The deficient element was identified in accordance with the evaluation results of Model B. In the tension only X-braced frame, Model C included the inelastic response of braces and columns; while, in the Model C of the chevron braced frame, the inelastic response was provided for braces and beams. In Model D, braces, columns and beams could exhibit inelastic response for both braced frames. Model D was used to consider all possible deficiencies that could occur in the structural members.

The seismic response of both concentrically braced frames was evaluated using NBCC 2010, ASCE 41 LDP and ASCE 41 NDP using the models that described earlier. Different evaluation results were obtained by the application of each method; therefore, several retrofit schemes would be required for each procedure. Among the application of NBCC 2010, ASCE 41 LDP and ASCE 41 NDP, the model with inelastic response for braces (Model B) can be used for the explicit evaluation of inelastic deformation demands on the braces which are deformation-controlled actions and monitor peak force demands on columns, beams and brace connections that are categorized as force-controlled actions. This model can provide realistic estimates of force-controlled actions, and it can be a time saving solution that gives rapid insight into potential deficiencies of these actions. Model B can simulate the intended structural response with inelastic deformations limited to deformation-controlled actions, and it does not stop as a result of a failure in the force-controlled actions. Thus, this model is adequate to develop a final retrofit scheme. The model with nonlinear modelling of both deformation- and force-controlled actions can provide more accurate representation of complex failure mechanisms; however, the analysis may need to be repeated several times, and update the model each time to retrofit the deficient structural members until the satisfactory response of the frame is obtained.

The evaluation results of 10- and 3-storey chevron braced frames using ASCE 41 NDP showed that the beam buckled in-plane over one half of its length before brace buckling for different probabilities of exceedance including 2%, 5% and 10% in 50 years. Thus, a detailed three-dimensional finite element analysis was performed in ABAQUS (Dassault 2012) to further validate the beam buckling response as observed in the OpenSees nonlinear time history

analyses. Note that the OpenSees models could not reproduce local buckling and lateral-torsional buckling modes, and it was assumed that beam buckling about weak axis and in torsion was fully prevented in these models. Therefore, it was required to perform more advanced analysis to simulate local buckling and lateral-torsional buckling modes of the beam. The description of modelling in ABAQUS is explained in APPENDIX B. The ABAQUS model of the chevron braced frame included beams, braces and gusset plates of the 1st and 2nd levels of the 10-story frame. The nonlinear static analysis was performed, and the geometric nonlinearity (large deformation) was considered in the finite element analysis. Two models were considered to investigate the impact of the concrete slab and the effect of lateral bracing on the beam response. In the first model, the lateral movement of the beam was restrained, and in the second model, both the lateral movement and torsion of the beam was restrained. These restrains were applied at the beam top flange only, as there was no connecting element between the beam bottom flange and the non-structural elements in the past practice. The comparison of time histories of OpenSees and ABAQUS results showed that the OpenSees models can be used to predict the occurrence of beam buckling and provide a reasonable estimate of beam post-buckling response.

3.1.2 Retrofit of an existing chevron braced frame

To improve the seismic response of the 10-storey chevron braced frame, several retrofit strategies were proposed. Model D with inelastic elements for braces, beams and columns were used for the assessment of the retrofitted frame. As the seismic assessment of this structure indicated that the light beams were the most deficient elements, these structural members were retrofitted first in compliance with ASCE 41-13 requirements. According to ASCE 41-13, beams of chevron braced frames should be evaluated as force-controlled actions to resist the unbalanced load effects in combination with gravity loads. The expected yield capacity of the brace in tension and 30% of the expected compression capacity of the brace in compression should be used to calculate the unbalanced load effects. To satisfy this criterion, large W-shaped sections would be required for the beams; however, this strategy may not be feasible in view of the impact on the clear story height, the difficulty in bringing and installing the heavy shapes in an existing building and the significant weight of the retrofitted beams in the braced frame. As the evaluation results showed the occurrence of column buckling, which led to frame collapse for this retrofit scheme, other retrofit strategies were considered.

To propose cost effective and efficient retrofit schemes, all possible stiffness that can be provided by gravity columns, fixity at the base and flexural continuity of column splices was employed in the modelling. Elastic beam-column elements were considered to model the gravity columns. These columns were pinned at the base, and pinned splices were considered at every two-story segments. The identical gravity columns were lumped together and the sum of the area and moment of inertia were assigned to the lumped columns. These more appropriate modelling assumptions lead to improved seismic response, but could not eliminate the need for further retrofit. Nevertheless, being more realistic, they were considered in the model for the next proposed schemes to reduce the required retrofit work and the cost.

In the original design of the chevron braced frame, the same brace cross sections were selected in the bottom five levels which made the frame prone to the drift concentration at the base. Also, large W-shaped sections were required to retrofit the beams with existing braces using the ASCE 41-13 acceptance criteria. Therefore, it was decided to use new braces to achieve more uniform inelastic deformations over the frame height and minimize variations in story drifts. The selected braces should also aim at minimizing the force demand on beams and columns to reduce the retrofit cost on these members. Therefore, circular hollow sections were considered for braces to provide several options of cross sections, with high demand-to-capacity ratio. Different schemes were considered to select the brace cross sections including the application of the m-factor specified in Equation 3 of Section 2.3.2, using the expected buckling strength of braces, P_{CE} and considering the expected post buckling strength of braces. In the latter case, the expected yield capacity of the brace in tension, T_{CE} and 30% of the expected compression capacity of the brace in compression, 0.3 P_{CE} are the tensile and compressive forces in the braces. The last retrofit scheme to select the bracing members was applying the post buckling strength of braces, while maintaining the imposed demand on the foundation below its capacity. For all mentioned cases, beams were designed in accordance with the ASCE 41 LDP, and the existing columns were evaluated for two critical loading conditions including reaching the expected buckling strength of braces, P_{CE} and post buckling strength of braces, T_{CE} and 0.3 P_{CE}. The most critical loading condition was considered for the assessment of columns. No column retrofit was required for any of the proposed schemes, and it was the last retrofit scheme that had the minimum number of collapse. This scheme was kept, as it was not required to retrofit the existing columns and the foundation, and also all possible capacities of the braces were used in this strategy.

To adjust the capacity of the retrofitted braced frame, with no alterations of the existing columns and the foundation, two-dual system options were examined. The first option was the application of a low-ductility steel moment frame, and the second choice was using a stiff truss. Two configurations were considered for the stiff truss: a continuous truss and a truss with a hinge at the mid-height. Figure 3.1 shows the details of the two-dual systems. In this figure, Retrofit D_1 is the application of a moment frame, while Retrofits D_2 and D_3 are a continuous truss and a truss with a hinge at the mid-height, respectively. Retrofit E consists of the application of the latter truss to retrofit the existing chevron braced frame.

Moment frame members were verified to ensure elastic response under combined axial and flexural load demands. This frame was designed such that the plastic shear resistance of the beams, V_P, was in the proportion of the expected buckling strength of braces, V_{CE}. To avoid the formation of plastic hinges in the moment frame columns, beams and columns were proportioned to satisfy the strong column/weak beam criterion used for ductile frames. Elastic column response was considered as a necessary measure for vertically distributing the inelastic demand in the braced frame and mitigating soft-story response. This frame was modelled using force based nonlinear beam-column elements for the beams whereas elastic beam-column elements were used for the columns. The moment resisting frame (MRF) columns were fixed at the base. To design a stiff truss, a stiff column with large moment of inertia was considered in Model D, and envelop of shear and bending demand of this column from a set of selected ground motions was used. W-shaped sections were considered for the truss members. Elastic beam-column elements were employed for the modelling, and the base of the truss was pinned. Rigid connections were used between the members of the truss.

A new configuration of a truss with a hinge at the mid-height can reduce the force demand in the truss members significantly. This configuration could reduce the required steel tonnage and the cost. Both of the moment resisting frame and the truss should be placed on the exterior of the building, and they should provide temporary lateral resistance during the retrofit of the braced frame.

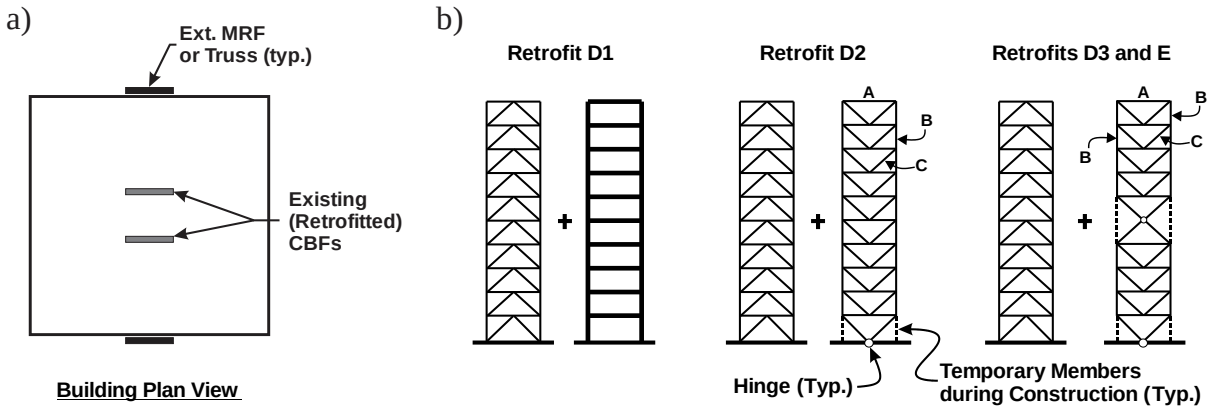

Figure 3.1: Dual retrofit options a) location of the external frames; and b) Retrofits D_1 to E.

The proposed retrofit strategies were compared to an option to build a new chevron braced frame designed by CSA S16-09 (CSA 2009). Contrary to the proposed retrofit strategies, it was found that the foundation of the new chevron braced frame would require repair. Also, the steel tonnage of the new braced frame was higher than the steel tonnage of the braced frame retrofitted by a truss with a hinge at the mid-height. Among all proposed retrofit schemes and the new chevron braced frame designed by CSA S16, the truss with a hinge at the mid-level was the most economical solution, and it needed the least retrofit work.

The truss with a hinge at the mid-height was used for the retrofit of existing chevron braced fame. Compared to all previous schemes, this retrofit uses the existing braced frames with limited strengthening as a result of the capacity of the truss to mitigate soft-story. Therefore, this solution requires the minimum steel tonnage compared to other options.

3.1.3 Assess the ductility of steel columns

According to ASCE 41, if the column axial load exceeds 50% of the lower-bound axial compressive strength, P_{CL}, the column should be considered force-controlled for both axial loads and flexure, and when the column axial load is less than 50% of the lower-bound axial column strength, the column should be considered deformation-controlled for flexure and force-controlled for axial compression. To evaluate the possible ductile flexural response of steel columns and investigate the appropriateness of the ASCE 41 acceptance criteria, a series of nonlinear static analyses was performed using OpenSees and ABAQUS. Seismic evaluation of

the tension-only braced frame with retrofitted columns in OpenSees showed that brace elongations at levels 8 and 9 induced flexural demands on the columns at levels 7 to 9. The columns at the 8th and 9th levels are the most critical columns in accordance with the ASCE 41 acceptance criteria and they would require significant strengthening if the flexural demand was considered in the evaluation. However, the OpenSees time history analysis showed that plastic hinging formed at both ends of the column and the column could carry the high axial compression without buckling. As the OpenSees model could not represent the local buckling effects on the column flexural strength and the possibility of flexural-torsional buckling, the ABAQUS model was used to provide a more realistic evaluation on the plastic rotation capacity of columns. In the first step, a series of analyses was performed in which storey drift was monotonically increased up to the failure of the column. A constant axial load varying from 0.1 to 0.9 P_{CL} was applied to the column model in ABAQUS and its boundary condition was fixed-fixed. In all cases, flange local buckling occurred in the end plastic hinges and no global buckling was observed. The analyses showed plastic rotation capacities for axial loads more than 0.5 P_{CL}. Also, the results indicated that plastic rotation capacities decreased by increasing the column axial compression. However, the columns with high axial compression equal to or greater than 0.5 P_{CL} had some ductility, which was contrary to the acceptance criteria of steel columns specified in ASCE 41.

In the second step, the seismic response of the column was evaluated in both OpenSees and ABAQUS models while undergoing flexural yielding due to brace yielding. For this aim, the column at the 8th level was evaluated by applying the time histories of the axial load, end displacements and end rotations imposed on the column as determined from the OpenSees model, and they were applied to the isolated ABAQUS finite element model of the column. The demands were determined from Model C with inelastic response for braces and columns. The moment-rotation responses from the OpenSees and ABAQUS models showed the same behaviour; however, the flexural resistance from ABAQUS reduced due to local buckling at large rotations. Note that local buckling could not be simulated in the OpenSees Model. The column in the ABAQUS model could resist that imposed axial compression demand without global buckling, even if large plastic rotations and pronounced local buckling occurred. These results indicated that plastic rotation or flexural strength can not be a good indicator for the assessment of braced frame columns that are not considered to have the contribution through bending to the

frame lateral resistance under a seismic event. Also, the ASCE 41 acceptance criteria specified for steel columns are conservative.

To validate the numerical study on the ductility of steel columns and assess the accuracy of ASCE 41 acceptance criteria, an experimental program was developed. Four full-scale W-shaped sections were considered and the experimental study was performed by the Multi-Directional Hybrid Testing System (MDHTS) at the Structural Engineering Laboratory of Polytechnique Montréal. The W250x101 column specimens were selected for this test program, which were classified as Class 1 in accordance with CSA S16. The plan of the experimental program is mentioned as follows: Two cyclic tests were performed about the weak axis of the column specimens. In the third test, the lateral displacement, rotation, and axial load of the tension-only X-braced frame column at the 8^{th} level determined from the OpenSees Model C was imposed about the strong axis of the specimen. In the last test, a loading protocol was developed that consisted of large lateral displacements and axial loads. This loading protocol was imposed about the strong axis of the specimen. For the first two tests, the end condition of the specimens was fixed-fixed; while for the 3^{rd} and 4^{th} tests, it was pinned-fixed to impose the demands to the steel column. Figure 3.2 shows the loading protocols that imposed to the specimens. The details of the experimental study are mentioned in APPENDIX A.

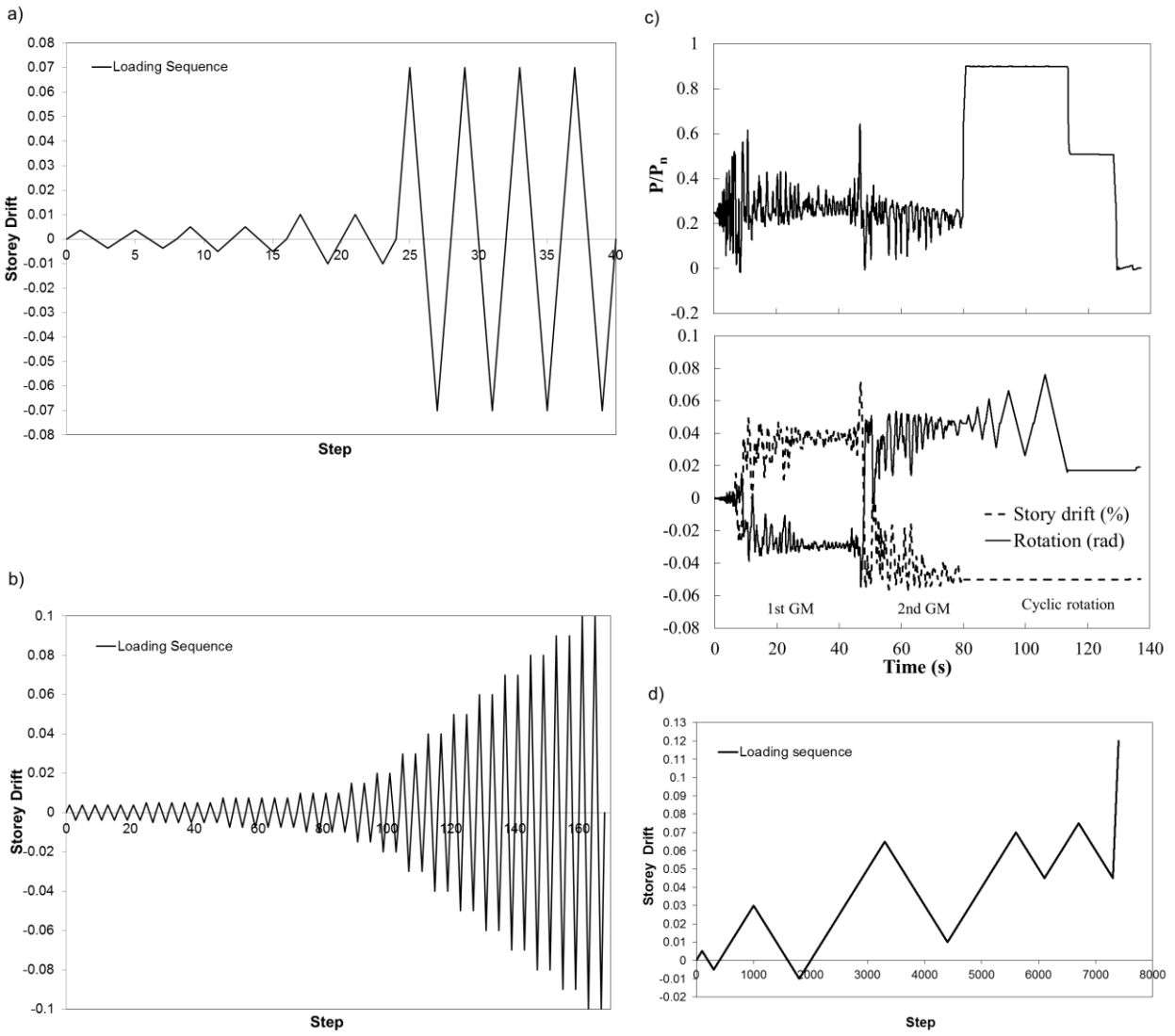

Figure 3.2: Loading protocol of a) Specimen CS5; b) Specimen CS6; c) Specimen CS7; and d) Specimen CS10.

3.2 Research activities

The main research activities of this Ph. D. thesis are seismic evaluation of existing chevron and tension-only X-braced frames designed in accordance with the 1980 Canadian code provisions, seismic rehabilitation of existing inverted-V bracing system and evaluate the appropriateness of acceptance criteria specified for steel columns in ASCE 41. The following activities have been performed over the course of this Ph. D. program:

- In fall 2010 and winter 2011, four courses were taken for credit including research methods: ING6900E (Polytechnique Montréal), Séminaires: CIV6904 (Polytechnique Montréal), Earthquake-Resistant Design: MGCIVE612 (McGill University) and Advanced Steel Structures Design: COCIVI691C (Concordia University).
- During winter 2011 and summer 2011, a literature review was carried out on the assessment and rehabilitation of existing concentrically braced frames. A 10-storey concentrically braced steel frame was designed using the design provisions of the 1980 NBCC and CSA-S16.1-M78 steel design standard. The studied building was evaluated by NBCC 2010 and CSA S16-09. The results were presented at the *STESSA 2012* conference (Jiang et al. 2012).
- From fall 2011 to summer 2012, a numerical model of back-to-back double angle braces was developed using the *OpenSees* platform. The existing tension-only braced frame was modelled in this program, while nonlinear elements were used for braces and elastic elements were considered for other structural members. The nonlinear time history analysis was performed for a group of three ground motion records, and the studied building was evaluated using the ASCE 41-06 standard. The results of this study were presented at the *CSCE 2013* conference (Balazadeh-Minouei et al. 2013).
- Several methods were used to evaluate the seismic response of the studied tension-only concentrically X-bracing system from fall 2012 to summer 2013. The studied building was assessed using current Canadian code provisions and linear dynamic and nonlinear dynamic analysis procedures of ASCE 41. Two types of nonlinear modelling were considered in nonlinear dynamic analysis method. In the first case, inelastic response was considered for the braces and elastic response was used for columns and beams; while, in the second case, inelastic response was applied to all structural members. Relevant acceptance criteria that were specified in the ASCE 41 standard were adapted to Canadian normative context. Also, the ACSE 41 performance criteria for columns were examined in the case of columns subjected to large drift induced flexural demands. The results of this study were presented in a paper entitled “Seismic Evaluation of a Steel Braced Frame using NBCC and ASCE 41.” (Balazadeh-Minouei et al., 2017a) published in *Journal of Constructional Steel Research*.
- In fall 2013 and winter 2014, the rehabilitation of existing tension only X-bracing system was studied to improve the seismic behaviour of the building. Also, the force-delivery

reduction factor that specified in the linear procedure of ASCE 41 was investigated. This study was published in the proceeding of the *10th National Conference on Earthquake Engineering* (Balazadeh-Minouei et al. 2014a). The seismic response of a tension-compression chevron-braced frame was evaluated using the nonlinear dynamic procedure proposed in the ASCE 41 standard. The nonlinear analysis was carried out for a group of seven historical ground motion records, and the study was focused on the response of braces and beams (Balazadeh-Minouei et al. 2014b).

- The seismic assessment of the 10-storey and 3-storey chevron braced frames was carried out using several methods including Canadian norms as well as linear and nonlinear procedures determined in the ASCE 41-13 standard during summer 2014. Different probabilities of exceedance including 2% in 50 years, 5% in 50 years and 10% in 50 years were used for the evaluation of the studied buildings. A comprehensive study was performed on the response of beams in chevron braced frames using *OpenSees* and *ABAQUS*. The results were submitted to the *Journal of Structural Engineering, ASCE*.
- In fall 2014 and summer 2015, the retrofit of existing chevron braced frame was studied. The seismic response of the existing chevron braced frame with retrofitted beams using ASCE 41 LDP was evaluated. Several schemes were considered to design the braces. Two retrofit solutions were proposed to improve the seismic behaviour of the tension-compression chevron braced frame. The most economical choice was determined. The results of this study were submitted to the *Journal of Structural Engineering, ASCE*.
- In winter and spring 2015, an experimental program was developed to evaluate the ductility of steel columns. The experimental study included four full-scale W-shaped sections was performed by the Multi-Directional Hybrid Testing System (MDHTS) at the Structural Engineering Laboratory of Polytechnique Montréal. The results of this study were presented at the 11th Pacific Structural Steel conference (Auger et al. 2016).

CHAPTER 4 ARTICLE 1: SEISMIC EVALUATION OF A STEEL BRACED FRAME USING NBCC AND ASCE 41

Yasaman Balazadeh-Minouei, Sanda Koboevic and Robert Tremblay

Department of Civil, Geological and Mining Engineering, Polytechnique Montreal, Montreal, QC, Canada

Published in *Journal of Constructional Steel Research*.

Abstract

The article presents the seismic evaluation and retrofit of a 10-storey steel building located in Vancouver, British Columbia, designed following the provisions of the 1980 NBCC and the CSA-S16.1-M78 steel design standard. Lateral resistance is achieved by tension-only X-bracing with back-to-back double angle members. Seismic evaluation is first performed in accordance with the recommendations of the User's Guide to NBCC 2010 using response spectrum analysis. A Tier 3 systematic evaluation according to ASCE 41-13 is then carried out using both linear and nonlinear dynamic analysis procedures. The performance objectives are set same as those implied in NBCC 2010. The ASCE 41 approach results in much less corrections to the structure. Using the mean results from 10 ground motions is also less stringent than using the maximum of three records. For this structure, nonlinear dynamic analysis permitted to identify the concentration of inelastic deformations demands on the braces along the frame height. This behaviour induced considerable bending moment demands on the columns not captured by linear dynamic analysis. Finite element analysis of the structure columns showed that columns of braced steel frames can exhibit higher ductility compared to acceptance criteria specified in ASCE 41.

Keywords: seismic evaluation, existing steel braced frame, columns, buckling, acceptance criteria, deformation capacity.

4.1 Introduction

New steel buildings designed according to the seismic provisions of the National Building Code of Canada (NBCC) (NRCC 2010) and the steel structures design standard CSA S16 (CSA 2009) are conceived to safely resist seismic loads and develop sufficient ductility while maintaining adequate strength and stiffness. While seismic design provisions were introduced in the 1941

edition of NBCC, it was only in 1989 that special seismic design and detailing requirements for steel structures were incorporated in the CSA S16 standard (Redwood and Channagiri 1991, Mitchell et al. 2010). Hence, steel buildings constructed before the 1990's may not develop the ductile seismic response implied by the reduced seismic loads specified in the NBCC.

In the 1980's, concentrically braced frames with tension-only X-bracing and chevron bracing were commonly used to resist lateral loads in steel buildings in Canada. Seismic evaluation of these framing systems for 4- and 10-storey sample buildings using the NBCC 2010 and CSA S16-09 provisions revealed that braces, brace connections, beams, and columns would require extensive retrofit (Jiang et al. 2012a). Similar deficiencies were observed in physical test programs on braced steel frames designed prior to implementation of seismic detailing requirements in the United States (Sen et al. 2014, Sloat 2014, Johnson et al. 2014). For such existing structures, it is essential to have appropriate seismic evaluation methods and criteria to properly identify their deficiencies and propose effective retrofit strategies to reduce seismic risk to an acceptable level.

Commentary L of NBCC 2010 provides information on structural evaluation and upgrading of existing buildings. For earthquake resistance, it refers to the 1993 Guidelines for seismic evaluation of existing buildings (NRCC 1993). In these guidelines, a load factor of 0.6 is applied to seismic loads for determining if upgrade is necessary, an approach that aimed at identifying severe deficiencies posing life-safety threats to building occupants. This reduced load level was comparable to those prescribed in contemporary U.S. seismic evaluation guidelines (e.g., BSSC 1992). The 1993 Guidelines also included system-specific checks based on experience in past earthquakes and defined expected deficiencies due to code changes. When required, upgrade design had to be performed based on a more detailed investigation and using higher seismic loads established with consideration of the future use of the building, control of seismic damage, and the differential in upgrading costs with force level. However, the 1993 Guidelines did not contain further guidance nor explicit criteria to complete this task. They were also developed based on the 1990 NBCC and have not been updated since. Hence, they do not include knowledge gained in the last 25 years and their application is difficult and questionable as they do not reflect current seismic design provisions and practice. Today, Commentary L of NBCC 2010 still recommends a seismic load factor of 0.6 for triggering seismic retrofit but upgrade must satisfy loading and resistance criteria specified in current NBCC and CSA S16 for new constructions, which may be difficult to implement in existing structures.

In the U.S., the ASCE 41-13 standard (ASCE 2013) has become the state-of-the-art reference for the seismic evaluation and retrofit of building structures. In ASCE 41, performance objectives, expressed through target structural and non-structural performance at defined seismic hazard levels, are selected to maximize benefits (e.g. improved safety or reduction of damage and downtime periods) with consideration of cost and feasibility. A three-tiered evaluation procedure is proposed to verify compliance to performance objectives: screening (Tier 1), deficiency-based evaluation (Tier 2), and systematic evaluation (Tier 3). In Tier 3, seismic demand is evaluated from structural analysis and the evaluation is performed at the components level by verifying acceptance criteria reflecting the expected capacity of the components. In retrofit design, the identified deficiencies are corrected until the structure is satisfactory, i.e. when all components meet their respective acceptance criteria. For existing buildings with severe deficiencies, it is expected that selecting proper performance objectives, performing a rigorous Tier 3 evaluation with advanced nonlinear analysis and adopting realistic component acceptance criteria will lead to targeted and effective retrofit solutions compared to simply applying seismic design provisions for new buildings.

Analysis procedures vary greatly in their complexity to represent structural behavior and their easiness of use in day-to-day application. In practice, the choice of the analysis method depends on the objectives and costs of the assessment program as well as the time available for the evaluation. Linear analysis is usually carried out for preliminary assessment and nonlinear analysis methods are subsequently performed to evaluate the imposed demand more realistically. Nonlinear analysis also provides a better insight into structural deficiencies and efficient retrofit strategies. Because linear analyses methods are commonly used in practice, it is useful to establish whether seismic structural assessment based on such analyses is consistent with one performed using more sophisticated nonlinear analysis methods. Callister and Pekelnicky (2011) showed that existing steel braced frames with deficient brace connections could satisfy basic life safety performance objectives when ASCE 41 nonlinear static analysis procedure is applied. Harris and Speicher (2015) evaluated steel concentrically braced frames designed according to modern U.S. codes. The study showed notable variations in performance assessment depending on the analysis method used. Acceptance criteria for steel columns were questioned, including the combinations of member stability and section yielding and of weak axis buckling and strong axis flexure in the interaction equations. Bech et al. (2015) examined past test results on steel columns and showed

that compact steel columns can exhibit dependable rotational ductility even when subjected to axial compression loads above 50% of their compressive strength. This is contrary to ASCE 41 criteria that state that such columns must be considered as force-controlled with no plastic flexural capacity. In New Zealand steel structure standard (NZS 1997), although limited, rotational capacity is permitted for columns supporting up to 0.8 times their axial strength.

Seismic evaluation and retrofit of existing structures designed according to past Canadian norms using the component-based ASCE 41 methodology has not been reported yet. In this article, ASCE 41-13 is used to evaluate the 10-storey building with tension-only concentrically X-bracing studied by Jiang et al. (2012a). The building is located in Vancouver, British Columbia, and was designed in accordance with the Canadian codes applicable in the early 1980's. The structure is first assessed based on current Canadian code provisions. ASCE 41 Tier 3 evaluation procedure is then applied using both the linear and nonlinear dynamic analysis procedures. For nonlinear analysis, different models are employed to examine the impact of considering nonlinear response only for the braces or for the braces and columns and beams. The effect of the number of ground motions considered in the analysis is also investigated. When developing the retrofit solution, the ASCE 41 performance criteria for columns subjected to combined high axial compression and large drift induced flexural demands are revisited using detailed finite element analysis.

4.2 Design of the Existing Building According to NBCC 1980

The plan view and frame elevation of the building studied is illustrated in Figure 4.1a. The 10-stories office building with an overall height of 40.23 m is located in Vancouver, British Colombia, on a firm ground site. Pairs of tension-only bracing with diagonals in the X configuration and chevron bracing provide lateral resistance in N-S and E-W directions, respectively. The X-braced frames are examined in this study. The structure was designed in accordance with the provisions of the 1980 NBCC (NRCC 1980) and the CSA-S16.1-M78 steel design standard (CSA 1978), thus before the implementation of seismic design and detailing requirements in CSA S16. The equivalent static force procedure (ESFP) was used to determine seismic effects, as was permitted for regular structures in NBCC 1980. The seismic base shear V was determined from:

[1] $V = ASKIFW$

where A is the design acceleration ratio, S is the seismic response factor, K is a coefficient to account for the material, type of construction, damping, ductility and/or energy-absorptive capacity of the structure, F is the foundation factor, I is the importance factor, and W is the seismic weight. In 1980, the acceleration ratio A was specified for a return period of 100 years and varied between 0 and 0.08 depending on the seismic zone. For Vancouver, A was equal to 0.08. The seismic response factor, S, was equal to $0.5/T^{0.5}$, where T is the building fundamental period, without exceeding 1.0 for short period structures. In NBCC 1980, the period could be determined from the empirical expression $T = 0.09 h_n / \sqrt{D}$, with h_n and D being respectively the building height and width, or from methods of mechanics. For this building, T = 2.77 s was determined using the Rayleigh method, as was suggested in the commentary to the NBCC, which gave S = 0.30. This period was much longer than the value of 0.54 s obtained from the code empirical equation. In NBCC 1980, K varied from 0.7 for the most ductile seismic force resisting systems to 2.0 for the least ductile ones. For tension-only braced frames K = 1.3 in view of their low energy dissipation capacity. For firm grounds, F could be taken equal to 1.0. Combining all factors, V = 0.032 W, and the seismic weight W was equal to 91392 kN for the entire building.

For the braced frames studied, the aspect ratio h_n/D_s is equal to 4.4. Because this ratio exceeds three, a concentrated load, $F_t = 0.004V (h_n/D_s)^{0.5} = 0.077\ V$ had to be applied at the top of the structure to account for higher mode response. The remainder, V-F_t, was distributed among the structure levels as a function of their relative seismic weights and elevations from ground. A reduction in overturning moments of up to 20 % was permitted (J_{Base} = 0.8) for this building but its effects on column design was marginal when seismic and gravity loads were combined and it was therefore ignored. In-plane torsional moments due to an accidental eccentricity of 0.05 times the building dimension perpendicular to the loads were taken into account in design. The load combinations considered were: (i) 1.25D + 1.5L; (ii) 1.25D + 1.5E; and (iii) 1.25D + 0.7 (1.5L + 1.5E), where D, L and E are the specified dead, live (including snow), and earthquake loads, respectively. P-delta effects were considered in the combinations with seismic loads. The resulting factored design storey shears per frame, including torsion and P-delta effects, are plotted in Figure 4.1b (ESFP 1980). Factored column axial loads including gravity loads are given in Figure 4.1c.

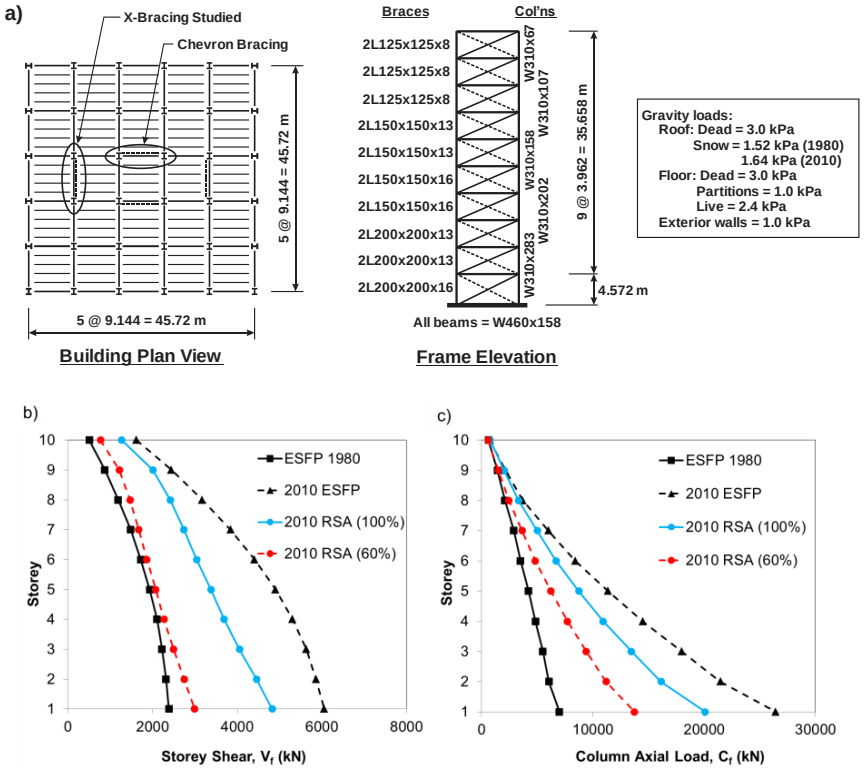

Figure 4.1: a) Plan view and braced frame elevations of the building studied; b) Design factored storey shear force per frame; and c) Design factored column axial loads.

The beams and columns are W sections whereas back-to-back double angles were used for the braces, reflecting construction practices of the 1980s. CSA-G40.21-300W steel was used for all members, with nominal yield stress F_y of 300 MPa and tensile strength F_u of 450 MPa. The columns were tiered in two-storey segments. The beams were assumed to be laterally supported by the floor slabs. The brace angles had equal legs and Class 3 sections (nonslender elements) were selected to prevent local buckling. Brace design was governed by strength requirements, except at the roof level where the brace slenderness limit of 300 controlled. Note that brace slenderness was determined assuming an unsupported length equal to half of the total brace length. At their ends, braces were connected to single gusset plates using ASTM A325 bolts, 19.1 mm in diameter. A single bolt line was used in all cases except that staggered or double row bolt configurations were specified for 127 mm and wider angle legs.

4.3 Seismic Evaluation Using NBCC 2010

Preliminary seismic evaluation of the braces, brace connections, columns, and beams was carried out using the current Canadian seismic design provisions for new buildings considering 100% and 60% of NBCC 2010 seismic loads. The latter was considered to determine if seismic upgrade would be needed according to NBCC 2010 Commentary L. In the 2010 NBCC, the base shear V is:

$$[2]\quad V = \frac{S(T_a) M_v I_E W}{R_d R_o}$$

where S is the design spectrum value at the period T_a, M_v is the factor accounting for the increase in base shear due to higher mode effect; I_E is structure importance factor; W is building seismic weight; R_d is the ductility-related force reduction factor and R_o is the overstrength-related force reduction factor. The S value is obtained by linear interpolation between uniform hazard spectral (UHS) accelerations that are specified at periods of 0.2, 0.5, 1.0, 2.0, and 4.0 s for a probability of exceedance of 2 percent in 50 years and modified to reflect soil conditions. For braced steel frames, the period T_a in NBCC 2010 is given by $T_a = 0.025\ h_n$. Alternatively, the period T_1 from dynamic analysis can be used without exceeding $0.05\ h_n$. For this frame, T_1 = 2.65 s and the upper limit $T_a = 0.05\ h_n$ = 2.01 s governed. For firm ground site conditions in Vancouver, S at this period is equal to 0.17. For this building, M_v = 1.0, I_E = 1.0, and W is 83756 kN. Because of the absence of seismic ductile detailing, the frame was assumed to be of the conventional construction (Type CC) category with R_d = 1.5 and R_o = 1.3. The resulting seismic force V is equal to 0.087 W, i.e., 2.7 times larger than the 1980 design value.

In NBCC 2010, the equivalent static force procedure (ESFP) is permitted for regular structures having a period T_a up to 2.0 s; otherwise, dynamic response spectrum analysis (RSA) is required. Since T_a = 2.01 s is close to the limit, both analysis methods were applied to see the impact of the analysis method on seismic evaluation. RSA was performed using the design spectrum $S(T)$ and the results were multiplied by I_E/R_dR_o to obtain design actions. Analysis results were then further adjusted such that the base shear from RSA was equal to 80% of V given by [3], as permitted in NBCC for regular structures.

In both analysis methods, a three-dimensional model of the entire structure was employed in ETABS (CSI 2008) to account for accidental torsion. Rigid diaphragms were considered at every level. One of the two intersecting braces at every level was removed to simulate tension-only response. Notional loads corresponding to 0.5% of gravity loads and P-delta effects as specified in CSA S16-09 have been added to seismic effects. The load combinations in NBCC 2010 are: (i) 1.25D + 1.5L+ 0.5S; and (ii) 1.0D + 0.5L + 0.25S + 1.0E, where S is the snow load. For Type CC structures having 40 m in height, CSA S16-09 requires that seismic effects be amplified by 1.5 to prevent excessive brace ductility demand from soft-storey response. Axial forces in columns induced by seismic loads must be further increased by 1.3 to ensure that the columns have relatively higher resistance compared to beams and bracing members.

These amplifications have been included and the final factored storey shear profiles and column axial loads from both seismic analysis methods are shown in Figures 4.1 (b) and (c). For RSA, the results are plotted for 100% and 60% of seismic loads. As shown, 100% NBCC 2010 design loads from RSA are lower than those obtained from ESFP, mainly because T_1 exceeds T_a and the RSA results could be scaled with respect to 0.8 V, rather than V. As shown, 60% of the 2010 seismic effects, even when obtained from dynamic analysis, exceed the 1980 design values at every level.

Seismic evaluation was performed based on the computed demand-to-capacity ratios (DCR) for the braces, columns, and beams presented in Figure 4.2. Force demands were those obtained from dynamic analysis for 60% and 100% NBCC 2010 seismic loads and capacities were the factored resistances of the components determined with CSA S16-09. As permitted in CSA S16,force demands on brace connections were limited to the probable yield tensile strength of the braces as determined with the brace probable yield strength R_yF_y = 330 MPa.

In Figure 4.2a, three limit states are examined for the bracing members: yielding of the member gross cross-section, and tension failure on net section and block shear failure at end connections. Beams are subjected to combined axial compression and flexure and the cross-section strength and overall member strength for buckling in the vertical plane is verified. For columns, buckling under compression axial loads is evaluated. As shown, brace yield tension resistances are less than the factored tension loads from 60% NBCC 2010 seismic loads at levels 1 to 3 and 8. Brace connection results are discussed in the next paragraph. The beam at the bottom floor and columns

in the first 7 storeys and at the 9th storey also have insufficient capacities to resist forces induced by gravity loads plus 60% NBCC 2010 seismic loads. Seismic retrofit would therefore be needed for this structure. DCRs under 100% seismic loads show that all frame members except beams in the top 5 levels and columns at the top storey would need to be strengthened or replaced. This represents a major structural upgrade that would require 18.4 tons of steel per braced frame, i.e. 55% of their original tonnage. From Figures 4.1b&c, it is clear that more drastic conclusions would have been drawn had ESFP been used for evaluation.

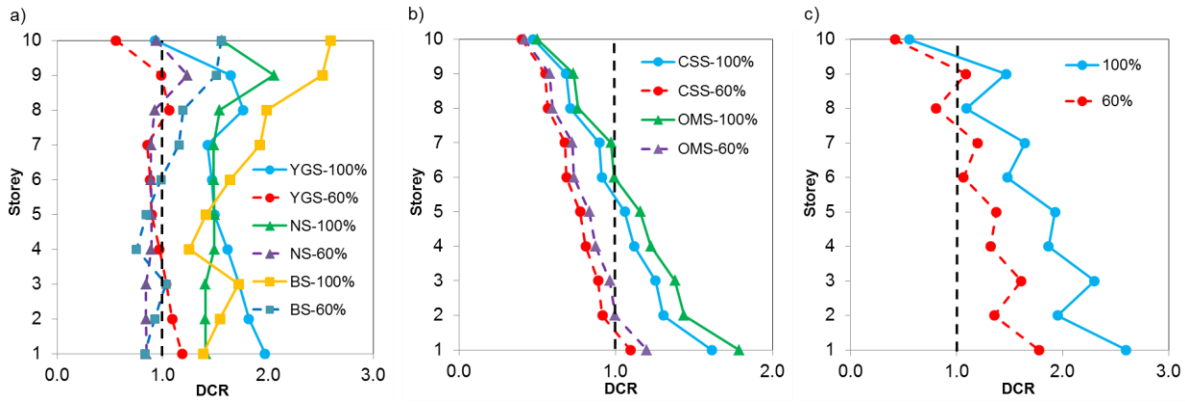

Figure 4.2: NBCC 2010 evaluation of the: a) Braces (YGS = yielding of gross section) and brace connections (NS = net section failure; BS = block shear failure); b) Beams (CSS = Cross Sectional Strength; OMS = Overall Member Strength); and c) Columns.

In Figure 4.2a, seismic evaluation of the braces is more critical when connection limit states are considered. As shown, under 60% 2010 NBCC loads, block shear failure (BS 60%) governs at levels 6-10 and net section failure (NS 60%) at levels 7, 9 and 10 are more severe than gross section yielding (YGS 60%). Deficiencies in block shear are anticipated due to the fact that this limit state was not covered in CSA S16.1-M78. For tension rupture on net section, current CSA S16 provisions are more stringent than in 1978 for angles connected by only one leg as shear lag effects on resistance must now be accounted for. Further detail on connection strength requirements is given in Section 4.5.

4.4 Seismic Evaluation Using ASCE 41

Seismic evaluation of the structure was also performed in accordance with ASCE 41-13 to examine if the approach could result in a more cost-effective retrofit. A brief overview of the approach is given in this section. Evaluation of the structure using linear and nonlinear analysis procedures are respectively presented in Sections 4.5 and 4.6, including acceptance criteria and evaluation results.

In ASCE 41, the evaluation process starts by selecting the performance objective which is defined by targeted performance levels for given earthquake hazard. For existing buildings, two basic performance objectives are proposed: life safety performance for 20% in 50 years seismic hazard (BSE-1E) and collapse prevention performance for 5% in 50 years hazard (BSE-2E). These objectives are less severe than the design objective for new buildings in NBCC: collapse prevention for 2% in 50 years hazard. This performance objective was adopted for the ASCE 41 evaluation to allow direct comparison with the seismic evaluation described in the previous section under 100% of the NBCC 2010 seismic loads.

The ASCE 41 procedure is a multi-tiered approach and the engineer has to select which tier will be used. In Tier-3 systematic evaluation, structural analysis must be performed to assess the demand on every component and the components are then evaluated using prescribed acceptance criteria. The Tier 3 evaluation was adopted herein to obtain a detailed comparison between the ASCE 41 and NBCC 2010 approaches and examine the influence of the analysis procedure on the evaluation results. Four analysis procedures are proposed in ASCE 41-13: linear static, nonlinear static, linear dynamic and nonlinear dynamic procedures. Although static procedures would be permitted for the regular structure studied, linear dynamic procedure (LDP) and nonlinear dynamic procedure (NDP) were used to obtain more realistic estimates of the seismic demand including dynamic effects. Details of the numerical models and seismic input used for each analysis procedure are given in the next sections. Because ASCE 41 procedures were applied for a structure constructed in Canada, the load factors for gravity and seismic loads were taken from the NBCC 2010 load combinations presented in the previous section.

In ASCE 41-13, structure evaluation is performed at the component level and the acceptance criteria depend on the component type, the structural action class, and the analysis procedure. For a braced frame structure, braces, brace connections, beams, and columns all classify as principal

components. Actions in components must be classified as either deformation-controlled or force-controlled actions. Deformation-controlled actions are those associated with ductile response whereas force-controlled actions are those which cannot classify as deformation-controlled. Brace tension yielding on gross section is a deformation-controlled action whereas axial compression in beams and columns as well as tension in brace connections are force-controlled actions. For the beams subjected to combined axial compression and bending moment, axial compression is a force-controlled action whereas flexure is treated as either a deformation- or force-controlled action depending on the level of axial load. Specific acceptance criteria for the applicable action types are given in the following sections.

Material properties used in the evaluation process also depend on action classification: lower-bound material properties are used for force-controlled actions whereas expected material properties (F_{ye} and F_{ue}) can be employed for deformation-controlled actions. Nominal steel properties (F_y = 300 MPa and F_u = 450 MPa) were used for the former. Values are proposed in ASCE 41-13 for the expected material strengths of various steel grades used in the U.S. No specific value is given for the CSA G40.21-300W steel and a value of 1.1 F_y was adopted for F_{ye}, as recommended in ASCE 41 for this situation. In ASCE 41, strengths of components are determined using AISC 360 Specification (AISC 2010a) with the applicable material properties, a resistance factor equal to 1.0, and a knowledge factor, κ. For application of ASCE 41 to a structure constructed in Canada, strengths of the frame components were determined using the CSA S16 standard rather than AISC 360. The value of the knowledge factor depends on the confidence with which the structural properties are known. For this study, κ = 1.0 was selected, as recommended in ASCE 41 for collapse prevention performance when the properties are obtained from structural documents.

4.5 ASCE 41 Evaluation using Linear Dynamic Procedure (LDP)

4.5.1 Analysis and modeling

In ASCE 41, either response spectrum analysis or response history analysis can be used for LDP. For simplicity, the former was adopted in this study. The analysis was performed with the three-dimensional structural model used for the NBCC evaluation. The frame model included the braces, beams, and columns and all components were represented using elastic frame elements.

Rigid column base was assumed. This model is subsequently referred to as Model A. The analysis was performed using the NBCC 2010 design spectrum S for the site. The building has no plan irregularities and the braced frame columns are not part of two intersecting seismic force resisting systems. Consequently, multidirectional seismic effects could be omitted and seismic analysis could be carried out independently along each principal direction of the structure. Seismic analysis parallel to the X-bracing is discussed herein.

4.5.2 ASCE 41 acceptance criteria for LDP

Deformation-controlled actions

In ASCE 41, the acceptance criteria for deformation-controlled is given by:

[3] $m\kappa Q_{CE} \geq Q_{UD}$

where m is the capacity modification factor that reflects the expected component for the selected structural performance level, κ is the knowledge factor, Q_{CE} is the expected strength of the component, and Q_{UD} is the action in the component due to gravity and earthquake loads ($Q_G \pm Q_E$).

For tension in bracing members, the basic m factor for collapse prevention objective is equal to 7.0 in ASCE 41. This value had to be multiplied by 0.5 because the braced frame is a tension-only bracing system and 0.8 because double-angle sections are used for the braces. Moreover, brace connections do not satisfy the special seismic detailing requirements of AISC 341-10 for SCBFs (AISC 2010b) and an additional factor of 0.8 had to be applied, which resulted in a final m factor of 2.24 (= 7.0 x 0.5 x 0.8 x 0.8).

Force-controlled actions:

For force-controlled axial compression in columns and tension in brace connections, acceptability in ASCE 41 is verified using:

[4] $\kappa Q_{CL} \geq Q_{UF}$

where Q_{CL} is the lower-bound strength of the component and Q_{UF} is the maximum action when all components delivering force to the component under consideration reach their expected

strength. Q_{UF} can be determined from a limit or plastic analysis of the inelastic mechanism of the structure, similar to the analysis performed when applying capacity design principles for new buildings. Alternatively, Q_{UF} may be determined based on the smallest demand-capacity ratio (DCR = Q_{UD}/Q_{CE}) of all components in the load path including force to the component under consideration. This alternative value can be computed from:

[5] $$Q_{UF} = Q_G \pm \frac{Q_E}{C_1 C_2 J}$$

In this equation, Q_G and Q_E are respectively the forces due to gravity and seismic loads, C_1 is a factor that accounts for the difference between expected maximum inelastic displacements to displacements calculated for linear elastic response, C_2 accounts for the component hysteretic response on maximum displacement response, and J is the force delivery reduction factor, which corresponds to the smallest DCR of the components delivering force to the component. Values of C_1, C_2 and J are discussed below when evaluating the braced frame columns.

Components under combined axial compression and flexure:

For the beams subjected to combined axial compression and flexure, the acceptance criterion depends on the ratio between the applied axial load and the beam lower-bound axial compressive strength, P_{UF}/P_{CL}. When the ratio is less than or equal to 0.1, the beam is considered as a beam in a moment frame and axial load action is ignored and flexure is considered as a deformation-controlled action. If P_{UF}/P_{CL} is comprised between 0.1 and 0.5, the beam is considered as a column in a moment frame and compression is considered as force-controlled whereas flexure is considered as deformation-controlled. For this case, acceptance for W shape beams under strong axis bending in ASCE 41 is verified using:

[6] $$\frac{P_{UF}}{2P_{CL}} + \frac{M_x}{m_x M_{CEx}} \le 1.0 \qquad \text{when: } \frac{P_{UF}}{P_{CL}} < 0.2$$

[7] $$\frac{P_{UF}}{P_{CL}} + \frac{8}{9}\frac{M_x}{m_x M_{CEx}} \le 1.0 \qquad \text{when: } 0.2 \le \frac{P_{UF}}{P_{CL}} \le 0.5$$

where M_x is the bending moment due to gravity and earthquake loads, M_{CEx} is the beam expected bending strength, and m_x is the ductility capacity factor for bending. The *m* factors depend on the beam cross-section slenderness and the level of axial load. For W shapes and collapse prevention objective, ASCE 41 specifies the following values for *m*:

For P_{UF}/P_{CL} less than 0.2:

[8] $if\ \ b/2t \le 136/\sqrt{F_{ye}}\ \ and\ \ h/w \le 787/\sqrt{F_{ye}}:\ \ m = 8$

[9] $\text{if } b/2t \ge 170/\sqrt{F_{ye}} \text{ or } h/w \ge 1210/\sqrt{F_{ye}}:\ m = 2$

For P_{UF}/P_{CL} between 0.2 and 0.5:

[10] $\text{if } b/2t \le 136/\sqrt{F_{ye}} \text{ and } h/w \le 682/\sqrt{F_{ye}}:\ m = 12\left[1 - \left(5/3\right)^{P_{UF}/P_{CL}}\right]$

[11] $if\ \ b/2t \ge 170/\sqrt{F_{ye}}\ \ or\ \ h/w \ge 1050/\sqrt{F_{ye}}:\ \ m = 1.5$

For intermediate values of P_{UF}/P_{CL} and cross-section slenderness, *m* can be obtained from linear interpolation. If P_{UF}/P_{CL} exceeds 0.5, beams are also considered as a moment frame columns but both axial compression and flexural are force-controlled actions. In this case, the *m*-factor does not apply and the ASCE 41 acceptance criterion for strong axis bending becomes:

[12] $\dfrac{P_{UF}}{P_{CL}} + \dfrac{M_{UFx}}{M_{CLx}} \le 1.0$ when: $\dfrac{P_{UF}}{P_{CL}} > 0.5$

where M_{UF} is the moment in the beams and M_{CL} is the lower-bound bending strengths of the beams.

4.5.3 Evaluation of bracing members using LDP

The bracing members were evaluated using Eq. 3 with Q_{CL} equal to the factored tension resistance T_r for gross section yielding in CSA S1-09 computed with the expected yield strength F_{ye} and ϕ = 1.0, Q_{UD} from response spectrum analysis, κ = 1.0, and *m* = 2.24. The results are presented in Figure 4.3a. On the horizontal axis, "Evaluation Results" corresponds to the ratio

$Q_{UD}/m\kappa Q_{CE}$ and a value equal to or less than 1.0 indicates acceptable performance. As shown, all braces are expected to have adequate performance and no strengthening would be needed.

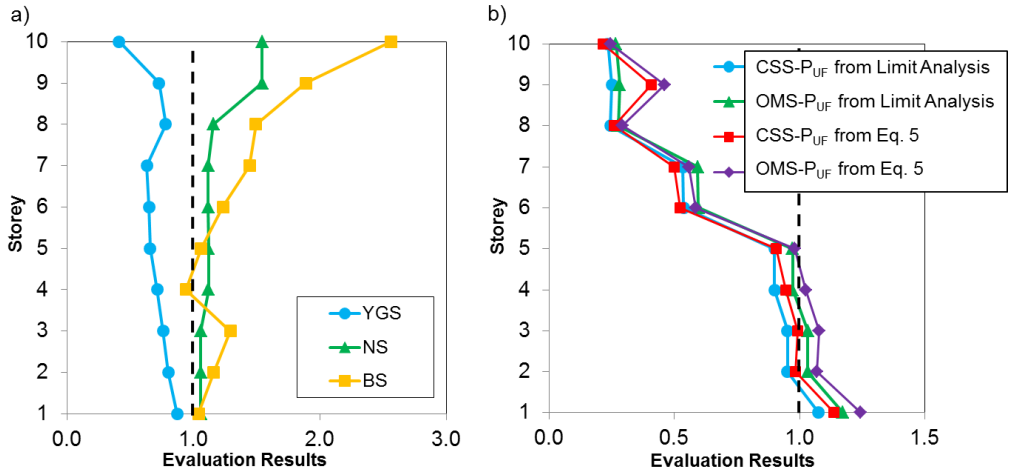

Figure 4.3: ASCE 41 LDP evaluation of the: a) Bracing members (YGS) and brace connections (NS and BS); and b) Beams (CSS and OMS).

This evaluation is less severe than the evaluation under 60% NBCC 2010 seismic loads (YGS-60%) in Figure 4.2a. In ASCE 41, the force demand is based on the elastic spectrum (R_oR_d = 1.0) and brace capacities are obtained with F_{ye} = 1.1 F_y, ϕ = 1.0, and ductility of 2.24. In the 60% NBCC 2010 evaluation, brace forces are those from 60% of seismic loads determined with R_dR_o = 1.95 and then amplified by 1.5, thus seismic loads corresponding to R_dR_o = 1.95/0.6/1.5 = 2.17, while the capacity is based on factored resistance (0.9 F_y). For this example, ASCE 41 is therefore 26% less critical than 60% NBCC.

4.5.4 Evaluation of brace connections using LDP

Force-controlled tension in brace connections was evaluated using Eq. 4. Tension rupture on net section (NS) and block shear failure (BS) were examined. For each limit state, the lower-bound strength Q_{CL} was determined using the nominal material properties and the resistance factor ϕ_u = 1.0 in the equations given in CSA S16-09:

[13] $$T_{CL} = \phi_u A_{ne} F_u$$

[14] $$T_{CL} = \phi_u \left[U_t A_n F_u + 0.6 A_{gv} \left(\frac{F_y + F_u}{2} \right) \right]$$

In these expressions, A_{ne} is the effective net area reduced for shear lag effects, A_n and A_{gv} are respectively the net area in tension and the gross area in shear for block shear failure, and U_t is the efficiency factor. In CSA S16, for angles connected by one leg, U_t = 0.6 and the shear lag reduction factor is equal to 0.8 when the connection includes four or more bolts and 0.6 when fewer bolts are used.

For each connection, Q_{UF} in Eq. 4 is the maximum force that can be imposed by the connected brace, i.e. the expected brace force Q_{CE}. The evaluation results ($Q_{UF}/\kappa Q_{CL}$) are presented in Figure 4.3a. As shown, strengthening of brace connections would be needed at every level, as was also predicted in the 60% NBCC 2010 evaluation. Block shear failure dominates in most cases, likely because that limit state was not considered in the original design as explained earlier. Compared to the 100% NBCC evaluation, ASCE 41 would require lighter connection reinforcement because the resistance factor is equal to 1.0 when assessing connection capacities.

4.5.5 Evaluation of beams using LDP

Beams were evaluated as described in Section 4.5.2 except that the interaction equations were adapted to reflect those prescribed in CSA S16-09. For the case where P_{UF}/P_{CL} is equal to or less than 0.5, Eqs. 6 and 7 were then replaced by:

[15] $$\frac{P_{UF}}{P_{CL}} + \frac{0.85 U_{1x} M_x}{m_x M_{CEx}} \leq 1.0$$

[16] $$\frac{M_x}{m_x M_{CEx}} \leq 1.0$$

Eq. 16 ensures that the applied moment does not exceed the flexural capacity of the beams and the most critical result from Eqs. 15 and 16 was retained. When P_{UF}/P_{CL} > 0.5, Eq. 12 was replaced by:

[17] $$\frac{P_{UF}}{P_{CL}} + \frac{U_{1x} M_{UFx}}{M_{CLx}} \leq 1.0$$

In these equations, similar to brace connections, the beam compression load P_{UF} was taken as the horizontal component of the expected yield tensile strength of the tension brace framing from below. The alternative value Q_{UF} from Eq. 5 was also considered for evaluating P_{UF}. In the equation, Q_E is the horizontal component of the force in the brace framing from below and the force delivery reduction factor is the minimum of the DCR values for the braces below and above. The beams are simply supported and bending moments M_x and M_{UFx} were same and equal to the maximum moments caused by the gravity loads.

P_{CL} is the beam axial resistance taken equal to the factored axial resistance C_r in CSA S16-09 determined with the nominal F_y value and $\phi = 1.0$, and the flexural strengths M_{CEx} and M_{CLx} were the factored bending resistances M_r in CSA S16-09 computed with the expected and nominal material properties, respectively, and $\phi = 1.0$. Equations 15 and 17 were applied twice, the first time to verify cross-section strength (CSS) and, the second time, to verify overall member strength (OMS) for buckling in the vertical plane. For the first verification, P_{CL} was determined without consideration for buckling (slenderness = 0). For the second verification, it was computed for beam flexural buckling about strong axis. In Eqs. 15 and 17, U_{1x} was taken equal to:

[18] $$U_{1x} = \frac{\omega_{1x}}{1 - P_{UF} / P_{ex}}$$

where ω_{1x} is the equivalent uniform bending coefficient (= 1.0 for beams subjected to multiple point loads – see Figure 4.1), and P_{ex} is the beam Euler load about strong axis. Beams were assumed to be laterally supported and M_{CEx} and M_{CLx} were determined for the yielding limit state. In Eqs. 15 and 16, m_x was determined with Eqs. 8 to 11.

Evaluation results are presented in Figure 4.3b for both values of P_{UF}. For beams at levels 6 to 10, the ratio P_{UF}/P_{CL} was less than 0.5 and only Eqs. 15 and 16 were used, while Eq. 17 was applied at levels 1 to 5. In the upper levels, values of m_x varied from 3.10 to 7.40 as a function of P_{UF}/P_{CL}, with the maximum value at the roof level where P_{UF}/P_{CL} was minimal. In Figure 4.3b,

"Evaluation Results" corresponds to the left-hand side (LHS) of Eqs. 15 to 17, depending on which one governed. At all levels, the two P_{UF} values from limit analysis and Eq. 5 were close and resulted in similar evaluations. The beam located at the 1st level is expected to have inadequate performance for both limits states (CSS and OMS) and for both values of P_{UF}. At levels 2 and 3, beams have insufficient resistance against in-plane buckling (OMS), regardless of the P_{UF} value. As opposed to the braces, evaluation of the beams with ASCE 41 LDP is similar to or more severe than the 60% NBCC evaluation. However, beam strengthening required by ASCE 41 would be much less than that needed to resist 100% NBCC 2010 seismic loads.

4.5.6 Evaluation of columns using LDP

Columns are considered as force-controlled and were verified using Eq. 4 with Q_{UF} being the maximum axial compression P_{UF} expected in the columns. P_{UF} was evaluated from a limit analysis assuming that braces at all levels have reached their expected yield tension strengths Q_{CE}. P_{UF} at a given level was then equal to the gravity induced axial compression plus the sum of the vertical components of the forces acting in the tension braces above and at the level under consideration.

Alternatively, P_{UF} could be taken as Q_{UF} from Eq. 5 with Q_E taken as the column axial load from response spectrum analysis. In ASCE 41, the C_1 and C_2 coefficients are equal to 1.0 if the structure fundamental period is longer than 1.0 and 0.7 s, respectively. For the structure studied, T_1 = 2.65 s and C_1 and C_2 were set equal to unity. The parameter J is the smallest DCR value (= Q_{UD}/Q_{CE}) of all braces contributing to the earthquake column axial load at the level under consideration. For this structure, brace DCRs vary from 1.0 at the roof level to 1.94 at the structure base. Because the smallest value is for the braces at the roof level, J = 1.0 applies for P_{UF} at all levels. In Figure 4.4a, P_{UF} from limit analysis is compared to P_{UF} from Eq. 5. As shown, the latter resulted in higher force demands. Considering that similar effort is needed to compute either set of P_{UF} values, limit analysis is recommended wherever possible as it provides a more realistic estimate of the maximum expected column loads.

In Eq. 4, the lower-bound strength Q_{CL} was taken as the CSA S16-09 factored compressive resistance C_r for flexural buckling about weak axis with a resistance factor of 1.0. Results of the seismic evaluation for the columns using the two P_{UF} values are presented in Figure 4.4b. In this figure, values of the acceptance criteria correspond to the ratios $Q_{UF}/\kappa Q_{CL}$. As shown, only the

columns at the top and 8th levels are expected to have adequate performance. All other columns would require strengthening. This evaluation is same as obtained under 60% NBCC seismic loads in Figure 4.2c. As was the case for the beams, however, column strengthening for 100% NBCC loads would be more significant.

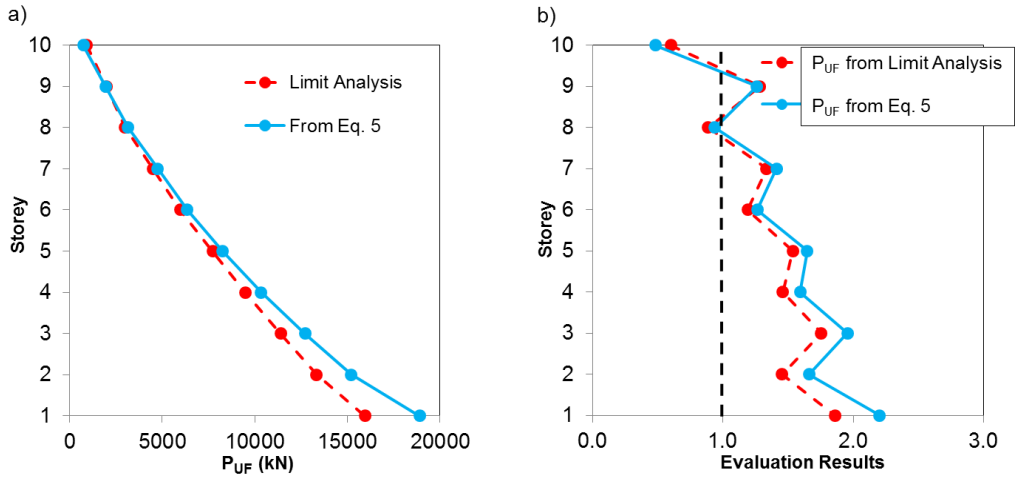

Figure 4.4: ASCE 41 LDP evaluation for the columns: a) Values of P_{UF}; and b) Acceptance criteria.

4.6 ASCE 41 Evaluation using Nonlinear Dynamic Procedure (NDP)

4.6.1 Analysis and modeling for NDP

Nonlinear response history analysis was performed using a two-dimensional numerical model of one of the two X-braced frames studied. The analyses were conducted using the *OpenSees* finite element platform (McKenna and Fenves, 2004) and three different numerical models were used to examine the influence of the extent of nonlinear modelling on seismic evaluation. In Model B, elastic beam elements were used for beams and columns and only inelastic brace behaviour was represented. In Model C, representation of inelastic response was added for the columns. In Model D, braces, columns, and beams could exhibit inelastic response. Details for each model are given below. The ground motion records used are described at the end of this section.

The structure studied is symmetrical and has no inherent torsion. For this situation, ASCE 41-13 allows two-dimensional models if the structure has rigid diaphragms and the torsional amplification multiplier for displacements due to total in-plane torsional moments does not exceed 1.1 at any floor. The displacement multiplier is the ratio between the maximum

displacement at any point on the floor diaphragm to the average floor displacement ($\delta_{max}/\delta_{avg}$) in a 3D analysis with 5% accidental mass eccentricity. For the building studied, the maximum displacement multiplier was 1.09 over the frame height, allowing simpler, two-dimensional nonlinear analysis. P-delta effects were included by adding a leaning column carrying gravity loads that was linked to the frame at every level. Mass proportional damping corresponding to 3% of critical in the first structure mode was specified in all three models. Stiffness proportional damping was not considered to avoid unrealistic excessive damping associated with inelastic response of structural members.

Model B

In Model B, nonlinear force-based beam-column elements are used for the braces whereas elastic beam-column elements are used for the columns and beams. The model therefore allows explicit assessment of inelastic deformation demands on the braces (deformation-controlled actions) while monitoring peak force demands on brace connections, beams, and columns (force-controlled actions). The brace model by Jiang et al. (2012b) was employed. Each angle of the bracing members is composed of 16 nonlinear beam-column elements, each with 4 integration points and fiber discretization of the cross-section to reproduce distributed plasticity. The two angles forming the braces are connected at their ends and at the locations of the stitch connectors. The Giuffré-Menegotto-Pinto (Steel 02) material with expected brace yield strength F_{ye} and kinematic and isotropic hardening properties are assigned to the fibers. Residual stresses and member initial out-of-straightness are also included. Zero length nonlinear spring elements are used to represent the flexural strength and stiffness of the gusset plates. The model allows for buckling of the individual angle member between the stitches and global in-plane and out-of-plane buckling of the double angle brace members (Balazadeh-Minouei et al. 2013). Zero-length elements with high axial and negligible flexural stiffness were considered to model the beam-to-column connections. For all models, column bases were assumed to be pinned and the columns were continuous over two consecutive storeys.

Models C and D

Model C is identical to Model B except that columns at every storey are represented by 10 nonlinear force-based beam-column elements with 4 integration points and fiber discretization. Steel 02 material with kinematic and isotropic hardening properties was also selected for the

columns. The nominal steel yield strength was specified and the residual stress pattern by Galambos and Ketter (1958) was assigned to the cross-section fibers of the columns (Lamarche and Tremblay 2011). The model can account for flexural buckling about both axes and half-sine out-of-straightness deformation with maximum amplitude of 1/1000 of the unsupported member length was initially applied along both orthogonal directions. As shown in Figure 4.1a, the columns are oriented such that their web is in the plane of the frame and strong axis bending due to uneven storey drifts could lead to flexural-torsional buckling. However, that failure mode could not be predicted by the column model used in this study.

Model D is identical to Model C except that nonlinear force-based beam-column elements are also used for the beams to represent possible beam buckling failure mode. The beam model is same as for the columns except that out-of-plane buckling is prevented by the horizontal restraint provided by the floor. Hence, initial beam out-of-straightness was only considered in the plane of the frame.

Ground motions

The response analysis was carried out for an ensemble of three site representative historical ground motion records scaled to match the 2010 NBCC design spectrum. The number of records is the minimum required in ASCE 41-13. They were selected from a broader ensemble of 20 far-field records matching the dominant magnitude-distance scenarios proposed by Atkinson (2009) for western Canada. Following the procedure described in this reference, the three selected records were those having the lowest standard deviation (SD) of the ratio between the NBCC and ground motion spectra ($S/S_{a,gm}$) in the 0.2-1.5 T_1 period range and a mean $S/S_{a,gm}$ value between 0.5 and 2.0 in that period range. The three records were scaled such that the average spectrum did not fall below the NBCC 2010 spectrum in the 0.2-1.5 T_1 period range. The spectra of the three individual scaled records and the average spectrum of the scaled records are shown in Figure 4.5. Ground motion properties and applied scaling factors (SF) given in Table 1. Since only three records were used, the maximum response from the three records was considered for seismic evaluation, as required in ASCE 41. In Figure 4.5, the average spectrum of a second set of 10 ground motions is also shown. This second ensemble is discussed in Section 4.7.

Table 4.1: Characteristics of the three selected ground motion records

Record No.	Event Name	Year	Recording Station	Mean $S/S_{a,gm}$	SD $S/S_{a,gm}$	SF
1	Imperial Valley	1979	El Centro	0.74	0.17	0.95
2	Superstition Hills	1987	El Centro Imp.Co	0.84	0.20	1.69
3	Superstition Hills	1987	Poe Road	1.06	0.22	1.36

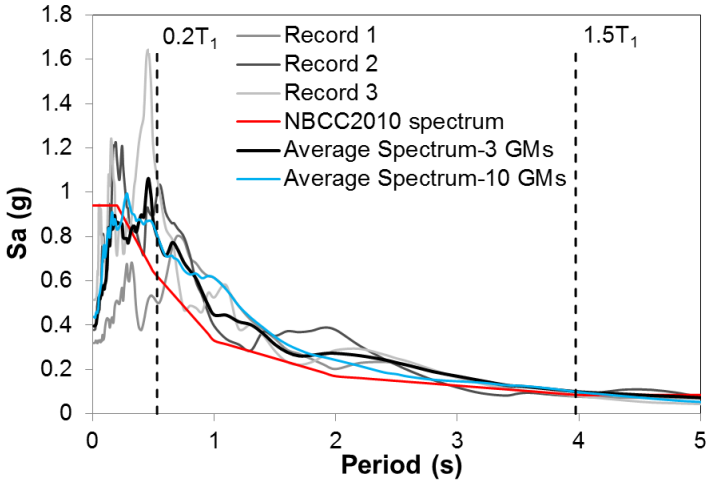

Figure 4.5: NBCC spectrum and 5% damped absolute acceleration spectra of the selected ground motions.

4.6.2 ASCE 41 Acceptance criteria for NDP

Deformation-controlled actions

When using NDP in ASCE 41, acceptance for the bracing members is based on their inelastic axial deformation capacity. For the collapse prevention performance level, the basic plastic deformation capacity of double angle braces in tension is equal to 12 Δ_T, where Δ_T is the brace axial deformation at the expected yield tensile load. For tension-only bracing, this value must be divided by 2.0 and a factor 0.8 is further applied because the connections do not meet the special seismic detailing requirements of AISC 341-10. This gives a plastic deformation capacity of 4.8 Δ_T.

Flexure in beams and columns subjected to axial compression and flexure is also considered as deformation-controlled action if $P_{UF}/P_{CL} < 0.5$. In that case, the peak plastic rotation θ_p in the member is compared to a permissible plastic rotation that varies with the member cross-section slenderness and the P_{UF}/P_{CL} ratio, similar to the *m* factor in LDP. Eqs. 8 to 11 can then be used to determine the limit on plastic rotation by replacing *m* by θ_p in all four equations, replacing the limits in Eqs. 8, 9 and 11 by 11 θ_y, 4 θ_y, and 1.2 θ_y, respectively, and replacing the limit in Eq. 10 by 17 (1- 5/3 P_{UF}/P_{CL}) θ_y. For W shapes, the yield rotation θ_y is determined from:

$$[19] \qquad \theta_y = \frac{ZF_{ye}L}{6EI}\left(1 - \frac{P_{UF}}{P_{ye}}\right)$$

where *A*, *I* and *Z* are the cross-section area, moment of inertia and plastic section modulus, respectively, and P_{ye} is the member expected yield axial strength (AF_{ye}). That rotation is for a fixed-fixed member when the end moments reach the member plastic moment reduced by axial load. If P_{UF}/P_{CL} is larger than 0.5, flexure is considered as force-controlled action with zero plastic rotation capacity.

Force-controlled actions

For force-controlled actions, the acceptance criteria described for LDP were used except for the following:

- In the analysis with Model B, the columns developed significant bending moments about strong axis due to non-uniform storey drift demands and were evaluated using the approach for components subjected to axial compression and bending moments described in section 4.5.3. Since axial loads and bending moments vary continually during the analysis, acceptance was verified at every time step of the response history and the largest result was retained for each level. When applying Eqs. 15 to 17, flexural-torsional buckling was also examined when evaluating the columns. For this failure mode, P_{CL} in the equations was determined for buckling about weak axis and flexural capacities M_{CL} and M_{CE} were determined with consideration of lateral-torsional buckling.

- In Models B and C, beams were evaluated using the acceptance criteria defined for LDP. Since beam moments are due to gravity loads only and do not vary, the evaluation was performed only at the time of maximum axial compression.
- In Models C and D, column failure was explicitly modelled in the analysis and the acceptance criteria for LDP were not verified. Similarly, when the analysis was performed using Model D, LDP acceptance criteria were not applied for the beams.

4.6.3 Evaluation of bracing members and brace connections using NDPs

In the frame studied, the brace length at level 2 and above is 9965 mm and F_{ye} = 330 MPa, which gives Δ_T = 16.4 mm. The plastic deformation capacity of the braces is therefore equal to 4.8 x 16.4 = 78.7 mm. When reaching this value, the total brace deformation is 5.8 Δ_T, which corresponds to a shear storey drift, excluding storey drift due to column axial deformations (overall frame bending), of 2.6 % of the storey height. Braces in level 1 are slightly longer and the corresponding higher deformation capacities were used in the evaluation.

Acceptance for the bracing members was verified using Model B and the ratio between peak brace plastic deformations during the response history and the brace plastic deformation capacities are plotted in Figure 4.6a. The peak axial load Q_{UD} normalized to the brace expected yield strength Q_{CE} is also given to inform on the peak loads reached in the braces. For both parameters, the maximum value from the three ground motion records is presented. As expected from LDP evaluation, brace tension forces reached Q_{CE} at all levels in the structure. More importantly, significant variation in brace plastic deformations is observed along the frame height with demands exceeding brace plastic capacities at levels 8 and 9 while no or limited brace ductility developed at other levels. This concentration of inelastic demand coincides with the marked reduction in brace sizes between levels 7 and 8 (see Figure 4.1a). Slightly higher demand-to-capacity ratios were obtained at the same two levels from NBCC response spectrum analysis in Figure 4.2a (YGS) and ASCE 41 LDP in Figure 4.3a, but linear dynamic analysis could not predict the pronounced differences in brace responses shown in Figure 4.6a. In the figure, the frame deformed shape when the braces at levels 8 and 9 reach a peak under the more critical record no. 2 suggests that higher modes likely contributed to the concentration of brace yielding. This NDP evaluation of the braces is markedly different from those obtained using

NBCC 2010 (all braces need to be strengthened) and ASCE 41 LDP (none of the braces had to be strengthened).

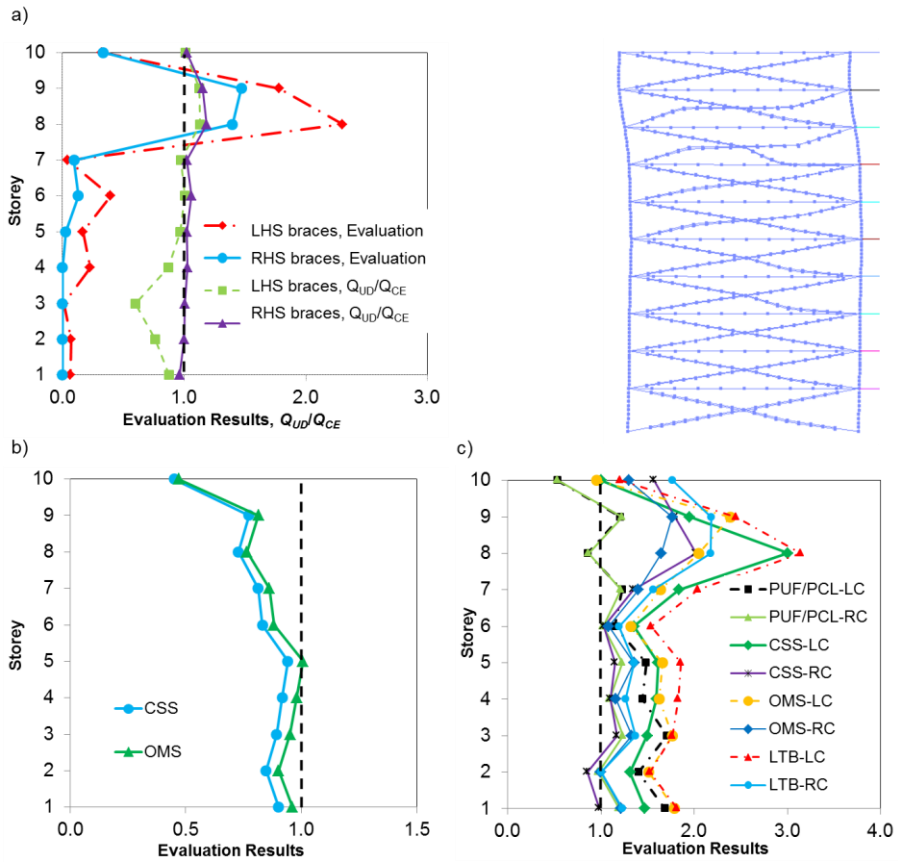

Figure 4.6: ASCE 41 NDP evaluation using Model B for the: a) Braces (with structure deformed shape at t = 13.7 s under record no. 2); b) Beams (CSS, OMS); and c) Columns (LTB = Lateral torsional buckling, LC = LHS column and RC = RHS column).

Because brace forces attain Q_{CE} in all braces, the force demand in the brace connections is same as considered in the NBCC and ASCE 41 LDP evaluations. At levels 8 and 9, strain hardening took place in the braces due to the large plastic deformations, which resulted in additional force demands not considered in NBCC and ASCE 41 LDP.

4.6.4 Evaluation of beams and columns using NDP

Evaluation of the beams and columns from Model B are presented in Figures 4.6b and 4.6c, respectively. The results correspond to the LHS of Eqs. 15, 16 or 17, as applicable. In Figure 4.6c, $P_{UF}/\kappa P_{CL}$ ratios are also given. Beam seismic evaluation using this model is close to that

obtained from LDP, mainly because beam moments are same and peak axial compression in beams are close to those predicted using brace forces Q_{CE} in LDP. At every level, in-plane buckling (OMS) is the governing failure mode. In the bottom floor, however, the force demand from ASCE 41 NDP is slightly lower and none of the beams would require retrofit.

In Figure 4.6c, the $P_{UF}/\kappa P_{CL}$ ratios exceed 1.0 in all columns except at levels 8 and 10. In the bottom 6 levels, the LHS column sustained higher axial load demand. Due to the large brace axial deformations at levels 8 and 9, significant strong axis bending moments developed in the columns from levels 7 to 10. Column condition is then more critical when assessing the columns as components subjected to combined axial compression and flexure. At all levels, peak P-M demands occurred when P_{UF}/P_{CL} was larger than 0.5. Flexure was thus considered as force-controlled action and the evaluation was based on Eq. 17. At all levels, lateral torsional buckling (LTB) limit state was critical, but CSS and OMS were not satisfied either at most levels. When considering moments, the most critical columns are those at level 8, which is contrary to the LDP evaluation in Figure 4.4b (or NBCC evaluation in Figure 4.2c) based on axial load actions only. Column flexural demand could only be observed when explicitly modelling brace nonlinear response in the analysis with Model B.

Model B predicted column failure by instability and this behaviour is examined further using Model C. In Figure 4.7, the response history from Models B and C under the most critical ground motion no. 2 is compared to study column responses. The ground motion is plotted in Figure 4.7a and roof lateral displacements from the two models are given in Figure 4.7b. From Model B, significant roof displacements are observed at approximately 13 and 20 s, as a result of considerable inelastic deformations developing in the braces at the 8^{th} and 9^{th} levels, as illustrated in Figure 4.7c for one of the two braces at these two levels. Similar roof displacement is obtained from Model C, but this analysis was halted at 13.3 s due to buckling of the LHS column as discussed next. In Figures 4.7d and 4.7e, the history of the action ratios P_{UF}/P_{CL} and M_{UF}/M_{CL} and the result of P-M interaction equations (Eq. 15 or 17, as applicable) are plotted for the LHS column at levels 8 and 1, respectively. The values are those obtained from Model B when verifying OMS (in-plane buckling) limit state. Column buckling could not be reproduced with this model but, for both columns, P-M interaction results exceed 1.0 at approximately 13 s, suggesting that column failure would have happened at this time. At the 8^{th} level in Figure 4.7d, peaks in the P-M interaction history coincide with peaks in the axial load ratio P_{UF}/P_{CL} but this

ratio remains below 0.84 and column overloading is largely caused by the large bending moments induced by the large storey drifts resulting from brace yielding at that level. For the LHS column at level 1, the demand essentially arises from axial loads and the P_{UF}/P_{CL} ratio reaches 1.5.

In the analysis with Model C, buckling of the LHS column occurred at level 1 as a result of the large axial compression demand predicted by Model B at 13.3 s. Column buckling in Model C produces the sudden increase in column axial deformation in Figure 4.7f. The column axial load-deformation response is plotted in Figure 4.8a. Buckling occurred at a load of 1.2 P_{CL}, which is higher than P_{CL} likely because of the rotational restraint provided at the upper end of the column by the continuity of the column. The analysis with Model C stopped at 13.5 s, when the column post-buckling compressive resistance had degraded below gravity induced axial loads, and convergence was no longer possible. With Model C, brace deformations at levels 8 and 9 remained small in Figure 4.7c and the large roof displacement in Figure 4.7b was mainly caused by buckling of the LHS column at level 1, though rigid body response of the structure above level 1 rather than by inelastic stretching of the braces at levels 8 and 9. Consequently, as shown in Figure 4.8b, the flexural demand on the columns at level 8 reduced significantly compared to that obtained with Model B in Figure 4.7d.

When using Model C, column buckling was also observed under earthquake record no. 3. This other column failure occurred at the 3rd level. For this structure, seismic induced column buckling observed with Model C at the first and third levels due to excessive axial load demand could be predicted in the evaluations performed using Model B as P_{UF}/P_{CL} ratios in Figure 4.6c are largest at these levels. Evaluation using 2010 NBCC in Figure 4.2c and ASCE 41 LDP in Figure 4.4b also indicated that the columns at these two levels would the most critical ones for resistance to axial compression.

Although the more comprehensive Model C could show column buckling and give a more realistic prediction of the anticipated frame behaviour, this example shows that the use of simpler analysis procedures, such as RSA and NDP with partial nonlinear response such as Model B, should not be undervalued in seismic evaluation. Here, for instance, NDP with partial nonlinear modelling limited to deformation-controlled actions (Model B) could provide a quick estimate of realistic forces for all force-controlled actions. Such a model is also sufficient to develop and

validate a final retrofit solution as it can adequately simulate the intended structural response with inelastic deformations limited to deformation-controlled actions.

This example also illustrates that NDP with nonlinear modelling of both deformation-and force-controlled actions may be used to refine the evaluation by predicting more accurately the strength of force-controlled members. In this case, however, the analysis may need to be repeated several times, updating the model each time to include the retrofit measures required by the previous analysis, until satisfactory nonlinear seismic performance is achieved. This progressive approach is essential as early failures of a deficient component may eclipse other deficiencies present in the structure or result in lower force demand on other components. When Model C was used for the frame under study, building failure was caused by column buckling at level 1. The large inelastic deformations in the braces at levels 8 and 9 and their possible consequences on the performance of the columns at these levels could not be predicted because the analysis stopped after buckling of the column at level 1, before these problems could be identified. Similarly, when using Model D, beam buckling response could not be fully evaluated because the analyses could not be pursued after column buckling.

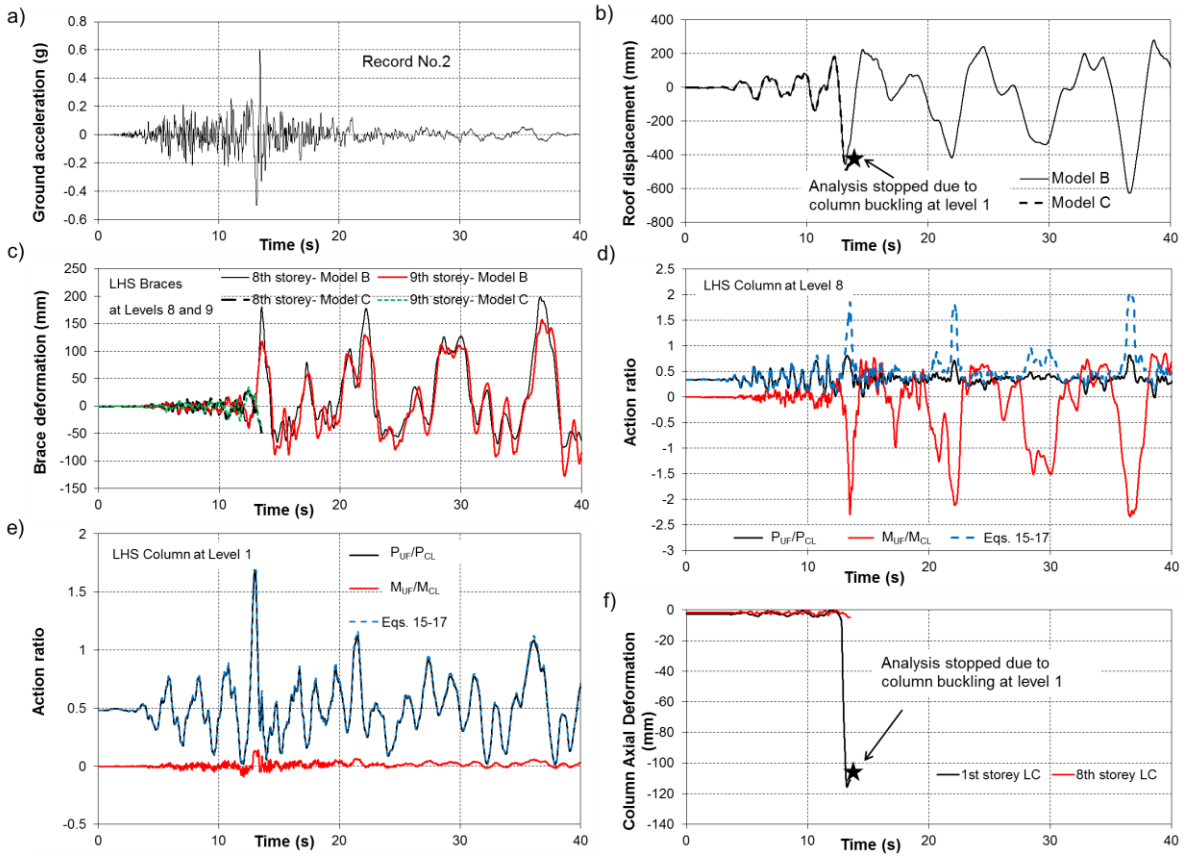

Figure 4.7: Response history response using Models B and C: a) Record no. 2; b) Roof displacements from Models B & C; c) Deformations of LHS braces at levels 8 and 9 from Models B & C; d) Evaluation of the LHS column at level 8 from Model B; e) Evaluation of the LHS column at level 1 from Model B; and f) Axial deformation of the LHS column at level 1 from Model C.

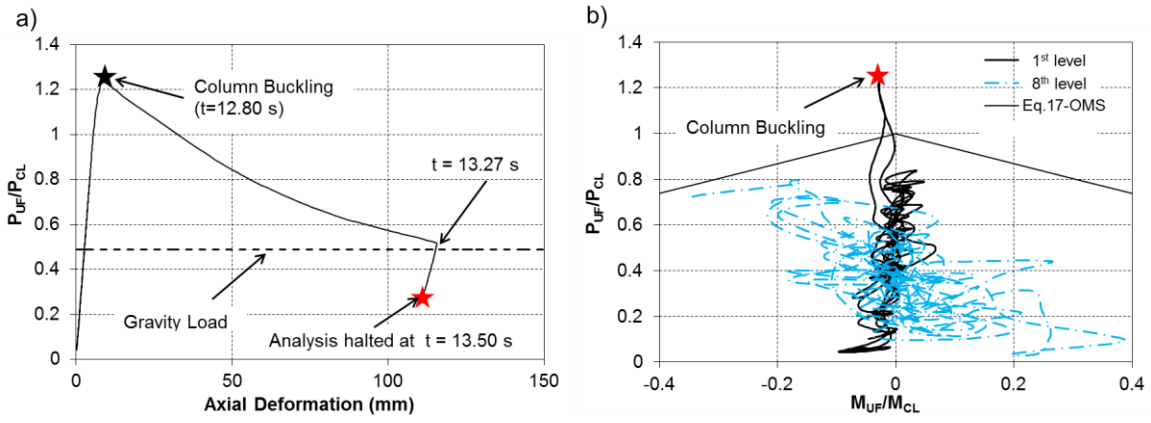

Figure 4.8: Response and demand for the LHS columns from Model C: a) Axial load-axial deformation response at level 1; b) P-M interaction at the 1st and 8th levels.

4.7 Seismic Retrofit using ASCE 41 NDP

4.7.1 Seismic retrofit using ASCE 41 NDP with nonlinear models B and C

Seismic retrofit of the frame was performed using ASCE 41 NDP with partial nonlinear modelling (Model B), as recommended in the previous section. For the retrofit design, the evaluation procedure was however modified as follows to identify the structure deficiencies more realistically and propose cost-effective retrofit actions:

- Knowing that brace connections would have to be retrofitted to resist forces corresponding to the brace expected strengths Q_{CE}, the 0.8 factor used in the calculation of the brace plastic deformation capacity for connections not complying with current seismic detailing provisions was omitted. This gave a higher plastic deformation capacity of $4.8\ \Delta_T / 0.8 = 6.0\ \Delta_T$.
- The demand from the most critical of 3 ground motions records was found severe and the analyses were redone using 7 additional ground motions such that the average demand from 10 records could be used in the evaluation. The average spectrum of the 10 scaled ground motions is shown in Figure 4.5. For the three records common to both ensembles, the scaling factors when part of the 3 motion and 10 motion sets were different. Impacts of using the average demand from 10 records rather than the maximum response from 3 records are discussed in this section.
- From the study by Bech et al. (2015), it was assumed that the columns would possess sufficient rotational ductility capacity to accommodate the flexural demand through yielding, even when subjected to high axial compression ($P_{UF}/P_{CL} > 0.5$). Hence, the columns were evaluated and retrofitted for axial compression only (P_{UF}/P_{CL}), ignoring the flexural demand. Validation of this approach and comparison with current ASCE 41 acceptance criteria are presented in this section.

With these modifications, braces and beams required no strengthening but column reinforcement was needed at levels 1 to 7 and at level 9. The retrofit scheme for the columns consisted in welding reinforcement steel plates to the flanges, as shown in Figure 4.9a. Because bending inelasticity was expected in the columns, a final evaluation of the retrofitted frame was performed

using ASCE 41 NDP with Model C simulating the nonlinear response of the bracing members and the columns. The results are presented in Figures 4.9 and 4.10.

In Figure 4.9b, brace evaluation using the average deformation demand from 10 ground motion records is satisfactory and no retrofit is required. This is partly due to the higher plastic capacity adopted for the braces (6.0 Δ_T *vs* 4.8 Δ_T) but the main difference comes from ground motion selection and scaling. In Figure 4.9b, evaluation results of the retrofitted frame under the 3 initial records are also given for comparison. In one case, the 3 records were scaled as part of the 10 record set (3 GMs). In the second case, the original scaling factors of Table 1 were used (3 OGMs). In both cases, record no. 2 was the most critical and the results from this motion are shown in the figure. In the first case, a reduced scaling factor (SF) of 1.59 compared to the original value of 1.69 was applied and the demand is higher but still close to the mean of the 10 ground motions. The evaluation with SF = 1.69 for record no. 2 is more critical, even more than computed with Model B in Figure 4.6b. Figure 4.9c shows that the slightly higher record amplitude was sufficient to trigger plastic hinging at both ends of the columns at the 8^{th} level, which created soft-storey response, a behaviour that could not be predicted with Model B under the same record because the columns were modelled with elastic frame elements. The time history of the brace deformations at level 8 is plotted in Figure 4.9d. With SF = 1.69, near collapse response with large permanent offset and progressive drifting in one direction is obtained, contrary to the more stable response with SF = 1.59 or the response from Model B in Figure 4.7c. For this frame, modelling the nonlinear response of the columns in NDP affected the distribution and amplitude of brace inelasticity response in the frame, an indication of the sensitivity of inelastic braced frame response to column modelling assumptions. The example also shows how ground motion selection and scaling can impact evaluation and retrofit as the brace performance ranges from acceptable to unsatisfactory with excessive ductility demand causing undesirable near collapse soft-storey response when changing the number of records from 10 to 3 or slightly increasing the amplitude of the critical record of a 3-record set.

Beam evaluation with the LDP acceptance criteria is presented in Figure 4.9d. Beam reinforcement is not needed when considering the 10-record ensemble. As shown, strengthening would have been required at levels 1, 4, and 5 for a set of 3 records. Effects of ground motion selection and scaling are less pronounced for the beams because axial force demand in beams is

bounded by the braces expected yield strengths and beam flexure is not affected by ground motions.

As shown in Figure 4.10a, the columns as retrofitted have sufficient axial strength P_{CL} to resist the gravity and seismic induced axial demands P_{UF} and no flexural buckling was observed in the 10 ground motions. As was the case for the beams, axial loads in columns are higher when considering the 3-record set and greater strengthening efforts would have been needed in the bottom storeys had the evaluation and retrofit been performed using that smaller ensemble. In all columns, the mean axial load ratio P_{UF}/P_{CL} under the group of 10 motions is however always larger than 0.5 and ASCE 41 would require that flexure in columns be considered as force-controlled action. The evaluation for combined axial and flexure is performed with this assumption in Figure 4.10d. As shown, flexural demand significantly impacts the evaluation at levels 8 and 9, where the large brace deformations at level 8 caused bending in the continuous columns. At levels 8 and 9, the columns do not meet the ASCE 41 criteria for LDP (Eqs. 15-17). It is noted that values presented in Figure 4.10b are not strictly correct as column moments are limited by the column capacities in Model C used in the evaluation. Higher values would have been obtained with Model B, as was presented in Figure 4.6c. Nonetheless, the results show that the columns as retrofitted would likely experience flexural yielding under the mean seismic demand. Model C could predict well cross-section yielding (CSS) and inelastic flexural buckling (OMS) but could not reproduce local buckling and lateral-torsional buckling modes and more advanced analysis was performed to further evaluate the column expected performance, as discussed next.

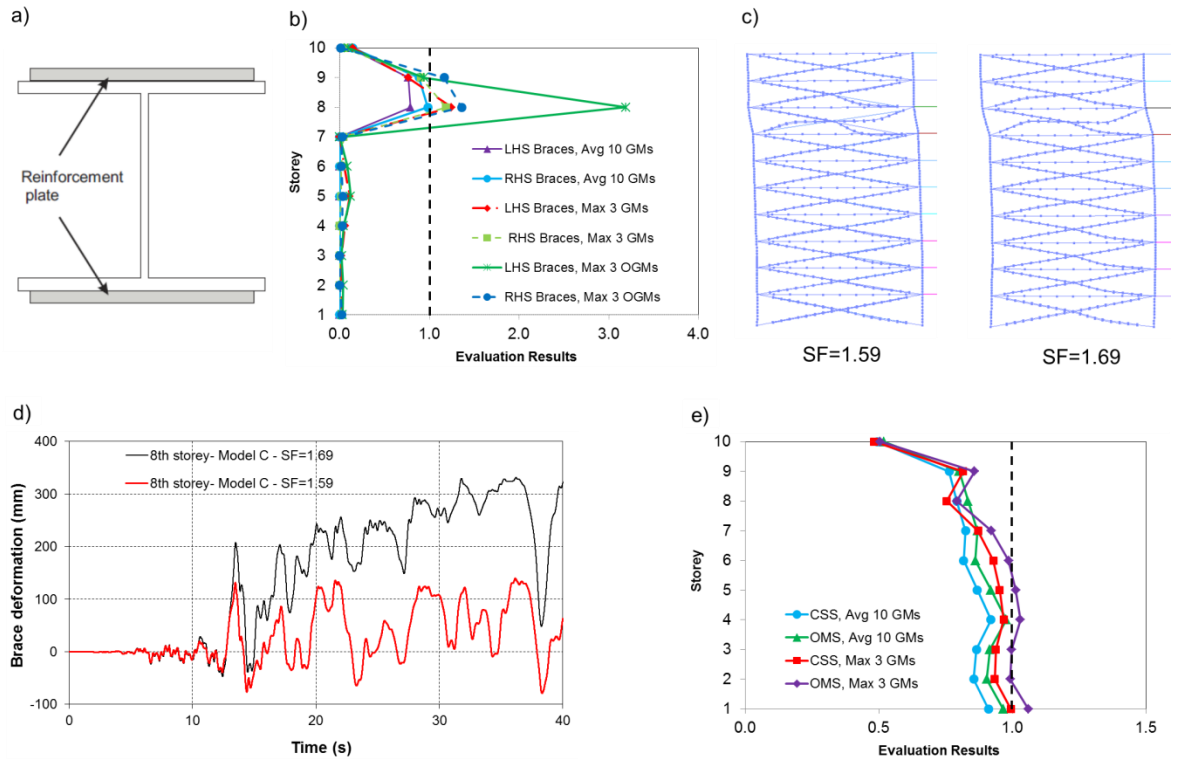

Figure 4.9: ASCE 41 NDP evaluation of the retrofitted structure using Model C: a) Column reinforcement; b) Braces; d) Structure deformed shape at t = 13.7 s under record no. 2 with SF = 1.59 and 1.69; d) Axial deformation time history of the LHS brace at level 8 under record no. 2 with SF 1.59 and 1.69; and d) Beams (CSS, OMS).

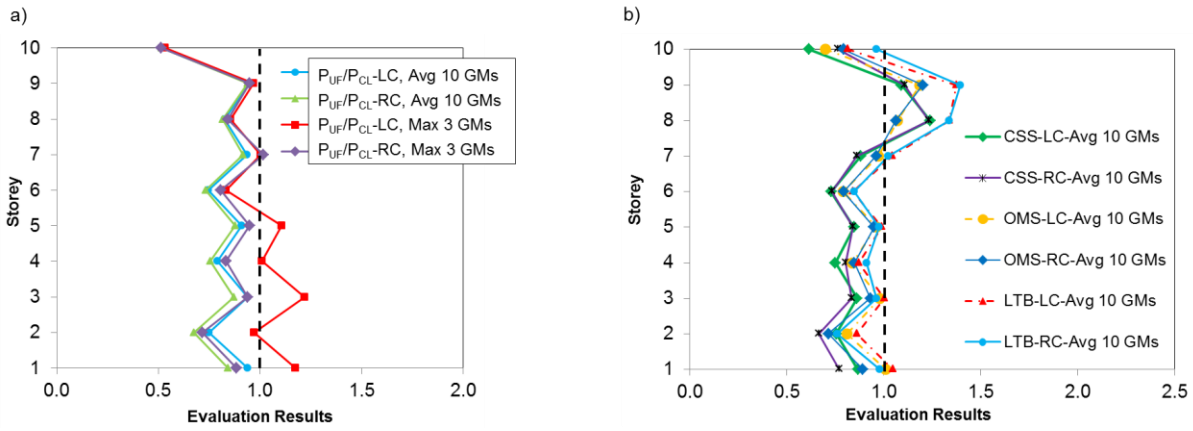

Figure 4.10: ASCE 41 NDP evaluation of the retrofitted structure using Model C: a) Columns based on axial compression only; and b) Columns using current ASCE 41 criteria for axial compression and flexure (LTB = Lateral torsional buckling, LC = LHS column and RC = RHS column).

4.7.2 Column rotation ductility

Column rotation capacity is studied herein for the columns at level 8 which did not need reinforcement based on axial load demand only. The column is a W310x107 section with $b/2t$ = $8.97 = 163/\sqrt{F_{ye}}$ and h/w = $25.5 = 463/\sqrt{F_{ye}}$. For KL = 3962 mm, P_{CL} = 0.75 P_{ye} and θ_y = $0.0078(1\text{-}P/P_{ye})$ from Eq. 19. Using these values in Eqs. 8-11, plastic rotation capacities are limited by flange local buckling and total rotation capacities ($\theta_y + \theta_p$) are plotted in Figure 4.11a for the entire range of P_{UF}/P_{CL}. As shown, the rotation limit decreases from 0.051 to 0.013 when P_{UF}/P_{CL} is increased from 0 to 0.5. Beyond that value, plastic rotation is not allowed and the rotation capacity corresponds to θ_y. Detailed finite element analysis was performed with the *ABAQUS* program (Dassault 2012) to verify those rotation capacities. A three-dimensional model of an individual column having 3.962 m in height (equal to h_s) was developed using four-node shell elements with reduced integration. Residual stresses from Galambos and Ketter (1958) as well as initial local flange imperfections and global out-of-straightness imperfections as specified in ASTM (2002) and CSA (2009) were considered. The model could therefore predict flexural buckling, local buckling, and lateral torsional buckling. A first series of analyses was performed in which the storey drift was monotonically increased up to failure while the column was carrying various levels of a constant axial load from 0.1 to 0.9 P_{CL}. Monotonic loading was adopted because large flexural demands on braced frame columns generally occurred only one or two times in response history analyses. The results are plotted in Figure 4.11c. In all cases, flexural strength was limited by flange local buckling occurring in the end plastic hinges (Figure 4.11b), which led to the degradation shown. Global buckling was not observed, although predicted when using Eqs. 15-17. Total rotations when peak flexural strength was reached and after 20% strength degradation were determined and the values are plotted in Figure 4.11a. Rotation capacities at maximum moment are generally close to the ASCE 41 limits. The analyses however clearly show plastic rotation capacities for axial loads above 0.5 P_{CL}. Much higher rotation capacities are obtained if degradation is acceptable. These results also indicate that plastic rotation capacities steadily decrease as axial compression is increased but columns carrying high axial compression equal to or greater than 0.5 P_{CL} do possess some ductility, contrary to current ASCE 41 criteria. These findings are consistent with the conclusions by Bech et al. (2015).

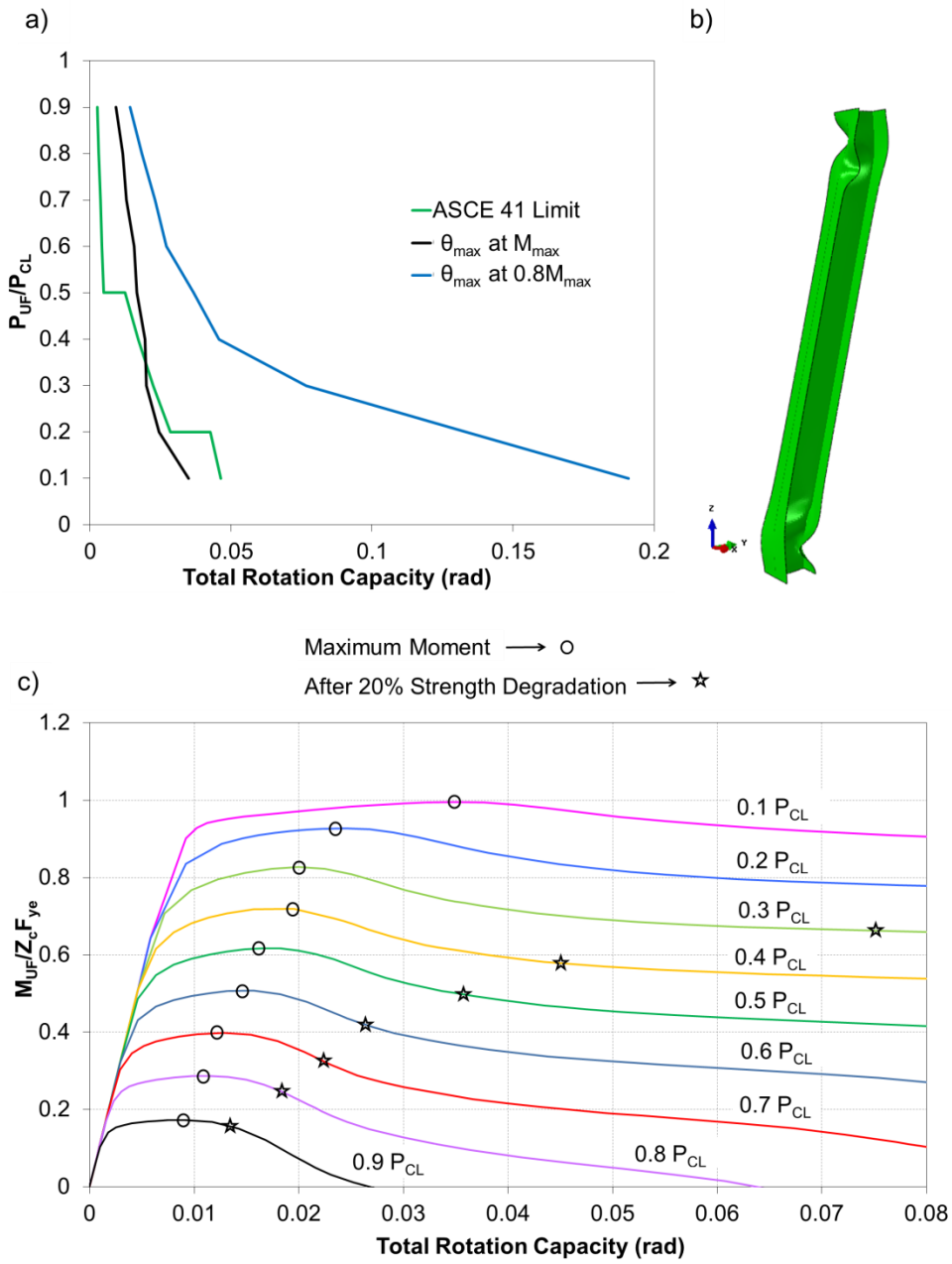

Figure 4.11: Column rotation ductility: a) From ASCE 41-13 and finite element analyses; b) Damaged column (case shown: P_{UF}/P_{CL} = 0.5 at θ = 0.22 rad); and c) Moment-rotation responses from finite element analysis.

To evaluate if the column at level 8 can withstand the seismic induced axial compression without failure while undergoing flexural yielding due to brace yielding, the time histories of the axial load, end displacements and end rotations imposed on the LHS column under record no. 2, as obtained from the analyses with OpenSees Model C, were applied to the isolated *ABAQUS* finite

element model of the column. The axial load *vs* total rotation traces from Model C are plotted in Figures 4.12a and 4.12d for the record scaling factors of 1.59 and 1.69, respectively. In both cases, the demand exceeded the capacities specified in ASCE 41 and the limits from finite element obtained in Figure 4.11c. The moment-rotation responses from Model C and *ABAQUS* are compared in Figures 4.12b and 4.12e. Both responses are similar except that the flexural resistance from *ABAQUS* reduces due to local buckling when large rotations are imposed. This effect is more pronounced when SF = 1.69 is applied to the ground motion record. The axial load-moment responses from both models and for both ground motion amplitudes are compared in Figures 4.12c and 4.12f. The axial loads in both models are same because the axial load demand from Model C was imposed to the *ABAQUS* model. However, the column in *ABAQUS* could resist that axial compression demand without global buckling for the entire duration of the two ground motions, even if large plastic rotations and pronounced local buckling occurred. This suggests that plastic rotation or flexural strength are not good indicators for the evaluation of columns not considered to contribute through bending to the frame lateral resistance to earthquakes. For these columns, such as gravity columns or braced frame columns, the level of axial compression they can safely carry when being subjected to seismically induced plastic hinging would probably better reflect the role of the columns and should be used as an acceptance criterion. It is noted that the flexural stiffness and strength of these columns can help mitigating soft-storey response; however, unless this second role is necessary to maintain structural integrity, it should not be considered in the seismic evaluation.

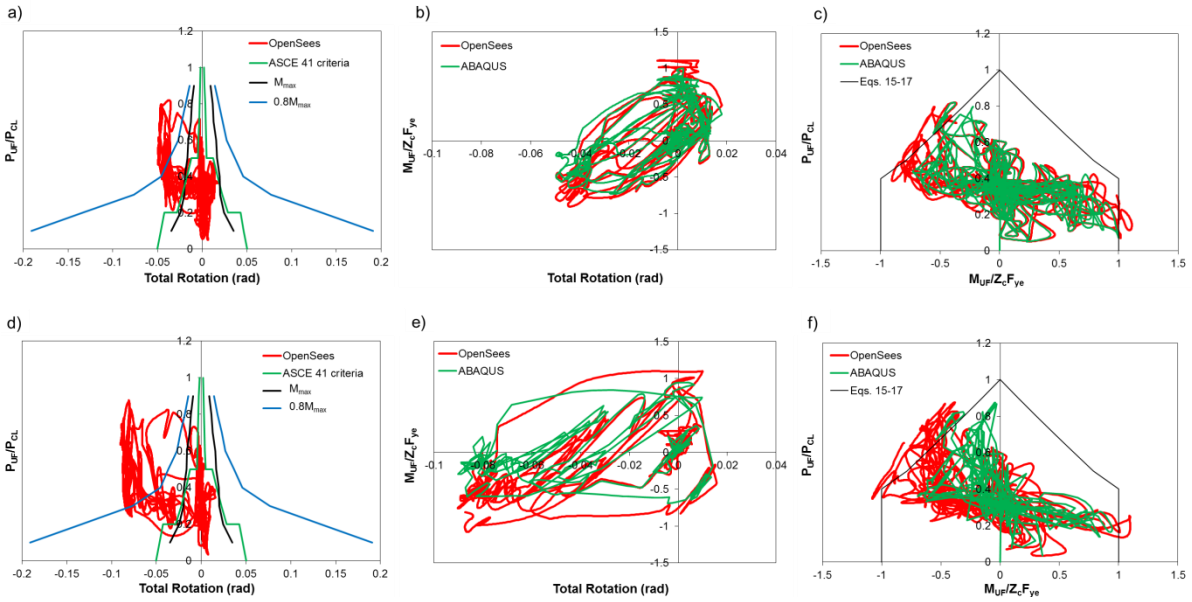

Figure 4.12: Response history response of the LHS column at level 8 from *Opensees* Model C and *ABAQUS* analysis under record no. 2: a) Axial load-rotation response of the column, SF=1.589; b) Moment-rotation response of the column, SF=1.589; c) Axial load-moment response of the column, SF=1.589; d) Axial load-rotation response of the column, SF=1.695; e) Moment-rotation response of the column, SF=1.695; and f) Axial load-moment response of the column, SF=1.695.

Further numerical simulations and experimental investigations are needed to develop acceptance criteria for columns whose main function during an earthquake is to resist axial loading. For the braced frame studied herein, the limited study presented here does not suffice to conclude that the retrofit scheme studied is sufficient to achieve the intended level of performance. In particular, the possibility of soft-storey response at the 8th level is of concern and the braces and/or columns could be strengthened to mitigate this undesirable response. Nonetheless, when compared to the retrofit currently required under NBCC 2010 (18.4 tons of steel), the retrofit scheme discussed in this section only requires 4.3 tons of steel, which clearly indicates that using ASCE 41-13 for seismic evaluation, including relaxations on plastic rotation capacities for columns subjected to high axial loads, can lead to more cost effective retrofit solutions in Canada.

4.8 Conclusions

The seismic performance of 10-storey tension-only steel X-braced frame with back-to-back double angle braces was evaluated using different methods. The structure was designed in accordance with the 1980 NBCC for a site class C in Vancouver, British Columbia, Canada. The evaluation approaches proposed in the 2010 NBCC and the ASCE 41-13 Tier 3 procedures were used. The former was performed using results from the equivalent static force procedure (ESFP) and response spectrum analysis (RSA). ASCE 41 evaluation was done using both linear and nonlinear dynamic analysis procedures (LDP and NDP). For NDP, models reproducing nonlinear responses associated to deformation-controlled actions in the bracing members and models accounting for nonlinear response for both deformation- and force-controlled actions in primary components were used. The ASCE 41 methodology was adapted for Canadian application. The following conclusions can be drawn from this study:

- Evaluation of the structure for 60% of the 2010 NBCC seismic loads using both static (ESFP) and dynamic (RSA) analysis procedures revealed that seismic retrofit was needed. When considering 100% of NBCC 2010 loads, both analysis methods indicated that most braces and columns would need strengthening. All brace connections were also found to have inadequate capacity and some of the beams had insufficient strength. The evaluation was generally less severe when using RSA.
- For the structure studied, the evaluation using ASCE 41 LDP was less severe than the one performed under 100% NBCC 2010 seismic loads. It could predict well the force demand on force-controlled actions obtained from NDP ASCE 41 with nonlinear modelling of deformation-controlled actions.
- When evaluating force-controlled actions using ASCE 41 LDP, limit analysis should be preferred to elastic analysis with the force delivery factor J as the former results in more realistic and lower force demands while requiring comparable computational efforts.
- NDP with partial nonlinear modelling limited to deformation-controlled actions effectively provides realistic estimates of all force-controlled actions and thus allows a rapid insight into potential seismic deficiencies related to force-controlled actions. Because the model can adequately simulate the intended structural response with inelastic

deformations limited to deformation-controlled actions, it is sufficient to develop and validate a final retrofit solution.

- NDP with nonlinear modelling of both deformation-and force-controlled actions permits more accurate representation of complex failure mechanisms and thus provides a more accurate prediction of the structure capacity. In this case, however, the analysis may need to be repeated several times, updating each time the model to include retrofit measures required from previous analysis, until satisfactory nonlinear seismic performance is achieved. This progressive approach is essential as early failure of a component may eclipse other deficiencies possibly present in the structure ore result in lower force demands on other components.
- Selection of ground motions may have a significant impact on evaluation performed using the ASCE 41 nonlinear dynamic analysis procedure. For the structure examined in this study, the average demand from 10 records was significantly less than the maximum value from 3 records.
- Current ASCE 41 LDP acceptance criteria for components subjected to axial compression and flexure appears to be too conservative for columns of steel braced frames. Further study is needed to assess the axial load carrying capacity as a function of the expected cyclic plastic rotation demand of these columns.

4.9 Acknowledgments

The authors gratefully acknowledge the financial support provided by the Natural Sciences and Engineering Research Council of Canada (NSERC) for the Canadian Seismic Research Network (CSRN).

4.10 References

AISC. 2010a. Specification for structural steel buildings, ANSI/AISC 360-10, American Institute of Steel Construction, Chicago, IL.

AISC. 2010b. Seismic provisions for structural steel buildings, ANSI/AISC 341-10, American Institute of Steel Construction, Chicago, IL.

ASCE. 2013. Seismic evaluation and rehabilitation of existing buildings, ASCE/SEI 41-13. American Society of Civil Engineers, Reston, VA.

ASTM. 2002. Standard specification for general requirements for rolled structural steel bars, plates, shapes and sheet piling, ASTM A 6/A 6M – 02. American Society for Testing and Materials, West Conshohocken

Atkinson, G.M. 2009. Earthquake time histories compatible with the 2005 national building code of Canada uniform hazard spectrum, Can. J. of Civ. Eng., 36(6): 991-1000.

Balazadeh-Minouei, Y., Koboevic, S., and Tremblay, R. 2013. Seismic evaluation of existing steel braced frames designed in accordance with the 1980 Canadian code requirements using nonlinear time history analysis. Proc. CSCE 2013 Annual Conf., Montreal, Canada, Paper No. DIS-58.

Bech, D., Tremayne, B., and Houston, J. 2015. Proposed changes to steel column evaluation criteria for existing buildings. Proc. Second ATC & SEI Conf. on Improving the Seismic Performance of Existing Buildings and Other Structures, American Society of Civil Engineers, San Francisco, CA.

BSSC. 1992. NEHRP Handbook for the Seismic Evaluation of Existing Buildings. Report No. FEMA 178, developed by the Building Seismic Safety Council for the Federal Emergency Management Agency, Washington, DC.

Callister, J.T., and Pekelnicky, R.G. 2011. Seismic Evaluation of an Existing Low Ductility Braced Frame Building in California. Proc. ASCE Structures Congress 2011, Las Vegas, NV.

CSA. 1978. Limit states design of steel structures, CAN3-S16.1-M78. Canadian Standards Association, Rexdale, ON.

CSA. 2009. Design of Steel Structures, CSA-S16-09, Canadian Standards Association, Mississauga, ON.

CSI. 2008. ETABS Computer Software, Version 9.5.0. Computers and Structures, Inc., Berkeley, CA.

Dassault. 2012. ABAQUS-FEA/CAE. Dassault Systemes Simulia Corp., RI, USA.

Galambos, T.V., and Ketter, R.L. 1958. Columns under combined bending and thrust. Fritz Engineering Laboratory Report No. 205A.21, Bethlehem, PA.

Harris III, J.L., and Speicher, M.S. 2015. Assessment of First Generation Performance-Based Seismic Design Methods for New Steel Buildings; Volume 2: Special Concentrically Braced Frames, NIST Technical Note 1863-2, National Institute of Standards and Technology, Gaithersburg, MD.

Jiang, Y., Balazadeh-Minouei, Y., Tremblay, R., Koboevic, S., and Tirca, L. 2012a. Seismic assessment of existing steel braced frames designed in accordance with the 1980 Canadian code provisions. Proc. 7th Stessa Conf., Santiago, Chile, 531-537.

Jiang, Y. and Tremblay, R, and Tirca, L. 2012b. Seismic assessment of deficient steel braced frames with built-up back-to-back double angle brace sections using OpenSees modelling. Proc. 15th World Conf. on Earthquake Eng., Lisbon, Portugal, Paper No. 4416.

Johnson, M., Sloat D., Roeder C.W., Lehman D.E, and Berman J.W. 2014. Seismic performance evaluation of concentrically braced frame connections. Proc. 10th National Conf. on Earthquake Eng., Earthquake Engineering Research Institute, Anchorage, AK, Paper No. 1168.

Lamarche, C.-P., and Tremblay, R. 2011. Seismically induced cyclic buckling of steel columns including residual-stress and strain-rate effects. J. Constr. Steel Res., 67(9):1401-1410.

McKenna, F. and Fenves, G.L. 2004. Open System for Earthquake Engineering Simulation (OpenSees). Pacific Earthquake Engineering Research Center (PEER), University of California, Berkeley, CA. (http://opensees.berkeley.edu/index.html)

Mitchell, D., Paultre, P., Tinawi, R., Saatcioglu, M., Tremblay, R., Elwood, K., Adams, J., and DeVall, R. 2010. Evolution of seismic design codes in Canada. Can. J. of Civ. Eng., 37(9):1157-1170.

NRCC. 1993. Guidelines for the seismic evaluation of existing buildings. Publication no. NRCC 36941, Institute for Research in Construction, National Research Council of Canada, Ottawa, ON.

NRCC. 1980. National building code of Canada 1980, 8th ed., National Research Council of Canada, Ottawa, ON.

NRCC. 2010. National building code of Canada 2010, 13th ed., National Research Council of Canada, Ottawa, ON.

NZS. 1997. NZS 3404, Steel Structures Standard. Standards New Zealand, Wellington, New Zealand.

Redwood, R.G., and Channagiri, V.S. 1990. Earthquake resistant design of concentrically braced steel frames. Can. J. of Civ. Eng., 18(5): 839-850.

Sen, A.D., Pan, L., Sloat, D., Roeder, C.W., Lehman, D.E., Berman, J.W., Tsai, K.C., Li, C.H., and Wu, A.C. 2014. Numerical and experimental assessment of chevron braced frames with weak beams. Proc. 10th Nat. Conf. on Earthquake Eng., Earthquake Engineering Research Institute, Anchorage, AK, Paper No. 961.

Sloat, D.A. 2014. Evaluation and Retrofit of Non-Capacity Designed Braced Frames. M.Sc. Thesis, Dept. of Civil and Environmental Eng., Univ. of Washington, Seattle, WA.

CHAPTER 5 ARTICLE 2: SEISMIC ASSESSMENT OF EXISTING STEEL CHEVRON BRACED FRAMES

Yasaman Balazadeh-Minouei[1], Sanda Koboevic[2] and Robert Tremblay[3]

[1]Ph.D. Candidate, Dept. of Civil, Geological and Mining Engineering, Polytechnique Montreal, Montreal, QC, Canada H3C 3A7 (Corresponding author). Email: yasaman.balazadeh-minouei@polymtl.ca

[2]Assistant Professor, Dept. of Civil, Geological and Mining Engineering, Polytechnique Montreal, Montreal, QC, Canada H3C 3A7.

[3]Professor, Dept. of Civil, Geological and Mining Engineering, Polytechnique Montreal, Montreal, QC, Canada H3C 3A7.

Submitted to the *Journal of Structural Engineering, ASCE.*

Abstract

The seismic response of 3- and 10-story typical chevron type steel braced frames located on the west coast of Canada is examined to identify potential deficiencies. The structures were designed in accordance with the 1980 National Building Code of Canada (NBCC). They did not include any specific seismic ductility considerations for braces, brace connections or floor beams. The frame beams are light beams. The evaluation was performed using the procedures of NBCC 2010 and ASCE 41-13 standard. Response spectrum analysis and nonlinear time-history analysis (NLTHA) methods were conducted. Different numerical models were used for NLTHA to verify the impact of the nonlinear response of different components on seismic response. NBCC evaluation required strengthening of all braces in both structures whereas all braces were found to be acceptable by the ASCE 41 linear dynamic procedure (LDP). However, ASCE 41 nonlinear dynamic procedure (NDP) revealed high inelastic demand in the upper and lower levels of the 10-story frame, in excess of the brace deformation capacities. From both ASCE 41 LDP and NDP, beams are expected to fail by strong axis buckling prior to brace buckling, a behavior confirmed by detailed finite element analysis. LDP showed that columns are also deficient. Columns could not be assessed using NDP because of beam buckling occurring first in the analyses. For the 10-story frame with retrofitted beams, NDP showed the possibility of column buckling.

Key words: seismic evaluation, existing steel braced frame, force-delivery reduction factor, probability of exceedance, nonlinear time history analysis.

5.1 Introduction

In the United States and Canada, chevron-type braced frames have been commonly used to resist lateral loads in steel buildings because of their structural efficiency and architectural flexibility. Many of these frames were built before special seismic design and detailing requirements were incorporated into U.S. and Canadian codes in the late 1980s (ICBO 1988, CSA 1989). In addition to problems related to non-ductile connection detailing and inadequate brace section compactness, one main shortcoming of this system is that the beams were not designed to resist the loads arising from the difference between the forces in tension and compression braces after brace buckling. Under unbalanced brace loads and gravity loads, beams can develop plastic hinging, which can lead to soft-story response and compromise the system gravity load resisting capacity (Khatib et al. 1988). This deficiency is common to old chevron braced frames in the U.S. and Canada as both were conceived following similar design procedures.

An extensive study was undertaken in the U.S. (Roeder et al. 2012) to investigate the seismic vulnerability of pre-1990s non-ductile concentrically braced frames (NCBFs) found in older buildings. Tests by Sloat (2014) confirmed the likelihood of non-ductile failure modes in connections of NCBFs. From numerical analyses calibrated against experimental results, Hsiao et al. (2014) found that brace or connection failures are expected in NCBFs under moderate earthquakes and collapse can occur for these structures when exposed to maximum considered earthquakes. Sen et al. (2016) evaluated experimentally the seismic performance of two-story non-ductile chevron-type braced frames with weak beams, not compliant with the current beam strength requirements of ANSI/AISC 341 (AISC 2010). Tests showed that, while inadequate brace compactness and brace connection details led to fractures at small drifts, unbalanced brace loads acting on the beams did not have a negative impact on the system ductility. In fact, for the cases tested, beam flexural yielding provided additional energy dissipation. The authors conclude that, although beam-yielding mechanism performed well and has potential to reduce retrofit costs, additional studies are needed to investigate the impact of such behavior on system response before the concept can be widely applied. The study reported herein addresses this issue. The focus is put on light beams as they may fail by instability prior to developing ductile flexural

yielding, with detrimental consequences on frame response. This more critical failure mode has not been investigated in the past and this study can provide additional data needed to establish the limits on acceptable beam demand-to-capacity ratios.

In the U.S, seismic evaluation of existing buildings is carried out using the requirements and procedures defined in the ASCE 41-13 standard (ASCE 2013). To satisfy the basic performance objective (BPOE), an existing building must attain life safety performance level for seismic hazard with probability of exceedance of 20% in 50 years and collapse prevention level under the seismic hazard with probability of exceedance of 5% in 50 years. ASCE 41 also specifies acceptance criteria for existing structures that are different from those used for new structures. Less stringent performance objectives compared to new constructions account for the facts that: (i) existing buildings have a shorter remaining life, (ii) more recent constructions do not become deficient with every more conservative changes in design codes, and (iii) the high cost associated with the higher level of performance cannot be justified in view of the incremental benefit. In Canada, according to NBCC 2010 (NRCC 2010), initial assessment is carried out using reduced loads corresponding to 60% of earthquake loads prescribed for new buildings that are established for a probability of exceedance of 2% in 50 years. Thus, unlike in the U.S., the seismic hazard used for the assessment of existing buildings is not related to a specific probability of exceedance. When triggered, the retrofit should be designed for higher force levels, preferably meeting the performance objective for new buildings, i.e. collapse prevention for a probability of exceedance of 2% in 50 years, taking into considerations of future building use, control of seismic damage and the differential in upgrading costs with force levels (Allen et al. 1992). Acceptance criteria used for assessment and retrofit are those prescribed for new constructions.

Past studies (e.g., Harris and Speicher 2015, Speicher and Harris 2016, Balazadeh-Minouei et al. 2017) have shown that the seismic assessment of steel concentrically braced frames is heavily influenced by the analysis method used. Evaluation procedures using linear analysis can yield less or more conservative results compared to nonlinear analysis, depending on the components being verified. Harris and Speicher (2015) also concluded that nonlinear procedures provide a more rigorous assessment compared to linear procedures and that more research is needed to determine appropriate acceptance criteria for beam-columns.

In this study, seismic response of non-ductile chevron braced frames is evaluated using 10- and 3-story buildings located in Vancouver, British Columbia. Seismic conditions at this site are

similar to those that prevail in Northwestern United States. The frames have light floor beams to investigate possible instability failure modes. Initial assessment is carried out in compliance with NBCC 2010 requirements for existing buildings, i.e. under 60% of seismic loads calculated for a probability of exceedance of 2% in 50 years. To investigate the extent of required upgrades, the seismic assessment is redone under 100% of the NBCC 2010 seismic loads. To explore the potential for savings when using specific provisions for seismic evaluation and retrofit, the evaluation under 100% NBCC seismic loads is also carried out using the Tier 3 ASCE 41 procedure. The linear dynamic procedure (LDP) is applied first. To understand better the frame behavior and identify more precisely possible failure mechanisms, nonlinear dynamic procedure (NDP) is also applied. Special attention is given to the evaluation of the beam response using distributed plasticity and 3D detailed finite element models. Nonlinear column modeling was also considered to examine the possibility of column inelastic buckling under combined axial and flexural demands. This article focuses on the evaluation of the structures; the seismic retrofit of the 10-story frame is discussed in a separate paper.

5.2 Original Design of the Building Studied

The original design was performed in accordance with the 1980 NBCC (NRCC 1980) and the CSA-S16.1-M78 (CSA 1978) steel design standard. The building plan view and frame elevations are illustrated in Fig. 5.1. The building is located in Vancouver, BC, on firm ground site. Chevron-type braced frame that provides seismic resistance in the E-W direction is examined in this study. The seismic base shear, V, was determined from the equivalent static force procedure, as permitted in NBCC 1980 for regular structures:

[1] $V_{1980} = ASKIFW$

In this equation, A is the design acceleration ratio, S is the seismic response factor for building period T ($S = 0.5/T^{0.5}$), K is a coefficient accounting for ductility in function of the type of construction, I is the importance factor, F is the foundation factor and W is the seismic weight. In this study, $A = 0.08$, $S = 0.35$ and 0.80 for the 10- and 3-story frames, $K = 1.0$, $I = 1.0$, $F = 1.0$, and $W = 91390$ and 26450 kN for the 10- and 3-story buildings, respectively. Note that the fundamental periods were 2.0 s and 0.39 s for the 10- and 3-story buildings, respectively. They were estimated using the Rayleigh method as was allowed in NBCC 1980 and would have been used in practice. These periods are significantly longer than 0.54 s and 0.17 s obtained from the

NBCC 1980 empirical expression $T_{emp} = 0.09h_n/D^{0.5}$ with h_n and D are the building height and plan dimension. The resulting seismic force coefficients, V_{1980}/W, were equal to = 0.029 (10-story) and 0.064 (3-story). Note that in the contemporary UBC 1979 (ICBO 1979), comparable base shears equal to 0.027 and 0.053 *W* would have applied to the two structures if located in seismic zone 2.

To account for higher mode effects, concentrated lateral forces, F_t = 7.74% *V* and 0.74% *V*, were applied at the roof level of the 10- and 3-story buildings, respectively. In-plane torsion and P-delta effects were considered in design. The overturning moment reduction factor, *J*, was taken equal to 1.0. In 1980, the load combinations were: (i) 1.25D + 1.5L; (ii) 1.25D + 1.5E; and (iii) 1.25D + 0.7 (1.5L + 1.5E), where D, L and E are the specified dead, live (including snow), and earthquake loads, respectively.

Design of frame members was carried out following CSA-S16.1-M78 steel design standard. The selected members are given in Fig. 5.1. They are made of CSA-G40.21-300W steel (F_y = 300 MPa, F_u = 450 MPa), as was the practice in the 1980's. All bracing members are double angle sections with equal legs in back-to-back position. Class 3 sections were used to control width-to-thickness ratios. The overall slenderness ratio was limited to 200. One stitch was considered at mid-length of the bracing members to satisfy individual buckling requirements. The vertical legs of the angles were connected to single vertical gusset plates using high strength A325 bolts, 19.1 mm in diameter. A typical connection detail is shown in Fig. 5.1. The design of the bracing members was governed by axial strength requirements, except at the roof level where the braces were selected to meet the maximum brace overall slenderness limits. CSA S16.1-M78 did not consider shear lag effects and block shear failure for bolted connections, which resulted in smaller brace connections compared to what would be needed today. Beams and columns were W-shapes and the columns were tiered in two-story segments. Simple shear connections with bolted web angles were used between beams and columns. The beams were assumed to be laterally supported out-of-plane by the floors, vertically supported by the braces. They were selected to resist shear and flexure from gravity loads and strong-axis buckling under combined axial compression and bending from gravity plus seismic loads.

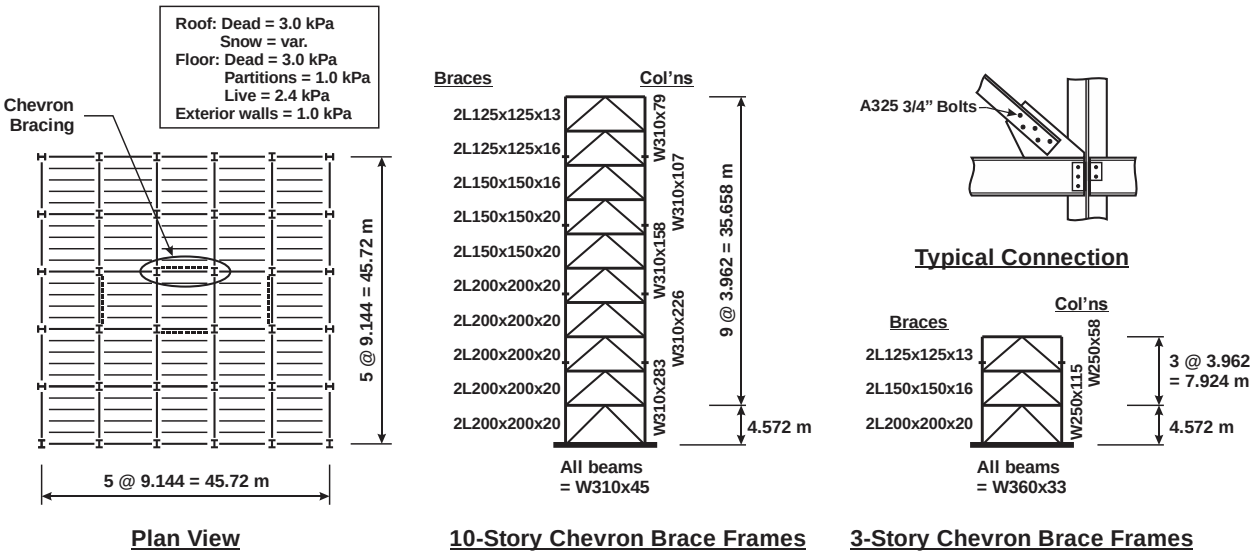

Figure 5.1. Plan view, braced frame elevations and typical connection of the 3- and 10-story buildings.

5.3 Seismic Evaluation using NBCC 2010

5.3.1 NBCC 2010 Seismic Loads for Evaluation

To determine if retrofit is required, initial assessment of the structures is carried out following provisions of NBCC 2010 and 2009 CSA S16 standard (CSA 2009) under 60% of the NBCC 2010 seismic loads. Seismic loads in NBCC 2010 are determined using a 2% in 50 years uniform hazard design spectrum. That spectrum is plotted in Fig. 5.2 for the site studied. As also shown in the figure, the 60% reduced seismic force demand for this site lies between those associated to seismic hazard levels with 5% and 10% probabilities of exceedance in 50 years. The seismic base shear in NBCC 2010 is given by:

$$[2]\quad V_{2010} = \frac{S(T_a) M_v I_E W}{R_d R_o}$$

where S is the design spectral acceleration value at the fundamental period T_a, M_V is a factor that accounts for higher mode effects on base shear, I_E is the importance factor and R_d and R_o are the ductility- and overstrength-related force modification factors. For the 10- and 3-story buildings, T_a = 2.01 and 0.62 s, respectively, and M_v and I_E are equal to 1.0 for both structures. Seismic weight calculations in NBCC changed between 1980 and 2010 and the 2010 values are 83760

and 24880 kN for the 10- and 3-story buildings, respectively. The frames are considered to be of the NBCC 2010 Conventional Construction (Type CC) category as their original design did not include any special seismic detailing. For this system category, R_d = 1.5 and R_o = 1.3. With these values, V_{2010} from Eq. 2 are 0.087W and 0.288W for the 10- and 3-story frames, respectively. For seismic evaluation, seismic effects were determined from response spectrum analysis (RSA) using a three dimensional model to account for accidental torsion. Elastic frame elements were used to model braces, beams and columns, and rigid diaphragm response was considered at every level. This model is named Model A. Base shears from RSA, respectively 0.0887W and 0.286W for 10- and 3-story frames, exceeded 0.8V_{2010} and the RSA results were therefore used without scaling, as required by NBCC. Notional loads and P-delta effects were also included in the analysis as specified in CSA S16-09. The load combinations in NBCC 2010 are: (i) 1.25D + 1.5L + 0.5S; and (ii) 1.0D + 0.5L + 0.25S + 1.0E. Additional details on NBCC 2010 loading are given in Jiang et al. (2012) and Balazadeh-Minouei et al. (2017). When considering all differences between seismic loads in 1980 and 2010 NBCC provisions, the factored design base shears in 2010 for the 10- and 3-story frames are respectively 2.83 and 3.88 times the 1980 values. The differences result from changes in seismic data, force reduction factors and period calculations (Mitchell et al. 2010).

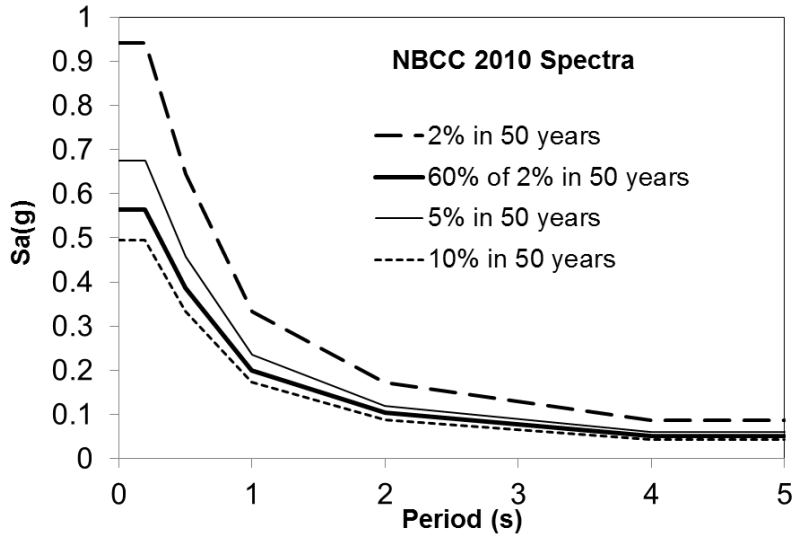

Figure 5.2. NBCC 2010 spectral accelerations for different probabilities of exceedance.

For the 10-story frame, seismic loads need to be amplified by 1.5 as required in CSA S16-09 to prevent excessive local ductility demands resulting from concentration of inelastic deformations along the frame height. For this frame, CSA S16-09 also requires that the seismic induced axial loads in columns be further increased by 1.3 to improve the robustness of the system. For the lower 3-story building, the 1.5 amplification factor need only be applied to seismic forces in brace connections to avoid non-ductile failures in connections. In both frames, brace connection forces were limited to the brace probable yield strengths determined with $R_y F_y$ = 330 MPa.

5.3.2 NBCC Seismic Evaluation Procedure and Results

In NBCC, seismic evaluation is performed by comparing factored load effects to factored resistances and the FLR (factored load to resistance) ratio is therefore used herein to present evaluation results. Figure 5.3a shows FLR ratios for the braces of the 3- and 10-story frames. For the braces in tension, two limit states related to brace connections are examined: tension failure on net section (NS) and block shear failure (BS). Braces in compression are evaluated for failure by buckling (BC), either flexural or flexural-torsional buckling depending which one governs. The corresponding factored resistances as specified in CSA S16-09 are given in Eqs. 3 to 5. Brace tension yielding on gross cross-section is not given as it did not control brace design.

[3] $T_r = \phi_u A_{ne} F_u$

[4] $T_r = \emptyset_u \left[U_t A_n F_u + 0.6 A_{gv} \frac{(F_y + F_u)}{2} \right]$

[5] $C_r = \emptyset A F_y (1 + \lambda^{2n})^{-1/n}$

In these expressions, A is the brace gross section area and A_{ne} is the brace effective net area reduced for shear lag, A_n and A_{gv} are respectively the net and gross areas governing block shear failure, U_t is an efficiency tension factor for block shear failure, λ is the brace slenderness ratio, n is the parameter for compressive resistance (n = 1.34), F_y and F_u are the specified minimum yield and tensile strengths, and ϕ and ϕ_u are resistance factors.

In Fig. 5.3a, all braces of the 10-story braced frame except the braces at the 5th level and all braces of the 3-story braced frame are inadequate in compression under 60% NBCC seismic loads. For the 10-story building, BC is the critical failure mode, with significant variations of FLR values along the height resulting from differences between analysis methods used in the original design (static) and the evaluation (RSA) and the step variations in brace sizes along the frame heights (Fig. 5.1). The largest FLR values are at levels 1 and 9. The 3-story frame exhibits

similar FLR values for BC, with the maximum at the top floor. When brace connection failure modes are considered, block shear (BS) limit state is more problematic than net section failure for both frames and is more critical than BC in the bottom two stories of the 3-story frame.

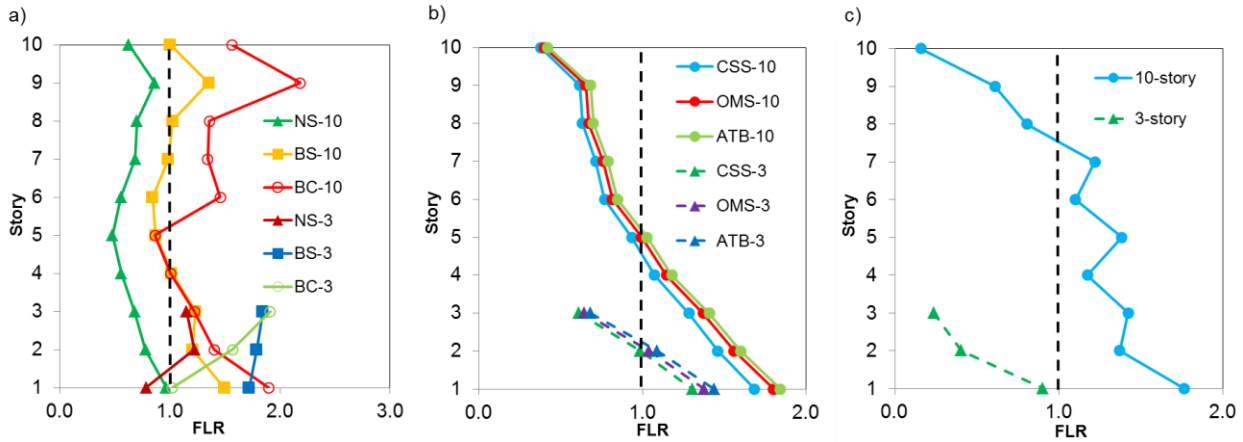

Figure 5.3. NBCC evaluation results under 60% of NBCC 2010 seismic loads for: a) Braces (BC = Buckling in compression) and brace connections (NS = net section failure; BS = block shear failure); b) Beams (CSS = Cross Sectional Strength; OMS = Overall Member Strength; ATB = Axial Tension and Bending); and c) Columns.

The beams are verified for three limit states including: cross-sectional strength (CSS), overall member strength (OMS) for buckling in the vertical plane under combined compression and bending, and combined axial tension and bending moments (ATB). Because the frame is classified as Type CC, all frame members including braces are assumed to remain essentially elastic. Stability effects were therefore determined assuming a beam buckling length equal to half the frame width and brace unbalanced load effects were not considered. Figure 5.3b shows that CSS, OMS, and ATB are not satisfied for the 1st to 5th level beams in the 10-story building. For the 3-story frame, OMS and ATB limit states are critical for beams at levels 1 and 2 whereas CSS is not satisfied at the 1st level. Noncompliance is due to the much higher axial loads imposed in beams by NBCC 2010 compared to NBCC 1980, as illustrated in Fig. 5.4 for the first level beam of the 10-story frame. Moments are due to gravity loads and only slightly differ because of differences in load combinations.

Axial compression FLR ratios for the bracing bent columns are given in Fig. 5.3c. Columns at the 1st to 7th levels in the 10-story building have insufficient strength. All columns of the 3-story building have sufficient strength.

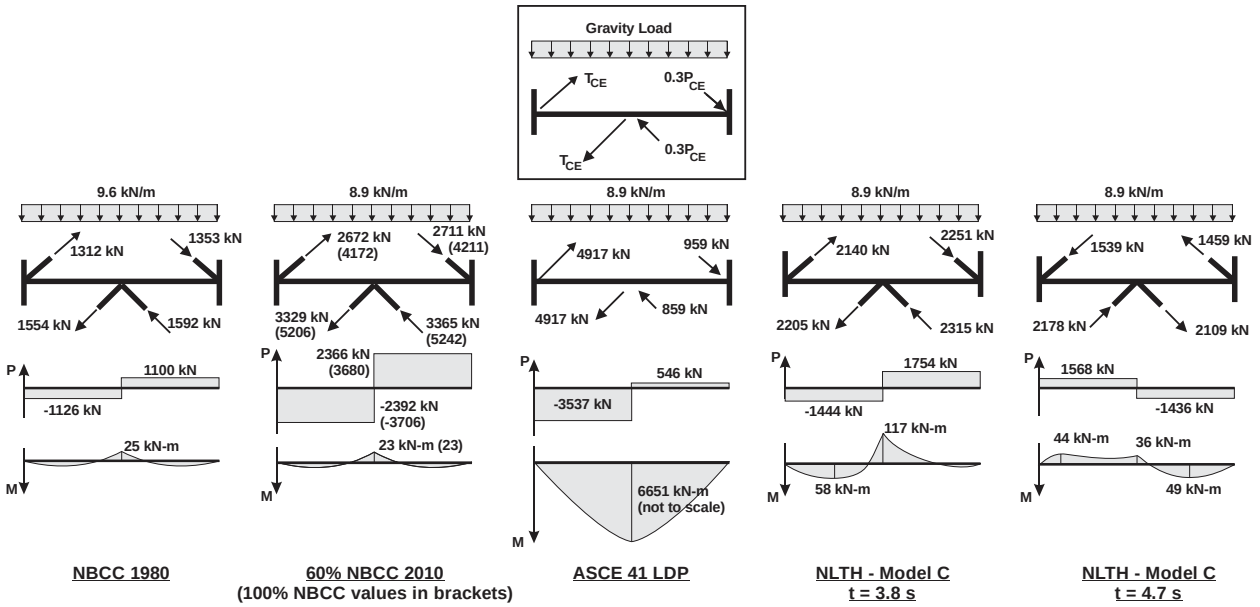

Figure 5.4. Axial loads and bending moments in the beam at level 1 of the 10-story frame. (*Note: horizontal loads from floor diaphragms not shown*)

5.4 NBCC Evaluation under 100% NBCC 2010 Seismic Loads

The initial assessment suggests that major retrofit would be needed for these buildings as nearly all braces and their connections must be strengthened and more than 50% of the beams need reinforcement for the two structures. For the 10-story frame, 70% of the columns also require strengthening. According to NBCC 2010, the retrofit solution has to be preferably designed for 100% of the NBCC 2010 seismic loads established for a 2% in 50 years probability of exceedance. In this study, it was assumed that this load level applies and the extent of retrofit that would be required is evaluated in this section.

The results are presented in Fig. 5.5. All braces of the two buildings, beams in the bottom 7 levels of the 10-story building and all beams of the 3-story building, and columns in the first 8 stories of the 10-story building and in the first story of the 3-story building have inadequate resistance for forces induced by 100% NBCC seismic loads. As expected, this evaluation is more critical than

the initial assessment and the required retrofit will be difficult to implement in practice. It is therefore of interest to examine the possibility of reducing the amount of work by using an evaluation procedure dedicated to existing structures, such as ASCE 41-13. This is presented in the next section.

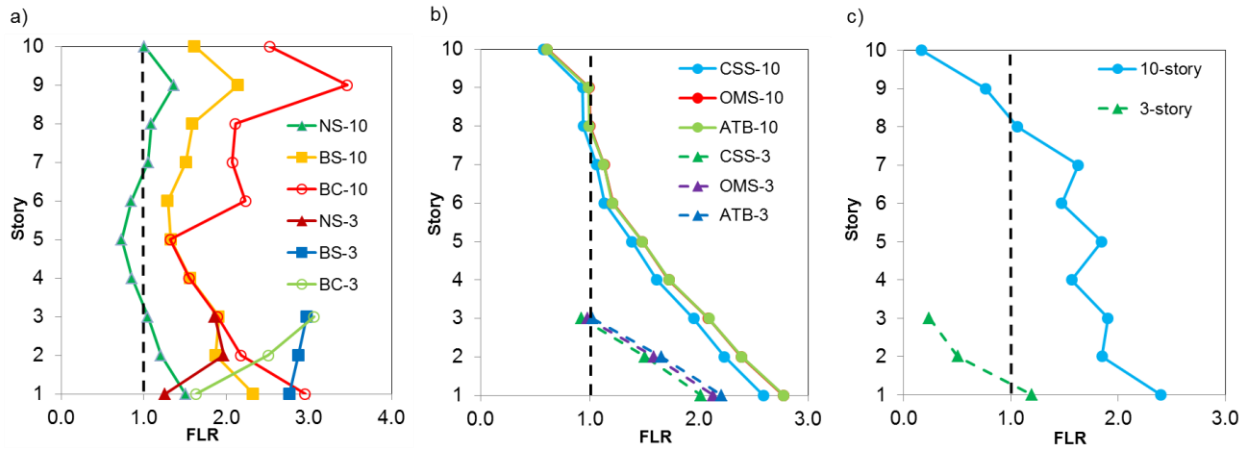

Figure 5.5. NBCC evaluation results under 100% of NBCC 2010 seismic loads: a) Braces (BC = Buckling in compression) and brace connections (NS = net section failure; BS = block shear failure); b) Beams (CSS = Cross Sectional Strength; OMS = Overall Member Strength; ATB = Axial Tension and Bending); and c) Columns.

5.5 ASCE 41 Evaluation under 100% NBCC 2010 Seismic Loads

For this application of ASCE 41, the performance objective to determine the extent of retrofit work required is set as collapse prevention performance for a hazard level with a probability of exceedance of 2% in 50 years to comply with NBCC design objective. The seismic demand is therefore determined using the NBCC design spectrum for 2% in 50 years probability of exceedance, without the additional amplification factors required in CSA S16. This allows an evaluation of the seismic response of deficient chevron braced frames for the maximum considered earthquake (MCE) level ground motions. Both linear and nonlinear dynamic procedures are applied to examine the impact of the analysis technique on the assessment results. Nonlinear dynamic procedure also provides a better understanding of the frame behavior and more precise identification of possible failure mechanisms.

5.5.1 Linear Dynamic Procedure (LDP)

Response spectrum analysis (RSA) was carried out using Model A described in Section "Seismic Evaluation using NBCC 2010" and the NBCC 2010 design spectrum for 2% in 50 years hazard level illustrated in Fig. 5.2. For evaluation, ASCE 41 classifies actions in structural components as either deformation-controlled (ductile) or force controlled (non-ductile) actions. In the linear dynamic procedure, components are evaluated using:

Deformation-controlled actions:

[6] $m\kappa Q_{CE} \geq Q_{UD}$

Force-controlled actions:

[7] $\kappa Q_{CL} \geq Q_{UF}$

where m is the component demand modification factor to account for the expected ductility related to a given action at the selected structural performance level, κ is the knowledge factor, Q_{CE} is the expected strength of a component at the deformation level under consideration for deformation-controlled actions, Q_{UD} is the deformation-controlled design action due to gravity loads (Q_G) and earthquake loads (Q_E), and Q_{CL} is the lower-bound strength of a component for force-controlled actions. Q_{UF} can be determined from a limit or plastic analysis of the inelastic mechanism of the structure, similar to the analysis performed when applying capacity design principles for new buildings. Alternatively, Q_{UF} can be determined based on the smallest demand-capacity ratio ($DCR = Q_{\mathrm{UD}}/Q_{\mathrm{CE}}$) of all components in the load path delivering forces to the component under consideration. This alternative value can be computed from:

[8] $Q_{UF} = Q_G \pm \frac{Q_E}{C_1 C_2 J}$

where C_1 is the modification factor that relates the expected maximum inelastic displacements to displacements calculated using linear elastic response, C_2 is a modification factor that considers the effect of pinched hysteresis shapes, cyclic stiffness degradation, and strength deterioration on maximum displacement response, and J is the force delivery reduction factor, calculated as the smallest DCR of all components delivering forces to the component. In ASCE 41-13, $C_1 = C_2 =$ 1.0 for periods longer than 1.0 s and 0.7 s, respectively.

For the frames studied, the knowledge factor, κ, is taken equal to 1.0 assuming all required data is available. For the m-factor, braces, beams and columns are considered as primary structural components. The member capacities are determined from the CSA S16 standard considering a

resistance factor equal to 1.0. For the braces, Q_{CE} is computed with the expected steel yield strength F_{ye} taken as 1.1 times the nominal yield value (F_{ye} = 1.1 x 300 = 330 MPa), as recommended for materials not listed in ASCE 41. For beams, columns and brace connections, the lower bound steel yield strength (F_y = 300 MPa) is used to determine Q_{CL}.

Axial tension and compression demands in braces are considered as deformation-controlled and Eq. 6 is therefore used for evaluation of the braces. *DCR* values for the braces in compression and tension are presented in Fig 5.6a. As shown, *DCR* > 1 for all braces of the two frames, which means that brace buckling is expected at every level. In tension, all braces of the 3-story frame will reach their expected yield strength. For the 10-story building, the results show that this will be the case only in the bottom two floors. However, force redistribution after brace buckling is expected to result in higher tension force demands compared to the values predicted from linear analysis and it can be expected that all braces of the 10-story frame would likely reach their expected yield tensile strengths.

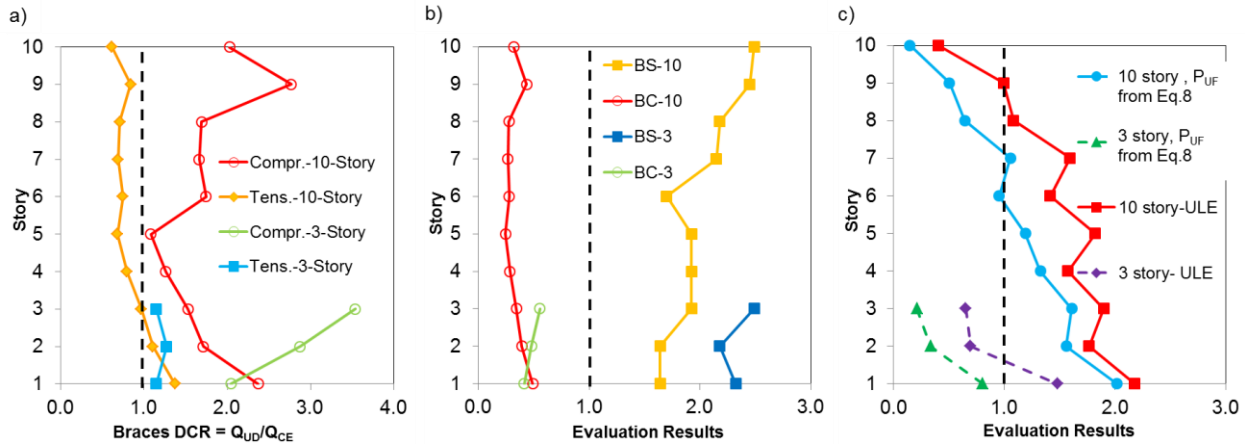

Figure 5.6. ASCE 41 linear assessment: a) Q_{UD}/Q_{CE} ratios of the braces in tension and compression; b) Assessment of the braces in compression (BC) and brace connections (BS = block shear failure); and c) Assessment of the columns (ULE = Unbalanced Load Effect) for 3-story and 10-story buildings using ASCE LDP (Model A).

For braces in compression, the *m*-factor is determined considering the slenderness ratio and cross-section of the members. Connection robustness, section compactness, and stitch requirements for built-up members also influence the value of *m*. For stocky and slender double angle compressive braces with in-plane buckling, the *m*-factor is equal to 7.0 and 8.0,

respectively, for collapse prevention objective. For braces with intermediate slenderness, linear interpolation is used. The *m*-factors were then reduced because the braces did not meet the high ductility compactness requirements and connection strength requirements specified for SCBFs in AISC 341-10. Stitch spacing, although not satisfying SCBF requirements, did not affect the ductility factors as brace buckling is expected in the plane of the frame. The resulting *m*-factors varied from 4.4 to 6.4 and from 5.0 to 6.4 for the 10- and 3-story frames, respectively. Evaluation of the braces in compression (BC) is given in Fig 5.6b. The values shown are the ratios between the right-hand side and left-hand side terms of Eq. 6.All braces of both frames are found adequate in compression (BC) by a comfortable margin, which drastically differs from the NBCC evaluation of Fig. 5.5a for the same seismic hazard level. Contrary to NBCC, it is concluded from ASCE 41 LDP evaluation that none of the braces of the two frames would need to be strengthened or replaced.

Evaluation of the brace connections was performed using Eq. 7 and the results are plotted in Fig. 5.6b for block shear (BS) failure under tension, the most critical limit state for connections. In the verifications, connection tension forces Q_{UF} were limited to the expected brace strength Q_{CE} when *DCR* was larger than 1.0 in tension, as permitted in ASCE 41. As shown, similar to the NBCC evaluation of Fig. 5.5a, none of the brace connections have sufficient capacity against block shear failure. Different from NBCC, the ASCE 41 evaluation procedure leads to a sharp distinction between deformation- and force-controlled actions: clearly, ductility (in braces) is rewarded while emphasis is put on the prevention of less ductile limit states such as failure in connections.

In chevron braced frames, beams, their connections, and supporting members must resist unbalanced brace load effects in combination with gravity loads considered as forced-controlled actions. This is shown in the upper part of Fig. 5.4, where P_{uf} and M_{UF} are determined under gravity loads plus a tension brace force equal to the brace expected yield strength T_{CE} and a compression brace force equal to 30% of the brace expected compression strength P_{CE} in the post-buckling range. As discussed earlier, the demand on braces indicate that this brace force scenario is expected for the two frames studied and the acceptance criterion for beams is then:

[9] $\frac{P_{UF}}{\kappa P_{CL}} + \frac{M_{UF}}{\kappa M_{CL}} \leq 1$

Because braces have buckled in compression, they no longer provide a vertical support at mid-span of the beams after buckling and the beams are therefore considered as simply supported over their full lengths (9.144 m) when determining P_{CL} for strong axis buckling in the frame vertical

plane. The resulting axial and moment demands for the first level beam of the 10-story frame are illustrated in Fig. 5.4. As illustrated, most of the story shear is resisted in compression by the beam segment located between the tension braces framing from above and below the beam, and unbalanced brace loads induce bending moments that significantly exceed those obtained from linear analysis (NBCC 1980 & 2010). For the W310x45 section originally selected for this beam, P_{CL} = 1168 kN (with KL_x = 9144 mm) and M_{CL} = 212 kN-m. The value of M_{CL} is obtained from the beam plastic moment as lateral torsional buckling of the beam is prevented. Hence, axial and flexural capacities are exceeded by 3.03 and 31.4 times, suggesting that beam hinging will govern beam inelastic response. Note that beams in these frames are light beams supporting limited tributary gravity loads and were not originally designed to resist such unbalanced brace loads. Rather, they were designed assuming that elastic braces could provide a vertical support at mid-span. This loading condition led to excessively high values for axial compression-bending interaction (Eq. 9) and the results are not plotted in Fig. 5.6. It is noted that beams in chevron braced frames are in compression over half their length and tension in the other half. Hence, using KL = 9144 mm for calculating the beam compressive strength and P-δ amplification probably lies on the conservative side.

Differences between force demands on beams from NBCC 2010 and ASCE 41 in Fig. 5.4 arise mainly because CSA S16 does not include any special requirements for beams of Type CC chevron braced frames regarding unbalanced brace loads and loss of support at beam mid-spans after brace buckling. The analysis and evaluation are then performed assuming elastic brace response. Although this approach led to comparable axial compression loads, bending moments from brace unbalanced loads in ASCE 41 are much more critical, which leads to a more severe assessment than NBCC. For this beam example at the first level of the 10-story frame, a W840x576 section would be needed to replace the existing W310x45 section to satisfy the ASCE 41 acceptance criteria of Eq. 9, which represents major retrofit action, probably not feasible in practice because of the impact on clear story height and the difficulty in bringing and installing such heavy shapes in an existing building. Recent experiments by Sen et al. (2016) showed that beams in chevron braced frames can undergo ductile flexural deformations without compromising the structure integrity, a behavior that can provide for additional energy dissipation and ductility capacity. The beam nonlinear response is studied further in sections “Nonlinear Dynamic Procedure” and “Three-Dimensional Finite Element Analysis of Beam

Buckling Response" to examine if beam ductile flexural hinging is possible for the studied frames.

In ASCE 41, axial compression in columns is also considered as force-controlled action. For chevron braced frames, columns must be considered as supporting members for beams and column axial compression P_{UF} must then be determined from limit analysis for the loading case resulting from the unbalanced brace loads and gravity loads on beams. Note that column moments from RSA are small and are neglected in the assessment. Figure 5.6c shows the evaluation results from Eq. 7 when using column loads from this analysis. Columns in levels 1 to 8 of the 10-story building and the first level of the 3-story building do not meet the ASCE acceptance criteria. NBCC and ASCE 41 evaluations lead to the same conclusions. This is however coincidental considering that the calculation of the axial load demands from the two procedures is different and, contrary to CSA S16, no resistance factor is applied to determine P_{CL} in ASCE 41.

As mentioned, column axial loads P_{UF} in ASCE 41 can also be determined using Eq. 8. In this equation, the parameter J is based on the *DCR* values of the braces contributing to the axial loads in the column under consideration. In the procedure, the *DCR* value at a given level is the largest of the values computed for the tension and compression braces. In Fig. 5.6a, compression braces have higher *DCR* values at all levels of both frames. For the 10-story building, *DCR* are equal to 2.03, 2.77, 1.69, 1.66, 1.75, 1.08, 1.26, 1.53, 1.71, and 2.37 from the 10^{th} to first levels. Hence, J = 2.03 for the 9^{th} and 8^{th} levels, 1.69 for the 7^{th} level, 1.66 for the 6^{th} and 5^{th} levels, and 1.08 for the remaining lower levels. J = 1.0 for level 10 as braces do not induce axial compression in the columns at this level. Similar calculations were performed for the 3-story building and column evaluation results using P_{UF} from Eq. 8 are plotted in Fig. 5.6c for comparison. As shown, evaluation using this approach is less severe than the evaluation resulting from limit analysis and the chevron braced frames beam loading condition. This difference is examined further in the last section of the article.

For the structures studied, NBCC and ASCE 41 LDP resulted in similar retrofit needs for brace connections and columns. From ASCE 41, braces would not require modifications but all beams would need to be replaced, which is different from NBCC. In ASCE 41, it is noted that force demands on force-controlled components depend on the capacities of the bracing members. For the two structures, the extent of retrofit predicted by ASCE 41 would reflect the final changes as

braces need no reinforcement. In cases where larger braces are required, the evaluation must be redone with the retrofitted braces, which is expected to result in more extensive retrofit.

5.5.2 Nonlinear Dynamic Procedure (NDP)

5.5.2.1 Modeling

For nonlinear dynamic analysis, a two-dimensional model of the frame was developed using the OpenSees platform (McKenna et al. 2004). Three modeling options with varying degree of complexity, Models B, C, and D, are employed. In Model B, the braces are represented with force-based nonlinear beam-column elements whereas elastic beam-column elements are used for the beams and columns. The model allows explicit evaluation of the inelastic deformation demands on the braces and gives more realistic force demands on brace connections, beams, and columns. In Model C, force-based nonlinear beam-column elements are employed for both the braces and the beams, giving a possibility to predict beam limit states such as flexural yielding and/or buckling in the vertical plane. Out-of-plane flexural buckling and lateral-torsional buckling are assumed to be prevented by floor and roof diaphragms. In Model D, force-based nonlinear beam-column elements are employed for all frame members so that column yielding and in-plane and out-of-plane flexural buckling modes can also be reproduced. Prediction of column buckling with this model has been validated by Lamarche and Tremblay (2011). In all models, beams are pin-connected to the columns. Brace connection limit states were not explicitly modelled in these models to focus on member responses. Additional detail on modeling assumptions can be found in Balazadeh-Minouei et al. (2017).

5.5.2.2 Ground Motion Records

The target spectrum S_{targ} for selection and scaling of the ground motions is the 2% in 50 years NBCC 2010 design spectrum of Fig. 5.2. The period range of interest spans between 0.2 T_1 and 1.5 T_1, where T_1 is the computed period of the 10-story structure (T_1 = 2.05 s). Twenty pairs of orthogonal horizontal ground motion components from historical earthquakes compatible with site conditions were initially selected considering the two magnitude-distance scenarios (M6.5 at 17-23 km and M7 at 28-35 km) dominating the seismic hazard at the site (Atkinson, 2009). The records were selected from the following earthquake events: 1994 Northridge, 1989 Loma Prieta, 1992 Landers, 1971 San Fernando, and 1999 Hector Mine earthquakes. Out of the twenty pairs,

the ten pairs with records that best matched the target spectrum within the period range of interest were retained.

Scaling was performed using the procedure described in ASCE 41-13. This procedure assumes 3D analysis under pairs of orthogonal components and a unique scaling factor is applied to both components of each pair. Because 2D analysis is conducted in this study, one record for each pair was selected and scaled using the following adapted procedure. A square root of the sum of the squares (SRSS) spectrum was constructed for each of the 10 pairs of horizontal components. Each pair was scaled such that the average of the SRSS spectra of all pairs was above the target spectrum. For each pair, the component with the response spectrum closest to the average of the SRSS spectra over the period range of interest was then selected. As shown in Fig. 5.7, the average spectrum of the 10 selected components fell below the target spectrum at the long period end of the period range considered. Thus, a second, final scaling factor was applied to bring the average spectrum above the target spectrum. For simplicity and ease of comparison in this study, the same scaling factors were used for both braced frames although their fundamental periods are different.

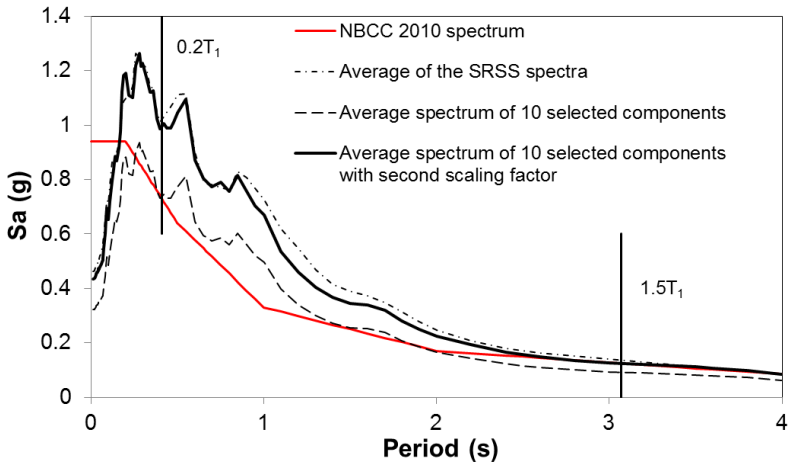

Figure 5.7. Scaling of the selected ground motions for the 10-story building.

5.5.2.3 Evaluation Results from ASCE 41 NDP

When using the most comprehensive Model D, nonlinear analysis revealed global structural collapse under all ground motions for the 10-story frame and under 5 ground motions for the 3-story one. The failure modes causing collapse varied, however, depending on the ground motions. For the 10-story frame, buckling of the braces developed in the upper stories in five of the 10 ground motions, which caused a large flexural demand on the adjacent beams and

eventually led to the formation of soft-story response and collapse. For two ground motions, buckling of a column was recorded. In the remaining three records, the first-story beam buckled in-plane over one half of its length. In these cases, brace buckling did not occur and frame collapse occurred due to the story drift resulting from post-buckling beam axial and flexural deformations. For the 3-story frame, buckling of the braces, soft-story response and collapse developed at the top level in three of the 10 ground motions. For two other ground motions, collapse was the results of in-plane beam buckling occurring at the first level, over one half of the beam length. No collapse was observed for the remaining five records. All these limit states were expected based on previous LDP assessment; although flexural yielding rather than buckling was anticipated for the beams. Failure modes and global responses also varied depending on the model used as beam inelastic response could not be reproduced in Model B and column buckling could only be simulated in Model D. In this section, examples of time history responses are presented for both frames under one of the most demanding ground motions. The selected responses illustrate cases where beam buckling occurred as this behavior had not been reported or documented in past similar studies. For the 10-story frame, responses obtained from the three models are presented so that the influence of the numerical modeling technique can be examined.

Out of the ten ground motion records, one of the most critical ones (H02: 1994 Northridge earthquake, Beverly Hills - 14145 Mulhol, 009°) was considered for the seismic evaluation of the 10- and 3-story buildings. Responses of the 10-story frame to ground motion no. H02 are presented in Fig. 5.8 for Models B to D. In Fig. 5.8a, all models predicted large story drifts in the first level of the structure under this record. The other plots in the figure therefore focus on the responses computed at this level. With Model B, story drift in level 1 starts increasing at t = 5.26 s as a result of buckling of the RHS brace at that level, as shown in Fig. 5.8b. In that figure, brace capacity in tension as limited by block shear (BS) failure is also indicated. Prior to t = 5.2 s, brace axial loads approached and reached P_{CE} in both braces, inducing large axial compression in the LHS and RHS beam segments at t = 3.9 s and at 4.2 s in Figs. 5.8c & 8d, respectively. However, brace buckling did not occur or was limited as beam moments in Fig. 5.8c remained small and nearly unchanged. At t = 5.2 s, large beam moments developed and beam deflected downward, which led to the large story displacement. In Fig. 5.8b, because of the beam flexibility, tension in the braces barely reached BS capacity and remained well below $T_{CE} = A_g F_{ye}$. In Figs. 5.8c & 8d, beam P_{CL} = 1168 kN is used to evaluate the beam capacity, as determined with KL_x = 9144 mm,

because braces buckled early (at t = 5.2 s) and could not vertically support the beam afterwards. In these figures and Fig. 5.8e, the "P-M ratio" is obtained from Eqs. (9-10) and (9-12), as applicable, in ASCE 41. In Fig. 5.8c, beam axial compression reaches nearly 2.0 P_{CL} at t = 3.9 s, suggesting that beam buckling would happen before beam flexural yielding caused by brace buckling. In Fig. 5.8e, the lower bound axial strength P_{CL} of the RHS column is also exceeded at t = 3.91 s, indicating that column buckling may also occur at about the same time.

Beam yielding and buckling were explicitly modelled in Model C. As expected from the response of Model B, buckling of the LHS beam segment occurred at t = 3.8 s followed by buckling of the RHS segment at t = 4.7 s upon load reversal. In Fig. 5.8b, brace loads in Model C were limited by beam buckling and never reached P_{CE}. In both directions, beam buckling therefore developed over half the beam span because braces were still unbuckled and provided positive vertical support at beam mid-span. Axial loads and moments in beams at the two beam buckling occurrences from Model C are illustrated in Fig. 5.4. As shown, beam compression loads reached values close to P_{CL} at buckling and moments were still small compared to the anticipated moment from expected brace unbalanced loads. Substantial story drift at level 1 in Model C started to develop towards the left (negative) after buckling of the beam RHS segment. At t = 6.5 s, story drift increased further in that direction to eventually lead to structure collapse when story shear acting in the same direction in a subsequent loading cycle worsened buckling of the RHS beam segment. Collapse of the frame took place without brace buckling nor block shear failure in brace connections. As shown in Fig. 5.8e, column axial load demands reduced and remained close to P_{CL} due to beam buckling; however, the columns sustained large bending moments as a result of the large story drift, which could affect their stability.

Column inelastic buckling was considered in Model D. During the analysis with this model, buckling of the RHS column initiated at t = 4.0 s, soon after buckling of the LHS beam segment at t = 3.8 s, but column buckling was interrupted because of load reversal. In the subsequent axial compression excursion, complete column buckling of the RHS column occurred at 5.4 s, which triggered the second buckling occurrence of the RHS beam segment and structure collapse earlier than in Model C. Again, brace buckling did not occur in that analysis and large story drift leading to collapse would be expected to occur due to beam and column buckling prior to failure in brace connections.

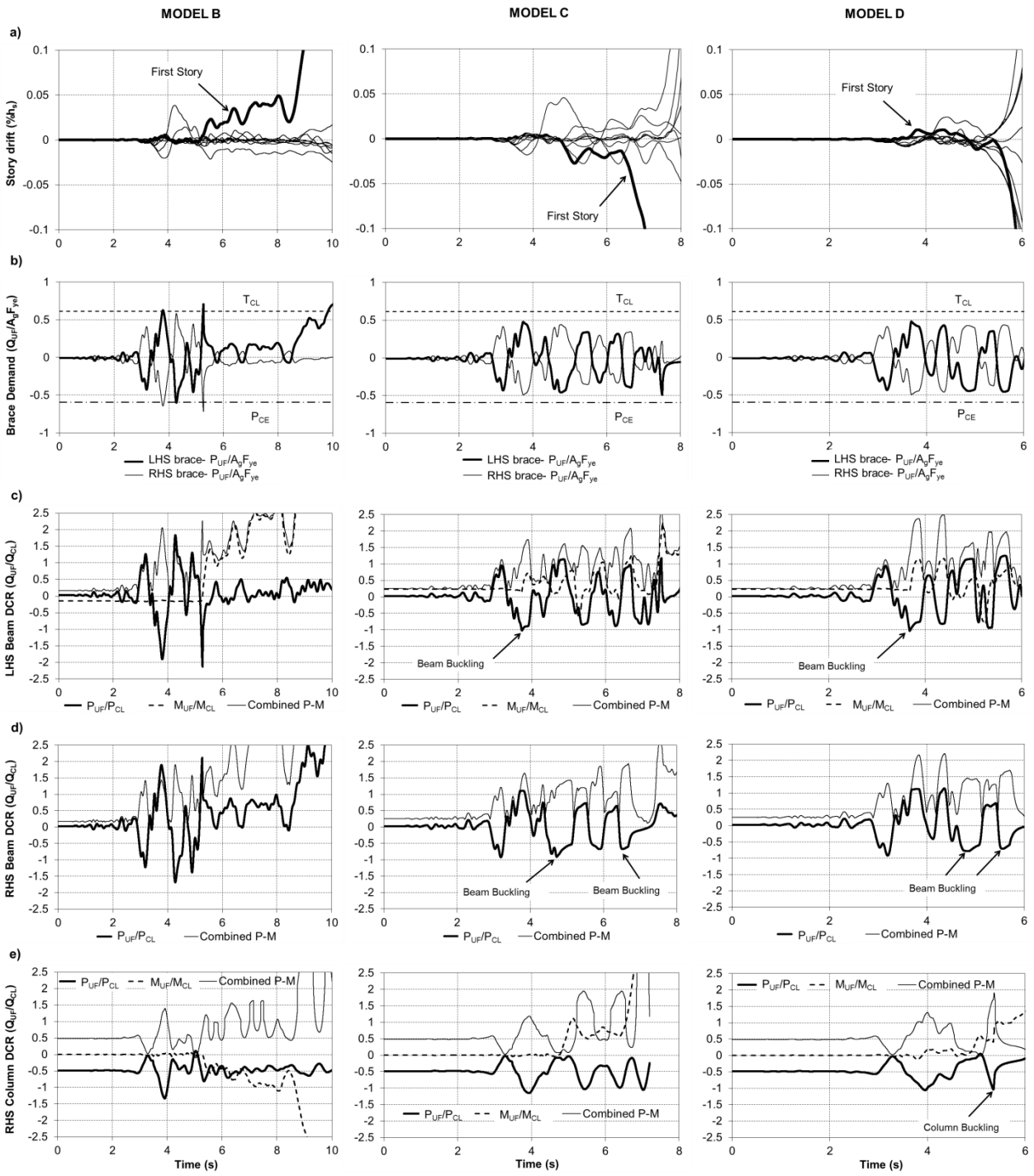

Figure 5.8. Response time history results for the 10-story frame under GM no. H02 from Models B, C, and D: a) Story drifts; b) Brace axial force demands at level 1; c) Axial and flexural demands in the LHS segment of the beam at level 1; d) Axial and flexural demands in the RHS segment of the beam at level 1; and e) Axial and flexural demands in the RHS column at level 1.

Figure 5.9 shows the same time history results from the analysis of the 3-story frame under the same ground motion and using the most comprehensive Model D. For this frame, brace buckling occurred early in level 3 and, then, level 2, which resulted in large drifts in these two stories. In Fig. 5.9a, brace buckling at the third level induced large bending demand on the roof beam. As in the 10-story frame, brace buckling was not observed in the first story but soft-story response developed in that level as a result of buckling of the beam RHS segment at t = 6.4 s. Again, as shown in Fig. 5.9c, beam buckling occurred while the flexural demand on the beam was insignificant. High flexural demand was induced in the RHS column as a result of the large story drift caused by beam buckling. However, the column did not buckle immediately because the axial load demand remained small (below 0.5 P_{CL}) due to the limited contribution from the buckled braces in levels 2 and 3. Instead, ductile column flexural yielding developed at the beam level, as predicted by ASCE 41 for components subjected to flexure and low axial load demand. In the figure, results are plotted until t = 8 s when drifts became excessive. As was the case for the 10-story frame, it is expected that seismic performance of that 3-story frame would not be influenced by failures of brace connections.

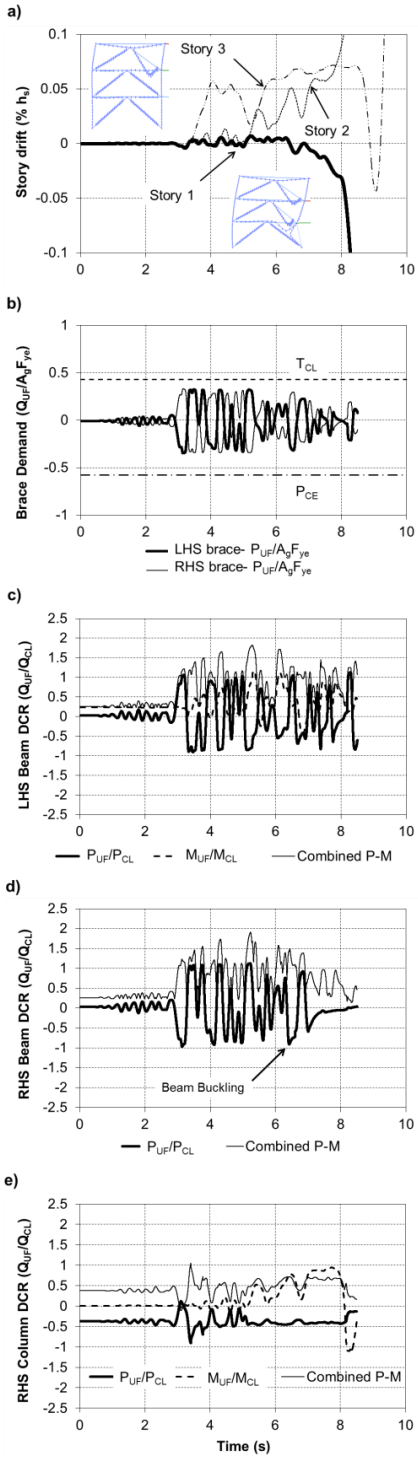

Figure 5.9. Response time history results from Model D for 3-story frame under GM no. H02 a) Story drifts; b) Brace axial force demands at level 1; c) Axial and flexural demands in the LHS beam segment at level 1; d) Axial and flexural demands in the RHS beam segment at level 1; and e) Axial and flexural demands in the RHS column at level 1.

5.5.2.4 Evaluation for lower hazard levels

Nonlinear dynamic analysis of the frames was repeated with Model D and ground motions scaled against the spectra for 5% and 10% probabilities of exceedance in 50 years in Fig. 5.2 to verify if the deficiencies would remain the same under reduced seismic demands as permitted when using ASCE 41 in the U.S. or NBCC for initial evaluation in Canada. As mentioned, 5% probability of exceedance is used to verify collapse prevention performance of the BPOE for existing structures in the U.S. and 60% of the NBCC seismic loads lies between the spectra for the two probability levels. For both lower hazard levels, collapse occurred under 8 and 3 ground motions, respectively, for the 10- and 3-story buildings. The failure modes causing collapse are same as those observed for a probability of exceedance of 2% in 50 years, i.e., soft-story due to beam buckling or brace buckling for both frames, and column buckling for the 10-story frame, indicating that these limit states could still trigger seismic retrofit under reduced seismic demand.

5.5.2.5 Discussion

When compared to NBCC and ASCE 41 LDP evaluations for the 10-story frame, NDP with Model B indicated excessive brace demand at the top and base of the structure. Model B confirmed that the force demands on the beams would exceed their capacities; it also showed that the high flexibility of the beams was sufficient to trigger soft-story response and collapse. NDP with Models C and D revealed that the beam could fail by in-plane buckling over half the frame width and ductile flexural yielding. In both cases, the beam response led to frame collapse. Model D also confirmed the need to strengthen columns in the lower levels as predicted by the NBCC and ASCE 41 LDP.

In Models C and D, beam buckling in torsion and about weak axis was fully prevented. In reality, the beam bottom flange is free to move laterally and out-of-plane forces may develop at the brace-to-beam connections, which may affect beam stability. Beam stability is examined further in the next section using three-dimensional finite element modeling. It was also noted that beam buckling and flexural yielding reduced the force demands on braces, brace connections, and columns. Since the beams will need to be strengthened, higher demands will be imposed to adjacent frame components and a complete, more realistic evaluation of these components should include nonlinear dynamic analyses of frames with retrofitted beams. This analysis is presented for the 10-story frame in the last section of the article.

5.6 Three-Dimensional Finite Element Analysis of Beam Buckling Response

A three-dimensional finite element analysis was performed to further validate the beam buckling response as observed in the OpenSees nonlinear dynamic analyses. As shown in Fig. 5.10a, the model included the beams, braces and gusset plates at the 1st and 2nd levels of the 10-story frame. Four-node shell elements with reduced numerical integration of the stiffness matrix were used for all components. The geometry of the braced bay, material properties, initial imperfections and residual stresses were same as in the OpenSees model. Pinned beam-to-column connections were also used as in the OpenSees model. Geometric nonlinearities (large deformations) were considered in the analyses.

Gravity loads were first applied to the beam at the 1st level. The lateral displacement time histories at mid-span of the 1st and 2nd level beams were then applied, together with the time histories of the vertical displacements at beam-to-column joints at both levels, as obtained from the OpenSees nonlinear seismic analysis with Model D illustrated in Fig. 5.8. Lateral displacements were applied at gusset plate-to-beam connections. To investigate the impact of the concrete slab and the effect of lateral bracing on the beam response, two models were used: (i) a model where the lateral movement of the beam was restrained (LR); and (ii) a model where both the lateral movement and torsion of the beam were restrained (LTR). These restraints were applied at the beam top flange only.

Responses of the LHS and RHS braces from the OpenSees and ABAQUS (Dassault 2012) models are compared in Fig. 5.10b. In the two plots, the P_{CE} value of the braces was calculated using the net length of the braces considering the size of brace connections and an effective length factor of 1.0. In the ABAQUS model, the braces were shorter and exhibited higher stiffness and generally attracted higher axial loads compared to those in the OpenSees model. Their buckling resistance was also higher and all braces remained elastic, even if P_{CE} was slightly exceeded, as was the case in the OpenSees analysis. Beam buckling in the ABAQUS analysis occurred approximately at the same times and following the same sequence as in the OpenSees analysis, as shown in Fig. 5.11a. The buckled shapes in the plane of the frame are also very similar. The deformed shapes from ABAQUS in Fig. 5.11a are those obtained from Model LR and include some torsional deformations of the beam, which could not be predicted by the OpenSees model. The cross-section views in the figure show that the beam top flange is laterally restrained but the bottom flange moved laterally. Torsional deformations are less pronounced in

ABAQUS Model LTR. Axial load responses in the LHS and RHS beam segments from OpenSees and both ABAQUS analyses are compared in Fig. 5.11b. As expected, all three analyses yield same beam axial resistances until the first occurrence of buckling at t = 3.8 s. In the post-buckling range, beam strengths from OpenSees are higher as local buckling is not considered in that model. However, the errors are generally small. As also anticipated, Model LTR results in higher beam resistance compared to Model LR because of the additional restraint but the differences are small. From this study, it can then be concluded that OpenSees fiber based models can be used to predict occurrence of beam buckling and provide a reasonable estimate of beam post-buckling response.

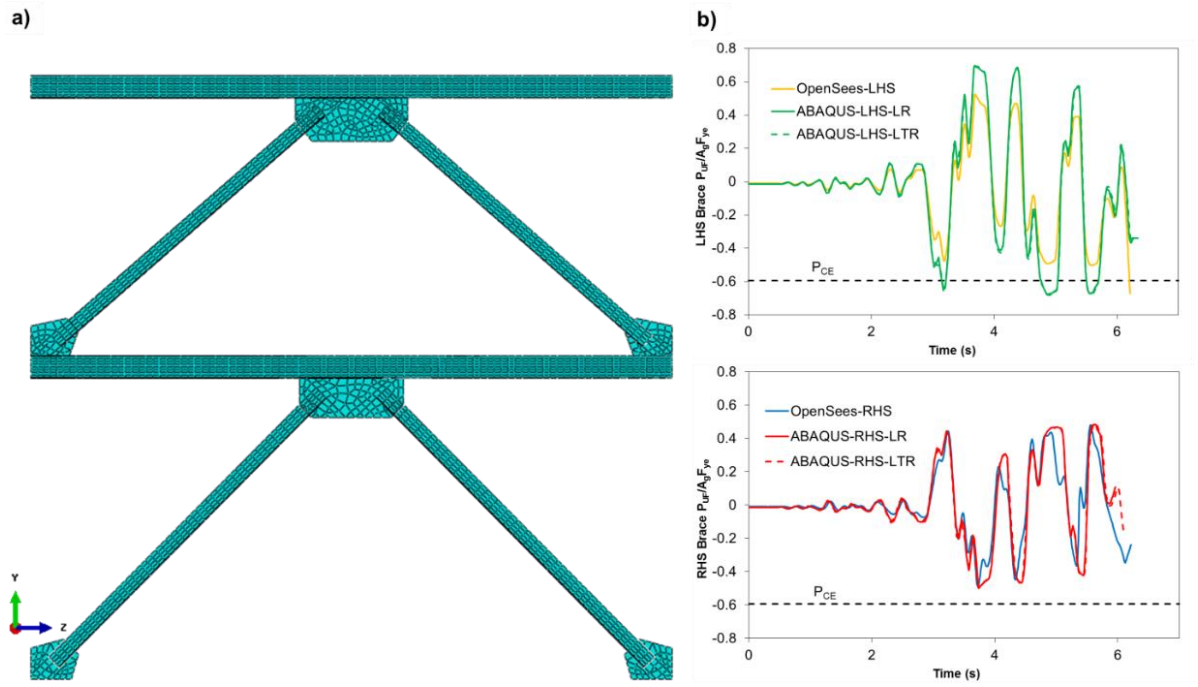

Figure 5.10. a) Finite element modelling of the 2-story chevron braced frame sub-assembly; b) Responses of the LHS and RHS braces from OpenSees and ABAQUS (LR = Lateral displacement of beam top flange restrained; LTR = Lateral displacement and torsion of beam top flange restrained).

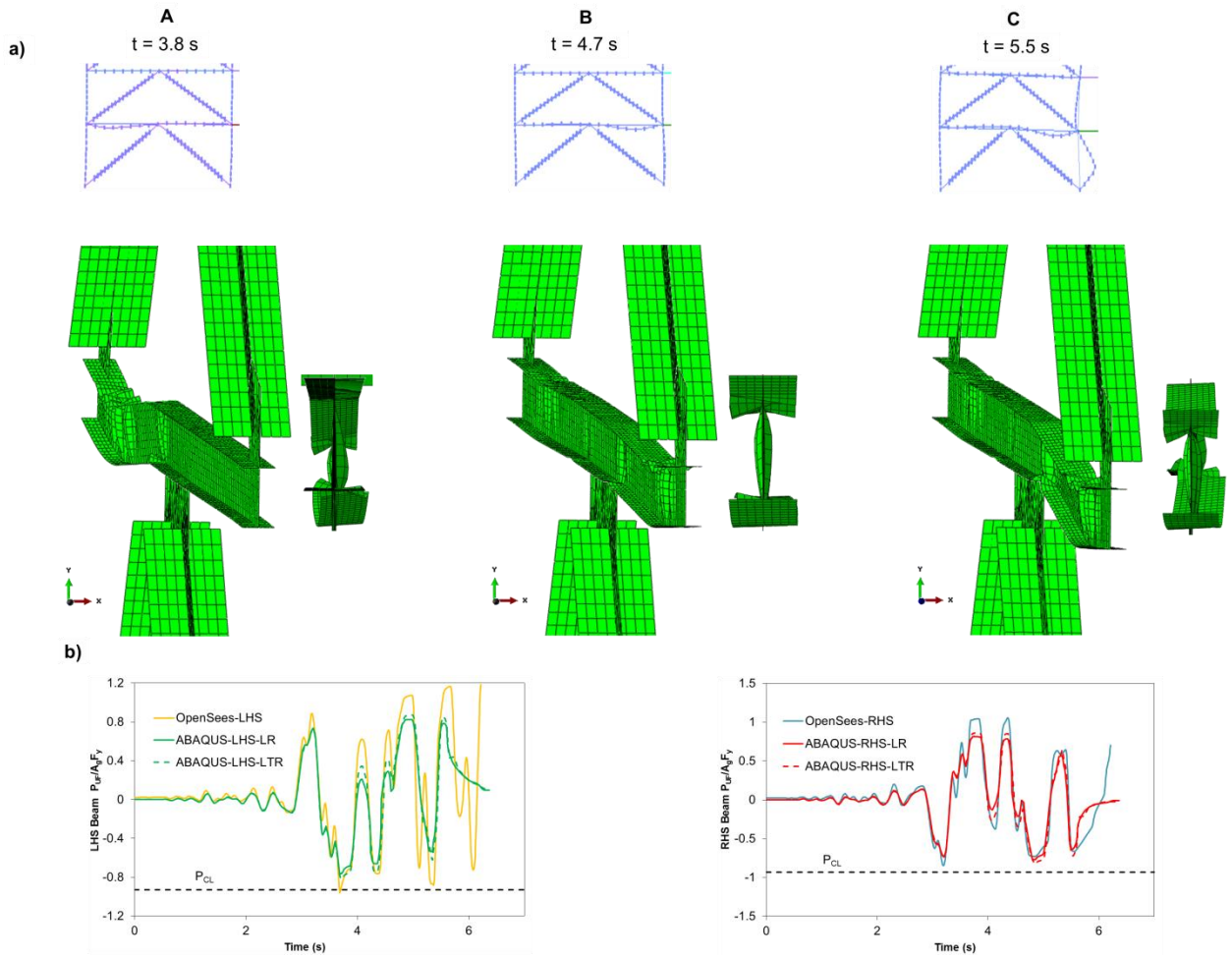

Figure 5.11. a) Evolution of beam buckling deformed shapes from OpenSees and ABAQUS; and b) Comparison of LHS and RHS beam buckling response in OpenSees and ABAQUS (LR = Lateral displacement of beam top flange restrained; LTR = Lateral displacement and torsion of beam top flange restrained).

5.7 ASCE 41 NDP Evaluation of the 10-story Frame with Retrofitted Beams

In this section, beams in the 10-story braced frame are retrofitted to satisfy the acceptance criteria given by Eq. 9 such that more realistic seismic demand can be obtained for the other components. The following beam sizes were selected to comply with Eq. 9: W840x576 for the 1st to 5th levels, W840x433 for the 6th to 9th stories and W840x299 at the roof level. Since columns of this partially strengthened structure would likely be still deficient, Model D was not a good candidate to obtain the required information as the analyses could be terminated early in ground motions due to non-convergence upon column buckling. Instead, Model B with elastic beams and

columns was selected for a first evaluation as it would generate upper bound estimates of the demand imposed on braces, their connections, and columns. A second series of analyses was then performed using Model D to verify the possibility of column buckling.

In Fig. 5.6b, ASCE 41 evaluation using LDP predicted satisfactory response for all bracing members of the 10-story frame. However, nonlinear dynamic analysis in section "Nonlinear Dynamic Procedure" indicated that brace inelastic response could concentrate in a few stories, which could lead to excessive brace ductility demand, large story drifts and, possibly, structural collapse. Nonlinear dynamic analysis with Model B did not reveal any structural collapse but inelastic brace deformations concentrated in the first and ninth levels, which resulted in large story drift demands. NDP evaluation results for the braces from Model B are presented in Fig. 5.12a. Plotted values represent the mean peak inelastic brace axial deformations from analysis normalized to the respective brace plastic deformation capacities. As was the case for the *m* factor in LDP, plastic deformation capacities in ASCE 41-13 vary with brace slenderness, brace cross-section compactness, and brace connection capacities. For the braces in their existing conditions, capacities ranged between 6.4 and 8.0 times Δ_C in compression, and was equal to 9.6 Δ_T in tension (Δ_C and Δ_T are brace axial deformations under loads P_{CE} and T_{CE}, respectively). As shown, braces in compression at levels 1, 9, and 10 need to be retrofitted while little or no plastic demand was observed at levels 2 to 5. This frame was prone to drift concentration at the base because the same brace cross-section was originally selected in the bottom five levels (Fig. 5.1) and the braces in the first level had relatively lower compressive resistance due to their greater length. This is also illustrated in Fig. 5.12b which compares frame story shear strengths V_{CE} and V'_{CE} reflecting the conditions before and after brace buckling to story shears V_E from RSA, where:

[10] $V_{CE} = 2\ P_{CE}\ cos\theta$

[11] $V'_{CE} = (0.3P_{CE} + T_{CE})\ cos\theta$

In these expressions, P_{CE} and T_{CE} are the brace expected strengths and θ is the brace inclination. As shown, capacity and demand profiles are quite different, and *DCR*s are larger at levels 1 and 9 compared to other levels. In the bottom levels, post-buckling strength V'_{CE} is also less than V_{CE}, another condition that can promote damage concentration. In Fig. 5.6a, braces at the 9th level also have relatively higher *DCR* compared to adjacent stories, which also has potential for soft-story response.

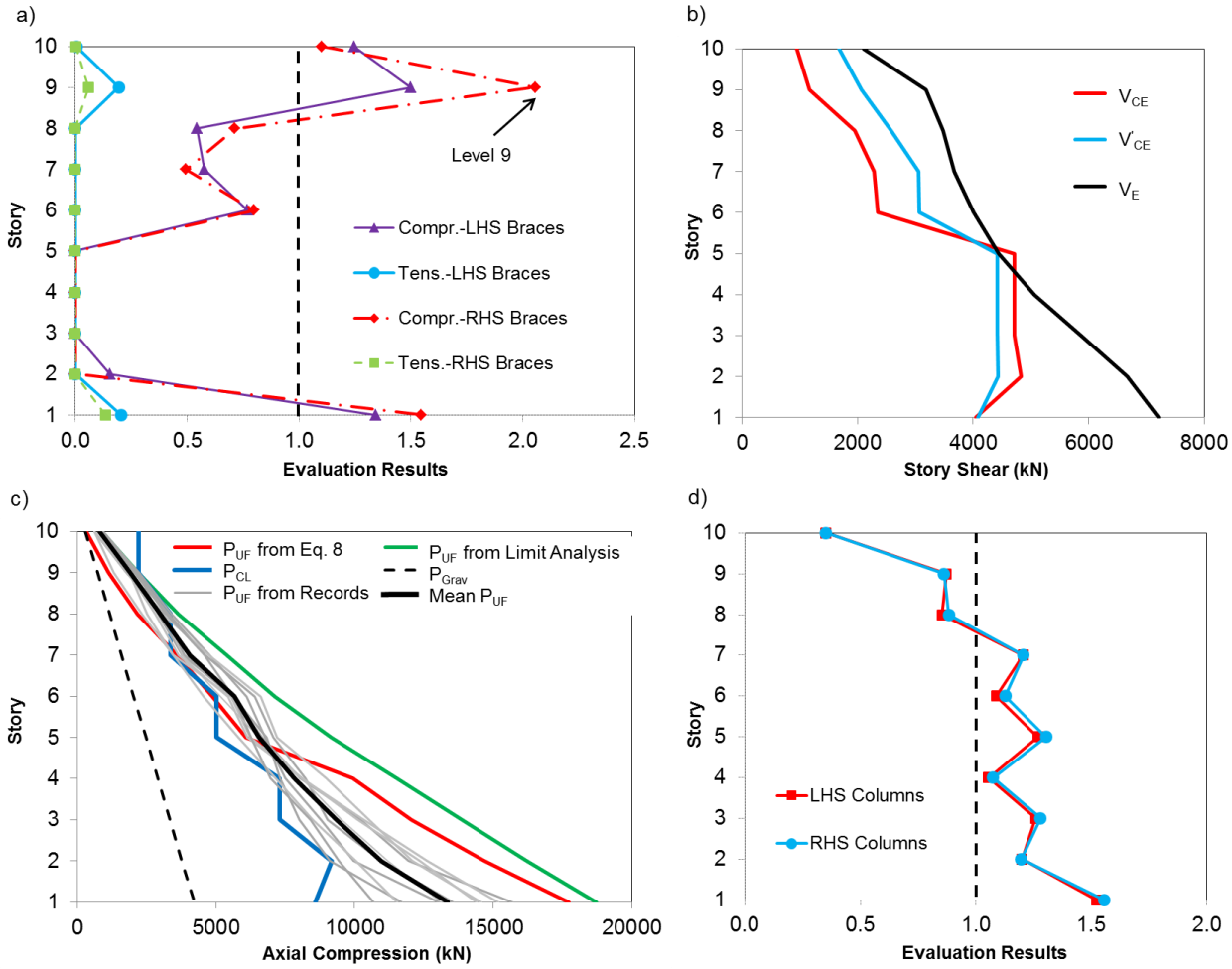

Figure 5.12. Evaluation of the 10-story frame with retrofitted beams using Model B: a) ASCE 41 NDP evaluation of the braces; b) Story shear demand and capacities from the braces; c) Axial force demands on the columns; and d) LDP evaluation of the columns.

Axial compression demand P_{UF} from Model B analyses is compared to column capacity P_{CL} in Fig. 5.12c. As shown, mean demand exceeds the column strength in all levels except in level 8 to 10, comparable to the evaluation from LDP in Fig. 5.6c. Predictions of P_{UF} from Eq. 8 with the J factor and from a limit analysis using the loading condition for beams of chevron braced frames are also plotted for comparison. As was observed in LDP, the former underestimates the column force demand whereas limit analysis provides a conservative force estimate. In Fig. 5.12d, LDP evaluation of LHS and RHS columns shows that the columns at the 1st to 7th levels have insufficient strength, and the most critical column is located at the 1st story, two conclusions that

are comparable to those from ASCE 41 linear assessment in Fig. 5.6c and 100% NBCC 2010 evaluation in Fig. 5.5c.

Figure 5.13 shows time history response of the frame from Model B under the ground motion considered in Figs. 5.8 and 5.9. In this case, significant drift reaching approximately 6% developed in the first level (Fig. 5.13a). In Fig. 5.13b, axial forces in the braces in the first level reached P_{CE} and T_{CE} and buckling and tension yielding of the two braces occurred which caused the observed large story drift at this level. Significant strain hardening developed in the LHS brace due to the several large yield tension excursions experienced by that brace. Block shear capacity of the connections of both braces was also attained and exceeded several times during the ground motion, meaning that brace connections would need to be strengthened to safely withstand the higher brace force demand resulting from using stiffer and stronger beams. In Figs. 5.13c and 5.13d, the retrofitted beam sustained relatively low axial load demands P_{UF}/P_{CL} due to their much larger sizes but the limit of Eq. 9 was exceeded at several instances due to the high flexural demand resulting from the larger than expected brace unbalanced load imposed by the strain hardened brace in tension. This high demand would probably be reduced if brace inelastic demand was better distributed over the frame height. As shown from Fig. 5.12c, axial compression in the RHS column in the 1st story in Fig. 5.13e exceeds the column axial strength P_{CL}, suggesting that column retrofit would be necessary. As was shown in Fig. 5.8e, Fig. 5.13e shows high flexural demand developing in the column at 8.9 s due to story drift response, which could also contribute to column failure by buckling at this level. Analysis using Model D confirmed the possibility of column buckling for this structure. Out of the 10 analyses, collapse of the frame was observed under seven records as a result of column buckling at the first level. Column buckling at the 5th and 6th levels caused the collapse of the frame for two other ground motions. In the 10th ground motion, the structure did not collapse although column buckling had occurred at the first level.

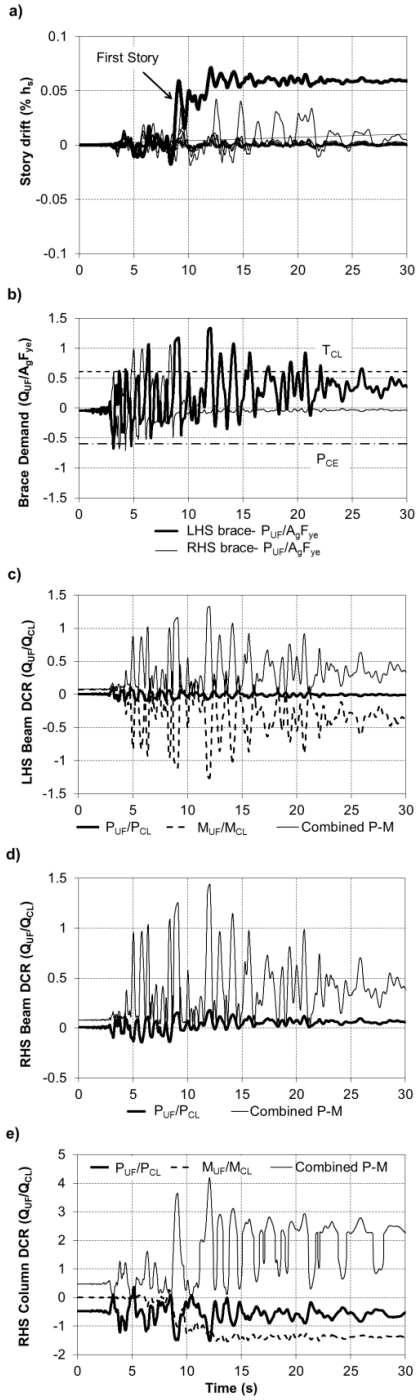

Figure 5.13. Response time history results from Model B for the 10-story frame with retrofitted beams under GM no. H02: a) Story drifts; b) Brace axial force demand at level 1; c) Axial and flexural demands in the LHS segment of the beam at level 1; d) Axial and flexural demands in the RHS segment of the beam at level 1; and e) Axial and flexural demands in the RHS column at level 1.

5.8 Conclusions

The seismic evaluation of 10- and 3-story steel chevron braced frames designed prior to implementation of special seismic design procedures was performed. The structures were originally designed in accordance with the 1980 NBCC for a site class C in Vancouver, British Columbia, Canada. The evaluation was carried out in accordance with NBCC 2010 for a probability of exceedance of 2% in 50 years. The ASCE 41-13 Tier 3 procedure was then applied to examine the possibility of reducing the extent of retrofit. ASCE 41 evaluation was done using both linear (LDP) and nonlinear dynamic analysis procedures (NDP). For NDP, models reproducing nonlinear responses associated to deformation-controlled actions in the bracing members and models accounting for nonlinear response related to force-controlled actions in beams and columns were used. This evaluation permitted to investigate the seismic response of deficient chevron braced frames under MCE level ground motions and validate the application of ASCE 41 for this type of braced frame. The following conclusions can be drawn from this study:

- Evaluation for 60% of NBCC seismic load showed that the two frames need to be retrofitted. For both frames, most braces and brace connections as well as some of the beams have inadequate resistance. Also, most of the columns of the 10-story frame are overloaded. The extent of the retrofit, determined by examining the response of the frames under 100% of NBCC seismic loads, would be extensive as all braces and brace connections and most of the beams should be strengthened for both frames. Most columns of the 10-story frame and columns at the bottom of 3-story building would also be required an upgrade.
- The evaluation using ASCE 41 LDP showed that all braces of both frames would be adequate, which is less stringent than NBCC evaluation. All brace connections and beams would however have inadequate resistance and would need to be strengthened. Most of the columns in the 10-story building and columns at the base of the 3-story frame show insufficient capacities. Evaluation of beams per ASCE 41 is more severe compared to the evaluation under 100% of NBCC loads, because the former explicitly accounts for unbalanced brace load effects anticipated after brace buckling has occurred.
- As was expected from past studies, deficient beams in existing chevron braced frames may detrimentally impact the frame seismic performance. In this study, the braced frames included light beams supporting limited gravity loads. For these beams, strong axis buckling in the vertical

plane occurred prior to brace buckling. This failure mode was confirmed through detailed 3D finite element analysis. Beam ductile flexural yielding was also observed. Both beam buckling and yielding led to frame collapse. In analyses where beams were modeled elastically, significant downward deflection of the beams occurred that led to soft-story response. Brace tension yielding could not develop because of the beam flexibility. This deficiency cannot be identified when verifying the ASCE 41 strength acceptance criteria for beams of chevron braced frames that account for brace buckling and yielding.

- In NDP, failure of beams by buckling was also observed under ground motions with reduced amplitudes scaled to match design spectra corresponding to 5% and 10% in 50 years probabilities of exceedance. Therefore, this deficiency should be considered when performing seismic evaluation under reduced seismic demands as permitted in ASCE 41 in the U.S. or when using 60% of the NBCC seismic loads in Canada.
- Column axial load demands determined from LDP and the force-delivery reduction (J) factor in ASCE 41 were smaller than those obtained from nonlinear time history analysis. For chevron braced frames, column axial loads must also be determined with consideration of the loading scenario corresponding to brace post-buckling conditions as specified for beams and their supporting members in ASCE 41.
- NDP evaluation of the 10-story frame with retrofitted beams showed that the frame was prone to concentration of inelastic brace deformations and large story drifts. This response led to excessive brace plastic deformations as well as large bending moments in the braced frame columns that may contribute to column failure by instability. This behavior could not be predicted from LDP.

5.9 Acknowledgments

The authors gratefully acknowledge the financial support provided by the Natural Sciences and Engineering Research Council of Canada (NSERC) for the Canadian Seismic Research Network (CSRN).

5.10 References

AISC (American Institute of Steel Construction). (2010). “Seismic Provisions for Structural Steel Buildings.” *ANSI/AISC 341-10*, Chicago, IL.

Allen, D. E., Rainer, J.H. and Jablonski, A. M. (1992). “Guidelines for the Seismic Evaluation of Existing Buildings.” Institute for Research in Construction, National Research Council Canada, NRCC 36941.

ASCE (American Society of Civil Engineers). (2013). “Seismic evaluation and rehabilitation of existing buildings.” *ASCE/SEI 41-13*, Reston, VA.

Atkinson, G.M. (2009). “Earthquake time histories compatible with the 2005 national building code of Canada uniform hazard spectrum.” *Canadian Journal of Civil Engineering*, 36(6), 991-1000.

Balazadeh-Minouei, Y., Koboevic, S., and Tremblay, R. (2017). “Seismic evaluation of a steel braced frame using NBCC and ASCE 41.” *Journal of Constructional Steel Research*, http://dx.doi.org/10.1016/j.jcsr.2017.03.017.

CSA (Canadian Standards Association). (1978). “Limit states design of steel structures.” *CAN3 S16.1-M78*, Toronto, ON.

CSA (Canadian Standards Association). (1989). “Limit states design of steel structures.” *CANJCSA-S16.1-M89*, Rexdale, ON.

CSA (Canadian Standards Association). (2009). “Design of Steel Structures.” *CSA-S16-09*, Toronto, ON.

Dassault. (2012). “Dassault Systemes Simulia Corp.” *ABAQUS-FEA/CAE*, RI, USA.

Harris III, J.L., and Speicher, M.S. (2015). “Assessment of First Generation Performance-Based Seismic Design Methods for New Steel Buildings; Volume 2: Special Concentrically Braced Frames, NIST Technical Note 1863-2.” *National Institute of Standards and Technology*, Gaithersburg, MD.

Hsiao, P. C., Lehman, D. E., Berman, J. W., Roeder, C. W., and Powell, J.(2014). “Seismic vulnerability of older braced frames.” J. Perform. Constr. Facil., 10.1061/(ASCE)CF.1943-5509.0000394, 108–120.

ICBO (1979, 1988) Uniform Building Code 1979, 1988. “International Conference of Building Officials (ICBO)”, Long Beach, California.

Jiang, Y., Balazadeh-Minouei, Y., Tremblay, R., Koboevic, S., and Tirca, L. (2012). "Seismic assessment of existing steel braced frames designed in accordance with the 1980 Canadian code provisions." In Behaviour of Steel Structures in Seismic Area: *Proc., 7th Int. Conf., STESSA 2012*, Santiago, Chile, 531-537.

Khatib, I.F.. Mahin, S.A., and Pister, K.S., (1988). "Seismic behavior of concentrically braced steel frames." Report UCB/EERC-88/01. *Earthquake Engineering Research Center*, University of California, Berkeley, CA.

Lamarche, C., and Tremblay, R. (2011). "Seismically induced cyclic buckling of steel columns including residual-stress and strain-rate effects." *Journal of Constructional Steel Research*, 67(9), 1401-1410.

McKenna, F. and Fenves, G.L. (2004). "Open System for Earthquake Engineering Simulation (OpenSees)." *Pacific Earthquake Engineering Research Center (PEER)*, University of California, Berkeley, CA. (http://opensees.berkeley.edu/index.html)

Mitchell, D., Paultre, P., Tinawi, R., Saatcioglu, M., Tremblay, R., Elwood, K., Adams, J., and DeVall, R. (2010). "Evolution of seismic design codes in Canada." *Canadian Journal of Civil Engineering*, 37(9), 1157-1170.

NRCC (National Research Council of Canada). (2010). (1980). "National building code of Canada 2010, 13th ed., 1980, 8th ed." Ottawa, ON.

Roeder, C.W., Lumpkin, E.J., and Lehman, D.E. (2012). "Seismic performance assessment of concentrically braced steel frames." *Earthquake Spectra, Earthquake Engineering Research Institute*, 28(2),709-727.

Sen, A.D., Roeder, C.W., Berman, J.W., Lehman, D.E., Li, C-H., Wu, A-C. and Tsai, K-C. (2016). "Experimental Investigation of Chevron Concentrically Braced Frames with Yielding Beams." Journal of Structural Engineering." *ASCE*., http://dx.doi.org/10.1061/(ASCE)ST.1943-541X.0001597.

Sloat, D. A. (2014). "Evaluation and Retrofit of Non-Capacity Designed Braced Frames." M.Sc. thesis, Univ. of Washington, Seattle.

Speicher, M.S., and Harris III, J.L., (2016). "Collapse prevention seismic performance assessment of new special concentrically braced frames using ASCE 41." *Engineering Structures*, 126 (2016), 652-666.

CHAPTER 6 ARTICLE 3: SEISMIC RETROFIT OF AN EXISTING 10-STORY CHEVRON BRACED STEEL FRAME

Yasaman Balazadeh-Minouei[1], Robert Tremblay[2] and Sanda Koboevic[3]

[1]Ph.D. Candidate, Dept. of Civil, Geological and Mining Engineering, Polytechnique Montreal, Montreal, QC, Canada H3C 3A7 (Corresponding author). Email: yasaman.balazadeh-minouei@polymtl.ca

[2]Professor, Dept. of Civil, Geological and Mining Engineering, Polytechnique Montreal, Montreal, QC, Canada H3C 3A7.

[3]Assistant Professor, Dept. of Civil, Geological and Mining Engineering, Polytechnique Montreal, Montreal, QC, Canada H3C 3A7.

Submitted to the *Journal of Structural Engineering, ASCE.*

Abstract

A seismically deficient 10-story chevron braced frame located on the west coast of Canada is retrofitted using different schemes. The building was designed in accordance with the Canadian codes applicable in the mid-1980s, prior to the implementation of the special seismic design provisions in the steel design standard. The ASCE 41 nonlinear dynamic procedure (NLP) was used to develop and validate the retrofit schemes. The performance objective was collapse prevention under seismic hazard with probability of exceedance of 2% in 50 years. Three retrofit solutions developed to satisfy the ASCE 41 component based criteria and achieve uniform demand to capacity ratios over the structure height exhibited inadequate global inelastic seismic response characterized by soft-story mechanisms and structural collapse. The same behavior was observed after having increased the lateral strength of the system by 80%, clearly indicating that ASCE 41 should include acceptance criteria aimed at verifying overall seismic response. Story drift concentration and structural collapse could be avoided by combining the retrofitted braced frame with a moment frame or an elastic vertical truss installed from outside along the perimeter walls. A vertical truss with a flexural hinge at mid-height was found to be the most cost-effective option. The exterior frames can serve as temporary lateral system during the repair of the existing braced frame.

Key words: Chevron Braced Frame, Seismic Evaluation, Seismic Retrofit, Elastic Truss, Nonlinear Time History Analysis.

6.1 Introduction

The seismic performance of a non-ductile 10-story chevron braced steel frame was evaluated by Balazadeh-Minouei et al. (2017a). The frame is illustrated in Fig. 6.1a. It was designed in accordance with Canadian codes applicable in the mid-1980's, prior to the implementation of the special seismic design provisions in the CSA S16 steel design standard (CSA 2009), for a class C site in Vancouver, British Columbia. The seismic loads and design requirements considered are comparable to those specified in UBC 1979 for chevron braced frames located in seismic zone 2 (ICBO 1979) and the findings presented herein may also apply to non-ductile chevron braced frames located in northwestern U.S. The seismic evaluation performed in accordance with the 2010 National Building Code of Canada (NBCC) (NRCC 2010) revealed several deficiencies that would trigger a seismic retrofit of the structure. In NBCC, seismic retrofit is preferably designed to achieve the performance level required for new constructions, i.e. collapse prevention under a seismic demand established for a probability of exceedance of 2% in 50 years. As an alternative to reduce retrofit costs, Balazadeh-Minouei et al. used the procedure of ASCE 41-13 standard (ASCE 2013) to identify the components that would require retrofit to achieve the target performance objective. Both the linear and nonlinear dynamic procedures (LDP and NDP) were applied. LDP showed that all braces were adequate; however, brace connections and beams at all levels and most of the columns would need to be strengthened. The beams were not initially designed for the expected brace unbalanced vertical loads. NDP using a frame model with elastic beams and columns revealed structural collapse due to soft-story response caused by the large flexibility of the beams. NDP with a model in which inelastic response of the beams was included showed that the beams either yielded in flexure or buckled in compression. Beam buckling occurred in the vertical plane over half the beam length and both beam failure modes resulted in soft-story response and frame collapse. Beam yielding and buckling was also observed under seismic ground motions scaled for lower seismic hazard with 5% and 10% probabilities of exceedance in 50 years. Nonlinear dynamic analyses were also performed using frame models in which the beams were strengthened to meet ASCE 41 acceptance criteria to allow the verification of the inelastic response of the braces and columns. These analyses revealed that braces at the

base and in top stories did not have sufficient plastic deformation capacities. When column inelastic response was included, column buckling occurred which led to frame collapse.

This article presents possible seismic retrofit solutions for this structure. Options were reported in past studies on deficient chevron braced frames. Rai and Goel (2003) proposed to extend the fracture life of the bracing members by using concrete-filled HSS braces and replace the chevron bracing configuration by a 2-story X to reduce the demand from the braces on the beams. From quasi-static cyclic testing on a 2-story non-ductile chevron braced frames, Sen et al. (2016) concluded that inadequate brace compactness and brace connection details should be addressed to prevent early fractures. The tests also revealed that flexural yielding of beams having insufficient strength to resist unbalanced brace loads could provide energy dissipation and did not impair the system ductility. Sen et al. (2017) experimentally validated several retrofit schemes including delaying of local buckling of HSS braces through brace replacement or concrete fill, and improving brace connection strength and deformation capacities. Alternative strategies to improve the global response have been proposed such as vertically tying together all beams of chevron braced frames at their mid-spans such that braces and beams at all floors are mobilized and soft-story response is mitigated (Khatib et al. 1988). The efficiency of this zipper system can be enhanced by anchoring the vertical ties to a stiff hat truss at the roof level (Yang et al. 2008). Forming a dual system by coupling concentrically steel braced frames and moment frames has been shown to improve the collapse prevention resulting from large story drift and brace fracture (Foutch et al. 1987, Whittaker et al. 1990). Other studies showed that drift concentration in new and existing steel braced frames can be prevented by adding a stiff elastic vertical truss, also referred to as a mast, spine or strongback (Martini et al. 1990, Tremblay 2003, Merzouq and Tremblay 2006, Lai and Mahin 2015, Qu et al. 2014, Pollino et al. 2017). Alternatively, techniques such as base isolation to reduce the seismic force demand on the existing frame members (e.g. Erduran et al. 2011) or addition of passive energy dissipation devices to control drifts (e.g., Symans et al. 2008, Sorace and Terenzi 2008) can be used to achieve enhanced braced frame response. Allowing the frame rocking is another approach for reducing the force demand on deficient steel braced frames (Mottier et al. 2017).

In this study, it was assumed that the existing chevron braced frame configuration had to be kept to meet architectural constraints and maintain current usage of the floor area in the building, eliminating the possibility of using 2-story X configuration, zipper systems or other similar more

effective structural systems. However, the use of dual systems with moment frames and/or vertical elastic trusses erected from outside of the building along the perimeter walls remained an acceptable option. All retrofit solutions were developed using the ASCE 41-13 procedure. Considering that all past studies had already proposed retrofit solutions at the components level, this study focused on proposing retrofit solutions that can exhibit proper global inelastic seismic response. In the first three solutions the beams were replaced to meet ASCE 41 acceptance criteria. Special consideration was also given to achieve uniform demand to capacity ratios (DCR) over the frame height to minimize concentration of inelastic demand, and the difference between the three retrofits resides in the parameter that was used to evaluate the target DCR. In these frames, the braces were also replaced with more effective circular HSS members to minimize the force demand on beams and columns although their response was found adequate as per ASCE 41. This led to minimum beam sizes and eliminated the need to reinforce the existing columns. Nonlinear dynamic analysis revealed story drift concentrations and structural collapse for these three retrofitted frames.

A fourth retrofit solution was designed using the same approach except that lateral strength of the system was increased by 80% as an attempt to prevent the undesirable response. That strength level was selected such that the existing braced frame columns and foundations could be kept without strengthening. This scheme did not result in acceptable global seismic response and thus two alternative dual framing systems were examined: one with moment frames and one with elastic vertical trusses, both placed along the exterior walls. The last, stronger braced frame retrofit was kept for these dual systems. For each system, the external frame would be placed on the building perimeter to limit disturbance on building usage and would serve as temporary lateral system during the retrofit of the existing braced frames. Both dual solutions were found to perform well and this motivated the examination of a last, simpler retrofit that consisted in adding a vertical elastic truss to the existing braced frames. For this structure, this solution would require minor strengthening of the members but would probably represent the most attractive retrofit approach.

The article describes the design and validation of each of the retrofit strategies that have been examined. The first section presents a brief description of the existing structure and summarizes the findings of the seismic evaluation initially performed by Balazadeh-Minouei et al. (2017a). Prior to presenting the different retrofit strategies, the redesign of the braced frame using current

Canadian code provisions for new constructions is introduced. That design was performed to assess the feasibility of this possible option for retrofit and obtain a reference basis that can be used to assess the effectiveness of the studied retrofit schemes. Details of retrofit strategies are then given. The required steel tonnage and force demands on the foundations for each retrofit solution are presented and discussed. The global seismic response for each retrofit is then investigated using detailed nonlinear dynamic analysis. It is noted that the retrofit solutions as described in the article are still preliminary and are presented to illustrate the concepts and identify possible advantages and shortcomings. In particular, the dual system solutions should be refined further to fully exploit the potential of the schemes and it is understood that additional design and construction constraints not considered in this study will likely impact the final retrofit designs.

6.2 Existing Building

Description of the structure

The structure plan view is shown in Fig. 6.1a. The building is an office building of the normal importance category situated on a class C site in Vancouver, British Columbia. In the E-W direction, lateral resistance is provided by the two chevron braced frames examined in this study. The building design followed the 1980 NBCC (NRCC 1980) and the CSA-S16.1-M78 (CSA 1978) steel design standard. The factored design base shear was 2253 kN per frame, corresponding to 2.5% of the seismic weight. The bracing members were back-to-back double angle sections whereas beams and columns were W shapes. All steel members were made from CSA-G40.21-300W steel (F_y = 300 MPa, F_u = 450 MPa), as was the practice. All connections were field bolted and beam-to-column joints were made with pairs of angles that were assumed to behave as pinned connections. Additional detail can be found in Balazadeh-Minouei et al. (2017a).

In Fig. 6.1a, it is noted that all braces in the first five stories are same due to the limited choice from available sections. The impact of this brace selection on the vertical distribution of the frame lateral resistance can be examined by looking at the frame expected story shear strengths V_{CE} corresponding to the compression braces reach their expected compressive strength (P_{CE}) and

V'_{CE} when the braces reach their expected tensile and post-buckling compressive strengths (T_{CE} and 0.3 P_{CE}), as defined in ASCE 41-13:

[1] $V_{CE} = 2P_{CE}\cos\theta$

[2] $V'_{CE} = \left(T_{CE} + 0.3P_{CE}\right)\cos\theta$

Values of P_{CE} and T_{CE} are determined using the expected yield strength F_{ye} = 330 MPa and θ is the brace inclination. As shown in Fig. 6.2, the computed V_{CE} and V'_{CE} do not exhibit smooth variations along the frame heights with relatively smaller values at the first level due to the taller story height, a constant value in levels 2 to 5, and a steep drop at level 6 followed by gradual reduction towards the roof level. This is a situation with strong potential for story drift concentration at levels 1 and 6 of the frame.

NDP evaluation

NDP evaluation results are summarized herein as they give a better insight of the structure deficiencies that need to be addressed in the structure retrofit. As discussed, the focus is on the system response and evaluation of brace connections is not discussed herein. The evaluation was performed with the OpenSees program (McKenna et al. 2004) using detailed models of the frame that accounted for geometric nonlinearities and inelastic response of the braces, beams, and columns. Models in which beams and columns were kept elastic were also used to isolate limit states in specific members. In addition to the braced frame, the models included a leaning column to include global P-delta effects. All columns were pinned at their bases and pinned connections were specified at column splices and beam-to-column joints. The models were subjected to an ensemble of 10 compatible historical ground motion time histories scaled with respect to the design spectrum of NBCC 2010 for 2% in 50 years probability of exceedance. Additional details are available in Balazadeh-Minouei et al. (2017a).

With a model using elastic beams and column elements, braces could not reach their expected tensile strengths under any of the ground motions due to the high flexibility of the beams. Large story drifts developed in the structure that led to collapse. This behavior is illustrated in Fig. 6.3a

under ground motion no. H02. Flexural buckling of the beams about strong axis was observed when using a model that included inelastic beam elements and elastic columns, as shown in Fig. 6.3b. In their study, Balazadeh-Minouei et al. (2017a) verified this limit state using detailed three-dimensional analysis. The OpenSees model with inelastic beams also revealed beam flexural yielding. Beam buckling and yielding resulted in large story drifts and structural collapse. These two limit states were also observed in models in which nonlinear response was assigned to all members. Beam flexural yielding with this model under ground motion (GM) no. H12 is illustrated in Fig. 6.3c. As seen in the same figure, column buckling was also observed with this model under GM no. H02.

In their study, Balazadeh-Minouei et al. also evaluated the response of the frame using a model in which the beams had been retrofitted to satisfy ASCE 41-13 criteria for beams of chevron braced frames. In ASCE 41, beams, their connections and supporting members in chevron braced frames must resist axial compression P_{UF} and moments M_{UF} resulting from unbalanced brace load effects in combination with gravity loads considered as forced-controlled actions. Unbalanced brace loads correspond to the expected yield strength (T_{CE}) for the brace in tension and 30% of the expected compression capacity of the brace in compression (0.3 P_{CE}). For the retrofit, the beams must then be satisfied the interaction equation:

$$[3]\ \frac{P_{UF}}{\kappa P_{CL}} + \frac{M_{UF}}{\kappa M_{CL}} \leq 1.0$$

Because of the high force demand imposed by the existing braces, very large W840 sections were needed at every level: W840x576 for the 1st to 5th levels, W840x433 for the 6th to 9th stories and W840x299 at the roof level. The existing and required beams are compared in Fig. 6.1b.

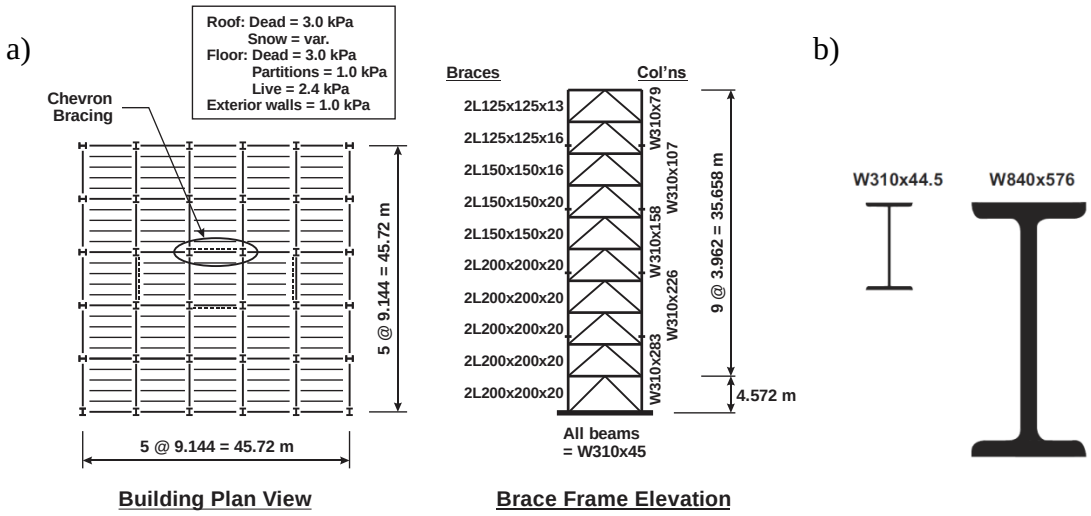

Figure 6.1. a) Plan view and braced frame elevations of the 10-story building, b) Required cross section of the beam at the 1st level of the chevron braced frame using ASCE 41-13.

The analysis of the frame with the retrofitted beams was performed using models with elastic and inelastic column elements. In both cases, beam buckling and yielding was eliminated, confirming the adequacy of the ASCE 41 criteria for beams. In the analyses with elastic columns, large story drifts still occurred in some levels due to inelastic deformations of braces. At the base and top levels, brace deformations exceeded the ASCE 41 plastic deformation limits for collapse prevention performance. Models with inelastic columns showed column buckling under all ground motions. Structural collapse due to this limit state was observed in 9 out of 10 ground motions.

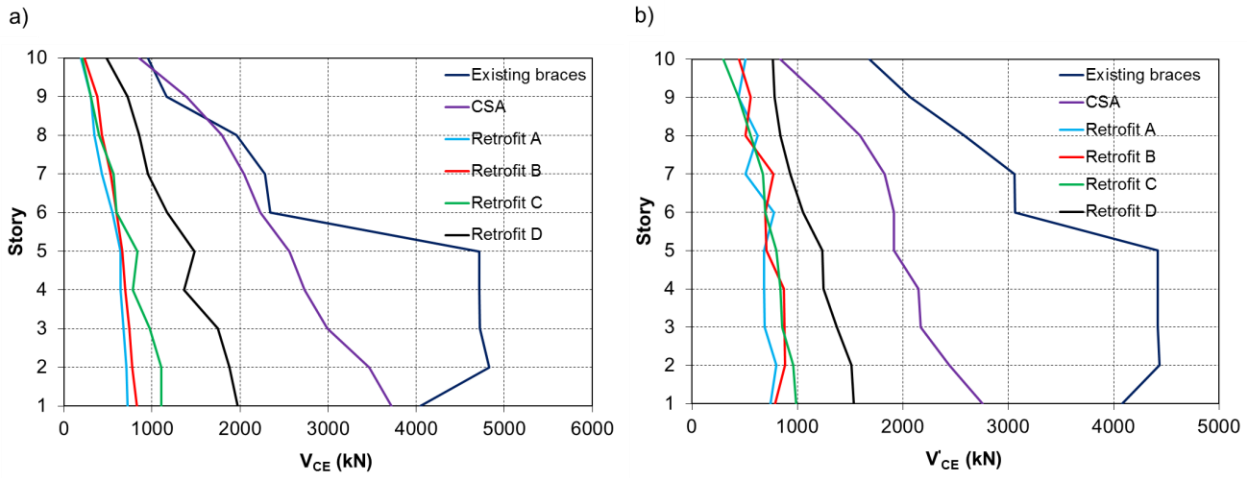

Figure 6.2.Expected story shear resistances from braces: a) at brace buckling (V_{CE}); and b) from braces in the post buckling range (V'_{CE}).

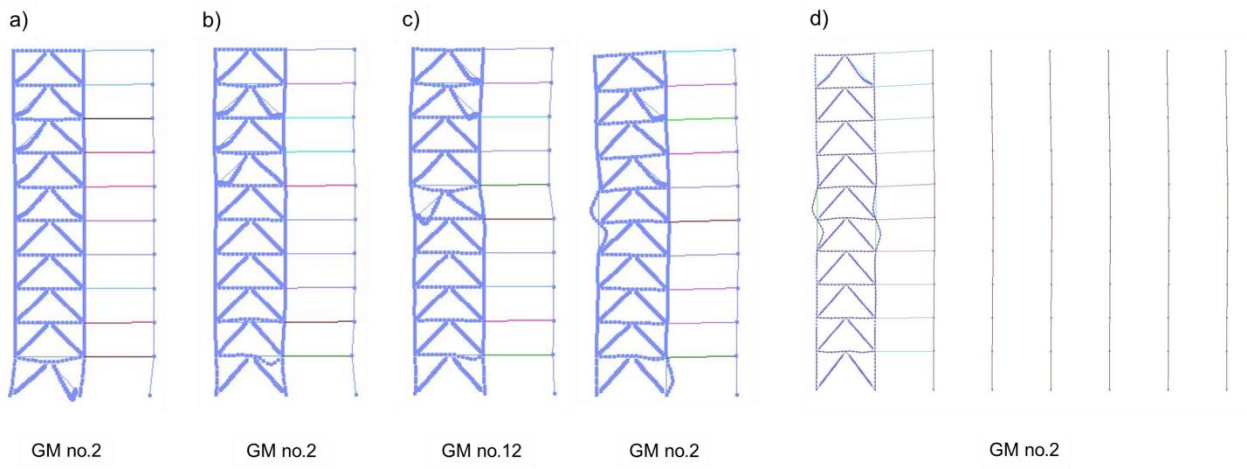

Figure 6.3. Seismic response of the existing braced frame using models with inelastic braces and: a) Elastic beams and columns; b) Inelastic beams and elastic columns; c) Inelastic beams and columns; and d) Inelastic beams and columns plus gravity columns.

Figure 6.4 presents time history response of the frame with retrofitted beams that collapsed under ground motion H02. In this case, column buckling occurred at levels 5 and 6 on the frame left-hand side (LHS), followed by buckling of the right-hand side (RHS) column at level 1 (Fig. 6.4a). In Fig. 6.4b, it is clear that buckling of both columns is in phase with the first mode oscillation of the building, and is the result of the accumulation of brace compression loads from

stories above failures. Strengthening the beams contributed to the development of larger brace forces compared to the existing frame in which beam buckling occurred. Load-deformation responses of the buckled columns are plotted in Fig.6.4c, showing the degradation of the column axial strength in the post-buckling range. In both cases, the capacity reduced below the axial loads from gravity (P_G). The story shear-story drift response at the first level is plotted in Fig. 6.4d. In both directions, the story shear could reach and exceed the expected story shear resistance V_{CE} (= 4049 kN) prior to column buckling at that level. Upon load reversal, the post-buckling story shear resistance V'_{CE} (= 4084 kN) was nearly attained when the story drift reached -40 mm towards the left. This shows that braces can develop their expected strength in tension and compression when beams are designed according to ASCE 41 criteria. These story shears exceed the factored base shear used in the original design of the structure (2253 kN), requiring that foundations be verified for this higher force demands. In Fig. 6.4d, the story shear capacity at level 1 reduced considerably after column buckling due to the fact that both braces must resist compression in the post-buckling condition due to gravity loads, thereby limiting their capacity to resist horizontal loads. As a consequence, large story drift developed that led to a sway collapse mode in that story. At the 5^{th} and 6^{th} levels, column buckling resulted in a vertical failure mode.

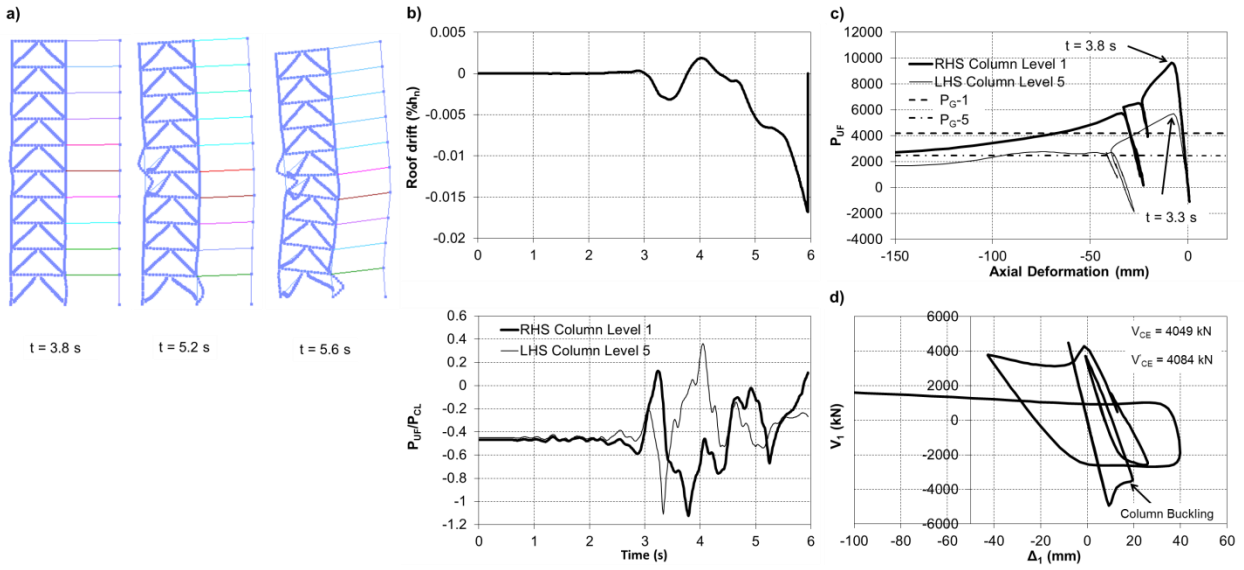

Figure 6.4. Response time history of existing braced frame with retrofitted beams under GM no. H02: a) Deformed shape of the frame; b) Roof drift and axial demands in the RHS column at level 1 and LHS column at level 5; c) Axial load-axial deformation response in the RHS column at level 1 and LHS column at level 5; and d) Base shear *vs*. lateral displacement.

6.3 Design of a new chevron braced frame using current CSA S16

The existing chevron braced frame was redesigned as a new structure using current NBCC 2010 and CSA S16-09. This design was performed to evaluate the feasibility of meeting the target requirement for retrofit recommended in NBCC, i.e. satisfying performance objectives for new structures. That frame design also served as a reference for assessing the effectiveness of the retrofit solutions presented later. For design, the frame was considered of the moderately ductile concentrically braced frame category with a ductility-related force modification factor R_d = 3.0 and over-strength-related force modification factor R_o = 1.3, which resulted in a factored design base shear of 2059 kN (2.3% of the seismic weight), including notional loads and P-delta effects. This is close to the base shear used in the original design but this similarity is only coincidental considering the numerous changes that took place in code provisions over the last three decades (Mitchell et al. 2010). As is the case in AISC 341 Seismic provisions for steel structures in the U.S (AISC 2010), new braced frames in CSA S16 must be designed using capacity design principles. Beams in chevron braced frames must resist gravity loads in conjunction with forces induced by the braces reaching their probable tensile resistance in tension and post-buckling

compressive resistance in compression. The selected members are given in Tables 6.1 to 6.3. Circular tubes were selected for the braces because of their high efficiency. This choice is discussed further later in the text. As expected from based shear values, Fig. 6.2a shows that the expected story shear strength V_{CE} of the new chevron braced frame is close to V_{CE} values of the existing braced frame at level 1 and at levels 6 to 10. However, the expected post buckling strength V'_{CE} of new bracing members is lower than the existing braces. This is because double angle members have relatively higher tensile to compressive strength ratio compared to CHS members. Beams and columns of the new frames are much larger than the corresponding existing frame members due to capacity design requirements. Overall, the new frame requires 55.9 t of steel, which is 1.94 times more than the 1980 frame.

Using this design as retrofit for this structure will pose major challenges for construction given the fact that heavy members will have to be manipulated in the building and column replacement will require temporary shoring. This will cause significant disturbance that may require vacating the building. Furthermore, the new frame will likely require strengthening of the foundations because of the maximum base shear it will impose during inelastic response. In CSA S16, this base shear would be based on brace probable resistances in tension and compression. To ease comparison with the other retrofit schemes designed using ASCE 41, it is determined herein using brace expected strengths:

[4] $$V_{CE,\,max} = \left(T_{CE} + P_{CE}\right)\cos\theta$$

The so-computed value of $V_{CE,max}$ is 4056 kN, higher than the factored load considered in the 1980 design. Similarly, the design overturning moment as per NBCC 1980 was 98317 kN-m which is 75% of the maximum base overturning moment that is induced when all braces reached their expected strengths, $OTM_{CE,max}$.

Table 6.1: Brace sections

Story	CSA S16	Retrofit A	Retrofit B	Retrofit C	Retrofit D
10	CHS 152.4x6.4	CHS 88.9x7.6	CHS 101.6x5.6	CHS 114.3x3.2	CHS 114.3x8.6
9	CHS 174.6x7.9	CHS 114.3x4.8	CHS 114.3x6	CHS 114.3x4.8	CHS 141.3x6.6
8	CHS 168.3x11	CHS 101.6x8	CHS 127x4.8	CHS 114.3x6	CHS 152.4x6.4
7	CHS 168.3x12.7	CHS 127x4.8	CHS 114.3x8.6	CHS 127x6.4	CHS 152.4x7.1
6	CHS 174.6x12.7	CHS 114.3x8.6	CHS 127x6.6	CHS 127x6.6	CHS 168.3x7.1
5	CHS 219.1x9.5	CHS 127x6.4	CHS 127x6.6	CHS 141.3x6.6	CHS 174.6x7.9
4	CHS 190.5x12.7	CHS 127x6.4	CHS 114.3x9.5	CHS 127x7.9	CHS 152.4x9.5
3	CHS 244.5x9.5	CHS 127x6.4	CHS 114.3x9.5	CHS 152.4x6.4	CHS 190.5x7.9
2	CHS 273.1x9.5	CHS 114.3x8.6	CHS 114.3x9.5	CHS 152.4x7.1	CHS 177.8x9.5
1	CHS 254x12.7	CHS 141.3x6.6	CHS 152.4x6.4	CHS 168.3x7.1	CHS 219.1x8.2

Table 6.2: Beam sections

Story	CSA S16	Retrofit A	Retrofit B	Retrofit C	Retrofit D	Retrofit D_1
10	W530x182	W410x149	W410x132	W410x100	W530x165	W690x802
9	W530x248	W410x132	W460x144	W410x114	W530x165	W690x548
8	W610x285	W460x158	W460x128	W460x144	W530x165	W690x548
7	W610x307	W410x132	W460x177	W460x158	W530x182	W690x548
6	W610x341	W460x177	W460x158	W460x158	W530x196	W690x323
5	W610x307	W530x138	W460x158	W460x177	W530x219	W610x455
4	W610x341	W460x144	W460x193	W530x165	W530x219	W610x455
3	W610x341	W460x144	W460x193	W460x177	W530x219	W690x500
2	W610x372	W530x165	W460x193	W530x165	W610x217	W690x500
1	W610x498	W530x165	W530x165	W530x196	W610x262	W760x582

Table 6.3: Column sections

Story	CSA S16	Retrofit A	Retrofit B	Retrofit C	Retrofit D	Retrofit D_1
9-10	W310x86	W310x79	W310x79	W310x79	W310x79	W920x1188
7-8	W310x143	W310x107	W310x107	W310x107	W310x107	W840x392
5-6	W310x253	W310x158	W310x158	W310x158	W310x158	W840x329
3-4	W310x342	W310x226	W310x226	W310x226	W310x226	W840x576
1-2	W360x509	W310x283	W310x283	W310x283	W310x283	W840x576

6.4 Proposed Traditional Retrofit Strategies

6.4.1 General

The retrofit strategies were developed with the main objective of addressing the component deficiencies and undesirable soft-story response identified in evaluation while limiting the extent of the retrofit work to reduce the repair costs and minimize disturbance to building occupants. This included reducing the required number of alterations to the existing frame, the number and size of replacement parts, and the amount of required additional structural steel. Consideration was also given to limit the force demands on the existing foundations to reduce impacts on building functionality. To achieve this, ASCE 41-13 was adopted to design the retrofits as it is the most comprehensive document providing acceptance criteria specifically developed for existing structures. In comparison, seismic retrofit provisions in NBCC are essentially based on requirements for new constructions are expected to result in less effective solutions. Because it is more convenient for design, ASCE 41 LDP was chosen to select both deformation- and force-controlled components, but NDP was applied to validate the retrofit solutions considering the inherent tendency for soft-story mechanism and structural collapse observed in evaluation.

In view of the key role played by the bracing members on the frame inelastic response, it was also decided to replace all bracing members even if not required from the evaluation. The new braces were carefully selected to achieve more uniform inelastic deformations over the frame height and reduce the force demands imposed on beams and columns. Circular hollow sections

(CHS) conforming to ASTM A500 were deemed to represent the best option considering the large numbers of available sections that permitted a stricter control on the demand to capacity ratios within the structure. These sections also offer the high compressive strength per unit cross-section area, resulting in minimum tension force demands on connections and unbalanced brace load effects on beams and columns. The nominal yield strength of ASTM A500, gr. C CHS is 317 MPa and the expected yield strength was taken equal to 1.1 F_y = 349 MPa, as recommended in ASCE 41-13.

In the next two sub-sections, four possible solutions are studied to achieve the stated retrofit objectives. In all four scenarios, response spectrum analysis was used and member sizes were optimized using an iterative procedure until ASCE 41 LDP criteria was met. The brace sections were selected first, preferably highly ductile members to permit higher ductility (*m*) factors or plastic deformation capacities in ASCE 41. After selection of the braces, beams and columns were verified and modified or replaced as necessary to satisfy the ASCE 41 LDP criteria. For the columns, axial load demand P_{UF} from the following two loading conditions was considered:

[5] $$P_{UF,i} = P_{G,i} + \sum_{x=i+1}^{n} P_{CE,x} \sin\theta_x$$

[6] $$P_{UF,i} = P_{G,i} + \sum_{x=i+1}^{n} 0.3P_{CE,x} \sin\theta_x + \sum_{x=i}^{n} \frac{(T_{CE,x} - 0.3P_{CE,x}) \sin\theta_x}{2}$$

Retrofit validation using ASCE 41 NDP was performed with the same OpenSees model and suite of 10 ground motion time histories developed in the seismic evaluation phase of the project. The model was however expanded to include all gravity columns tributary to the braced frame studied, in lieu of the single P-delta leaning column. The new gravity columns were represented with elastic beam-column elements and the columns were pinned at their bases and had pinned splices at every other level. In addition, the braced frame columns were assumed to have fixed bases and theirs splices were modeled with full flexural continuity. These changes influenced the frame response by affecting column buckling modes and variation of story drifts along the frame height. Changes to column buckling patterns can be seen by comparing Figs. 6.3c and 3d for the existing braced frame with inelastic members subjected to GM no. 2. Modelling of the braces

was also modified to reflect the use of CHS members' model. For these members, material properties were also adjusted to reproduce the limited amount of strain hardening response that is measured in tests due to cold-forming experienced by the steel during the rolling process (Packer et al. 2010). Evaluation and design using NDP are based on the mean seismic demand from the 10 ground motion time histories.

6.4.2 Retrofits A to C

These first three retrofit solutions were developed to take full advantage of the ASCE 41 procedure by selecting bracing members such that they just satisfy the LDP acceptance criteria without any other considerations. In Retrofit A, braces were chosen such that their demand-capacity ratios (*DCR*) were as close as possible to 1.0. Braces of braced frames classify as deformation-controlled components for which *DCR* is:

$$[7]\quad DCR = \frac{Q_{\mathrm{UD}}}{m\kappa Q_{\mathrm{CE}}}$$

where Q_{uD} is the brace axial force demand from gravity plus seismic loads, m is the ductility factor prescribed in ASCE 41, κ is the knowledge factor (equal to 1.0 in this study), and Q_{CE} is equal to P_{CE} or T_{CE} for compression and tension braces, respectively. The m-factor varies with the performance objective, whether the brace is in tension or compression, the brace slenderness, and the compactness of the brace cross-section. In the determination of m, no correction was considered for the connections assuming that they would be properly sized and detailed in the retrofitted frame. Figure 6.5a shows the *DCR* values of the selected compressive braces. As shown, the values vary from 0.8 to 1.0. The m-factors of these braces vary from 6.64 to 7.00 along the frame height. When acting in tension, m = 5.60 for all selected braces. An equivalent R-factor for the retrofit scheme can be established by multiplying the m-factor by the *DCR* and the values are plotted in Fig. 6.5b. For Retrofit A, R-factor based on the compression braces varies from 5.4 to 6.9 along the height of the frame, with an average value of 6.1.

In Fig. 6.5b, the R-factor changes along the height because braces were selected based on the m-factor which varies with the brace slenderness and the compactness, rather than being selected to satisfy strength requirements. As this variation could be a source of story drift concentration,

Retrofits B and C were developed using the same approach except that the braces were also chosen to achieve uniform V_{CE} and V'_{CE} values, respectively, over the frame height using a fixed value V_{uD}/V_{CE} = 6.0 for Retrofit B and V_{uD}/V'_{CE} = 5.0 for Retrofit C, where V_{uD} is the story shear from response spectrum analysis. As shown in Fig. 6.5b, this strategy was successful to achieve more uniform equivalent *R* factors for both retrofit designs, but at the expense of generally lower *DCR* values (Fig. 6.5a).

For these three retrofit schemes, the existing beams needed to be replaced at all floors but the existing columns could be kept intact, without strengthening. Brace and beam sections are given in Tables 6.1 and 6.2 and the total required additional steel tonnages and building fundamental periods are given in Table 6.4. The amount of steel is nearly the same for the three cases and varies between 28 and 31% of the steel needed for the new CSA S16 braced frame. Calculated expected maximum story shear and overturning moment at the base of the three retrofitted frames are also given in Table 6.4. In all cases, both reactions are less than the factored loads considered in the original 1980 design (2253 kN and 98317 kN-m), suggesting that repair work to the foundations would not be needed for these retrofits. The fact that the foundations and existing columns could be re-used without repair combined to the reduced amount of steel makes Retrofits A to C very attractive for this building.

Unfortunately, validation using ASCE 41 NDP showed inadequate performance with severe drift concentrations that caused structural collapse. Examples of story drift patterns just before collapse are presented in Fig. 6.6 for each retrofit solution and the numbers of collapse occurrences out of the 10 ground motions are given in Table 6.4. Figure 6.7 shows the time history response of Retrofit A under one ground motion causing frame collapse (H05). In Fig. 6.7a, large story drift occurred at the first level and the response of the structural members at this level is shown in the figure. In Fig. 6.7b, LHS and RHS braces at the 1st level reached T_{CE} and P_{CE}. No column buckling occurred in the LHS and RHS columns, as shown in Figs. 6.7c and 6.7d, respectively. When the brace in tension reached T_{CE} and stretched in the inelastic range after t = 6 s, plastic hinging formed in the columns and a plastic soft-story mechanism developed in the first level that led to frame collapse due to excessive P-delta effects in that level. The collapse mode of the Retrofit A under this ground motion is shown in Fig. 6.6. Figure 6.7e shows that the response of the retrofitted beam at the 1st level is satisfactory before the frame collapse.

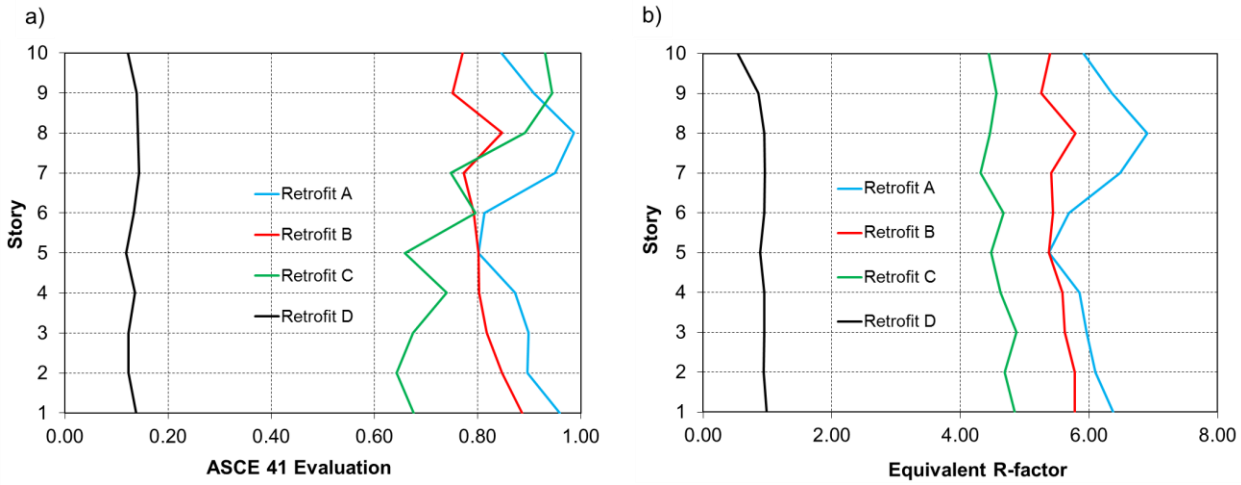

Figure 6.5. Retrofits A to D: a) Evaluation of braces using ASCE 41 LDP; and b) Equivalent R-factor.

Table 6.4: Maximum base shear, maximum overturning moment, steel tonnage, and number of collapse cases

Retrofit	$V_{CE,max}$ (kN)	$OTM_{CE,max}$ (kN-m)	Steel tonnage (t)	T_1 (s)	Number of collapse cases
CSA S16	4056	130343	55.9	2.02	0
Retrofit A	996	33492	15.6	2.97	5
Retrofit B	1079	37007	17.1	2.85	5
Retrofit C	1375	38592	16.2	2.82	6
Retrofit D	2226	63602	21.5	2.53	3
Retrofit D_1	2226	63602	$21.5^{(1)} + 93.9^{(2)}$	2.25	0
Retrofit D_2	2226	63602	$21.5^{(1)} + 30.1^{(2)}$	1.73	0
Retrofit D_3	2226	63602	$21.5^{(1)} + 18.5^{(2)}$	2.16	0
Retrofit E	6213	210001	$4.3^{(3)} + 18.5^{(2)}$	1.79	0

(1): Steel tonnage of retrofitted CBF and (2) Steel tonnage of additional MRF/Truss (3) Partial braced frame retrofit

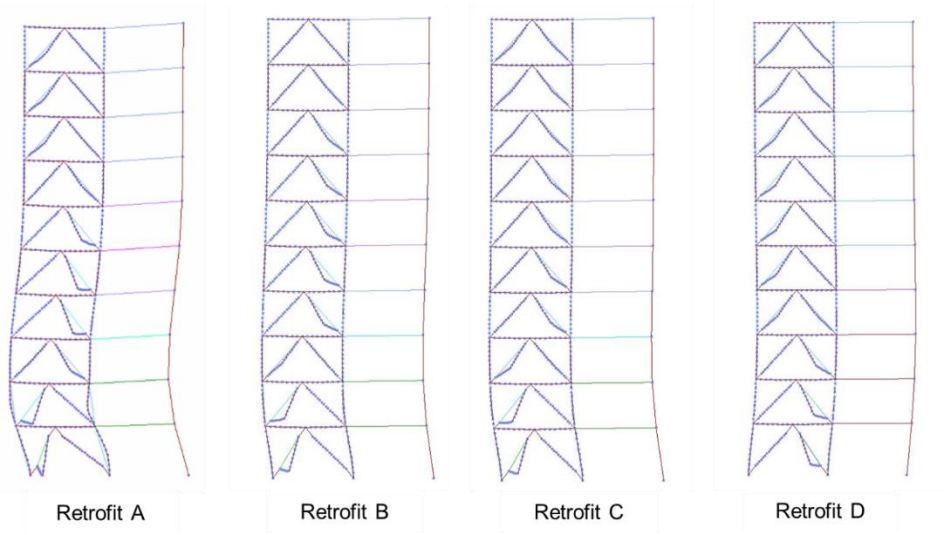

Figure 6.6. Deformed shape near collapse for Retrofits A to D under GM no. H05.

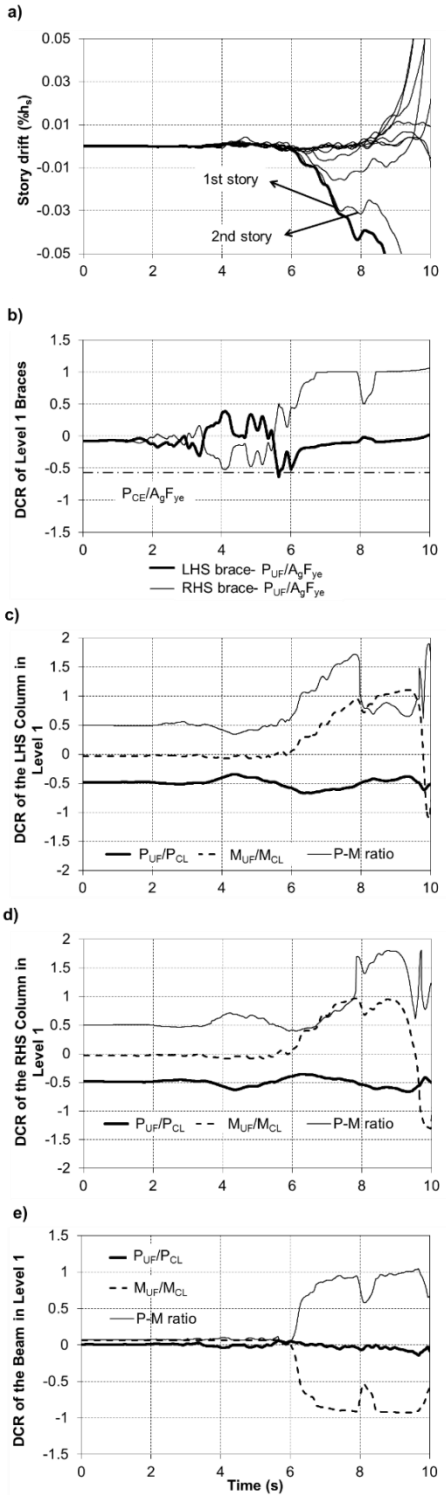

Figure 6.7. Response time history of Retrofit A under GM no. H05: a) Story drifts; b) Brace axial force demand at level 1; c) Axial and flexural demands in the LHS column at level 1; d) Axial and flexural demands in the RHS column at level 1; and e) Axial and flexural demands in the beam at level 1.

6.4.3 Retrofit D

Inadequate response of Retrofits A-C is attributed to the fact that ASCE 41 LDP used to select/verify the bracing members assumes a brace ductility demand uniform along the frame height with amplitude based on the equal displacement principle. The method omits important effects in the actual inelastic response such as concentration of inelastic deformations concentrating in weaker levels and P-delta effects on the inelastic response that contributed to observed collapses. For new buildings, such detrimental effects are taken into consideration through limits on design periods, design base shears, story drifts, etc., not present in ASCE 41, that provide the structure with sufficient lateral strength and stiffness to accommodate these effects and achieve proper response. Differences in lateral resistance and periods of Retrofits A-C and CSA S16 in Fig. 6.2 and Table 6.4 reflect the differences between the ASCE 41 procedure and current code provisions. As an attempt to investigate the possibility of avoiding soft-story response by providing minimum lateral resistance, Retrofit D is studied which corresponds to Retrofit C with a lateral resistance increased by approximately 80%. That limit was dictated by the capacity of the existing columns and foundations such that Retrofit D could maintain the same advantages of not requiring any repair to these critical components. The use of V'_{CE} instead of V_{CE} as the design parameter for verifying uniform lateral resistance was motivated by the fact that soft-story response at large drifts involves brace resistances that are associated to V'_{CE} rather than V_{CE}. In Table 6.4, the selected braces of Retrofit D were such that $V_{CE,max}$ is slightly less than the NBCC 1980 value of 2253 kN per frame and $OTM_{CE,max}$ value is less than the 98317 kN limit. These forces are much less than those imposed by the CSA S16 frame and the amount of additional steel required is still significantly lower (38%) than the one needed to build the CSA S16 frame, maintaining Retrofit D solution attractive in spite of its higher lateral capacity. In Fig. 6.5, the *m*-factor of the compressive braces varies from 5.6 to 7.0 along the frame height while the equivalent *R*-factor varies from 0.5 to 1.0.

Nonlinear time history analysis showed similar unsatisfactory response with collapses occurring for three out of ten ground motions. All collapses occurred as a result of soft-story mechanism, as shown in Fig. 6.6 under GM no. H05. This clearly shows that the component-based evaluation LDP procedure of ASCE 41-13 is not sufficient to prevent this global failure mode for chevron braced steel frames. This is in accordance with observations made by the authors in the

evaluation phase of this project. Speicher and Harris (2016) also concluded that linear assessment procedures may not be consistent with nonlinear procedures.

6.5 Alternative Retrofit Strategies with Backup External Frames

6.5.1 General

Seismic performance obtained for Retrofits A to D clearly indicated that a cost-effective traditional retrofit scheme consisting in solely strengthening the existing braced frame would be difficult to achieve. Alternative retrofit means capable of preventing soft-story response and structural collapse at a reasonable cost while maintain maximum building functionality during repair work had to be employed. Past studies had shown that inelastic seismic response of steel braced frames could be significantly enhanced by coupling them with a second lateral system to form a dual seismic force resisting system. Moment frames and vertical elastic trusses were deemed to be very suitable for this retrofit project. These additional frames would be constructed from outside of the building along the perimeter walls to limit the disturbance on the building usage (Fig. 6.8a). These external frames would be attached to the existing slab at every level to ensure interaction with the interior chevron braced frames. They would be erected on new foundations elements to be built against the existing foundations from the exterior. In the retrofit project, these frames can be constructed first; so that they can serve as temporary lateral resistance system during the repair of the existing braced frames. In this section, both the moment frame and elastic vertical truss options are examined (Fig. 6.8b). In both cases, it is assumed that the retrofit D solution would be applied to the existing braced frames as this retrofit provides the maximum lateral resistance without having to reinforce the existing braced frame foundations and columns. For the vertical truss, two different designs are investigated, one where the trusses are continuous over the full building height and one where the trusses are formed of two segments pinned at their mid-height. In the last sub-section, the potential for using the elastic vertical truss system in combination with the existing braced frames is also examined on a preliminary basis.

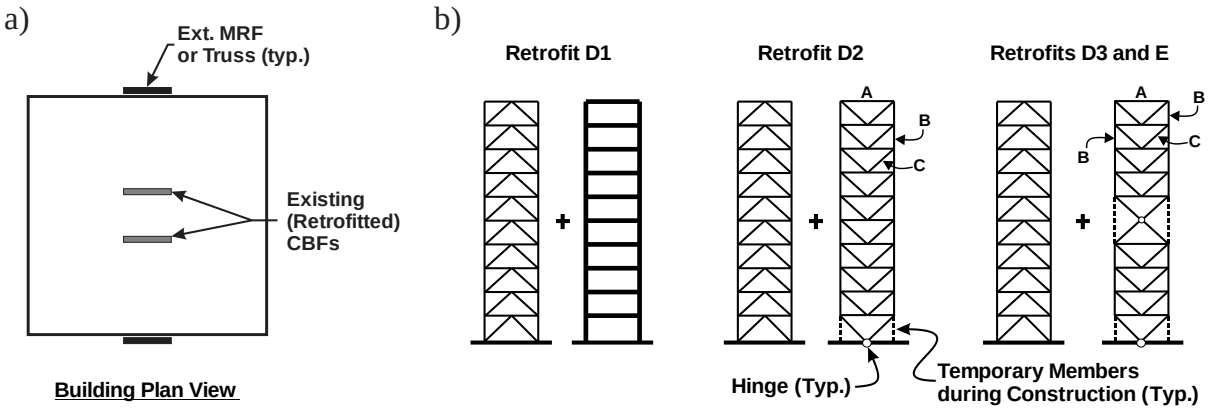

Figure 6.8. Dual system retrofit options: a) location of the external frames; and b) Retrofits D_1 to E.

6.5.2 Retrofit D_1

At first, the concept of forming a moment frame with the beams and columns of the chevron braced frames, as is often done in construction nowadays, was studied. However, it appeared that this strategy would be difficult to apply without major of the strengthening of the existing column because these columns in this particular case studied are oriented such that they would be bent about their weak axis. Rigid beam-to-column connections would be difficult to realize in practice because of the column orientation. The additional lateral load resisted by the moment frames would likely require strengthening of the foundations. For these reasons, the external moment frame option was retained for Retrofit D_1.

The moment frame members were selected by trial and errors until the Retrofit D braced frame members could satisfy ASCE 41 acceptance criteria. For the braces, inelastic axial deformations for analysis were compared to the applicable plastic deformation capacities. Conversely, beams and columns of the braced frame were evaluated as force-controlled components under combined axial load and bending moment demand from analysis. Moment frame members were also verified to ensure elastic response under combined axial and flexural load demands. To avoid the formation of plastic hinges in the moment frame columns, beams and columns were also proportioned to satisfy the strong column/weak beam criterion used for ductile frames. Elastic column response was felt to be a necessary measure for vertically distributing the inelastic demand in the braced frame and mitigating soft-story response and structural collapse. ASCE 41

evaluation of the braced frame members for the final moment frame design iteration is presented in Fig. 6.9. As shown, satisfactory behavior is anticipated for all members.

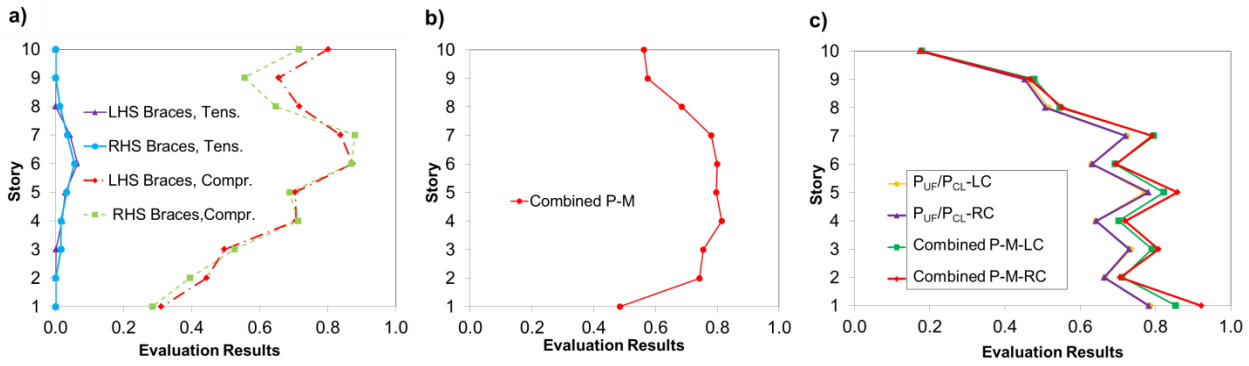

Figure 6.9. Evaluation of the Retrofit D braced frame in Retrofit D_1: a) NDP evaluation of the braces; b) LDP evaluation of the beams; and c) LDP evaluation of the columns.

In this final iteration, the moment frame plastic story shear capacity V_p in levels 1 to 6, as governed by plastic hinging of the beam, was equal to 1.8 times the braced frame V_{CE} value. In levels 7-10, that ratio increased to 5 as beams and columns of the moment frame had to be increased to limit plastic deformations in the braces. The required moment frame members are given in Tables 6.2-6.3. As shown in Table 6.4, the moment frame as designed required a substantial amount of steel. In total, 115 t of steel would be needed to construct one Retrofit D braced frame and one external moment frame, i.e. approximately twice the material required for the new CSA S16 braced frame. Hence, the solution cannot be qualified as cost-effective.

In the nonlinear response history analysis, moment frame columns were modeled as elastic beam column elements. In the analyses, stress levels in the frame members remained within the elastic range and the dual system exhibited stable inelastic seismic response under all 10 ground motions (no collapse). Other results from the nonlinear response history are reported in Table 6.5. The maximum base shear and overturning moment at the base of the braced frame reached values close to the maximum anticipated $V_{CE,max}$ and $OTM_{CE,max}$ values of Table 6.4, but well below the factored base shears and overturning moments considered in the design of the foundations (2253 kN and 98317 kN-m). Reactions at the base of the moment frames that would need to be considered for the design of the exterior foundations are also given. As also shown in the table,

an average peak roof drift was obtained 0.78% for this retrofit, which is less than the 1% limit specified in the 2010 NBCC for post-disaster buildings.

Table 6.5: Base shear, overturning moment, and roof drift from ASCE 41 NDP

Type of Retrofit	Base Shear (kN)		Base Overturning Moment (kN-m)		Roof Drift (% h_n)
	CBF	MRF/Truss	CBF	MRF/Truss	
Retrofit D_1	1946	3699	68855	46145	0.78
Retrofit D_2	1961	6246	71311	0	0.76
Retrofit D_3	1960	2098	70375	0	0.75
Retrofit E	5641	1886	128663	0	0.71

6.5.3 Retrofits D_2 and D_3

As illustrated in Fig. 6.8b, the vertical elastic truss in Retrofit D_2 has a pinned connection at its base and is continuous over the entire story height. Contrary to the dual system with the moment frame, the vertical truss does not provide additional lateral load resistance to the building. It is however designed with high shear and flexural stiffness such that the building structure is forced to respond essentially in its fundamental mode of vibration and thereby, prevent concentration of story drifts in individual stories. In Retrofit D_3, the truss is cut into two halves that are hinge connected at the building mid-height and each segment is designed to play the same role within the 5-story segment. The main advantage of the second design is that the force demand in the truss members can be significantly reduced (Chen et al. 2012, Tremblay et al. 2014). To act as temporary lateral system during construction, removable vertical members are used to form regular braced frame system with a fixed base and continuous overturning moment capacity (Fig. 6.8b).

For preliminary design, the vertical truss segments were represented by single elastic beam elements in the nonlinear model, which permitted to easily assess shear and bending moment demands on the truss and determine the truss stiffness required to achieve the desired

performance. Similar to the dual system with external moment frames, the design of the vertical truss was gradually improved through successive iterations until the Retrofit D braced frame members satisfied the ASCE 41 acceptance criteria. To ensure elastic truss response, the truss members were also designed to resist the maximum (envelop) force demands from the 10 ground motions. W sections were used for all members and the selected shapes are given in Table 6.6. Horizontal, vertical and inclined truss members are identified by labels A, B, and C, respectively (see Fig. 6.8b). As expected, in Table 6.4, Retrofit D_3 required less steel than Retrofit D_2: 40 *vs* 56.5 t in total. The actual cost difference between the two systems should however account for the increased complexity resulting from the second hinge required in Retrofit D_3. Retrofit scheme D_3 necessitates 28% less steel than the CSA S16 frame.

Table 6.6: Vertical truss members for Retrofits D_2 and D_3

Story	Retrofit D_2-A	Retrofit D_2-B	Retrofit D_2-C	Retrofit D_3-A	Retrofit D_3-B	Retrofit D_3-C
10	W410x100	W610x140	W410x85	W310x52	W410x53	W310x44.5
9	W410x100	W610x174	W410x75	W310x52	W610x113	W310x38.7
8	W410x85	W610x195	W410x60	W310x52	W530x82	W310x23.8
7	W410x67	W610x195	W310x52	W310x28.3	W610x125	W310x21
6	W410x53	W610x241	W310x52	W310x28.3	-	W310x28.3
5	W410x53	W610x241	W310x44.5	-	-	W410x114
4	W410x46.1	W610x241	W310x44.5	W410x132	W610x113	W410x67
3	W310x52	W610x241	W310x32.7	W310x86	W610x125	W310x44.5
2	W310x38.7	W610x241	W310x44.5	W310x52	W610x140	W310x38.7
1	W410x46.1	-	W610x285	W410x46.1	-	W610x140

In the final response history analyses, the trusses were modeled with elastic beam elements that were rigidly connected at the trusses nodes. Both retrofit truss systems showed adequate global response, with no collapses. Evaluation results for the Retrofit D braced frame members are given in Figs. 6.10 and 6.11 for two retrofit schemes. In Figs. 6.10a and 6.11a, axial force demand to capacity ratio based on lower bound strengths, P_{UF}/P_{CL}, are also given for selected vertical truss members. These ratios are close to 1.0. In Figs. 6.10b and 6.11b, the braces of the two frames showed adequate inelastic performance. Evaluation of beams and columns of the braced frame are given only for Retrofit D_3 as the demand was higher for this retrofit design. All beams and columns are expected to have adequate performance under combined axial and flexural demand. In Fig. 6.11d, evaluation results for the columns in the first story slightly exceed 1.0 due to the high flexural demands that developed at the column bases. As shown, the columns have sufficient axial load resistances at this level and recent studies have shown that ASCE 41 LDP acceptance criteria were probably too conservative for this situation as braced frame columns carrying axial compression can undergo significant inelastic end rotations without endangering their stability (Bech et al. 2015, Balazadeh-Minouei et al. 2017b).

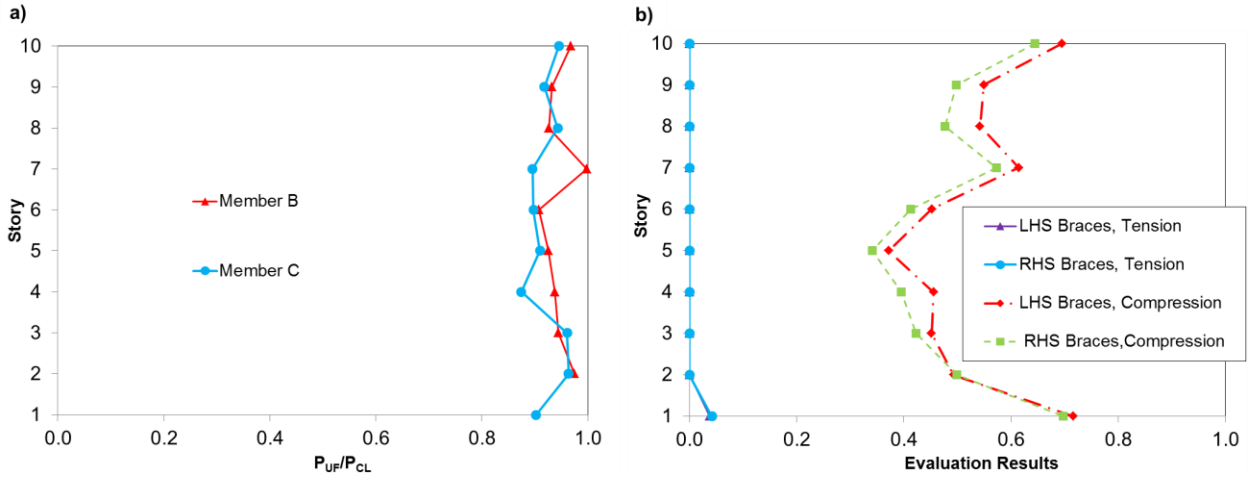

Figure 6.10. Evaluation of Retrofit D_2: a) *DCR* of selected truss members; and b) NDP evaluation of the braces.

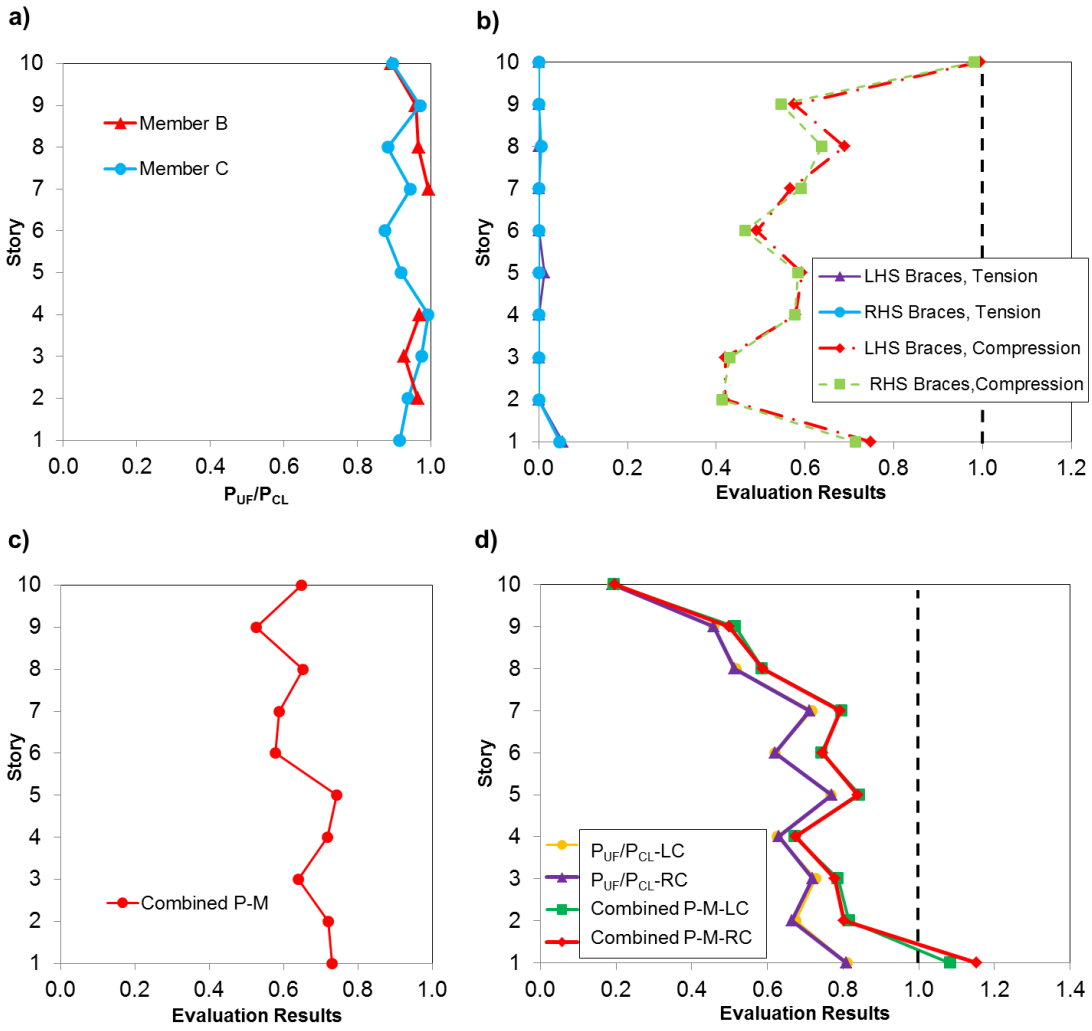

Figure 6.11. Evaluation of Retrofit D_3: a) *DCR* of selected truss members; b) NDP evaluation of the braces; c) LDP evaluation of the braced frame beams; and d) LDP evaluation of the braced frame columns.

In Table 6.5, reactions at the base of the Retrofit D braced frame for the two trussed retrofit options remained below the existing foundation capacities. The shear at the base of the vertical truss in Retrofit D_2 is higher than in Retrofits D_1 and D_3, likely due to the more pronounced higher mode response of the single continuous vertical truss. The horizontal reaction at the base of the vertical truss in Retrofit D_3 is less than the one obtained at the base of the moment frames of Retrofit D_1. Roof drifts experienced by the two truss retrofitted structures are same and are comparable to those obtained for the dual system with moment frames. In Table 6.5, the dual truss systems impose less base shears and no overturning moments to the new foundations to be built outside of the building.

6.5.4 Retrofit E

The promising response observed with Retrofit D_3 suggested that the same vertical truss solution could be directly applied to the existing deficient chevron braced frame. The potential of this option, referred to as Retrofit E, is examined herein on a preliminary basis. For this purpose, NDP was performed to assess the seismic behavior of this retrofit scheme using the vertical truss that was designed in Retrofit D_3. The evaluation showed column buckling occurrences at the bottom and middle levels of the braced frame under seven out of the ten ground motions. Structural collapse was observed in six of these cases. The columns of the braced frame were then retrofitted at levels 1 to 8 using ASCE 41 LDP requirements for chevron braced frames. The retrofit scheme for the columns consisted in reinforcement steel plates welded to the edges of the column flanges to form box sections with higher flexural stiffness and strength. This solution was found to be more effective than simply welding cover plates to the column flanges. The thickness of the reinforcement plates was selected such that their width-to-thickness ratio satisfied the limits for highly ductile members in AISC 341-10. Nonlinear response analysis of the braced frame with strengthened columns coupled with the segmented vertical truss showed that this scheme was sufficient to eliminate column buckling, soft-story response, and structural collapse.

Figure 6.12a however shows excessive plastic deformation demands on the existing double angle members at levels 1 and 8 to 10. This deficiency could be addressed by replacing the deficient braces by more effective members, as was done in other retrofits previously discussed in the article. Impact of implementing such new braces on frame response should then be verified. Figure 6.12b shows the evaluation of the retrofitted columns of the existing braced frame using the ASCE 41 LDP with force demand from the nonlinear analysis. The results confirm the adequacy of the adopted column strengthening approach. Similarly to Retrofit D_3, insufficient strength is predicted by ASCE 41 at the column bases; however, the nonlinear analyses with inelastic column models proved that this high demand was not detrimental to the stability of the columns.

In Fig. 6.12c, evaluation results for the beams are presented using two different effective length values for the calculation of the beam lower-bound axial strength P_{CL}: the total length of the beam with KL_x = 9144 mm, and half of this length, i.e. KL_x = 4572 mm. The corresponding values of P_{CL} are 1168 kN and 1582 kN, respectively. The evaluation results indicate that the

beams at all levels have insufficient strength to resist the combined axial compression and bending demands, regardless of the effective length used in the calculations. As also shown in the figure, P_{UF} /P_{CL} ratios exceed 1.0 at levels 1 to 4 even when assuming a buckling length KL_x = 4572 mm. The results are more critical when using KL_x = 9144 mm as P_{UF} /P_{CL} > 1.0 at all levels. Careful examination of the beam responses in the nonlinear analyses showed that beam buckling in fact occurred over half the beam length. The axial load-axial deformation response of the beam at level 2 that buckled under GM H01 is presented in Fig. 6.12d. The results clearly show inelastic buckling response of this member with a buckling load of 1630 kN, close to the P_{CL} value determined with KL_x = 4572 mm (1582 kN). This suggests that beam axial strengths could be calculated using half the beam span when evaluating beams of chevron braced frames. In this case, the beam exhibited stable hysteretic axial response up to axial compressive deformations of 40 mm, which suggests that some ductility could be associated to beam buckling in compression. Contrary to the response of the existing braced frame without vertical truss discussed in the first section of the article, beam buckling in this frame did not lead to structural collapse, likely because the elastic vertical truss distributed the frame inelastic response among several floors, and, thereby, limiting the extent and consequences of beam buckling on the frame overall response.

Beam buckling and its possible effects on frame response is a complex problem as it depends on several factors including the stiffness and strength of the vertical support provided by the braces responding in the nonlinear range, the possible horizontal restraint offered by floor slabs, surrounding columns and, for the retrofitted frames, the elastic vertical truss. This complex response will need further research before final recommendations can be formulated on beam inelastic axial response. This study indicates, however, that the addition of a soft-story restraining system such as the elastic vertical truss could be one possible means of permitting inelastic response in beams either in flexure, as suggested by Sen et al. (2016, 2017), or combined axial and flexure as observed herein. Until more information is available and considering that beam buckling is more likely to affect the integrity of the braced frame, it is recommended that the beams be reinforced to resist the anticipated axial load demand.

In Table 6.5, this retrofitted braced frame imposes a base shear of 5641 kN and an overturning moment of 128663 kN-m, both being larger that the forces used in the original design of the existing foundations. Foundation strengthening would then be required. In Table 6.4, the required

steel tonnage for this retrofit solution is 4.3 tons for the column strengthening and 18.5 t for the vertical truss, resulting in a total of 22.8 tons, the smallest among all other solutions presented in this article. Although this steel quantity does not include the material required to correct braces, brace connections and beams deficiencies, it shows that this retrofit strategy has potential for limiting alterations to an existing deficient structure.

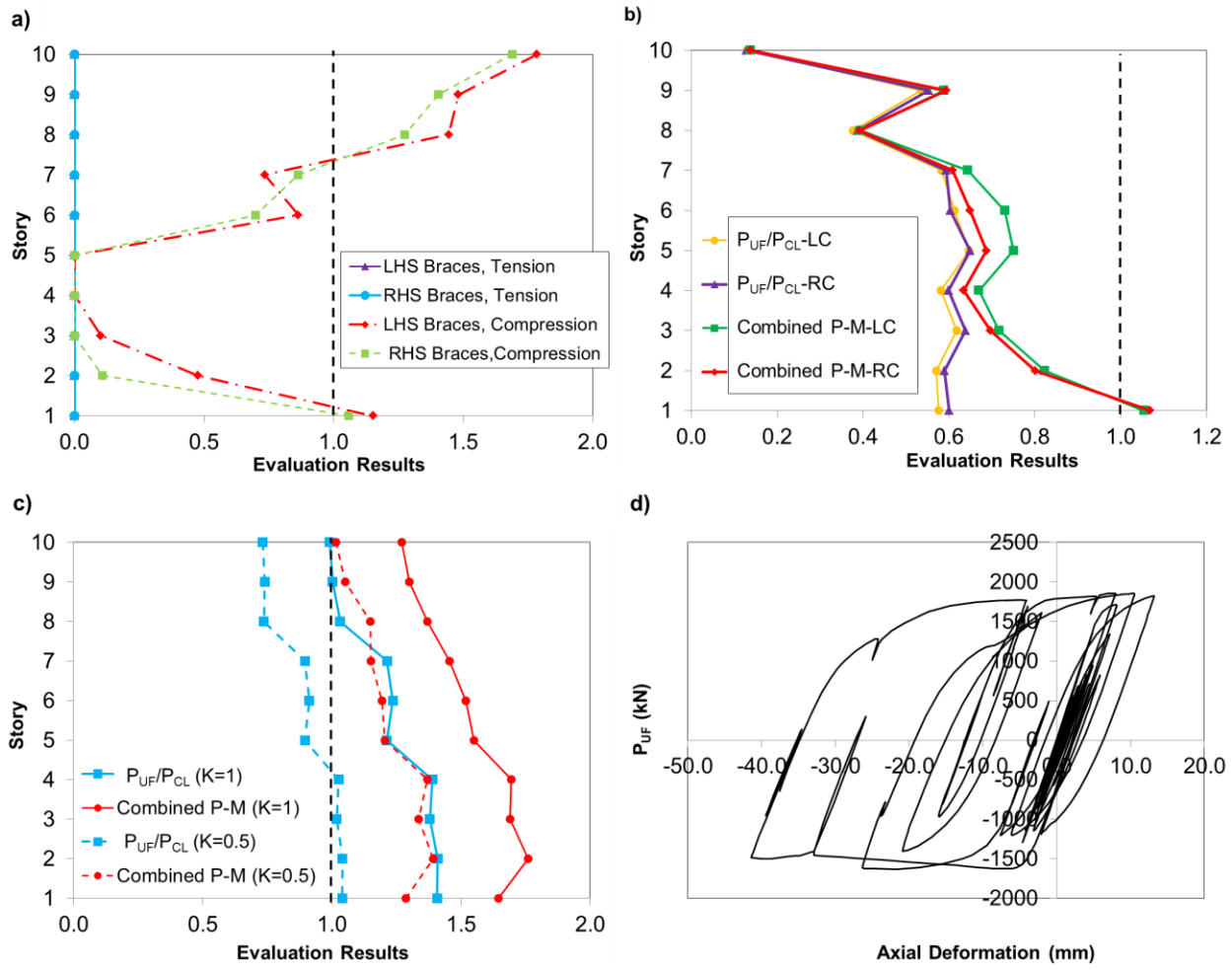

Figure 6.12. Evaluation of Retrofit E: a) ASCE 41 NDP evaluation of the braces; b) LDP evaluation of the columns; c) LDP evaluation of the beams; and d) Axial load-axial deformation response for the RHS beam at level 2 under GM no. H01.

6.6 Conclusion

The seismic retrofit of a 10-story steel existing chevron braced frame designed prior to implementation of special seismic design procedures was performed. The structure was originally designed in accordance with the 1980 NBCC for a site class C in Vancouver, British Columbia, Canada. Previous evaluation showed that all beams and a large number of the columns needed retrofit. A braced frame was first designed in accordance to provisions of current Canadian codes for new structures for reference purposes. Eight seismic retrofit strategies were then developed using the dynamic procedures of ASCE 41 with collapse prevention under a seismic demand with a probability of exceedance 2% in 50 years as performance objective. The first four retrofit solutions (A to D) consisted in modifying the members of the existing braced frames. The subsequent three solutions (D_1 to D_3) involved the addition of external lateral systems acting in parallel with braced frames retrofitted using the fourth (D) strategy. The last solution (E) was same except that the existing braced frame with strengthened columns was used. Validation of the retrofit schemes was performed using the nonlinear dynamic analysis procedure of ASCE 41 using a model that reproduced nonlinear behavior for the braces, beams and columns and elastic response for gravity columns. The following conclusions can be drawn from this study:

- Compared to other retrofit solutions, the braced frame designed in accordance with current Canadian provisions required the largest amount of steel (except for D_1) and imposed larger forces on the existing foundations. Its implementation would also require column replacement and strengthening of the existing foundation, which would represent major construction challenges.
- In retrofits A to C, braces were replaced with the main objectives of minimizing the force demand on beams, columns, and foundations while achieving uniform demand to capacity ratios along the frame height to avoid soft-story response. Beams were replaced but the existing columns could be kept. In all three cases, structural collapse was observed in 50% or more of the ground motions due to soft-story response. In Retrofit D, larger brace sizes were selected to increase the frame lateral resistance by up to 80% while keeping the expected base shear below the capacity of the existing foundations. This required larger beams compared to schemes A to C but the existing columns could still be maintained without strengthening. This stronger retrofit design also exhibited inadequate global response as structural collapse was observed under 30% of the ground motions. Such unacceptable response for Retrofits A to D show that structural

collapse by global instability is a possibility for steel braced frames that satisfy component based ASCE 41 acceptance criteria. Explicit verification of satisfactory global seismic response using NDP should be mandatory for retrofit design of these structures. Alternatively, ASCE 41 could include provisions such as maximum story drifts, minimum lateral strength or P-delta verification to achieve stable response when using LDP.

- Retrofit D_1 included moment frames along the exterior walls to control soft-story response and ensured that the inelastic brace axial deformations below ASCE 41 acceptance criteria. An iterative approach using nonlinear dynamic procedure was adopted to determine the required moment frame stiffness properties. Retrofit D for the braced frame was kept such that no alterations were required to the existing columns and foundations. Retrofit D_1 resulted in satisfactory global inelastic response (no collapse) but at the expense of a much larger amount of steel compared to all other retrofit schemes because of the large beam and column cross sections that were required. This dual system still represents an attractive solution because it imposes no disturbance on building usage and the moment frame can be installed first to provide temporary lateral resistance during the subsequent retrofit of the existing chevron braced frames.
- Retrofit D_2 and D_3 are also dual system options in which the external system consisted of pinned base, stiff elastic vertical trusses. For D_2, the trusses were continuous over the full building height whereas the trusses in D_3 were made of two 5-story segments pin-connected at the building mid-height to reduce force demands from higher modes. These trusses offer the same advantage as the D_1 solution in terms of obstruction and can also serve as temporary bracing. The same iterative approach was adopted to design the two truss systems but the trusses required significantly less steel because of their higher inherent lateral stiffness. The two systems achieved satisfactory global seismic response. The two external truss solutions also impose no overturning moments on external foundations. Among the two truss designs, D_3 is the most economical in terms of steel tonnage and impose less base shears than D_2.
- In Retrofit E, elastic vertical trusses with a hinge at the building mid-height developed in retrofit D_3 were used in combination of the existing frames. This scheme was found sufficient to eliminate soft-story response and, thereby, limit the extent of inelastic demand on individual frame members and structural collapse. Braces, beams, and columns of the braced frame would require strengthening to prevent member failure. For the beams, buckling should be prevented but

limited flexural yielding might be acceptable. Additional studies are needed to propose acceptance criteria for the beams.

6.7 Acknowledgments

The authors gratefully acknowledge the financial support provided by the Natural Sciences and Engineering Research Council of Canada (NSERC) for the Canadian Seismic Research Network (CSRN).

6.8 References

AISC (American Institute of Steel Construction). (2010a). "Seismic Provisions for Structural Steel Buildings." *ANSI/AISC 341-10*, Chicago, IL.

ASCE (American Society of Civil Engineers). (2013). "Seismic evaluation and rehabilitation of existing buildings." *ASCE/SEI 41-13*, Reston, VA.

Balazadeh-Minouei, Y., Koboevic, S., and Tremblay, R. (2017a). "Seismic Assessment of Existing Steel Chevron Braced Frames." Submitted to *Journal of Structural Engineering, ASCE*.

Balazadeh-Minouei, Y., Koboevic, S., and Tremblay, R. (2017b). "Seismic evaluation of a steel braced frame using NBCC and ASCE 41." *Journal of Constructional Steel Research,* http://dx.doi.org/10.1016/j.jcsr.2017.03.017.

Bech, D., Tremayne, B., and Houston, J. (2015). "Proposed changes to steel column evaluation criteria for existing buildings." *Proc. Second ATC & SEI Conf. on Improving the Seismic Performance of Existing Buildings and Other Structures*, American Society of Civil Engineers, San Francisco, CA.

Chen, L., Tremblay, R., and Tirca, L. (2012). "Seismic Performance of Modular Braced Frames for Multi-Storey Building Application," *Proceedings of the 15th World Conference on Earthquake Engineering*, Lisbon, Portugal, Paper No. 5458.

CSA (Canadian Standards Association). (1978). "Limit states design of steel structures." *CAN3 S16.1-M78*, Toronto, ON.

CSA (Canadian Standards Association). (2009). "Design of Steel Structures." *CSA-S16-09*, Toronto, ON.

Erduran, E., Dao, N.D., and Ryan, K.L. (2011). "Comparative response assessment of minimally compliant low-rise conventional and ase-isolated steel frames," *Earthquake Engineering and Structural Dynamics*, 40, 1123-1141.

Foutch, D.A., Goel, S.C., and Roeder, C.W. (1987). "Seismic testing of full-scale steel building—Part I." *Journal of Structural Engineering, ASCE*, 10.1061/(ASCE)0733-9445(1987)113:11(2111), 2111–2129.

ICBO (1979) Uniform Building Code 1979 "International Conference of Building Officials (ICBO)", Long Beach, California.

Khatib, I.F.. Mahin, S.A., and Pister, K.S., (1988). "Seismic behavior of concentrically braced steel frames." Report UCB/EERC-88/01. *Earthquake Engineering Research Center*, University of California, Berkeley, CA.

Lai, J.-W., and Mahin, S.A. (2015). "Strongback System: A Way to Reduce Damage Concentration in Steel-Braced Frames" *Journal of Structural Engineering, ASCE*, 141,9: DOI: 10.1061/(ASCE)ST.1943-541X.0001198.

Martini, K., Amin, N., Lee, P. L., & Bonowitz, D. (1990). "The Potential Role of Non-Linear Analysis in the Seismic Design of Building Structures," *Proceedings of Fourth U.S. National Conference on Earthquake Engineering*, 2, 67-76.

McKenna, F. and Fenves, G.L. (2004). "Open System for Earthquake Engineering Simulation (OpenSees)." *Pacific Earthquake Engineering Research Center (PEER)*, University of California, Berkeley, CA. (http://opensees.berkeley.edu/index.html)

Merzouq. S., and Tremblay, R. (2006), "Seismic Design of Dual Concentrically Braced Steel Frames for Stable Seismic Performance for Multi-Storey Buildings," *Proceedings 8th U.S. National Conference on Earthquake Engineering*, San Francisco, CA, Paper 1909.

Mitchell, D., Paultre, P., Tinawi, R., Saatcioglu, M., Tremblay, R., Elwood, K., Adams, J., and DeVall, R. 2010. Evolution of seismic design codes in Canada. *Canadian Journal of Civil Engineering*, 37(9):1157-1170.

Mottier, P., Tremblay, R., and Rogers, C. (2017). "Seismic Retrofit of Existing Low-Rise Steel Buildings in Eastern Canada using Rocking Braced Frame System." *Earthquake Engineering and Structural Dynamics* (submitted).

NRCC (National Research Council of Canada). (2010). (1980). "National building code of Canada 2010, 13th ed., 1980, 8th ed." Ottawa, ON.

Packer, J.A., Chiew, S.P., Tremblay, R., and Martinez-Saucedo, G. (2010). "Effect of material properties on hollow section performance." *Structures and Buildings*, 163, 6, 375-390. doi: 10.1680/stbu.2010.163.6.375.

Pollino, M., Slovenec, D., Qu, B., and Mosqueda, G. (2017). "Seismic rehabilitation of concentrically braced frames using stiff rocking cores." *Journal of Structural Engineering, ASCE*, 143, 9: DOI: 10.1061/(ASCE)ST.1943-541X.0001810.

Qu, B., Sanchez-Zamora, F., and Pollino, M. (2014). "Transforming Seismic Performance of Deficient Steel Concentrically Braced Frames through Implementation of Rocking Cores," *Journal of Structural Engineering, ASCE*., 141, 5: DOI: 10.1061/(ASCE)ST.1943-541X.0001198

Rai, D., and Goel, S. (2003). "Seismic evaluation and upgrading of chevron braced frames." *Journal of Constructional Steel Research*, 59, 971-994.

Sen, A.D., Roeder, C.W., Berman, J.W., Lehman, D.E., Li, C-H., Wu, A-C., and Tsai, K-C. (2016). "Experimental Investigation of Chevron Concentrically Braced Frames with Yielding Beams," *Journal of Structural Engineering, ASCE*, 142, 12, doi.org/10.1061/(ASCE)ST.1943-541X.0001597.

Sen, A.D., Swatosh, M.A., Ballard, R., Sloat, D., Johnson, M.M., Roeder, C.W., Lehman, D.E., and Berman, J.W. (2017) "Development and Evaluation of Seismic Retrofit Alternatives for Older Concentrically Braced Frames," *Journal of Structural Engineering, ASCE*, 143,5, doi: 10.1061/(ASCE)ST.1943-541X.0001738.

Sorace, S.and Terenzi, G. (2008) "Seismic Protection of Frame Structures by Fluid Viscous Damped Braces," *Journal of Structural Engineering, ASCE*, 134, 1, 45-55.

Speicher, M.S., and Harris III, J.L. (2016). "Collapse prevention seismic performance assessment of new special concentrically braced frames using ASCE 41." *Engineering Structures*, 126, 652-666.

Symans, M., Charney, F., Whittaker, A., Constantinou, M., Kircher, C., Johnson, M., and McNamara, R. (2008). "Energy Dissipation Systems for Seismic Applications: Current Practice and Recent Developments." *Journal of Structural Engineering, ASCE, DOI: 10.1061/(ASCE)0733-9445(2008)134:1(3)*

Tremblay, R. (2003). “Achieving a Stable Inelastic Seismic Response for Concentrically Braced Steel Frames.” *Engineering Journal, AISC,* 40, 2, 111-129.

Tremblay, R., Chen, L., and Tirca, L. (2014). “Enhancing the seismic performance of multi-storey buildings with a modular tied braced frame system with added energy dissipating devices,” *International Journal of High-Rise Buildings*, 3, 1, 21-33

Whittaker, A.S., Uang, C.-M., and Bertero, V.V. (1990), “Experimental Seismic Response of Steel Dual Systems.” *Proceedings Fourth U.S. National Conference on Earthquake Engineering*, Palm Springs, California, 2, 655–664.

Yang, C.S., Leon, R.T., and DesRoches, R. (2008) “Design and behaviour of zipper braced frames,” *Engineering Structures,* 30, 1092–1100.

CHAPTER 7 GENERAL DISCUSSION

This chapter presents a discussion on the assessment methods and rehabilitation strategies that have been addressed in Chapters 4 to 6. Additionally, some aspects that provide directions for future research in the field of evaluation and retrofit of existing steel braced frames are discussed.

7.1 Evaluation of existing steel braced frames

Several experimental and numerical studies were performed to assess the seismic response of conventional constructions in the United States; however, there is a limited study on the seismic evaluation of existing steel braced frames designed in Canada prior to introduction of seismic provisions and detailing. Hence, it is required to provide a comprehensive study on the seismic evaluation of existing bracing systems.

7.1.1 Impact of the selection of evaluation methods on assessment results

Following evaluation methods were used for the assessment of 10-storey tension-only X-bracing and tension-compression chevron bracing systems:

- NBCC 2010
- Linear dynamic procedure of ASCE 41
- Nonlinear dynamic procedure of ASCE 41

In the available Canadian documents for the seismic evaluation of existing structures, acceptance criteria are not specified for structural elements. According to NBCC 2010 (NRCC 2010), initial assessment should be carried out using reduced loads corresponding to 60% of earthquake loads prescribed for new buildings that are established for a probability of exceedance of 2% in 50 years. When the deficiencies are detected, the retrofit should be conceived for higher force levels, preferably meeting the performance objective for new buildings that is implicitly defined as collapse prevention for a probability of exceedance of 2% in 50 years. In the United States, the ASCE 41-13 standard (ASCE 2013) should be used for the seismic evaluation of existing buildings. In this standard, two cases should be satisfied for the basic performance objective of existing buildings (BPOE). The existing structure must attain life safety performance level for seismic hazard with probability of exceedance of 20% in 50 years and collapse prevention

performance level under the seismic hazard with probability of exceedance of 5% in 50 years. In ASCE 41, less stringent performance objectives are specified for existing buildings compared to new structures considering that: (i) existing buildings have a shorter remaining life, (ii) more recent constructions do not become deficient with every more conservative changes in design codes, and (iii) the high cost that associated with the higher level of performance which can not be justified in view of the incremental benefit. In this study, the existing concentrically braced frames were evaluated by NBCC 2010 to provide an initial assessment of these structures. As there are no specific acceptance criteria in the Canadian codes for the seismic evaluation of existing buildings, ASCE 41 was also selected to explore the potential for savings by the application of acceptance criteria specifically defined for the seismic assessment and retrofit.

Evaluation of both tension-only X-braced frame and tension-compression chevron braced frame for 60% of the 2010 NBCC seismic loads showed that the retrofits are required. For 100% of NBCC 2010 loads, the retrofit would be extensive. The evaluation results obtained for the tension-only X-braced frame using ASCE 41 LDP were less severe compared to those when 100% NBCC seismic loads were applied. Also, for both chevron braced frames studied the application of ASCE 41 LDP showed that all braces had adequate strength which was less severe than NBCC evaluation. However, the evaluation of beams per ASCE 41 LDP was more severe compared to that under 100% of NBCC loads; because, according to NBCC 2010, the beams are not evaluated for unbalanced brace load effects anticipated after brace buckling.

ASCE 41 NDP was performed using models reproducing nonlinear responses associated to deformation-controlled actions in the bracing members and models accounting also for nonlinear response related to force-controlled actions in beams and columns. NDP with partial nonlinear modelling limited to deformation-controlled actions provides realistic estimates of all force-controlled actions, and it permits a rapid insight into potential seismic deficiencies that are related to those actions. This model can simulate the intended structural response with inelastic deformations limited to deformation-controlled actions, and it can be used to develop a final retrofit scheme. NDP with nonlinear modelling of both deformation-and force-controlled actions allows more accurate representation of complex failure mechanisms, and it provides a more accurate estimation of the structure capacity. However, the failure in one component can halt the analysis; that element should be retrofitted and the analysis should be repeated, which can be a time consumption procedure. Contrary to the ASCE 41 LDP evaluation results, ASCE 41 NDP

with partial nonlinear modelling limited to deformation-controlled actions indicated that the braced frame was prone to concentration of inelastic brace deformations and large story drifts which led to the excessive brace plastic deformations as well as large bending moments in the braced frame columns. Also, ASCE 41 NDP evaluation results showed strong axis beam buckling in the vertical plane before brace buckling and beam ductile flexural yielding which led to frame collapse for both cases. The application of NDP with partial nonlinear modelling limited to deformation-controlled actions indicated significant downward deflection of the beams that led to soft-story response. In this model, brace tension yielding could not develop as a result of the beam flexibility. This deficiency can not be identified when the ASCE 41 LDP acceptance criterion is used for the assessment of beams in the chevron braced frames.

In general, NBCC 2010 provides more conservative assessment results of the concentrically braced frames compared to ASCE 41. However, this code is less conservative for the evaluation of the beams in the chevron braced frames. ASCE 41 LDP can not consider all possible failure modes that occurred in the beams of the chevron braced frames obtained by ASCE 41 NDP. Also, the ASCE 41 LDP assessment results on the braces of the chevron braced frame were less stringent than ASCE 41 NDP. NDP with partial nonlinear modelling limited to deformation-controlled actions can provide a rapid insight to identify the potential deficiencies of force-controlled actions, and it can be used to define a final retrofit solution. Note that these evaluation results are limited to a 10-storey tension-only X-braced frame and 10- and 3-storey chevron braced frames.

7.1.2 Influence of selection of selected ground motions in nonlinear dynamic analysis

To perform nonlinear time history analysis of the concentrically braced frames, a group of ground motion records were selected. For the assessment of the tension-only X-braced frame, two sets of three and ten records were considered. They were selected from a broader ensemble of 20 far-field records matching the dominant magnitude-distance scenarios proposed by Atkinson (2009) for western Canada. According to this reference, the selected records should have the lowest standard deviation (SD) of the ratio between the NBCC and ground motion spectra ($S/S_{a,gm}$) in the 0.2-1.5 T_1 period range and a mean $S/S_{a,gm}$ value should be between 0.5 and 2.0 in that period

range. So, the selected records were scaled such that the average spectrum did not fall below the NBCC 2010 spectrum in the 0.2-1.5 T_1 period range. T_1 is the period from dynamic analysis.

For the scaling of the records that have been used for the evaluation of the chevron braced frames, a procedure described in ASCE 41-13 was considered. This procedure assumes 3D analysis under pairs of orthogonal components and a unique scaling factor is applied to both components of each pair. As a two-dimensional analysis was considered for the assessment of the chevron braced frames, the procedure adapted for a 2D analysis and one record for each pair was selected. In this procedure, a square root of the sum of the squares (SRSS) spectrum was determined for each of the 10 pairs of horizontal components. Each pair was scaled such that the average of the SRSS spectra of all pairs was above the NBCC 2010 spectrum. For each pair, the component with the response spectrum closest to the average of the SRSS spectra was selected over the period range of interest. In this study, the average spectrum of the 10 selected components fell below the NBCC 2010 design spectrum of the period range considered. Therefore, a second scaling factor was applied to bring the average spectrum above the target spectrum. Note that the selected scaled records for the assessment of the chevron braced frames were also considered for the retrofit of the 10-storey tension-compression chevron braced frame.

For the assessment of the existing structures using ASCE 41, the mean results can be used from ten ground motion records, while the maximum response of the parameter should be considered for a set of three records. The assessment results of the ASCE 41 NDP on the tension-only X-braced frame showed that the selection of ground motions may have a significant impact on the evaluation results such as the assessment of braces, columns and beams.

As the number of selected records for the assessment and retrofit of concentrically braced frames is limited to ten, increasing the number of historical ground motion records can affect the evaluation results, and more or less cost effective retrofit solutions can be proposed. Note that the selected ground motions were recorded in past shallow crustal earthquakes, and two more scenarios that are common in the Vancouver area are not considered in this study. These scenarios are deep sub-crustal and large magnitude interface earthquakes (Tremblay et al. 2015). Thus, the consideration of the records from all three scenarios and using NBCC 2015 (NRCC 2015) to scale the records can impact the assessment and retrofit of concentrically braced frames.

7.1.3 Adaption of ASCE 41 linear procedure into Canadian normative context

As no acceptance criteria were specified for structural components in the Canadian documents, the available procedures of ASCE 41 were adapted to use in the Canadian normative context. For linear dynamic procedure, the response spectrum analysis method was performed using the NBCC design spectrum. The evaluation of deformation controlled actions was done using $R_d R_o = 1$ in Equation 2 of Section 4.3 to remove the effect of the ductility-related force reduction factor and the overstrength-related force reduction factor on the results, and then the m-factor was applied to account for the expected ductility of the member. This factor is specified in Equation 3 of Section 4.5.2. The expected material properties were also employed for deformation-controlled actions. For the assessment of brace connections, the nominal material properties were used and the resistance factor ϕ_u was taken equal to 1.0 in Equations 13 and 14 of Section 4.3.4. To evaluate beams and columns, Equations 15 to 17 was employed. In these equations, P_{CL} is the axial resistance of the member, and it should be taken equal to the factored axial resistance C_r in CSA S16-09 determined with the nominal F_y value and $\phi = 1.0$. The flexural strengths M_{CEx} and M_{CLx} are the factored bending resistances M_r in CSA S16-09 computed with the expected and nominal material properties, respectively, and $\phi = 1.0$. For nonlinear dynamic procedure, the design objective of new buildings in NBCC was adapted for the ASCE 41 evaluation, which is collapse prevention for the probability of exceedance of 2 % in 50 years. This performance objective can provide direct comparison with the seismic evaluation under 100% of the NBCC 2010 seismic loads.

7.1.4 Effect of the boundary condition on the seismic evaluation of concentrically braced frames

In the real structures, the bases of columns are not totally pinned. Also, the gravity columns are presented as part of the structures which can provide stiffness for the system. The splices of columns are not pinned in practice, and they can create the fixity at the ends of the columns. For the retrofit of the existing chevron braced frame, all parameters that mentioned above were considered to use all possible stiffness provided by the existing elements in the system. These factors could affect the seismic response of the 10-storey chevron braced frame; however, they were not sufficient to improve the seismic behaviour of the braced frame, extensively. For

example, the fixity of the column at the base of the chevron braced frame that retrofitted by a truss could prevent column buckling at this level.

As mentioned in Chapter 4, the column buckling occurred at the 1st level of the 10-storey tension-only X-braced frame using nonlinear dynamic procedure, while the columns were pinned at the base. In reality, the columns are not totally pinned at the base of the structures; therefore, the numerical models of these braced frames can be updated using the fixed boundary condition at the base of columns to reflect the extreme case scenario. This modification may affect the seismic response of steel columns at the bottom level of the studied frame.

7.1.5 Beam response in chevron braced frames

In the studied chevron braced frames, beams were light beams supporting limited gravity loads. The seismic evaluation of the 10- and 3-storey chevron braced frames using nonlinear dynamic procedure (NDP) showed strong axis beam buckling in the vertical plane which occurred prior to brace buckling. A detailed 3D finite element analysis was performed to further investigate the seismic response of the beam. The beam buckling over half of the total beam length was also confirmed by this analysis. Another type of failure mode that observed in the nonlinear time history analysis using OpenSees was beam ductile flexural yielding. Both beam buckling and beam yielding led to frame collapse. In the analyses, where elastic elements were used to model the beams, significant downward deflection of the beams occurred that led to soft-story response. As a result of the beam flexibility, brace tension yielding could not develop. This deficiency could not be identified using ASCE 41 LDP acceptance criteria for the assessment of beams of chevron braced frames. According to ASCE 41 LDP, beams of chevron braced frames should be evaluated as force-controlled, and they should resist unbalanced brace load effects in combination with gravity loads. The failure of beam buckling was also observed under ground motions with reduced amplitudes scaled to match design spectra corresponding to 5% and 10% probabilities of exceedance in 50 years. Note that 60% of NBCC seismic loads fell between 5% and 10% probabilities of exceedance in 50 years; hence, the beam buckling would also occur at this level of seismic load.

Experimental study performed by Sen et al. (2016a) on four full-scale two-storey chevron braced frame with weak beams showed that such beams in non-ductile chevron braced frames are not detrimental for frame behaviour. Sen argues that beam flexural yielding could provide additional

mechanism of energy dissipation. Figure 7.1 shows the test setup of first specimen representative of the non-seismic concentrically braced frame (NCBF). The beam sections were W16x45 (W410x67) and W24x94 (610x140) at the first and second levels, respectively, which were common cross sections for NCBFs. Test results showed that, while inadequate brace compactness and brace connection details led to fractures at small drifts, unbalanced brace loads acting on the beams did not have a negative impact on the system ductility. They concluded that the beams of such systems with axial-flexural demand-to-capacity ratios (DCRs) of 2.5 or less do not have the priority for seismic retrofit. Instead, potential brace fracture is the main deficiency of the frame, and thus braces should be retrofitted. Sen's study did not include light beams with smaller tributary gravity loads, and the quasi-static loading protocol was the only type of loading that applied to the braced frames. The study conducted within the scope of this thesis focused on beams that carried small tributary gravity load, which led to small sections (W310x44.5). This section is smaller than the sections that have been used in the experimental tests by Sen et al. (2016a); but could be found in existing chevron braced frames. Therefore, although beam flexural yielding could be beneficial to overall seismic response of non-ductile existing chevron braced frames, a caution should be exercised when dealing with light frame beams.

Figure 7.1: Overview of specimen (Sen et al. 2016a).

To verify the numerical results obtained for the existing chevron braced frame and validate the need to retrofit this frame, an experimental test could be performed. This test could produce the data for the evaluation of exiting chevron braced frames designed in 1980's. No experimental investigation on chevron braced frames designed in 1980's in Canada has been carried out so far. Such experimental study could be carried out on the first two storeys of the 10-storey braced frame. Data could be extracted from the nonlinear response history analysis of the steel braced frame using OpenSees, and the histories of lateral and vertical loads could be applied to the ends of the specimen. Such experimental results could be used to validate the numerical results and propose the required retrofit strategies.

As the lateral bracing of beams was not considered in 1980's design practice, the out of plane buckling of these structural members can cause a potential deficiency for the frame. In this thesis, a fibre-based (OpenSees) and a 3D finite element (ABAQUS) programs were used for the modeling of the braced frame. As the lateral torsional buckling and local buckling of structural

members can not be investigated by OpenSees, a 3D finite element analysis was considered to investigate the lateral torsional buckling and local buckling modes. Note that the modeling of all structural members in ABAQUS is complicated and time-consuming. Thus, the proposed model was limited to the modeling of braces and beams in the critical storey. The seismic demands obtained from the analysis of the frame in OpenSees were imposed to the 3D finite element model developed in ABAQUS. The response of beams and braces were monitored, while the failure occurred in the system. The ABAQUS results showed the possibility of lateral torsional buckling of beams. The retrofit strategies can be proposed to prevent this failure mode, and provide a cost-effective retrofit solution. For instance, the composite deck can provide the lateral bracing for the top flange of the beam. The effect of the composite deck should be modelled in detail in ABAQUS to evaluate the efficiency of the proposed retrofit scheme.

7.1.6 Connection modelling in braced frames

As mentioned in section 2.4, the inadequate capacity of brace connections was one of the most common deficiencies in exiting concentrically braced steel frames. Tremblay et al. (2012) performed a hybrid seismic simulation on a sub-structure of the fictitious 4-storey concentrically braced frame designed in accordance with NBCC 1980 (NRCC 1980) and CSA S16.1-M78 (CSA 1978). In this study, quasi-static cyclic tests were conducted on brace specimens. During the tests, failure was observed in the brace end connection, as shown in Figure 7.2. As these tests were performed on the braced frames designed by NBCC 1980 and CSA S16.1-M78, their results are valuable to be used in the numerical studies. In this research study, the sophisticated models included inelastic response for braces, beams and columns. However, elastic elements were considered for the modelling of brace connections. Therefore, the application of inelastic elements in accordance with the test results would be an interesting subject, as the effect of brace connections can be determined on the seismic response of the existing braced frames.

Figure 7.2: Failure in brace connection (Tremblay et al. 2012).

7.1.7 Force-delivery reduction factor

In ASCE 41, two methods are considered to determine the force-controlled action, Q_{UF}. In the first method, Q_{UF} should be taken as the maximum action that can be developed in a component based on a limit-state analysis. In this method, the expected strength of the components should be considered to deliver the force to the component under consideration, or the maximum action that can be developed in the component as limited by the nonlinear response of the structure. In the second method, Q_{UF} should be determined by Equation 1.

(1) $$Q_{UF} = Q_G \pm \frac{Q_E}{C_1 C_2 J}$$

In this equation, Q_E and Q_G are earthquake load and gravity load, respectively, C_1 is the modification factor that relates expected maximum inelastic displacements to displacements calculated for linear elastic response, C_2 is the modification factor to consider the effect of pinched hysteresis shape, cyclic stiffness degradation, and strength deterioration on the maximum displacement response, and J is the force delivery reduction factor, calculated as the smallest demand capacity ratio (DCR) of components in the load path delivering force to the component. In order to calculate the demand capacity ratio, DCR, the value of Q_{UD} should be divided by Q_{CE}.

Both methods were used to define the column forces in the existing tension-only X-braced frame and tension-compression chevron braced frame (Balazadeh-Minouei et al. 2017a and Balazadeh-Minouei et al. 2017b). Note that the first method was not considered in ASCE 41-06 (ASCE

2006). Therefore, a new approach was proposed to investigate the appropriateness of the force delivery reduction factor (Balazadeh-Minouei et al. 2014a). This approach was named J-Individual, and it was obtained from the concept of capacity design. J-Individual is calculated using the demand capacity ratio (DCR) of the components at each level to deliver the force to the component located at that level. The axial forces in the columns of the tension-only X-bracing system were calculated using the J-factor specified by ASCE 41 and J-Individual, as shown in Figure 7.3. In this figure, the J-factor calculated by Equation 1 is named J-Minimum. In Figure 7.3, the axial forces of the columns determined from J-Minimum are significantly higher than those calculated by J-Individual. The forces calculated by the J-Individual approach are similar to the maximum demands determined from the nonlinear response history analysis with Model B from the three selected ground motions. As it was expected, the demands determined from nonlinear time history analyses are the same as the demands defined by J-Individual, because this factor was defined by the concept of capacity design.

In ASCE 41, beams, their connections, and supporting members in chevron braced frames must resist unbalanced brace load effects in combination with gravity loads, and they should be considered as forced-controlled actions. The unbalanced load effects should be calculated using the expected yield capacity of the brace in tension and 0.3 of the expected capacity of the brace in compression. This procedure was named "P_{UF} from limit analysis" in Figure 7.4. It was obtained from the concept of capacity design, and it followed the same trend that was considered to define J-Individual. The ASCE 41 acceptance criterion was used to determine the column forces, and the demands were compared with the column forces defined by J-Minimum. Figure 7.4 shows the axial forces in the columns of inverted V-bracing system using J-Minimum, PUF from limit-state analysis and PUF from records. Predictions of PUF from J-Minimum underestimate the column force demand whereas limit analysis provides a conservative force estimate. The comparison of the column force demands using J-Minimum by the average axial compression demands from historical ground motion records showed that J-Minimum underestimates column axial forces at five levels of the braced frame.

These results indicated that the application of J-factor does not provide a realistic estimation of column axial forces in tension-only X-braced frame and tension-compression chevron bracing system. However, limit-state analysis can provide an appropriate assessment of structural

members. This method considers the expected strength of the deformation-controlled components to define the demands on force-controlled elements, which is the concept of the capacity design.

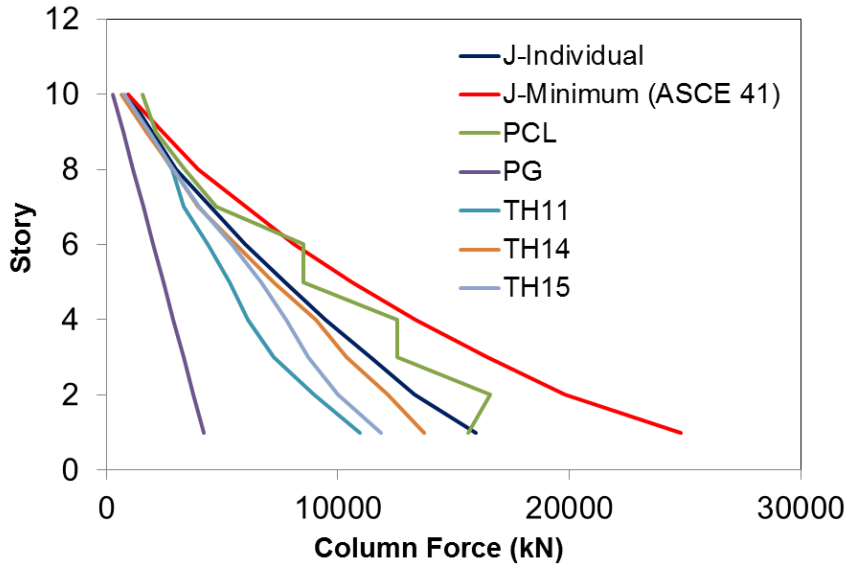

Figure 7.3: Axial force demands induced on the columns of tension-only X-braced frame.

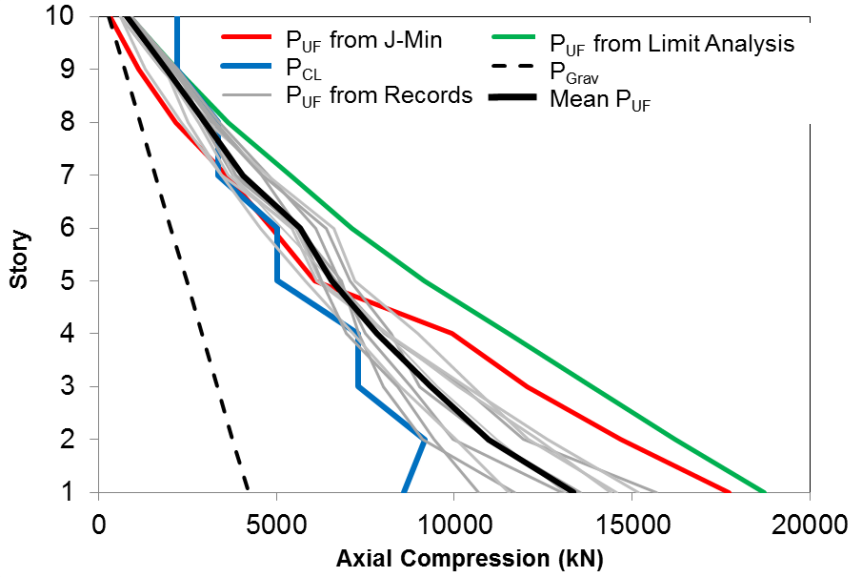

Figure 7.4: Axial force demands on the columns of chevron braced frame.

7.1.8 Ductility of steel columns

The seismic evaluation of steel columns of tension-only X-braced frame showed that the acceptance criteria specified in the current ASCE 41 for components subjected to combined axial compression and flexure in linear dynamic procedure are conservative. The results from a detailed 3D finite element analysis indicated that the steel column can exhibit a ductile response by the formation of plastic hinges at both ends of the member even when the ratio of column force to column lower-bound axial compressive strength exceeds 0.5. Also, the assessment of columns in the retrofitted chevron braced frame using a truss with a hinge indicated that the columns should be retrofitted at the first level in accordance with the ASCE 41 criteria. However, these columns had sufficient axial compressive strength, and no flexural buckling occurred in the nonlinear time history analysis. If the columns are retrofitted for the combined axial compression and flexure, the retrofit work on the existing columns will be extensive, and the imposed demands on the existing foundation will be increased; therefore, it may be required to retrofit the foundation.

To investigate the ductility of steel columns and validate the numerical results, a test program was developed. In this experimental program four full-scale W-shaped sections with 4m tall were tested. The W250x101 column specimens were selected, which were classified as Class 1 in accordance with CSA S16. The details of experimental study including the features of Multi-Directional Hybrid Testing System, the loading protocols and experimental results are mentioned in APPENDIX A.

7.2 Retrofit of existing steel braced frames

The seismic assessment of the existing 10-storey tension-only X-braced frame using NDP with partial nonlinear modelling limited to braces showed that the columns required to be retrofitted at levels 1 to 7 and at level 9. The results of this model were used for the retrofit of columns. The seismic performance of the retrofitted braced frame was evaluated using the model simulating the nonlinear response of the braces and columns, because bending inelasticity was expected in the columns. The evaluation results of the retrofitted tension-only X-braced frame showed that braces and beams had sufficient strength for a set of ten ground motions records. The columns had adequate axial strength; however, the assessment of columns for combined axial compression and

bending using ASCE 41 indicated that the columns were critical at levels 8 and 9. Note that the study on the ductility of steel columns showed that the ASCE 41 acceptance criteria are conservative for the evaluation of components subjected to axial compression and flexure. If a set of three records was considered for the assessment of the retrofitted braced frame, the braces at upper levels, and the beams at the bottom and at the middle levels had inadequate strength. The columns had insufficient axial strength at the bottom and middle levels. These results showed the sensitivity on the selection of number of ground motions to the extent of retrofit work. To provide the cost effective retrofit strategies to improve the seismic response of the existing 10-storey braced frame, using a set of ten records or more can provide a reasonable retrofit scheme compared to the application of a set of three records. As mentioned earlier, the braces were satisfactory for a set of ten records in accordance with ASCE 41 NDP; however, the existing braces did not provide uniform inelastic deformations over the frame height to minimize variations in story drifts that induce detrimental flexural demands on columns and cause the soft-storey response. Hence, satisfying the ASCE 41 acceptance criterion is not sufficient to provide a satisfactory global response.

The evaluation of the existing 10-storey chevron braced frame indicated that the beams are the most deficient elements in the system. Therefore, the first retrofit solution was the strengthening of these structural members. The ASCE 41 acceptance criteria specified for beams of chevron braced frames were used for the retrofit of these members. The application of ASCE 41 criteria showed that very large W-shaped beam sections are required, which may not be feasible in practice. The evaluation results of this retrofit strategy using Model D with inelastic response for all structural members showed that the column buckling occurred. The objective of this study was the application of the traditional approach and retrofit of the existing chevron braced frame using cost effective retrofit solutions. Thus, the retrofit of existing columns for the imposed high level of axial loads from the large beam cross sections can increase the extent of the retrofit work. The retrofit of the foundation may also be required as a result of large demands imposed to this element by the retrofitted chevron braced frame columns.

Four retrofit schemes were considered to modify the members of the existing braced frame. The braces were replaced with the main objectives of minimizing the force demand on beams, columns, and foundations while achieving uniform demand to capacity ratios along the frame height to avoid soft-story response. In the models, all possible stiffness that can be provided by

the system was considered to reduce the extent of the retrofit work and the cost, including gravity columns, fixity at the base and flexural continuity of column splices. In the last retrofit scheme, larger brace sizes were selected to increase the frame lateral resistance while keeping the expected base shear below the capacity of the existing foundation. In all four cases, the beams were replaced; however, the existing columns could be kept. For all strategies, frame collapse was observed as a result of a soft-storey response; however, the number of collapse of the last scheme was less than other strategies. This scheme was considered as a selected retrofitted braced frame.

Two-dual options were proposed in which the capacity of the selected retrofitted braced frame was adjusted such that no alterations required to the existing columns and the foundation. The selected options were the application of a low-ductility steel moment frame and also using a stiff truss to prevent the soft-storey response. Two configurations were proposed for the latter case including a continuous truss and a truss with a hinge at the mid-height. Among the selected retrofit strategies, the truss with a pin at the mid-height was the most cost-effective retrofit solution in terms of steel tonnage, and it imposed less base shears than other retrofit solutions.

Compared to other retrofit strategies, a new braced frame designed in accordance with the provisions of CSA S16 required the more steel except one case and it imposed larger forces on the existing foundation. It would require replacing the existing columns, and repairing the existing foundation, which would cause major challenges in the practice.

The truss with a hinge at the mid-height was considered for the retrofit of existing chevron braced frame. The evaluation results showed that columns required to be retrofitted. The seismic response of this retrofit scheme indicated that limited number of braces required to be retrofitted. Also, the beams at the first four levels should be repaired to prevent beam buckling. Therefore, the strengthening of the existing chevron braced frame was limited as a result of the capacity of the truss to mitigate soft-storey. The required steel tonnage of this retrofit was less than the braced frame that needed to change all braces and beams.

To retrofit the existing chevron braced frame, other options are possible:

1) This study was focused on the application of traditional approach and retrofit the existing chevron braced frame. However, other options including base isolation, rocking system and passive energy dissipation devices can be considered.

2) In this study, the selected historical ground motion records used to perform the assessment and retrofit of existing concentrically braced frames were scaled to match the 2010 NBCC design spectrum. The selected set of ground motions lack two scenarios including deep sub-crustal and large magnitude interface earthquakes (Tremblay et al. 2015). As such, the ground motion data can be improved to cover all three scenarios including shallow earthquakes, deep sub-crustal or in-slab events and large magnitude interface or subduction earthquakes, and use NBCC 2015 (NRCC 2015) for scaling the records. The application of all three scenarios can affect the required steel tonnage that is required for the retrofit of the existing chevron braced frame.

3) The beams should be retrofitted to prevent the in-plane instability. Several retrofit strategies including the application of composite action for beams and welding steel plates to the webs of these members can be used to increase their compressive resistance.

4) The beams can be retrofitted such that flexural plastic hinges form within the beams away from the columns such as the application of reduced beams section (RBS) connection shown in Figure 7.6. This retrofit scheme would result in increasing the flexural ductility of the beams as a part of the existing chevron bracing systems, while reducing the construction cost. This scheme can be effective if the frame collapse does not occur as a result of soft-storey response.

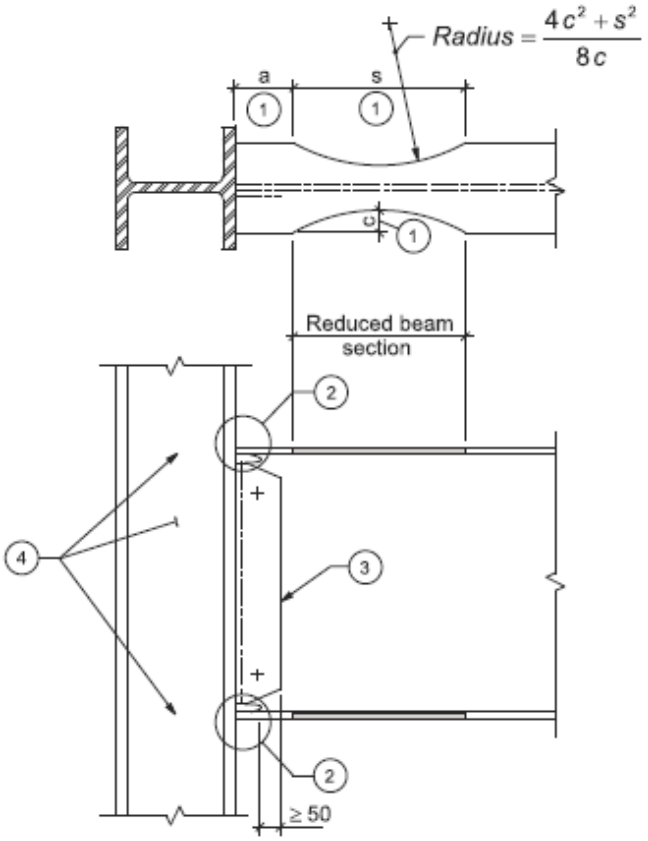

Figure 7.5: Reduced Beam Section (RBS) Connection (CISC 2008).

This study was performed for a 10-story chevron braced frame. Thus, the proposed retrofit solutions can be changed for low-rise and high-rise buildings, and other options can be used for these structures.

CHAPTER 8 CONCLUSION AND RECOMMENDATIONS

In this chapter, the main conclusions and findings of the research study are summarized and the areas that required further investigations are identified. The main objectives of this Ph. D. dissertation were:

1) Evaluate the seismic performance of multi-storey concentrically braced frames with focus on tension-only and chevron braced frames to identify the deficiencies of these systems and compare the assessment results obtained from NBCC 2010 and ASCE 41-13 evaluation methods. The evaluation should include an explicit verification of yielding and buckling limit states for the main structural components (braces, beams and columns) and examine the global stability performance of braced frames.

2) Examine the possibility of allowing flexural yielding in beams of chevron braced frames with consideration of the anticipated high compression force demand.

3) Assess the appropriateness of current ASCE 41 acceptance criteria for braced frame columns subjected the high axial compression combined with drift induced flexural demand and/or plastic rotations; and

4) Propose retrofit solutions using ASCE 41-13 procedures to improve the seismic response of seismically deficient chevron braced frames.

This chapter reviews the main conclusions of the study presented in the thesis. The recommendations for future investigations are also discussed.

8.1 Summary and conclusions

In Canada, seismic design provisions were introduced in the 1941 edition of NBCC, and special seismic design and detailing requirements for steel structures were incorporated in the CSA S16 standard in 1989. Thus, steel buildings constructed before the 1990's may not develop the ductile seismic response implied by the reduced seismic loads specified in NBCC 1980.

In the 1980’s, concentrically braced frames with tension-only X-braced frame and tension-compression chevron braced frame were commonly used to resist lateral loads in steel buildings in Canada. To assess the seismic response of such systems, a 10-storey tension-only X-braced frame and 10- and 3-storey chevron braced frames were selected in this research. The overall

height of the 10- and 3-storey braced frames were respectively 40.23 m and 12.49 m, and they were designed in accordance with the provisions of the 1980 NBCC and the CSA S16.1-M78 steel design standard. The structure was located on class C site in Vancouver, British Columbia, Canada. Back-to-back double angles were used for braces of concentrically braced frames to reflect construction practices of the 1980's.

The seismic performance of concentrically braced frames was examined using NBCC 2010 and ASCE 41-13. According to NBCC 2010, initial assessment was carried out for reduced loads corresponding to 60% of earthquake loads prescribed for new buildings that are established for a probability of exceedance of 2% in 50 years. If the deficiencies of existing structures are identified for this load level, the retrofit should be designed for higher force levels, preferably meeting the performance objective for new buildings, i.e. collapse prevention for a probability of exceedance of 2% in 50 years. Also, the ASCE 41-13 Tier 3 procedure was considered using both LDP and NDP to explore the potential for savings when using provisions specifically developed for seismic evaluation and retrofit. For ASCE 41 NDP, numerical frame models reproducing nonlinear responses associated to deformation-controlled actions in the bracing members only as well as frame models accounting for nonlinear response for both deformation- and force-controlled actions in primary components were used.

The following conclusions can be drawn from this study:

- The initial assessment of the existing tension-only X-braced frame and chevron braced frame using 60% of the 2010 NBCC revealed that both tension-only X-braced frame and chevron braced frame needed to be retrofitted. For the tension-only X-braced frame, the application of 100% of NBCC 2010 seismic loads to determine the extent of the retrofit showed that most braces and columns, all brace connections, and some of the beams would require strengthening. For the 10- and 3-storey chevron braced frames, all braces and brace connections and most of the beams should be repaired. Most columns of the 10-storey chevron braced frame and columns at the bottom of the 3-storey braced frame would also need strengthening.
- For both braced frame configurations, the ASCE 41 LDP evaluation was generally less severe compared to the evaluation under 100% NBCC 2010 seismic loads. However, the ASCE 41 assessment of the beams of the chevron braced frames was more critical because beams in

ASCE 41 must be verified for unbalanced brace load effects anticipated after brace buckling, which is not the case in the NBCC.

- The application of ASCE 41 NDP with partial nonlinear modelling limited to deformation-controlled actions provides realistic estimates of all force-controlled actions and allows a rapid insight into potential seismic deficiencies related to force-controlled actions. The frame model with inelastic deformations limited to deformation-controlled actions can simulate the intended structural response and can be used to develop a final retrofit solution.
- ASCE 41 NDP evaluation of concentrically braced frames showed pronounced concentrations of inelastic brace deformations and large storey drifts. This response could not be predicted by ASCE 41 LDP.
- When using the ASCE 41 LDP assessment of force-controlled actions in concentrically braced frames, a limit-state analysis is preferred to the elastic analysis with the force delivery reduction factor *J*, as limit-state analysis results in more realistic force demands.
- Failure of beams by buckling was observed in the nonlinear time history analysis using OpenSees and a detailed 3D finite element analysis. This limit states should be considered for the evaluation of chevron braced frames using ASCE 41 or NBCC.
- When elastic beams response was modelled in the analyses, the ASCE 41 NDP evaluation showed that beam flexibility in chevron braced frames may prevent the development of the brace yielding in tension, a behavior that could not be predicted by ASCE 41 LDP.
- Both numerical and experimental studies on steel columns showed that current ASCE 41 acceptance criteria for the evaluation of braced frame columns are too conservative. Steel columns could sustain large plastic rotations without buckling when supporting axial compression loads above $0.5\,P_{CL}$.
- For the retrofit of a 10-storey seismically deficient chevron braced frame, the addition of a stiff vertical elastic truss with a hinge at the building mid-height was found to form the most economical retrofit scheme in terms of steel tonnage and base reactions. With this retrofit solution, soft-storey response was eliminated, storey drifts were kept lower than the limit specified for post-disaster buildings, and the inelastic demand on individual frame components was minimized.

– Nonlinear dynamic procedure is required to verify soft-storey response and global collapse in the seismic evaluation and retrofit of steel concentrically braced frames.

8.2 Recommendations

The results of this study raised additional questions that should be addressed in future research regarding the seismic evaluation and retrofit of existing steel concentrically braced frames. These issues are summarized below:

– Additional experimental and numerical studies should be performed to propose more realistic acceptance criteria for braced frame columns.

– Further study should be performed to determine the height beyond which nonlinear dynamic procedure is needed for seismic evaluation and retrofit of concentrically braced frames.

– The selected historical ground motion records used in this study were scaled to match the 2010 NBCC design spectrum. The selected set of ground motions lack two scenarios including deep sub-crustal and large magnitude interface events that are expected in southwest British Columbia (Tremblay et al. 2015). As such, the ground motion data can be improved to cover all three scenarios, and the procedure given in NBCC 2015 can be applied to select and scale the ground motion records.

– The numerical models of concentrically braced frames could be improved by using nonlinear elements for brace connections and beam-to-column connections to evaluate the seismic performance of these components.

8.3 Original contributions

The following original contributions were made in this study:

– The seismic performance of a tension-only X-braced frame and chevron braced frames designed in accordance with NBCC 1980 and CSA S16.1-M78 was evaluated using NBCC 2010 and ASCE 41-13 Tier 3 procedures.

– The effect of nonlinearity of structural members on the response of the braced frames was examined.

- The ASCE 41 assessment and retrofit methodology was adapted for the application in Canada.
- The response of beams of chevron braced frames was evaluated, and the limitation of ASCE 41 LDP for verifying possible failure modes for beams was identified.
- Current ASCE 41 acceptance criteria for components of steel braced frames subjected to combined axial compression and flexure were investigated by means of numerical and experimental studies.
- The need for an explicit verification of the satisfactory global seismic response in the evaluation and retrofit of concentrically braced frames was identified.

BIBLIOGRAPHY

Adluri, S.M.R., and Madugula, M.K.S.1995. Residual Stresses and Initial Out-of-Straightness of Hot-Rolled Steel Angles. Proc. 1995 SSRC Annual Technical Meeting, Kansas City, MO: 115-126.

Aguero, A., Izvernari, C. and Tremblay, R. 2006. "Modelling of the seismic response of concentrically braced steel frames using the OpenSees analysis environment." Advanced Steel Construction, 2: p. 242-274.

AISC (American Institute of Steel Construction). 2010a. Seismic Provisions for Structural Steel Buildings, ANSI/AISC 341-10, American Institute of Steel Construction, Chicago, IL.

AISC (American Institute of Steel Construction). 2010b. Specification for Structural Steel Buildings. ANSI/AISC 360-10, Chicago, IL.

Allen, D. E., Bell, L., Cherry, S., Knoll, F., Lo, R., and Rainer, J.H. 1995. "Guideline for Seismic Upgrading of Building Structures." Institute for Research in Construction, National Research Council Canada, NRCC 38857.

Allen, D. E., Rainer, J.H. and Jablonski, A. M. 1992. "Guidelines for the Seismic Evaluation of Existing Buildings." Institute for Research in Construction, National Research Council Canada, NRCC 36941.

Anderson, J.C. 1975. Seismic behavior of K-braced frames. Journal of the Structural Division, ASCE, 101(10).

ASCE. 2013. Seismic evaluation and rehabilitation of existing buildings, ASCE/SEI 41-13. American Society of Civil Engineers, Reston, VA.

ASCE. 2010. Minimum design loads for buildings and other structures, ASCE/SEI 7-10, American Society of Civil Engineers, Reston, VA.

ASCE. 2006. Seismic Rehabilitation of Existing Buildings, ASCE/SEI 41-06. American Society of Civil Engineers, Reston, VA.

ASCE. 2003. Seismic evaluation of existing buildings, ASCE/SEI 31-03. American Society of Civil Engineers, Reston, VA.

ASCE. 1991. Guideline for Structural Condition Assessment of Existing Buildings. American Society of Civil Engineers, New York, New York.

Astaneh-Asl, A., S.C. Goel, and R.D. Hanson, 1985. Cyclic out-of-plane buckling of double-angle bracing. Journal of Structural Engineering, 111(5): p. 1135-1153.

Astaneh-Asl, A. and S.C. Goel, 1984. Cyclic in-plane buckling of double angle bracing. Journal of Structural Engineering, 110(9): p. 2036-2055.

ASTM (American Society for Testing and Materials). 2010. Standard specification for cold-formed welded and seamless carbon steel structural tubing in rounds and shapes. A500/A500M – 10a, West Conshohocken.

ASTM. 2002. Standard specification for general requirements for rolled structural steel bars, plates, shapes and sheet piling, ASTM A 6/A 6M – 02. American Society for Testing and Materials, West Conshohocken.

ATC-14. 1987. Evaluating the Seismic Resistance of Existing Buildings. Applied Technology Council Report ATC-14, Redwood City, California.

ATC-22. 1989. A Handbook for Seismic Evaluation of Existing Buildings (Preliminary). Issued by Federal Emergency Management Agency as FEMA-178. Washington, D.C.

Atkinson, G.M. 2009. Earthquake time histories compatible with the 2005 national building code of Canada uniform hazard spectrum, Can. J. of Civ. Eng., 36(6): 991-1000.

Auger, K., Balazadeh-Minouei, Y., Elkady, A., Imanpour, A., Leclerc, M., Lignos, D., Toutant, G., and Tremblay, R. 2016. Multi-directional structural component hybrid testing system for the assessment of the seismic response of steel I-shaped columns. Proc. of Eleventh Pacific Structural Steel Conference, Shanghai, China, 26-28 October, Paper No. 211.

Balazadeh-Minouei, Y., Koboevic, S., and Tremblay, R. 2017a. Seismic evaluation of a steel braced frame using NBCC and ASCE 41. *Journal of Constructional Steel Research,* http://dx.doi.org/10.1016/j.jcsr.2017.03.017.

Balazadeh-Minouei, Y., Koboevic, S., and Tremblay, R. 2017b. Seismic Assessment of Existing Steel Chevron Braced Frames. Submitted to *Journal of Structural Engineering, ASCE*.

Balazadeh-Minouei, Y., Tremblay, R., and Koboevic, S. 2017c. Seismic Retrofit of an Existing 10-Story Chevron Braced Steel Frame. Submitted to *Journal of Structural Engineering, ASCE.*

Balazadeh-Minouei, Y., Koboevic, S., and Tremblay, R. 2014a. Seismic assessment and rehabilitation of existing steel braced frames designed in accordance with the 1980 Canadian code provisions. In Proceedings of the 10th U.S. National Conference on Earthquake Engineering, Anchorage, AK, 21-25 July, Paper ID: 510.

Balazadeh-Minouei, Y., Koboevic, S., and Tremblay, R. 2014b. Seismic assessment of existing chevron braced frames designed in accordance with the 1980 Canadian codes requirements. In Proceedings of the Second European Conference on Earthquake Engineering and Seismology, Istanbul, Turkey, Paper No. 1857.

Balazadeh-Minouei, Y., Koboevic, S., and Tremblay, R. 2013. Seismic evaluation of existing steel braced frames designed in accordance with the 1980 Canadian code requirements using nonlinear time history analysis. *In* Proceedings of the CSCE 2013, Montreal, Canada, Paper No. DIS-58.

Bech, D., Tremayne, B., and Houston, J. 2015. Proposed changes to steel column evaluation criteria for existing buildings. Proceedings of the Second ATC & SEI Conference on Improving the Seismic Performance of Existing Buildings and Other Structures, American Society of Civil Engineers, San Francisco, CA.

Bertero, V-V., and Bozorgnia, Y. 2004. Earthquake Engineering from Engineering Seismology to Performance-Based Engineering, CRC Press LLC, Boca Raton, Florida, USA.

BSSC. 1992. NEHRP Handbook for the Seismic Evaluation of Existing Buildings. Report No. FEMA 178, developed by the Building Seismic Safety Council for the Federal Emergency Management Agency, Washington, DC.

Callister, J.T., and Pekelnicky, R.G. 2011. Seismic Evaluation of an Existing Low Ductility Braced Frame Building in California, Proc. ASCE Structures Congress 2011, Las Vegas, NV.

Cheng, X., Chen, Y., and Pan, L. 2013. Experimental study on steel beam-columns composed of slender H-sections under cyclic bending. Journal of Constructional Steel Research, 88: 279-288.

CISC. 2008. Moment connections for seismic applications, Canadian Institute of Steel Construction, Markham, ON.

CSA. 2009. Design of Steel Structures, CSA-S16-09, Canadian Standards Association, Mississauga, ON.

CSA. 2004. Design of Steel Structures, CSA-S16-04, Canadian Standards Association, Mississauga, ON.

CSA. 2001. Design of Steel Structures, CSA-S16-01, Canadian Standards Association, Mississauga, ON.

CSA. 1994. Limit states design of steel structures. Standard CAN/CSA-S16.1-94, Canadian Standards Association, Rexdale, ON.

CSA. 1989. Limit states design of steel structures. CANJCSA-S16.1-M89, Rexdale, ON.

CSA. 1978. Limit states design of steel structures, CAN3-S16.1-M78, Canadian Standards Association, Rexdale, ON.

CSI. 2008. ETABS Computer Software, Version 9.5.0. Computers and Structures, Inc., Berkeley, CA.

Dassault. 2013. 2012. ABAQUS-FEA/CAE. Dassault Systemes Simulia Corp., RI, USA.

Erduran, E., Dao, N.D., and Ryan, K.L. 2011. Comparative response assessment of minimally compliant low-rise conventional and base-isolated steel frames, Earthquake Engineering and Structural Dynamics, 40, 1123-1141.

FEMA. 1992a. NEHRP Handbook for the Seismic Evaluation of Existing Buildings. Federal Emergency Management Agency, Report FEMA-178, Washington, D.C.

FEMA. 1992b. NEHRP Handbook of Techniques for Seismic Rehabilitation of Existing Buildings. Federal Emergency Management Agency, Report FEMA-172, Washington, D.C.

Fogarty, J. and El-Tawil, S. 2015. Collapse Resistance of Steel Columns under Combined Axial and Lateral Loading. Journal of Structural Engineering, ASCE, http://dx.doi.org/10.1061/(ASCE)ST.1943-541X.0001350.

Foutch, D. A., Goel, S. C., and Roeder, C. W. 1987. Seismic testing of full-scale steel building—Part I. J. Structural Engineering, ASCE, 10.1061/(ASCE)0733-9445(1987)113:11(2111), 2111–2129.

Galambos, T.V., and Ketter, R.L. 1958. Columns under combined bending and thrust. Fritz Engineering Laboratory Report No. 205A.21, Bethlehem, PA.

Goel, SC. 1992. Cyclic Post Buckling Behavior of Steel Bracing Members. Stability and Ductility of Steel Structures under Cyclic Loading. CRC Press: Boca Raton, FL, pp. 77-104.

Gouvernement du Québec. 2015, Code de construction, Loi sur le bâtiment, Éditeur officiel du Québec, Québec, QC.

Harris III, J.L., and Speicher, M.S. 2015. Assessment of First Generation Performance-Based Seismic Design Methods for New Steel Buildings; Volume 2: Special Concentrically Braced Frames, NIST Technical Note 1863-2, National Institute of Standards and Technology, Gaithersburg, MD.

Hines, E.M., Appel, M.E. and Cheever, P.J. 2009. Collapse performance of low-ductility chevron braced steel frames in moderate seismic regions, Engineering Journal, AISC, Vol. 46, No.3, 3rd Quarter, pp.149-180.

Hsiao, P. C., Lehman, D. E., Berman, J. W., Roeder, C. W., and Powell, J. 2014. Seismic vulnerability of older braced frames. J. Perform. Constr. Facil., 10.1061/(ASCE)CF.1943-5509.0000394, 108–120.

Hsiao, P. C., Lehman, D. E., and Roeder, C. W. 2012. Improved analytical model for special concentrically braced frames. J. Constr. Steel Res., 73(Jun), 80–94.

ICBO. 1977, 1988. Uniform Building Code 1979, 1988. International Conference of Building Officials, Whittier, CA.

ICC. 2006. International Building Code, International Code Council, Falls Church, VA.

Imanpour, A. 2015. Seismic response and design of steel multi-tiered concentrically braced frames. Ph.D. dissertation, Polytechnique Montréal, Montréal, Canada.

Jiang, Y., Balazadeh-Minouei, Y., Tremblay, R., Koboevic, S., and Tirca, L. 2012a. Seismic assessment of existing steel braced frames designed in accordance with the 1980 Canadian code provisions. In Behaviour of Steel Structures in Seismic Area: In Proceedings of the Seventh International Conference STESSA 2012, Santiago, Chile, 531-537.

Jiang, Y., Tremblay, R., and Tirca, L. 2012b. Seismic assessment of deficient steel braced frames with built-up back-to-back double angle brace sections using OpenSees modelling, In Proceedings of the 15WCEE, Lisbon, Portugal, Paper No. 4416.

Johnson, M., Sloat, D., Roeder, C.W., Lehman, D.E, and Berman, J.W. 2014. Seismic performance of concentrically braced frame connections. Proc. 10th National Conference in Earthquake Eng., Earthquake Engineering Research Institute, Anchorage, AK, Paper No. 1168.

Khatib, I.F., Mahin, S.A. and Pister, K.S. 1988. Seismic behavior of concentrically braced steel frames, UCB/EERC Report 88/01, Earthquake Engineering Research Center, University of California, Berkeley, Richmond, CA, January.

Kiggins, S., and Uang, C.-M., 2006. Reducing Residual Drift of Buckling Restrained Braced Frames as a Dual System. Engineering Structures, 28(11),1525–1532.

Kim, J. and Choi, H. 2004. Response modification factors of chevron-braced frames. Engineering Structures, Vol. 27, pp. 285-300.

Lai, J.-W., and Mahin, S. A. 2015. Strongback System: A Way to Reduce Damage Concentration in Steel-Braced Frames. Journal of Structural Engineering, ASCE, DOI: 10.1061/(ASCE)ST.1943-541X.0001198.

Lai, J. 2012. Experimental and analytical studies on the seismic behaviour of conventional and hybrid braced frames. Ph.D. thesis, University of California, Berkeley, CA.

Lamarche, C. and Tremblay, R. 2011. Seismically induced cyclic buckling of steel columns including residual-stress and strain-rate effects. Journal of Constructional Steel Research, 67 (2011): 1401-1410.

MacRae, G. A., Carr, A. J., and Walpole, W. R. 1990. The seismic response of steel frames. Report No. 90-6, Department of Civil Engineering, University of Canterbury, Christchurch, U.K.

Mazzoni, S., McKenna, F., Scott, M. H., and Fenves, G. L. 2009. Open system for earthquake engineering simulation user command-language manual—OpenSees version 2.0, Pacific Earthquake Engineering Research Center, Univ. of California, Berkeley, CA.

McKenna, F. and Fenves, G.L. 2004. Open System for Earthquake Engineering Simulation (OpenSees). Pacific Earthquake Engineering Research Center (PEER), University of California, Berkeley, CA. (http://opensees.berkeley.edu/index.html)

Mitchell, D., Paultre, P., Tinawi, R., Saatcioglu, M., Tremblay, R., Elwood, K., Adams, J., and DeVall, R. 2010. Evolution of seismic design codes in Canada. Can. J. of Civ. Eng., 37(9):1157-1170.

Mottier, P., Tremblay, R., and Rogers, C. 2017. Seismic Retrofit of Existing Low-Rise Steel Buildings in Eastern Canada using Rocking Braced Frame System. *Earthquake Engineering and Structural Dynamics* (Submitted).

Nakashima, M. and Wakabayashi, M. 1992. Analysis and design of steel braces and braced frames in building structures. in Stability and Ductility of Steel Structures under Cyclic Loading, Fukumoto, Y. and Lee, G.C. editors, CRC Press, Boca Raton, FL, pp. 309-321.

Newell, J.D. and Uang, C.M. 2008. Cyclic behavior of steel wide-flange columns subjected to large drift, Journal of Structural Engineering, ASCE, 134(8): 1334-1342.

NRCC. 2015. 2010, 2005, 1980. National building code of Canada 2010, 13th ed., 2005, 1980, 8th ed. National Research Council of Canada, Ottawa, ON.

NRCC. 1993. Guidelines for the seismic evaluation of existing buildings. Publication no. NRCC 36941, Institute for Research in Construction, National Research Council of Canada, Ottawa, ON.

NRCC. 1993. Manual for Seismic Screening of Buildings for Seismic Investigation, National Research Council of Canada, Ottawa, ON.

NZS. 1997. Steel Structures Standard, NZS 3404, Standards New Zealand.

Packer, J. A., Chiew, S. P., Tremblay, R. and Martinez-Saucedo, G. 2010. Effect of material properties on hollow section performance. Proceedings of the Institution of Civil Engineers, Structures and Buildings 163, doi: 10.1680/stbu.2010.163.6.375.

Pollino, M., Slovenec, D., Qu, B., and Mosqueda, G. 2017. Seismic rehabilitation of concentrically braced frames using stiff rocking cores. Journal of Structural Engineering, ASCE, 143-9: DOI: 10.1061/(ASCE)ST.1943-541X.0001810.

Qu, B., Sanchez-Zamora, F., and Pollino, M. 2014. Transforming Seismic Performance of Deficient Steel Concentrically Braced Frames through Implementation of Rocking Cores, Journal of Structural Engineering, ASCE., 141, 5: DOI: 10.1061/(ASCE)ST.1943-541X.0001198.

Rai, D., and Goel, S. 2003. Seismic evaluation and upgrading of chevron braced frames. Journal of Constructional Steel Research, 59, 971-994.

Redwood, R.G., and Channagiri, V.S. 1990. Earthquake resistant design of concentrically braced steel frames. Can. J. of Civ. Eng., 18(5): 839-850.

Roeder, C.W., Lumpkin, E.J., and Lehman, D.E. 2012. Seismic performance assessment of concentrically braced steel frames. Earthquake Spectra, Earthquake Engineering Research Institute, 28(2),709-727.

Saatcioglu, M., Shooshtari, M., and Foo. S. 2013. Seismic Screening of Buildings based on the 2010 National Building Code of Canada. Can. J. of Civ. Eng., 40: 483-498. doi:10.1139/cjce-2012-0055.

SEAONC. 1982. Earthquake resistant design of concentric and K-braced frames. Structural Engineers Association of Northern California, Research Committee, July.

Sen, A.D., Roeder, C.W., Berman, J.W., Lehman, D.E., Li, C-H., Wu, A-C. and Tsai, K-C. 2016a. Experimental Investigation of Chevron Concentrically Braced Frames with Yielding Beams. Journal of Structural Engineering, ASCE, http://dx.doi.org/10.1061/(ASCE)ST.1943-541X.0001597.

Sen, A.D., Sloat, D., Ballard, R., Johnson, M.M., Roeder, C.W., Lehman, D.E. and Berman, J.W. 2016b. Experimental Evaluation of the Seismic Vulnerability of Braces and Connections in Older Concentrically Braced Frames. Journal of Structural Engineering, ASCE, http://dx.doi.org/10.1061/(ASCE)ST.1943-541X.0001507.

Sen, A.D., Ballard, R., Sloat, D., Johnson, M., Roeder, C.W., Lehman, D.E. and Berman, J.W. 2015. Seismic Evaluation and Retrofit of Older Concentrically-Braced Frames. Proceedings of the Second ATC & SEI Conference on Improving the Seismic Performance of Existing Buildings and Other Structures, American Society of Civil Engineers, San Francisco, CA.

Sen, A.D., Pan, L., Sloat, D., Roeder, C.W., Lehman, D.E., Berman J.W., Tsai, K.C., Li, C.H., and Wu, A.C. 2014. Numerical and experimental assessment of chevron braced frames with weak beams. Proc. 10th National Conference in Earthquake Eng., Earthquake Engineering Research Institute, Anchorage, AK, Paper No. 961.

Shiabata, M. and Wakabayashi, M. 1983a. Ultimate strength of K-Type braced frame. Transactions of the Architectural Institute of Japan, No. 326, pp. 1-9, (in Japanese).

Shiabata, M. and Wakabayashi, M. 1983b. Experimental study on the hysteretic behavior of K-Type braced frame subjected to repeated load. Transactions of the Architectural Institute of Japan, No. 326, pp. 10-16, (in Japanese).

Singh Huns, B., Grondin, G. and Driver, R. 2002. Block shear behaviour of bolted gusset plates. Structural Engineering Report No. 248. Department of Civil and Environmental Engineering, University of Alberta, Edmonton, AB.

Sloat, D.A. 2014. Evaluation and Retrofit of Non-Capacity Designed Braced Frames. M.Sc. Thesis, Dept. of Civil and Environmental Eng., Univ. of Washington, Seattle, WA.

Sorace, S.and Terenzi, G. 2008. Seismic Protection of Frame Structures by Fluid Viscous Damped Braces, Journal of Structural Engineering, ASCE, 134, 1, 45-55.

Speicher, M.S., and Harris III, J.L. 2016. Collapse prevention seismic performance assessment of new special concentrically braced frames using ASCE 41. Engineering Structures, 126 (2016), 652-666.

Symans, M., Charney, F., Whittaker, A., Constantinou, M., Kircher, C., Johnson, M., and McNamara, R. 2008. Energy Dissipation Systems for Seismic Applications: Current Practice and Recent Developments. Journal of Structural Engineering, ASCE., DOI: 10.1061/(ASCE)0733-9445(2008)134:1(3).

Tremblay, R., Atkinson, G., Bouaanani, N., Daneshvar, P., Leger, P., and Koboevic, S. 2015. Selection and scaling of ground motion time histories for seismic analysis using NBCC 2015, *In* Proceedings of the 11th Canadian Conference on Earthquake Engineering, 11CCEE, Victoria, Canada.

Tremblay, R., Jiang, Y., Leclerc, M. and Tirca, L. 2012. Seismic assessment of steel braced frames using advanced hybrid simulation techniques, *In* Proceedings of the 3rd International Structural Specialty Conference, CSCE 2012, Edmonton, Canada, Paper No. STR-1116.

Tremblay, R. and Merzouq, S. 2004. Dual Buckling Restrained Braced Steel Frames for Enhanced Seismic Response. Proc. Passive Control Symposium 2004, Tokyo Institute of Technology, Yokohama, Japan, 89-104.

Tremblay, R., and Poncet, L. 2004. Improving the seismic stability of concentrically braced steel frames. Proc., 2004 SSRC Annual Technical Session and Meeting, Long Beach, Calif, 19-38.

Tremblay, R. 2003. Achieving a Stable Inelastic Seismic Response for Concentrically Braced Steel Frames. Engineering Journal, AISC, Vol. 40, No. 2, pp. 111–129.

Tremblay, R. and Robert, N. 2001. Seismic performance of low- and medium-rise chevron braced steel frames, Canadian Journal of Civil Engineering, Vol. 28, pp.699-714.

Tremblay, R. 2001. Seismic behavior and design of concentrically braced steel frames, Engineering Journal, AISC, Vol. 38, No.3, 3rd Quarter, pp.148-166.

Tremblay, R. and Robert, N. 2000. Seismic design of low-and medium-rise chevron braced steel frames, Canadian Journal of Civil Engineering, Vol. 27, pp.1192-1206.

Uang, C.M., Ozkula, G. and Harris, J.L. 2015. Cyclic performance of deep wide-flange steel beam-columns, Proceedings of the Eight International Conference on Advances in Steel Structures, ICASS 2015, Lisbon, Portugal, Paper No. 104.

Uang, C.M. and Bertero, V. 1986. Earthquake simulation tests and associated studies of a 0.3-scale model of a six-story concentrically braced steel structure, UCB/EERC-86/10, Earthquake Engineering Research Center, University of California at Berkeley, Richmond, CA, December.

Whittaker, A.S., Uang, C.-M., and Bertero, V.V. 1990, Experimental Seismic Response of Steel Dual Systems. Proceedings Fourth U.S. National Conference on Earthquake Engineering, Palm Springs, California Vol. 2, pp. 655–664.

Zargar, S., Medina, R. A., and Miranda, E. 2014. Cyclic behavior of deep steel columns subjected to large drifts, rotations, and axial loads. Proc. 10th National Conference in Earthquake Eng., Earthquake Engineering Research Institute, Anchorage, AK.

APPENDIX A – EXPERIMENTAL STUDY OF STEEL COLUMNS

An experimental program was performed for cyclic testing of concentrically braced frame columns started in winter 2015 at the Structural Engineering Laboratory of Polytechnique Montréal. In this appendix, the objectives of the test program, the test setup, column testing and experimental results are presented.

A1. Objectives

As large scale physical tests offer a robust method to evaluate the response of steel structures under seismic loading, an experimental program was developed to evaluate the ductility of steel columns and verify the seismic response of these components determined from the numerical study.

A2. Multi-Directional Hybrid Testing System (MDHTS)

The Multi-Directional Hybrid Testing System (MDTHS) is an advanced large-scale structural testing system that designed to impose the combination of displacement and rotation to the test specimen along 6 Degrees-Of-Freedom using a sophisticated control system (Imanpour 2015). The MDTHS is attached to the L-shaped strong wall and strong floor using four horizontal and four vertical actuators, respectively. The base attachment platen is a 140 mm thick steel plate, named lower platen in Figure A.1. This system can be used to perform multi-axis static, quasi-static cyclic, pseudo-dynamic or hybrid tests on various structural components. This system can reproduce different end conditions such as fixed, pinned or semi-rigid condition using the movable upper platen. This platen can be controlled by specifying three translational and three rotational DOFs of the control point using load- or displacement-controlled or combination of these two modes.

The Multi-Directional Hybrid Testing System can reproduce different top end conditions. It can apply complex multi-directional loading histories to the specimens by controlling the upper platen. This system can be considered to test large scale structural components using different loading in load- or displacement-controlled mode or combination of these two modes at any of the six DOFs. The MDTHS can perform hybrid simulations, and it can record applied loads and 3-Dimensional (3D) positional information using global and local displacement coordinates.

The preliminary testing results confirmed the presence of friction forces developed in the MDHTS, which causes the difference between the measured and expected forces in the specimen. The value of friction force depends on the level of axial load applied to the specimen.

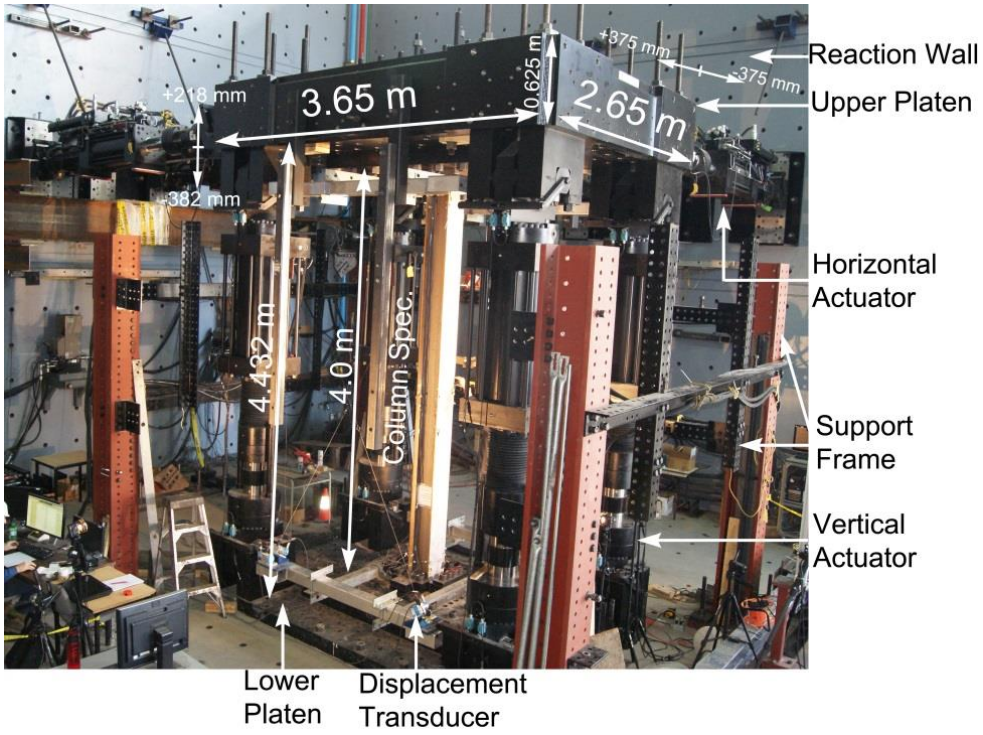

Figure A.1: Components of Multi-Directional Hybrid Testing System (Imanpour 2015).

A3. Column testing

In this section, the seismic response of full-scale steel wide-flange column specimens were evaluated under cyclic loading. The specimens were 4000 mm tall, and they represented the first storey column of concentrically braced frames. The cross section of all specimens was W250x101, which was categorized as Class 1 and highly ductile in accordance with the requirements of CSA S16 (2009) and AISC Seismic Provisions (2010a), respectively. All specimens were fixed at the base by attaching to the lower platen. The columns were tested in the vertical position, and they were subjected to various types of loading protocols. The specimens were not braced laterally along their lengths. The material properties of flange and web of column section were obtained from tension coupon testing, and ASTM A992 steel was specified for the wide-flange steel column sections. The material's yield and tensile strengths of the flange

were 398 and 554 MPa, respectively; while, the values of 402 and 556 MPa were obtained for the yield and tensile strengths of the web. The details of material properties of coupon tests are presented in Table A.1.

Table A.1: Material properties of coupon testing

Steel properties	
$F_{y\text{-Flange}}$	**398 MPa**
$F_{u\text{-Flange}}$	**554 MPa**
$\varepsilon_{sh\text{-Flange}}$	**0.0152 (mm/mm)**
$\varepsilon_{u\text{-Flange}}$	**0.139 (mm/mm)**
$\varepsilon_{rup\text{-Flange}}$	**0.2493 (mm/mm)**
$F_{y\text{-Web}}$	**402 MPa**
$F_{u\text{-Web}}$	**556 MPa**
$\varepsilon_{sh\text{-Web}}$	**0.0109 (mm/mm)**
$\varepsilon_{u\text{-Web}}$	**0.141 (mm/mm)**
$\varepsilon_{rup\text{-Web}}$	**0.2058 (mm/mm)**
E (Assumed)	**200,000 MPa**

The instruments including strain gauges and string pods were installed to the specimens, and they were monitored throughout each test. The strain gauges were located at the internal and external sides of flanges at three locations of the specimen including top, middle and bottom to define the strains at these points. The string pods were used at the middle and top of the specimen to measure the in plane and out of plane lateral displacements of the column. The initial out-of-straightness of each specimen was measured using theodolite, while no axial load was applied to the column. The residual stresses of flange and web were determined from individual strips using sectioning method. Table A.2 shows the residual stress measurements.

The measured dimensions of all specimens are mentioned in Table A.3. In this table, t_f is the thickness of the flange, t_w is the thickness of the web, b_f is the width of the flange, h_w is the height of the web and H is the height of the specimen.

Table A.2: Residual stress measurements determined from individual strips

Residual stress values	
$\sigma_{r,A}$	**-58 MPa**
$\sigma_{r,B}$	**74 MPa**
$\sigma_{r,C}$	**-181 MPa**
α	**0.1796**
β	**0.1666**

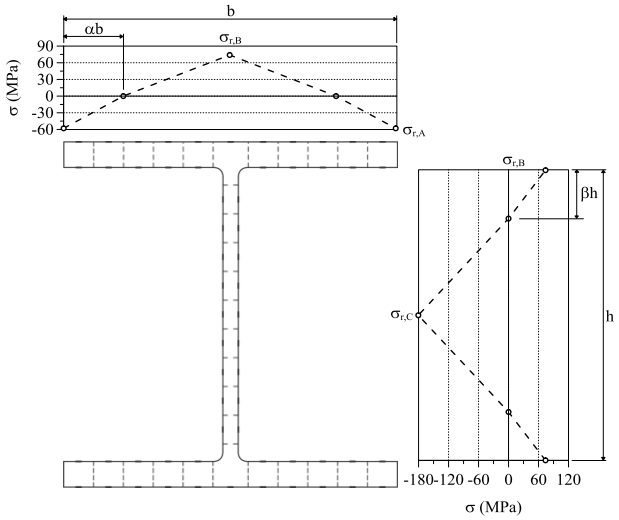

Table A.3: Measured dimensions of specimens

Specimen	t_f (mm)	b_f (mm)	t_w (mm)	h_w (mm)	H (mm)
CS5	20.4	255.1	12.7	228.3	269.1
CS6	20.7	256.8	12.7	228.4	269.7
CS7	20.2	254.9	12.4	228.7	269.2
CS10	20.2	256.5	12.1	229.3	269.8

A4. Experimental results

In this section, the results of four full-scale experimental tests are discussed. The shop drawing of the first specimen with the location of strain gauges is shown in Figure A.2. In the first test, specimen CS5 was subjected to the constant level of axial load, $0.7P_{CL}$, where P_{CL} was the lower-bound axial strength of the column and large cyclic lateral displacement equal to 7% storey drift that imposed about the weak axis of the member. At the beginning of the test, the system was

checked in the elastic range of the specimen using two cycles of 0.375%, 0.5% and 1% of storey drift. Then, the large cyclic lateral displacement was imposed to the column. Figure A.3 shows the applied loading protocol to specimen CS5. Regarding this figure, the column buckling occurred after three half large cycles of 7% storey drift.

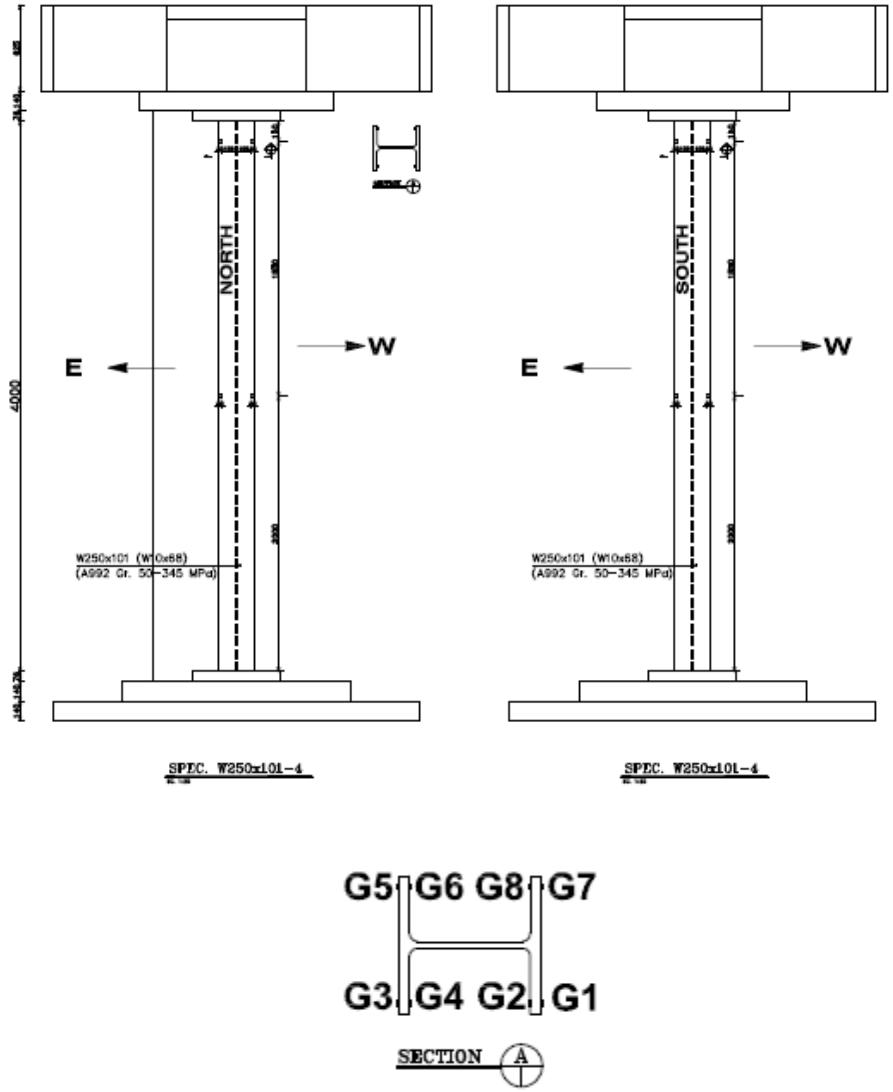

Figure A.2: Shop drawing of specimen CS5.

Figure A.4 shows the deformed shape of the column at the second cycle of 0.375%, and 0.5% storey drift. In these figures, the specimen is in the elastic range.

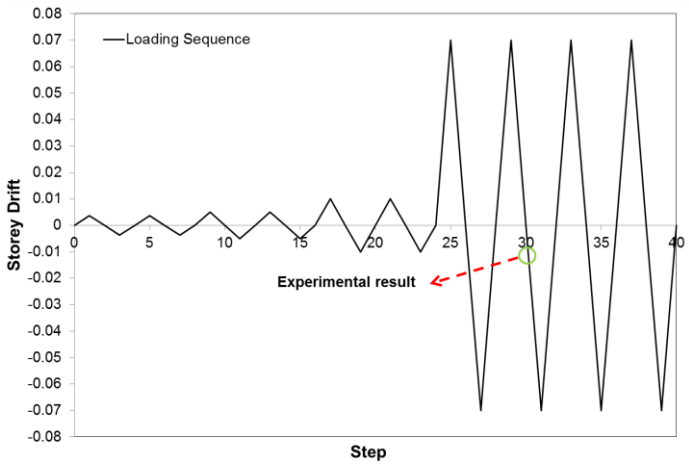

Figure A.3: Applied loading protocol to specimen CS5.

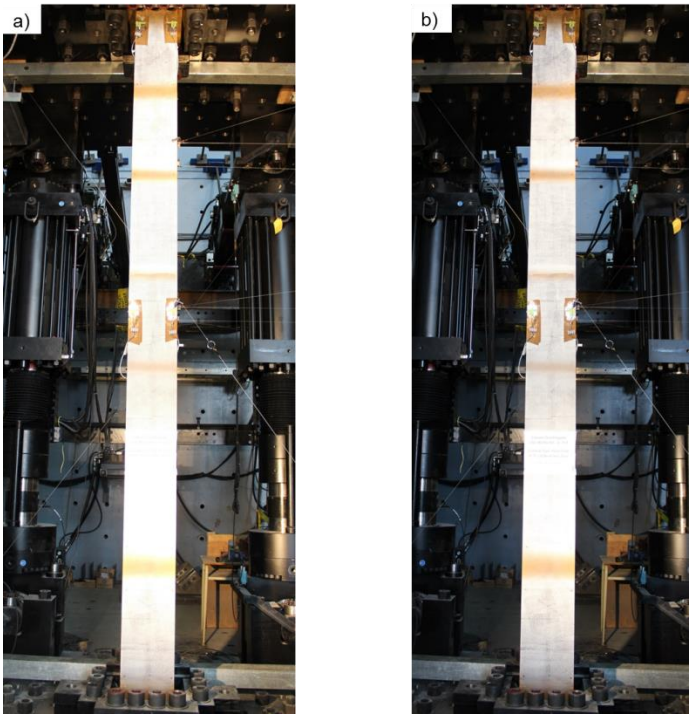

Figure A.4: Deformed shape of specimen CS5 at a) 0.375%; and b) 0.50% storey drift.

The deformed shape of the specimen at ±7% at the first and second cycles is shown in Figure A.5. In Figure A.5c, the initiation of formation of plastic hinges along the height of the column is observed.

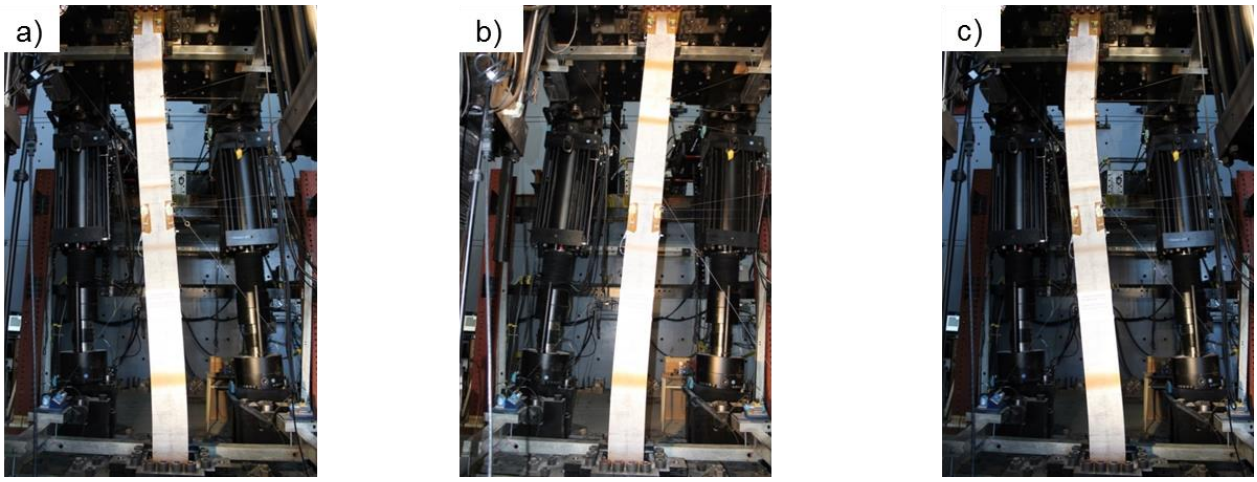

Figure A.5: Deformed shape of specimen CS5 at a) first peak +7.0%; b) second peak -7.0%; and c) third peak +7.0% storey drift.

Figure A.6a shows the buckling of the specimen about the weak axis. The deformed shape of the column was half-sine, and three plastic hinges were formed at the top, middle and bottom of the specimen. Local buckling was observed at the top and bottom of the column as shown in Figure A.6b. The normalized bending moment to the corresponding expected plastic bending moment, M_p, versus storey drift is shown in Figure A.7 for two cases including the presence of friction forces in the bending moment and removing the mentioned forces. In this figure, the effect of friction forces in the system on the flexural demand of the column at high level of axial load is obvious. The friction forces that were existed at each cycle of experimental results were removed, which has been shown in Figure A.7. The flexural strength degradation of the column could be as a result of local buckling of the specimen. The results of this test show that the steel column with compact cross section exhibits a ductile behaviour even at 0.7 of the lower-bound axial strength of the column.

Figures A.8.a, A.8.b and A.8.c show the axial shortening, rotation due to weak axis and axial load of specimen CS5. These measurements were recorded at top of the column.

Figures A.9.a to A.9.d present the measurement of strain gauges located at the top and middle of the column. The location of each strain gauge is shown in Figure A.2. In Figure A.9.a, the strain gauge of G8 was missed at the beginning of the test.

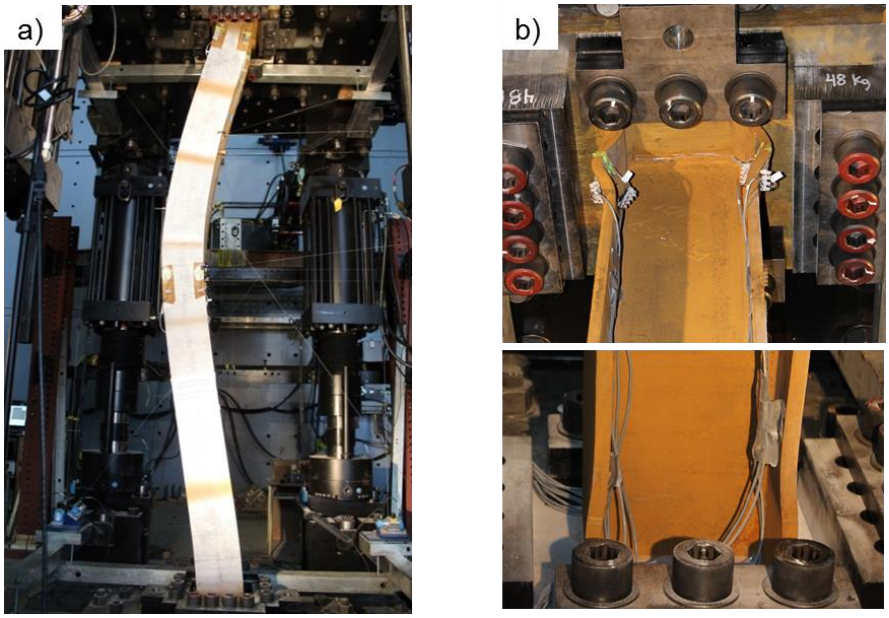

Figure A.6: Specimen CS5 at a) column buckling; and b) local buckling at bottom and top of specimen.

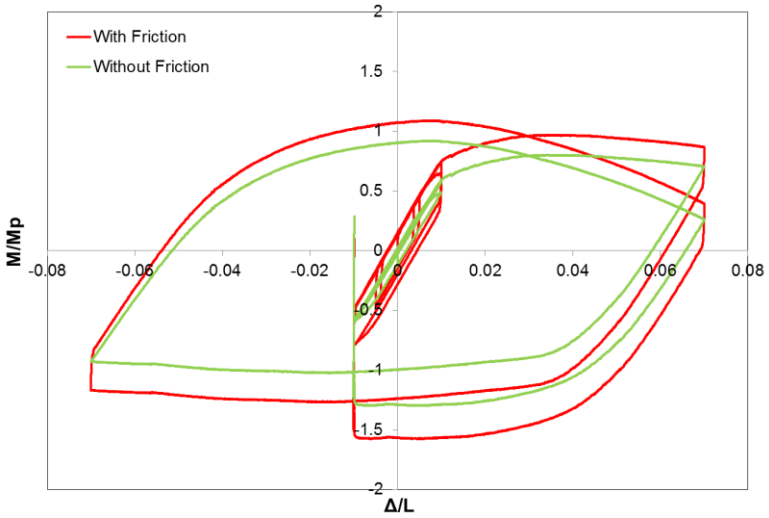

Figure A.7: Normalized flexural strength response versus storey drift of specimen CS5 with and without presence of friction forces.

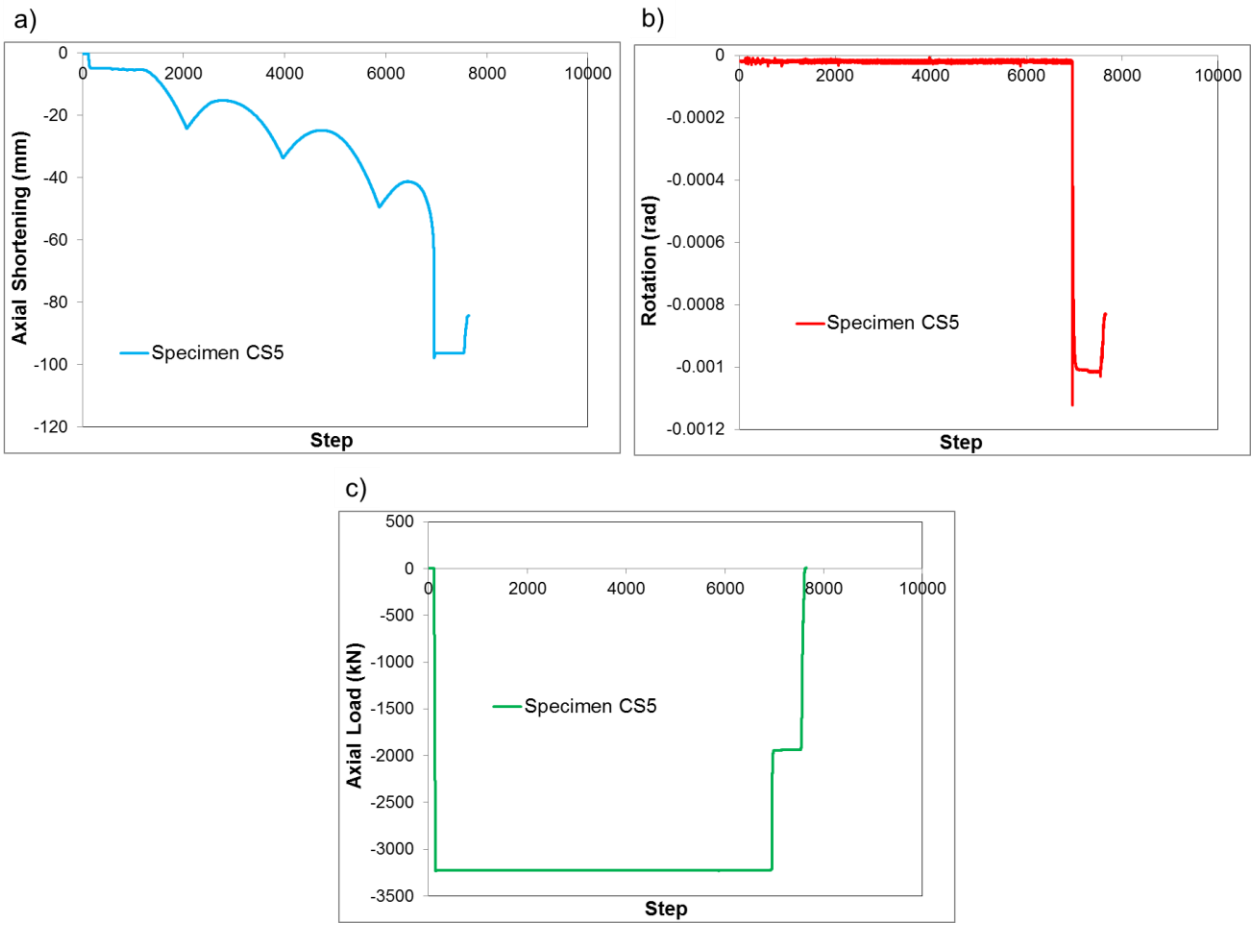

Figure A.8: a) Axial shortening; b) rotation; and c) axial load of specimen CS5.

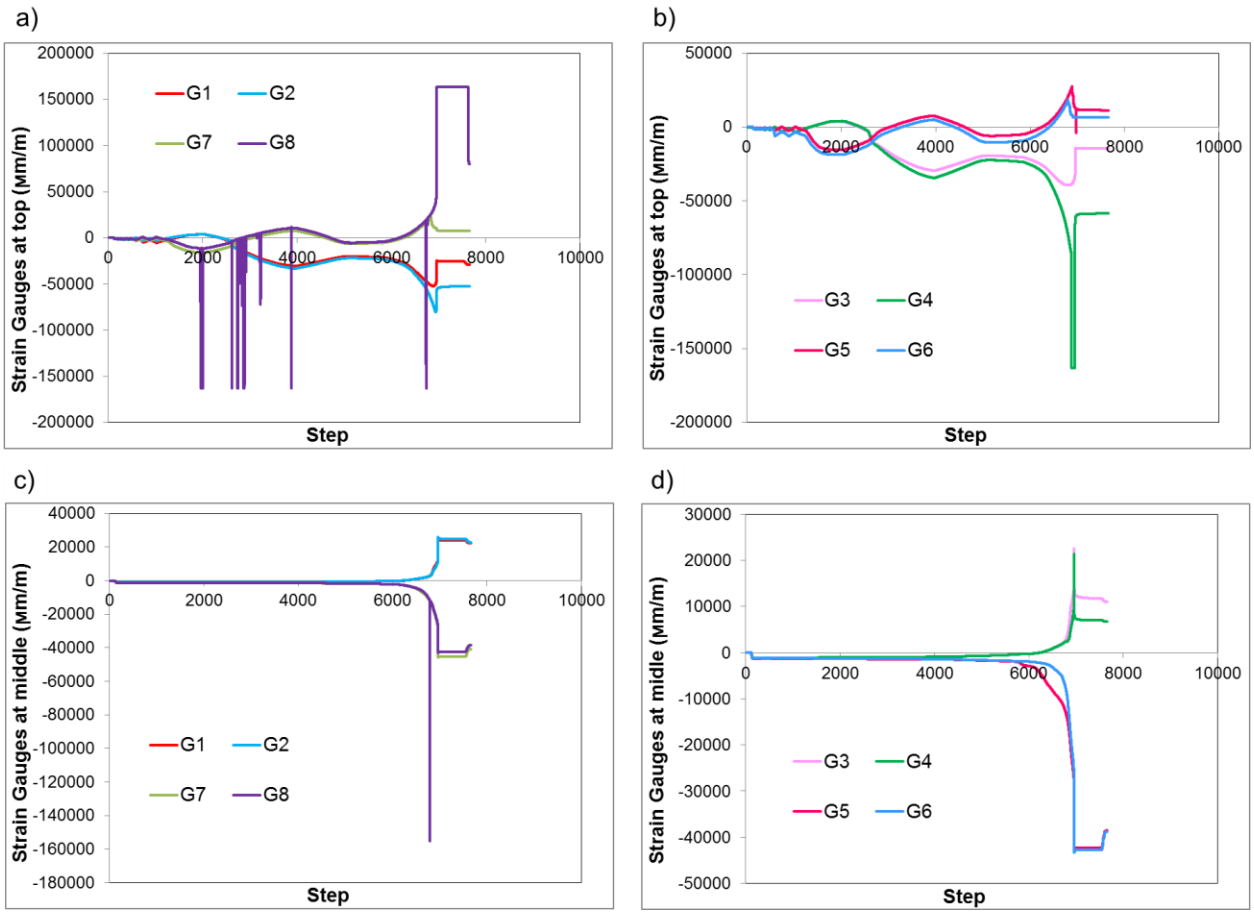

Figure A.9: Strain gauge measurements at top and middle of specimen CS5: a) G1, G2, G7, G8 (top); b) G3, G4, G5, G6 (top); c) G1, G2, G7, G8 (middle); and d) G3, G4, G5, G6 (middle).

In the second test, the imposed constant axial load demand to Specimen CS6 increased reaching 0.9 P_{CL}, and the AISC loading sequence was applied to the specimen. The lateral displacement was imposed about the weak axis of the column. The shop drawing of specimen CS6 is shown in Figure A.10. Figure A.11 shows the loading protocol of this test. According to this figure, the column buckled at 2% storey drift.

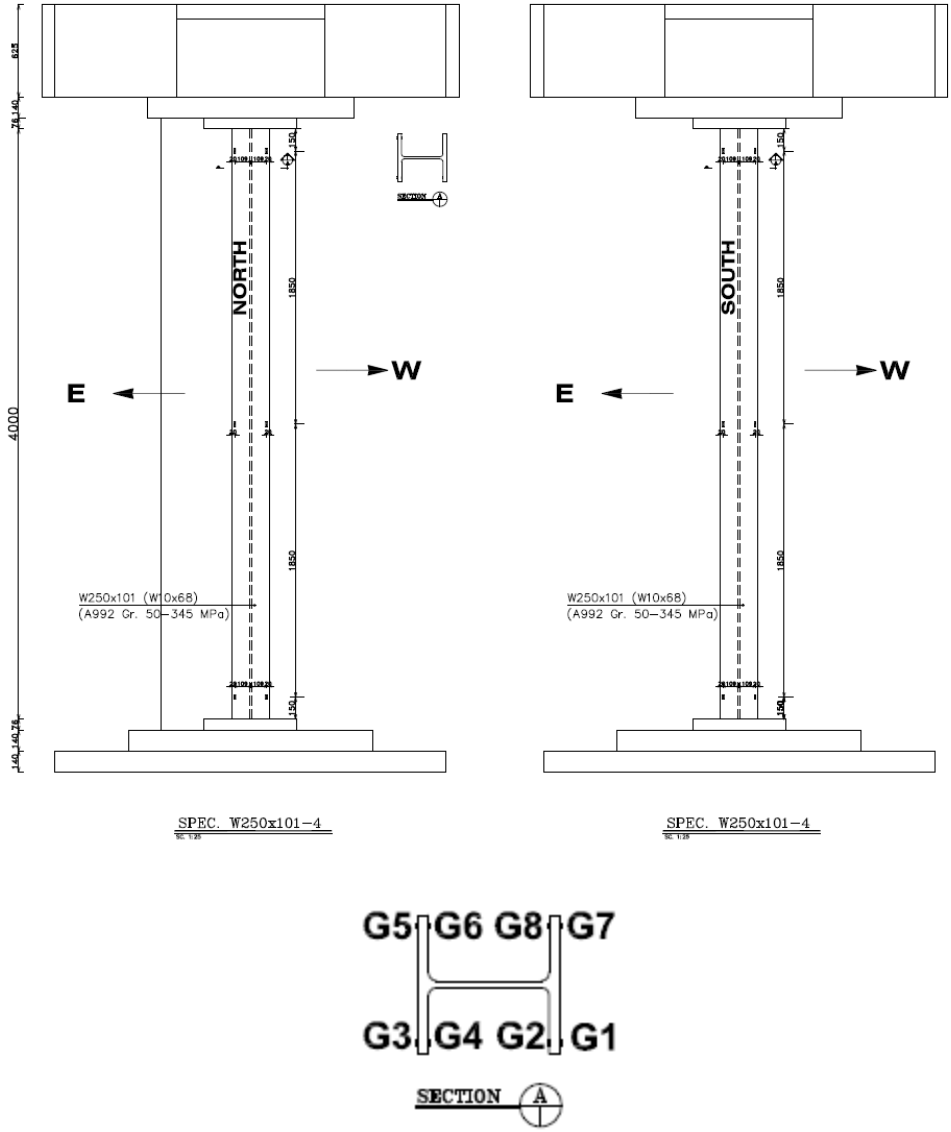

Figure A.10: Shop drawing of specimen CS6.

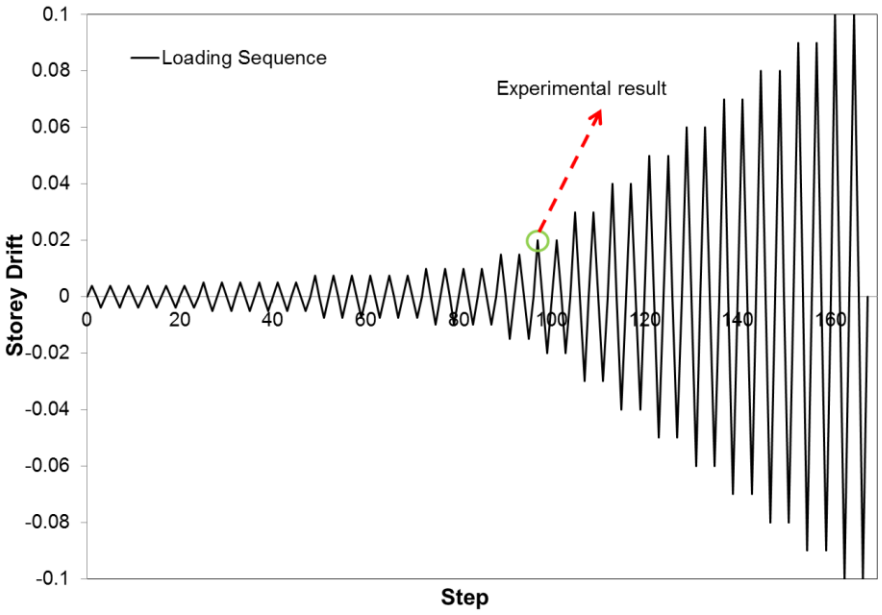

Figure A.11: Applied loading protocol to specimen CS6.

Figure A.12 presents the deformed shape of specimen CS6 at 0.375%, 0.5%, 0.75% and 1% storey drift. In this test, column buckling happened at 2% storey drift due to weak axis, and three plastic hinges formed at the bottom, middle and top of the specimen as shown in Figure A.13.a. Local buckling at the top, middle and bottom of the column is presented in Figure A.13.b.

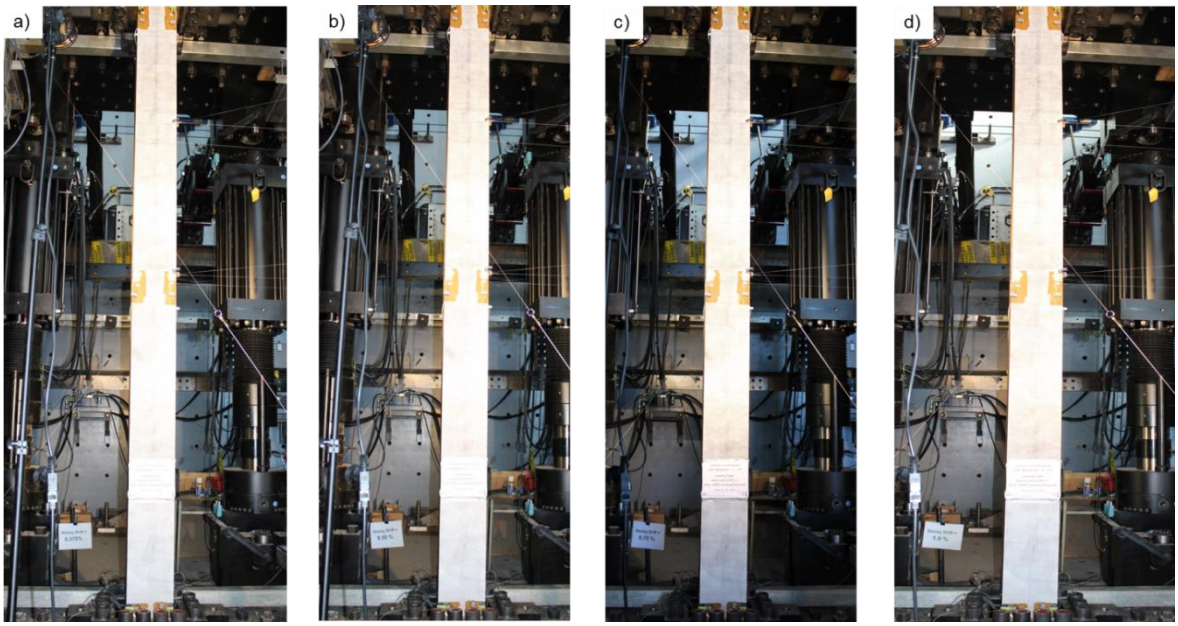

Figure A.12: Deformed shape of specimen CS6 at a) 0.375%; b) 0.5%; c) 0.75%; and d) 1% storey drift.

Figure A.14 shows the normalized flexural strength response versus storey drift of specimen CS6 for two cases: friction forces are presented in the experimental results, and these forces are removed from the results. The effect of friction forces on the results is obvious as a vertical line in the loading and unloading of the specimen. In Figure A.14, the rate of friction force has been changed for different amplitudes of AISC loading sequence, and the maximum bending moment is 107 kN.m due to the friction force, occurred at 0.75% storey drift. Figure A.15.a to A.15.c show the column axial shortening, rotation due to weak axis and column axial load of specimen CS6. In Figure A.16, the measurement of strain gauges located at top, middle and bottom of the column is presented. The strain gauge of G4 located at the bottom of specimen CS6 was missed during the test.

The experimental result of specimen CS6 shows that the ductility of column under high level of axial load such as 0.9 P_{CL} is limited.

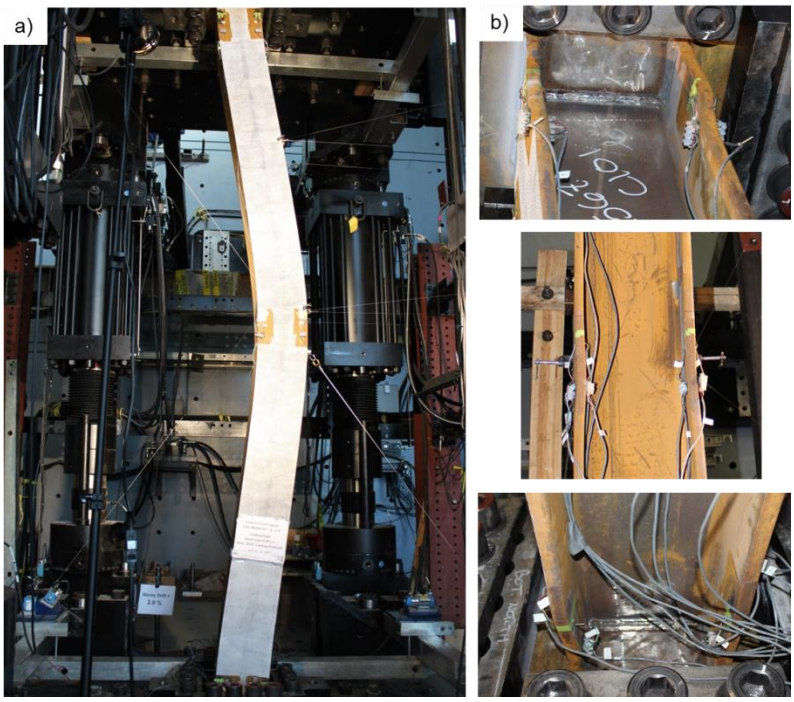

Figure A.13: Specimen CS6 at a) column buckling; and b) local buckling at bottom, middle and top of specimen.

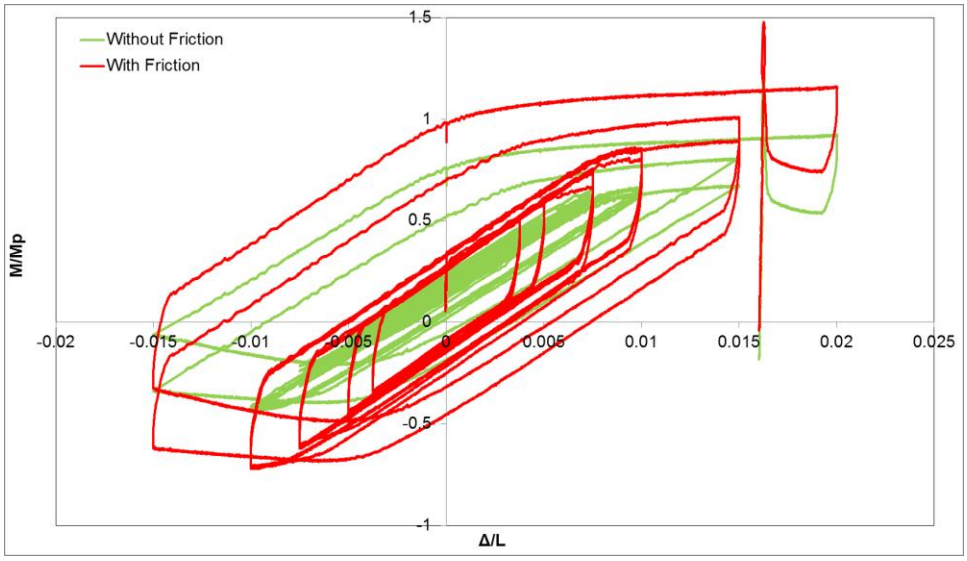

Figure A.14: Normalized flexural strength response versus storey drift of specimen CS6 with and without presence of friction forces.

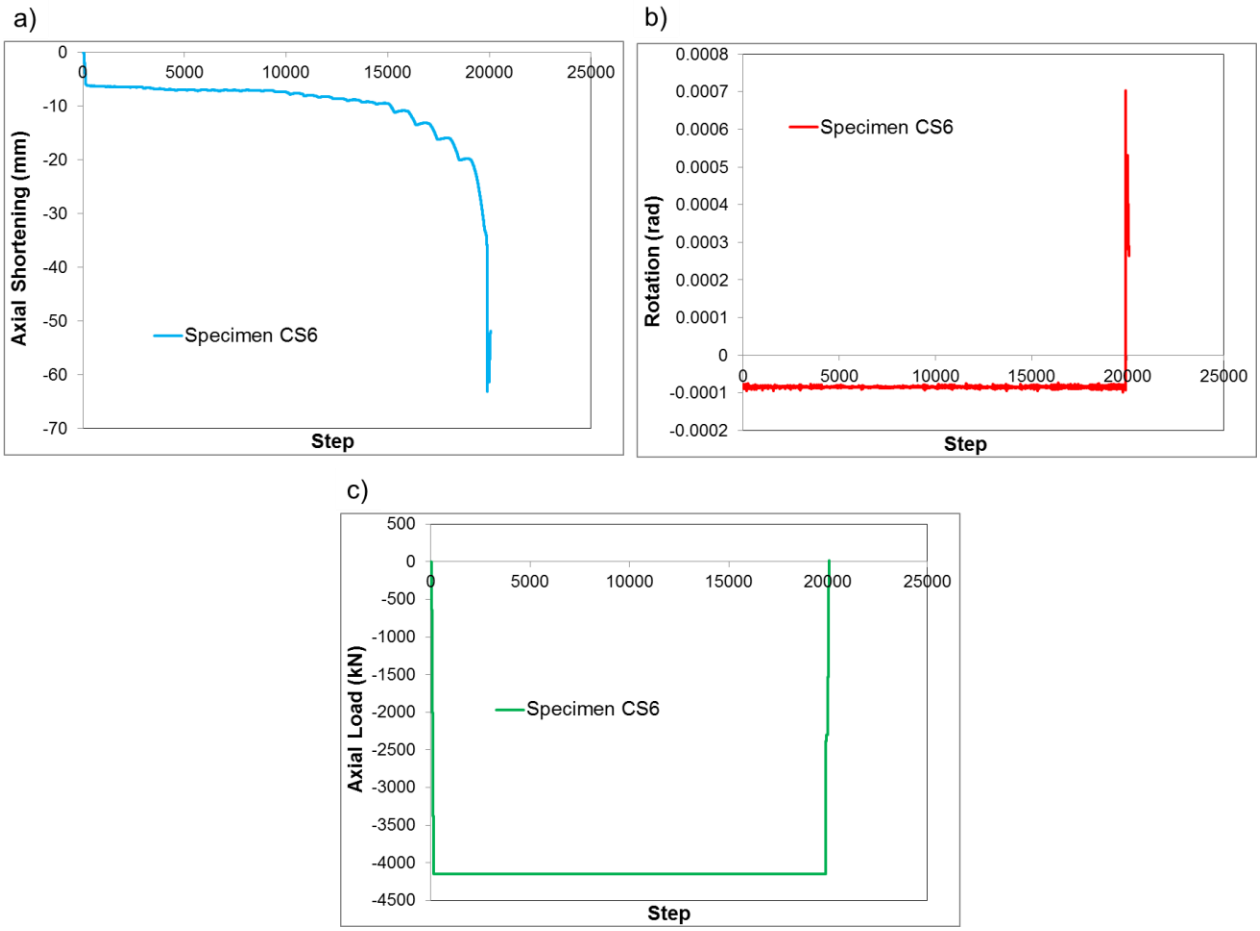

Figure A.15: a) Axial shortening; b) rotation; and c) axial load of specimen CS6.

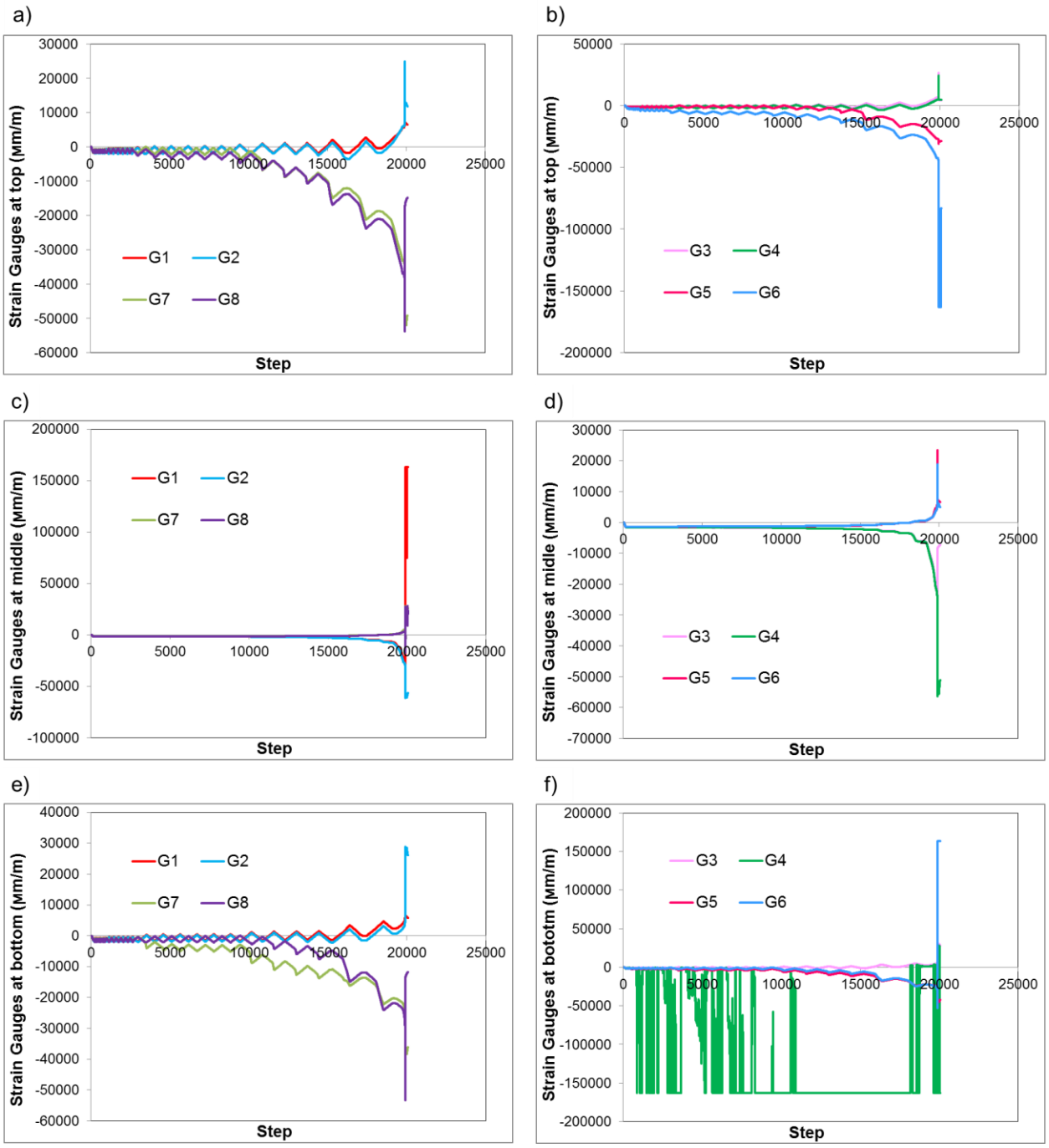

Figure A.16: Strain gauge measurements at top, middle and bottom of specimen CS6: a) G1, G2, G7, G8 (top); b) G3, G4, G5, G6 (top); c) G1, G2, G7, G8 (middle); d) G3, G4, G5, G6 (middle); e) G1, G2, G7, G8 (bottom); and f) G3, G4, G5, G6 (bottom).

In the third test, the accuracy of acceptance criteria specified for steel columns in ASCE 41 was evaluated (Auger et al. 2016). Figure A.17 shows the shop drawing of specimen CS7. The response of the column at the 8th storey of the tension-only X-braced frame was studied using OpenSees and ABAQUS. The numerical study showed the ductile response of this column by the formation of plastic hinges at both ends of the member. The loading protocol that applied to the column specimen is shown in Figure A.18.a. It was extracted from the nonlinear response history analysis of the steel braced frame modelled in OpenSees. The gravity load was first imposed to the specimen. Then, the histories of axial force, story drift and relative end rotation about strong axis resulting from two consecutive applications of the same ground motion were applied. The scale factor of the 2nd ground motion was two times of the scale factor of the first one. Finally, a constant axial load equal to 0.9 of nominal compressive strength of the column, P_n was applied together with stepwise increasing cyclic rotations at the column top end until column buckling. Axial forces were applied in load-controlled mode, whereas displacement-controlled mode was used to impose lateral displacements and end rotations to the specimen.

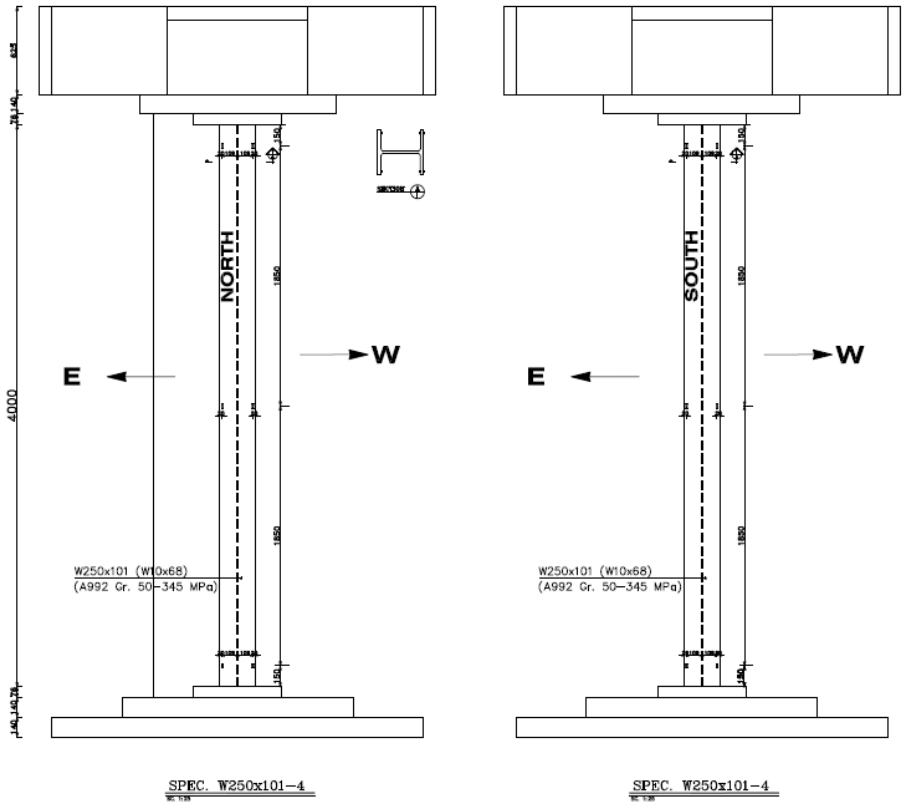

Figure A.17: Shop drawing of specimen CS7.

Figure A.18.b shows the measured top end, strong axis moment and column axial shortening as a function of strong axis to end rotation. The experimental results indicated that the column could withstand the two ground motion sequences without buckling and flexural strength degradation. During the first ground motion, the specimen experienced a total shortening of 20 mm. At the beginning of the second sequence, axial shortening continued but it was interrupted due to a large inelastic story drift and end rotation excursion that occurred in the opposite direction. The column could then maintain its axial and flexural resistances up to the end of the second ground motion.

In the processing of the results of two previous experimental tests (Specimens CS5 and CS6), it was found that frictional resistance by the test setup could affect the results, especially at very high axial loads. However, the frictional resistance was not significant for this test during the two ground motion histories as axial loads were relatively low and the column was bent about strong axis and offered much larger lateral resistance.

In the last part of the test, cyclic end rotation was applied in combination with high constant axial load. The specimen exhibited a reduced flexural strength and experienced additional axial shortening. The column eventually failed by weak axis flexural buckling with some torsional response, as shown in Figure A.18.c.

Figures A.19 and A.20 show the deformed shape of the specimen at several time steps of two sets of ground motions. In Figure A.21, the deformed shape of the column is shown at 0.9 of nominal compressive strength of the column, P_n and different cyclic rotations.

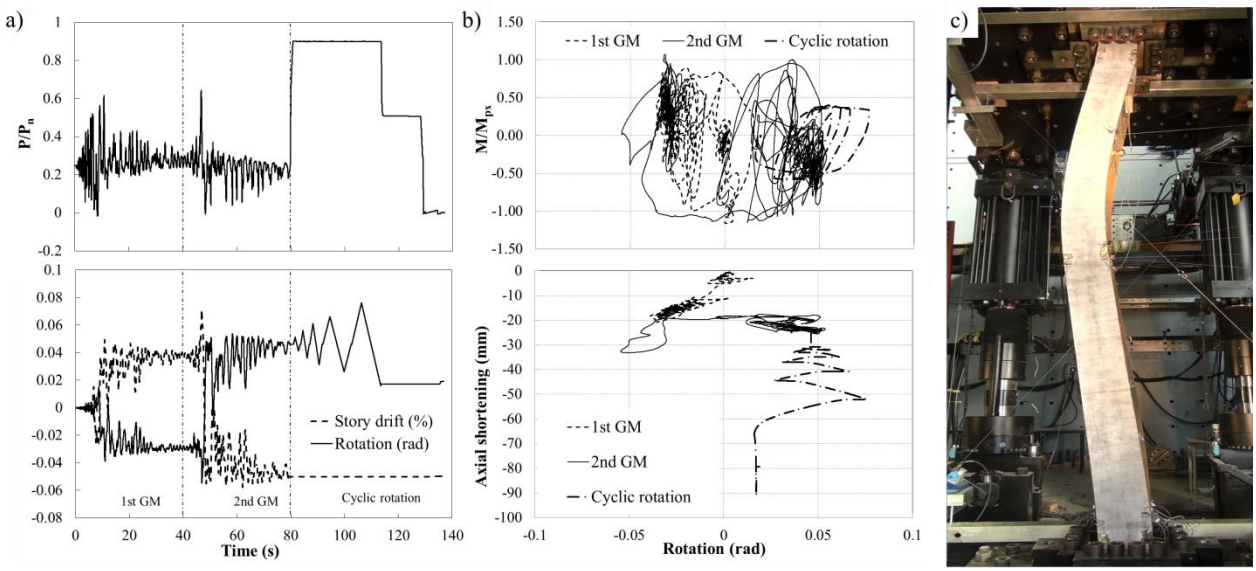

Figure A.18: a) Applied axial load, story drift and top end rotation; b) Top end moment about strong axis and axial shortening *vs* top end rotation; and c) Buckled shape at the end of the test.

The formation of plastic hinges at the bottom, middle and top of specimen CS7 is shown in Figure A.22. Figure A.23 shows the column axial shortening. In Figure A.24, the measurement of strain gauges at the top, middle and bottom of the specimen is presented. In Figure A.24.f, the strain gauge of G3 was missed during the experimental test.

Regarding ASCE 41, this column was not capable of sustaining any inelastic rotation demands. The experiment clearly showed that the column could achieve considerable rotational ductility, even when carrying a large compressive axial load.

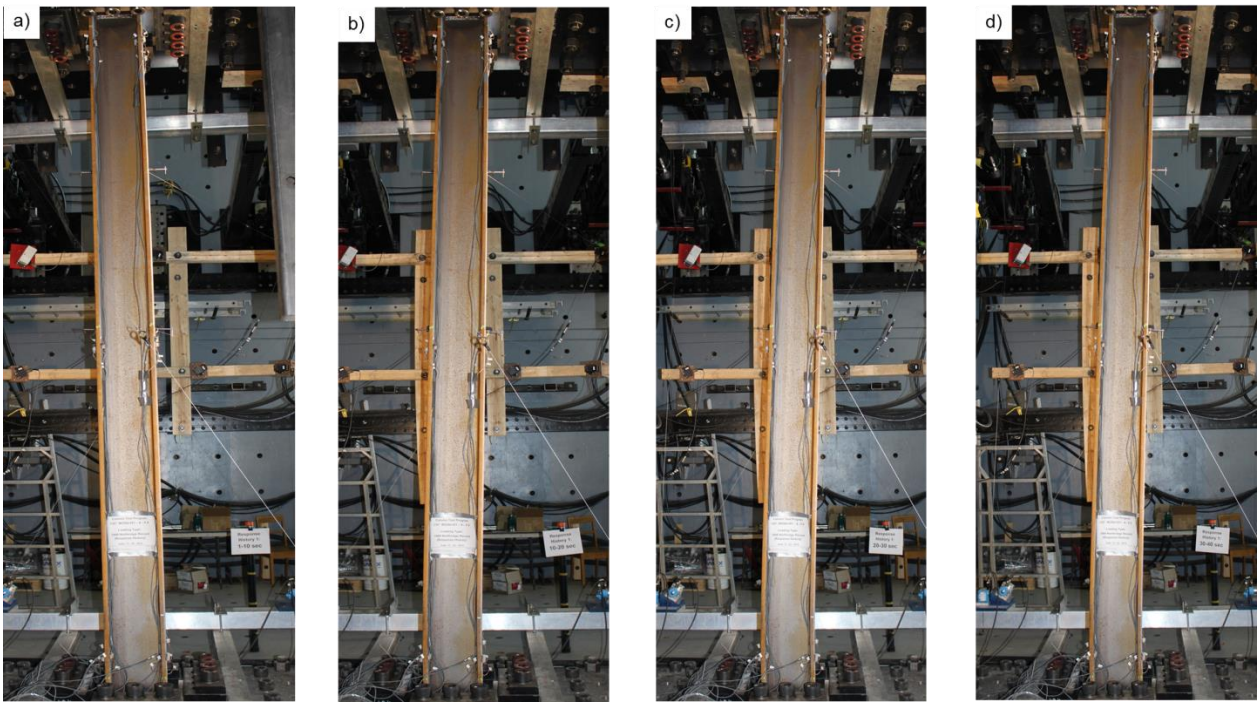

Figure A.19: Deformed shape of specimen CS7 under the first imposed ground motion at a) 1-10 sec; b) 10-20 sec; c) 20-30 sec; and d) 30-40 sec.

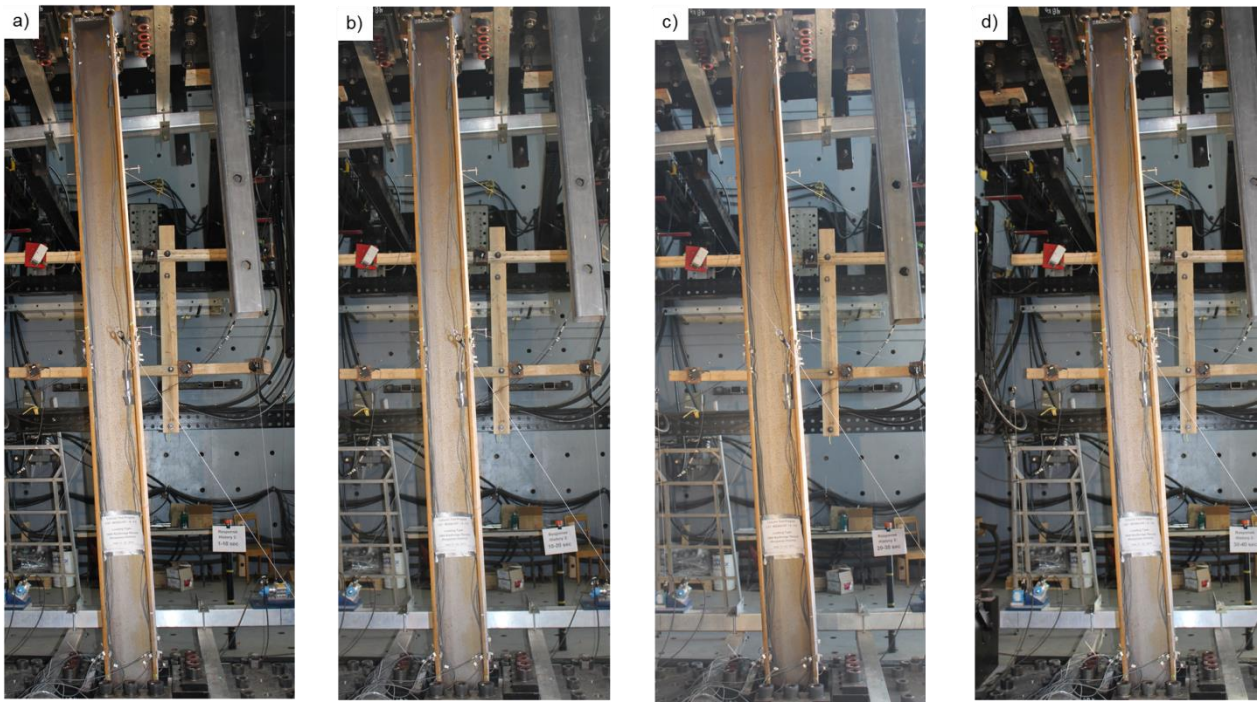

Figure A.20: Deformed shape of specimen CS7 under the second imposed ground motion at a) 1-10 sec; b) 10-20 sec; c) 20-30 sec; and d) 30-40 sec.

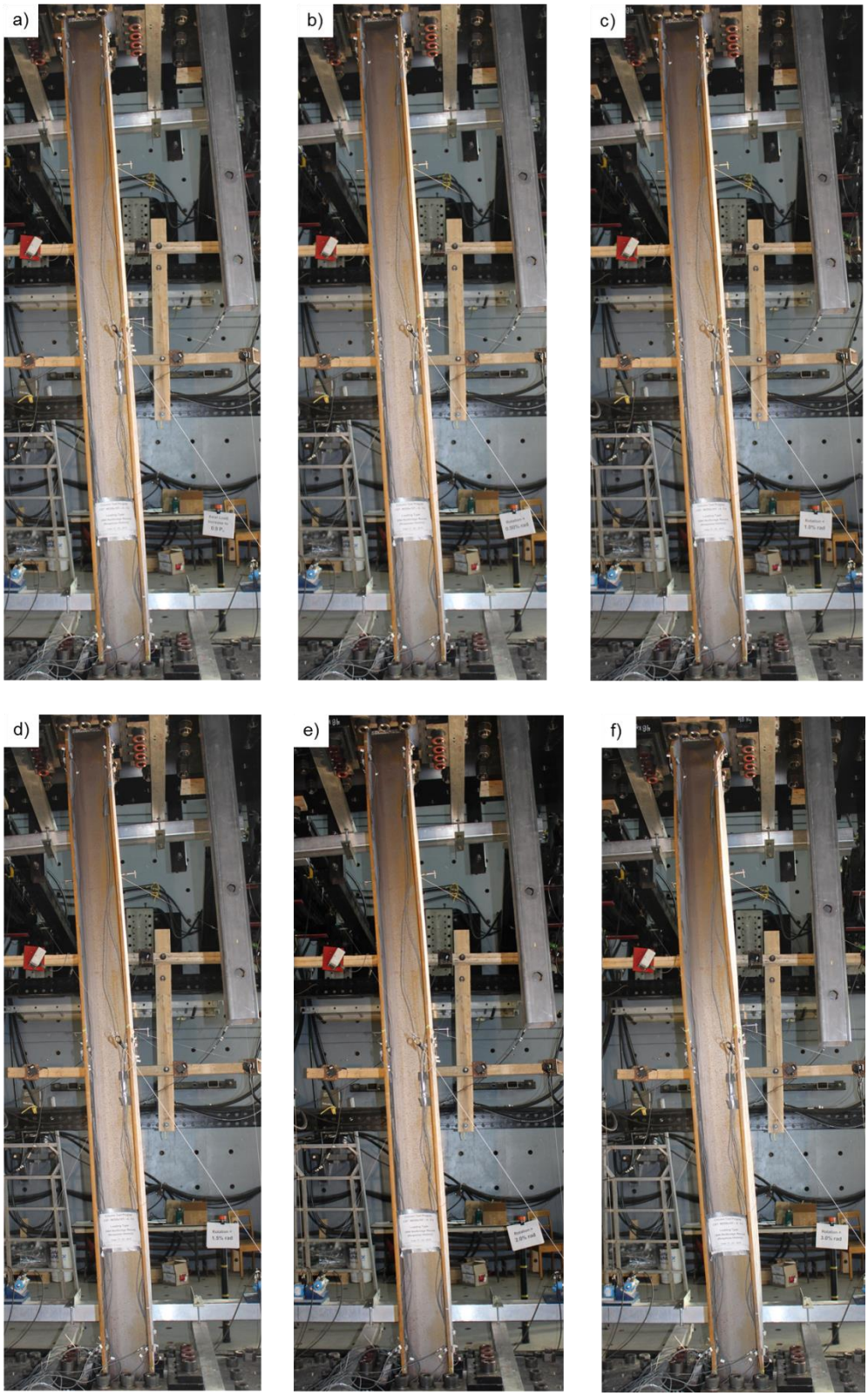

Figure A.21: Deformed shape of specimen CS7 at a) 0.9 P_{CL}; b) 0.5% rad; c) 1% rad; d) 1.5% rad; e) 2% rad; and f) 3% rad.

Figure A.22: Local buckling of specimen CS7 at a) bottom; b) middle; and c) top of column.

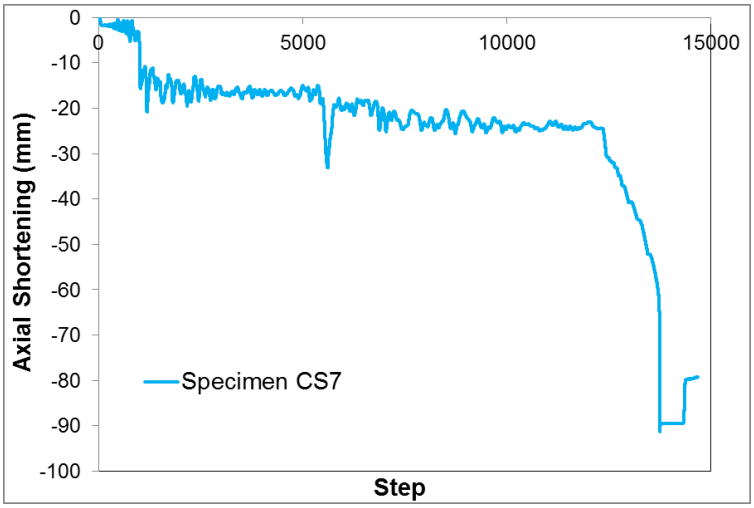

Figure A.23: Axial shortening of specimen CS7.

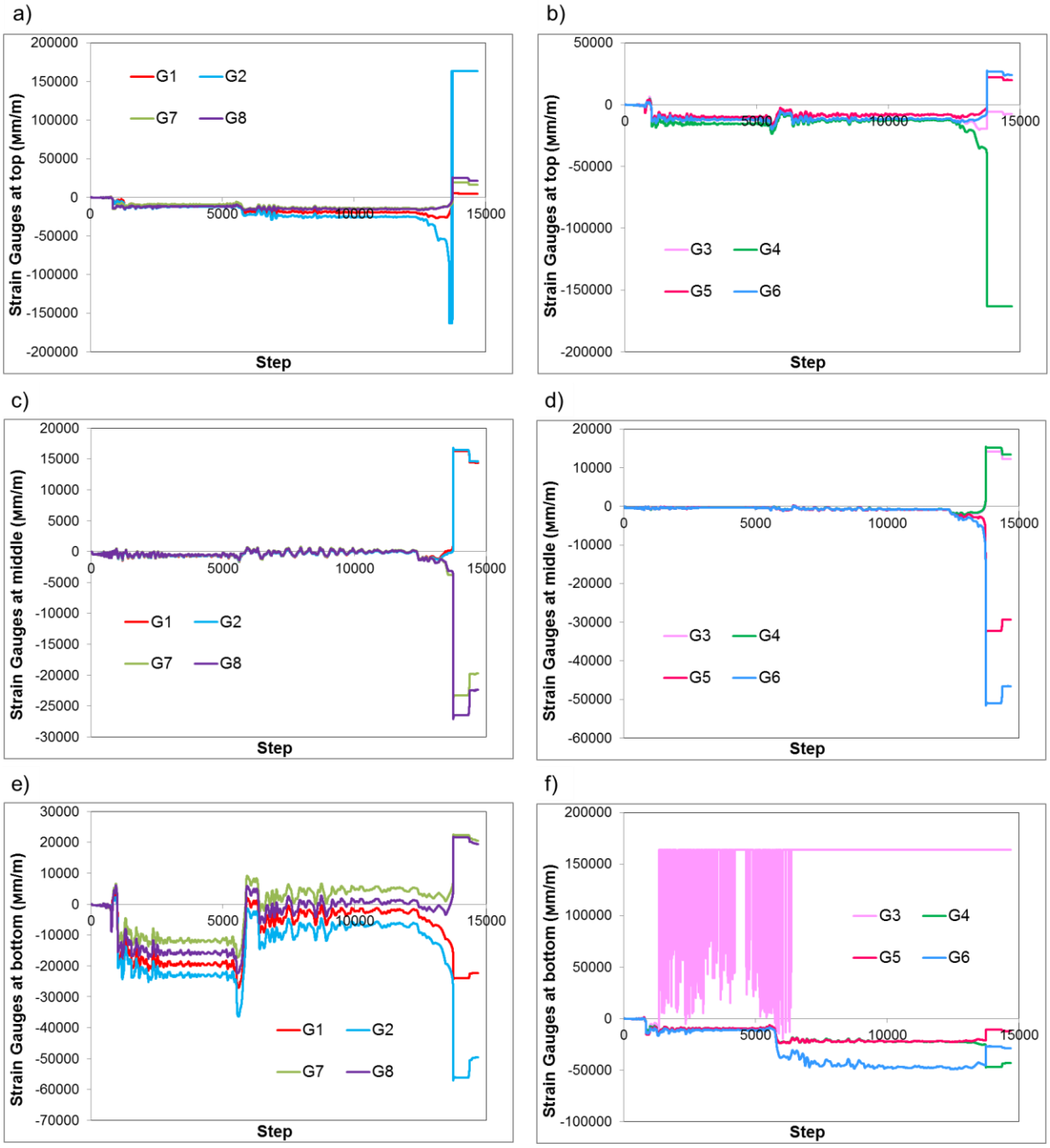

Figure A.24: Strain gauge measurements at top, middle and bottom of specimen CS7: a) G1, G2, G7, G8 (top); b) G3, G4, G5, G6 (top); c) G1, G2, G7, G8 (middle); d) G3, G4, G5, G6 (middle); e) G1, G2, G7, G8 (bottom); and f) G3, G4, G5, G6 (bottom).

The fourth test was designed for further investigation of the seismic response of the column at the 8th storey in the tension-only X-braced frame. The shop drawing of specimen CS10 is the same as specimen CS7. The loading protocol of this test was determined using the seismic response of the column modelled in OpenSees for a group of seven historical ground motion records. The worst case scenario that includes high level of axial loads and large lateral displacements was considered as the selected loading sequence. This loading protocol was imposed to the isolated column modelled in OpenSees with the section of W250x101 as shown in Figure A.25. Two braces with the sections of bracing members at the 8th storey of the studied frame were connected to the top of the column, and they were located at the left- and right-hand side of the structural member. The column was fixed in the model to simulate the boundary condition of Specimen CS10 in the lab. The measured material's yield strength, initial out-of-straightness and residual stress of the specimen were applied to the model. The gravity load of the column at the 8th storey was imposed. Then, several cycles of lateral displacements were applied to the column model. At the end of the loading protocol, a large lateral displacement was imposed to cause the column buckling. The axial loads and lateral displacements that recorded from the column model were imposed to the top of the specimen about its strong axis.

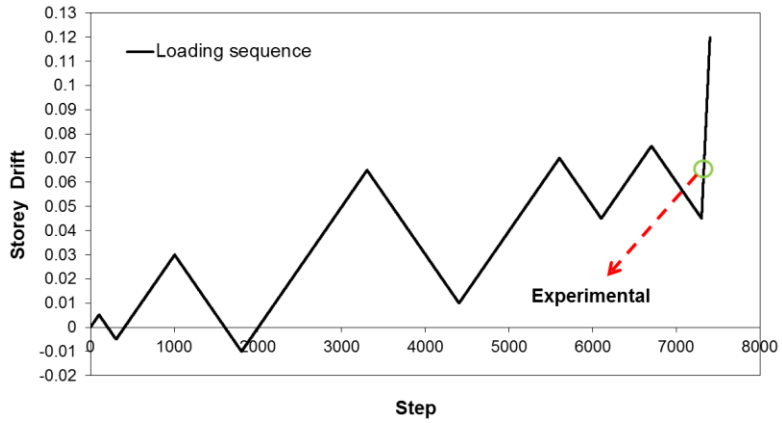

Figure A.25: Lateral displacement imposed to Specimen CS10.

Figure A.26 shows the normalized axial and flexural strength responses versus storey drift of specimen CS10. In Figure A.26.a, the column could carry high level of axial load at large lateral displacement. The results of Figure A.26.b include the friction forces that developed in the system. Regarding the results, the specimen could reach M_p at large storey drift.

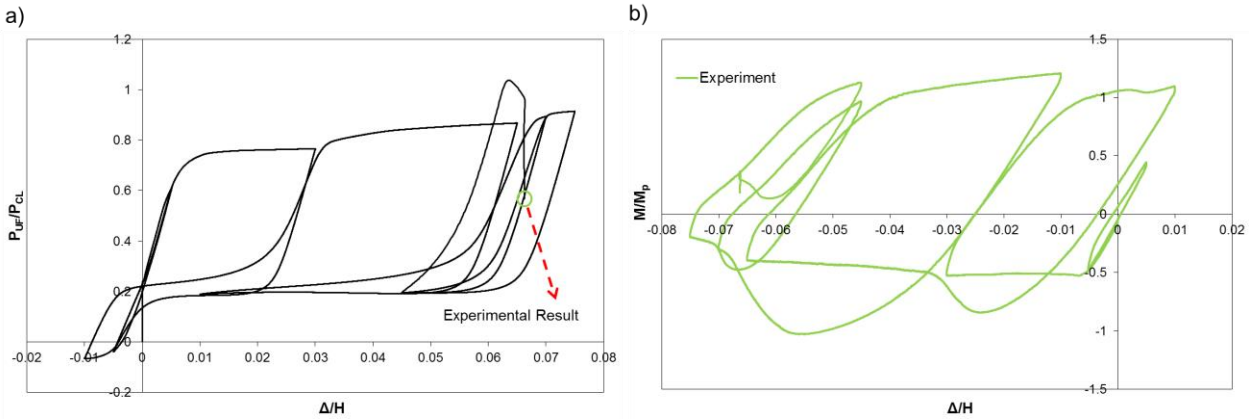

Figure A.26: Specimen CS10 a) normalized axial strength response versus storey drift; and b) normalized flexural strength response versus storey drift.

In Figures A.27 and A.28, the deformed shape of specimen CS10 is presented under several values of storey drift. Lateral torsional buckling of the column is obvious in Figure A.28. Figure A.28c shows that the specimen could carry 0.9 P_{CL} at 0.075 of storey drift without endangering the stability of column.

Figure A.29 shows the buckling of specimen CS10 at storey drift of 6.6% about the strong axis. The governed failure mode of the column was lateral torsional buckling. No local buckling was observed in this test. In Figure A.30, the column axial shortening and rotation due to strong axis are presented. Figure A.31 shows the measurement of strain gauges located at the top, middle and bottom of specimen CS10.

The experimental results of specimen CS10 indicate that the column can resist high level of axial load demand, while large lateral displacement is applied to the specimen. Thus, the column exhibits a ductile behaviour.

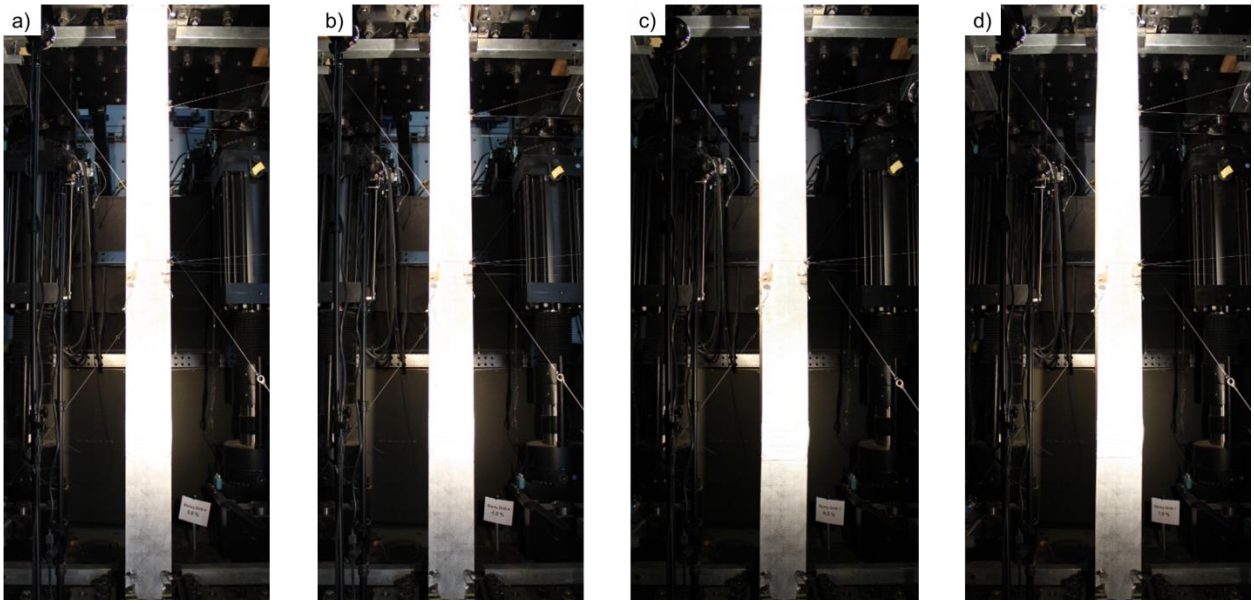

Figure A.27: Deformed shape of specimen CS10 at a) 0.03; b) -0.01; c) 0.065; and d) 0.01 storey drift.

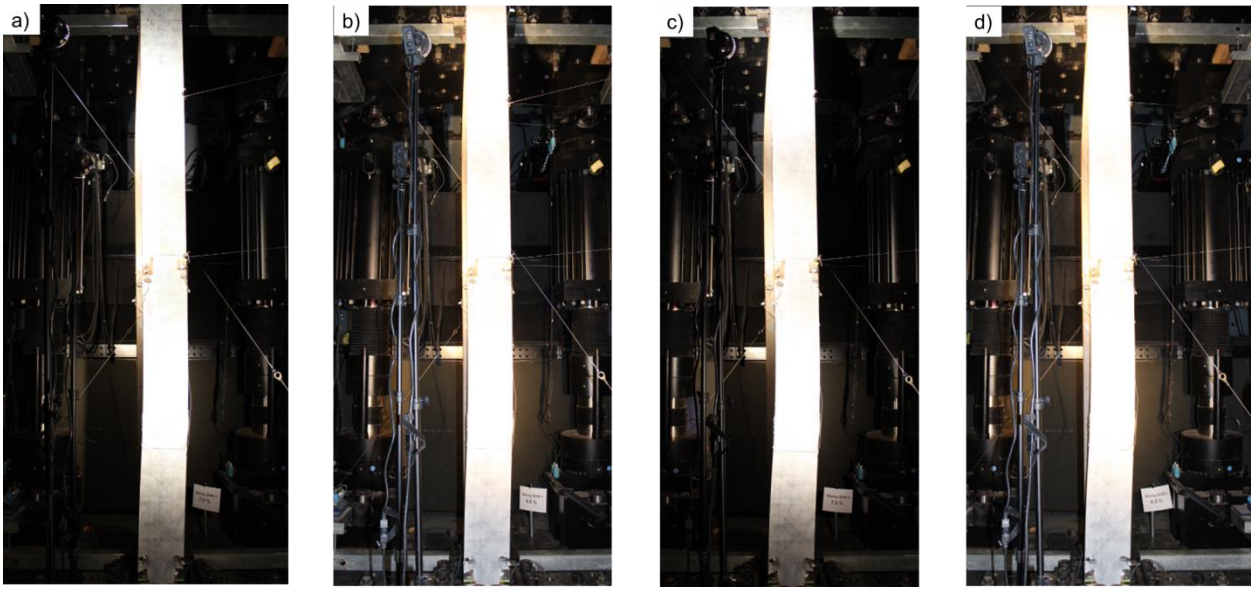

Figure A.28: Deformed shape of specimen CS10 at a) 0.07; b) 0.045; c) 0.075; and d) 0.045 storey drift.

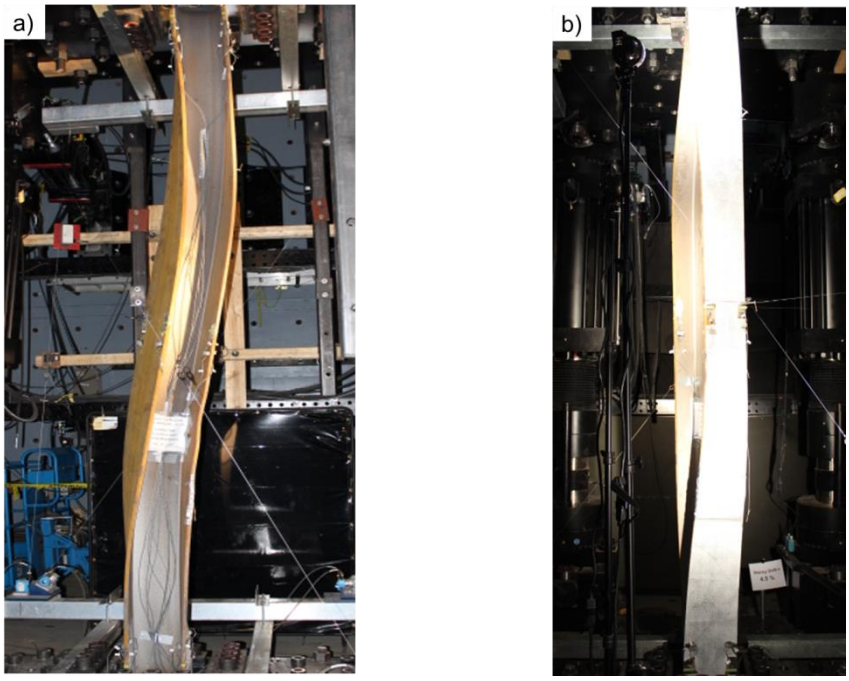

Figure A.29: Deformed shape of specimen CS10 at buckling a) web view; and b) flange view.

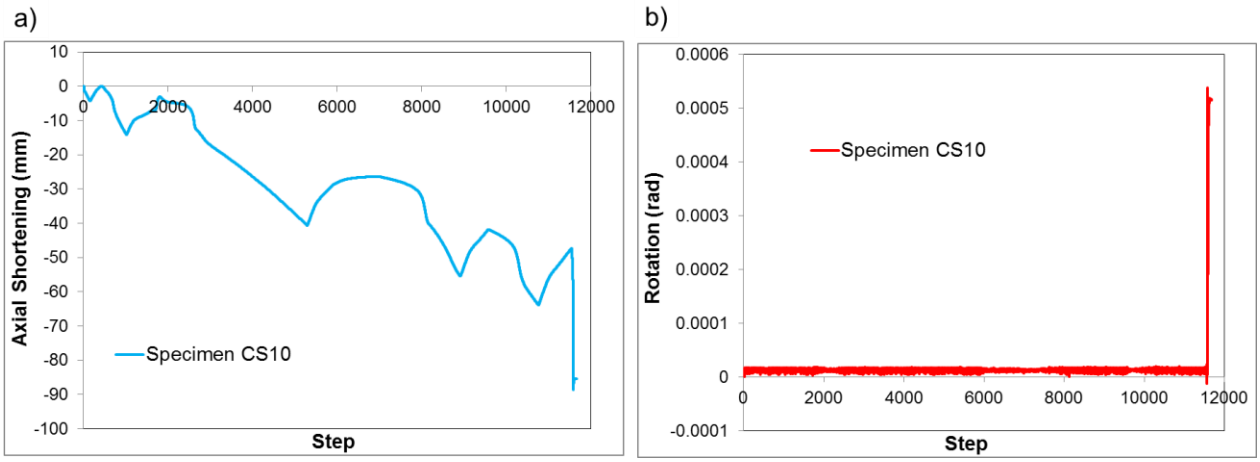

Figure A.30: a) Axial shortening; and b) rotation of specimen CS10.

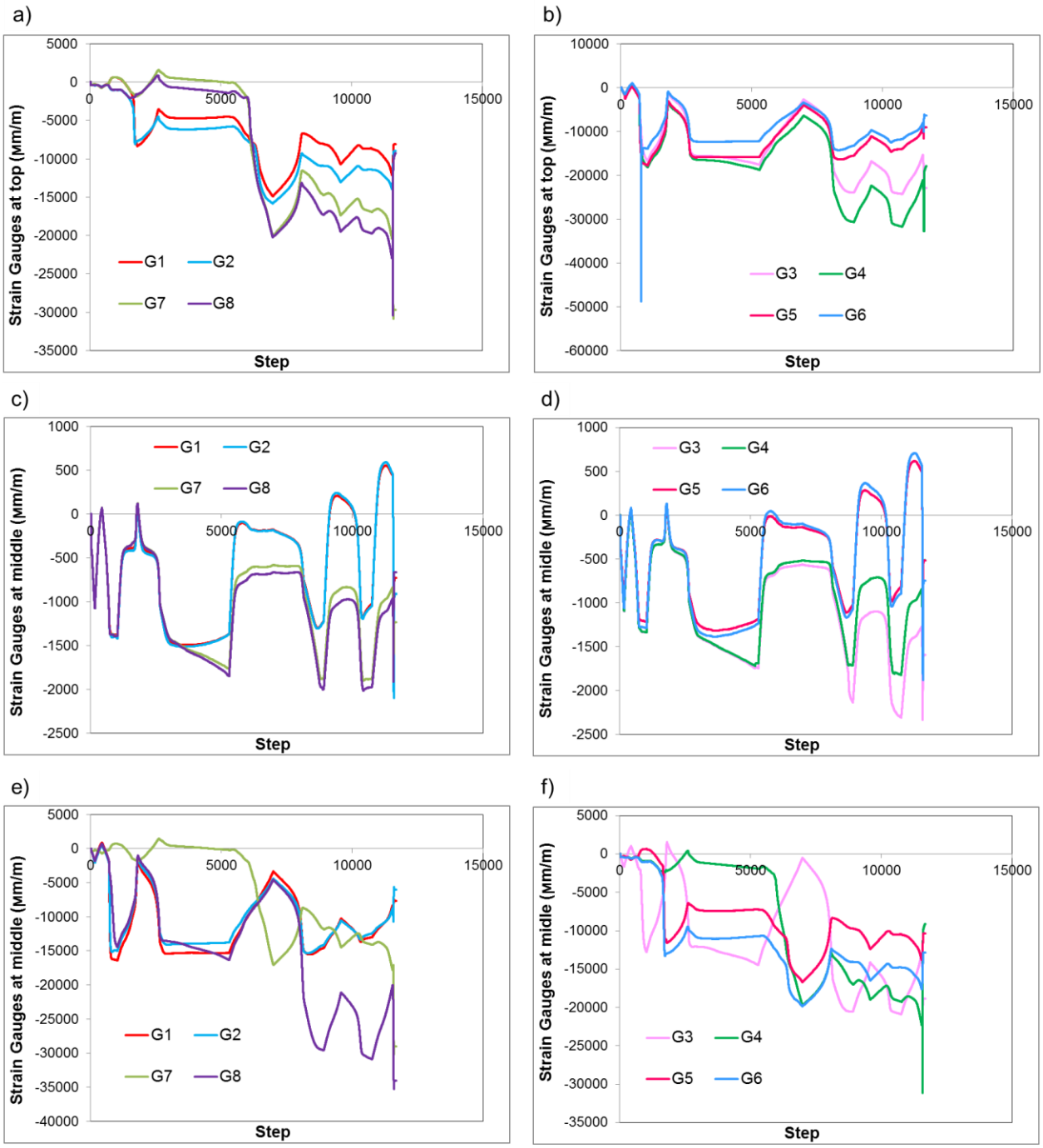

Figure A.31: Strain gauge measurements at top, middle and bottom of specimen CS10: a) G1, G2, G7, G8 (top); b) G3, G4, G5, G6 (top); c) G1, G2, G7, G8 (middle); d) G3, G4, G5, G6 (middle); e) G1, G2, G7, G8 (bottom); and f) G3, G4, G5, G6 (bottom).

APPENDIX B – MODELLING

In APPENDIX B, the details of modelling in OpenSees and ABAQUS are presented. Also, the information regarding double angle sections and brace connections is provided in this appendix.

B1. Modelling in OpenSees

All structural members of the tension-only X-braced frame and chevron braced frame were modelled in the OpenSees finite element platform (McKenna and Fenves 2004).

In all OpenSees models, nonlinear force-based beam-column elements were used to model bracing members. Each angle of the brace member was divided into 16 force-based beam-column elements with 4 integration points placed along each element (Bertero 2004). The cross section of each brace element was discretized by fibers using 20 segments across each leg and 12 layers of fibers across the angle thickness. The Giuffré-Menegotto-Pinto (Steel02) material model was selected to account for the Bauschinger effect and simulate both kinematic and isotropic strain hardening responses. The Giuffré-Menegotto-Pinto (Steel02) material was defined by specifying the yield stress, F_y, and the Young's modulus E (= 200 GPa). The strain-hardening ratio, b (= 0.75%) was considered to define kinematic hardening of the steel material, and three parameters including R_0 (= 30), cR_1 (= 0.925), and cR_2 (= 0.15) were used to simulate the transition from the elastic to inelastic phases. Four isotropic hardening parameters, a_1 (= 0.4), a_2 (= 22), a_3 (= 0.4), and a_4 (= 22) were applied to model the isotropic hardening of the steel material. A yield strength of 330 MPa corresponding to the minimum specified yield value was assigned to the material of the braces. Residual stresses were assigned to the cross-section fibers. They varied linearly along the width of the angle legs following the pattern observed experimentally by Adluri and Madugula (1995). A sinusoidal deformation with maximum amplitude of 1/1000 of the unsupported brace length was assumed for the initial out-of-straightness of the braces, as specified in CSA-S16.1-M78. The initial out-of- straightness was applied both for in-plane and out-of-plane directions. At every level in the tension-only X-braced frame model, the two braces were connected at the intersection point. According to CSA-S16.1-M78, the maximum slenderness ratio permitted for a tension member is 300, and it equals to 200 for a compression member. To satisfy this requirement, one stitch connector was required at mid-length of all braces in the tension-only X-braced frame and chevron braced frame. To model the stitch

connector, an elastic beam element was used to attach the individual angle members to each other. In the connection zone of the brace, the double angle sections in the model were linked to each other by means of elastic beam column elements with high axial and flexural stiffness.

In the OpenSees models, the connections of the braces to the gusset plates were represented by zero-length elements. These in turn were attached to the beams or columns by means of elastic beam column elements with high flexural and axial stiffness simulating the rigidity of the connection zones. The out-of-plane flexural response of the gusset plates was modeled using zerolength elements with uniaxial Giuffré-Menegotto-Pinto material (Steel02) for flexure. Elastic material was considered to simulate the torsional response in the connection regions.

In Model B, where nonlinear force-based beam-column elements were considered for braces, elastic beam-column elements were used for other structural members including beams and columns. Actual flexural and axial stiffness properties of the beams and columns were assigned to the beam-column elements and the zero-length element with high axial and negligible flexural stiffness was considered to model the beam-column connection. Column bases were assumed to be pinned.

Model C of the tension-only X-braced frame was identical to Model B except that columns at every storey were represented by 10 nonlinear force-based beam-column elements with 4 integration points and fiber discretization. Steel02 material with kinematic and isotropic hardening properties was also selected for the columns using the same values that considered for braces except the yield strength. The nominal steel yield strength of 300 MPa was specified for columns and the residual stress pattern by Galambos and Ketter (1958) was assigned to the cross-section fibers of these members (Lamarche and Tremblay 2011). For the columns, 20 segments were considered across the flange of the W-shaped section, and 10 layers of fibers were used across the thickness of the flange. The same assumption was considered for the web of the W-shaped section. The model can account for flexural buckling about both axes and half-sine out-of-straightness deformation with maximum amplitude of 1/1000 of the unsupported member length was initially applied along both orthogonal directions. In Model C of the chevron braced frame, force-based nonlinear beam-column elements were employed for both the braces and the beams, giving a possibility to predict beam limit states such as flexural yielding and/or buckling in the vertical plane. Out-of-plane flexural buckling and lateral-torsional buckling were assumed to be

prevented by floor and roof diaphragms. In this model, 16 nonlinear beam-column elements were used for the beam with 4 integration points placed along each element. Number of fibers used across the flange, web and thickness of the W-shaped sections of beams is the same as columns. As out-of-plane buckling of the beam was restrained by the floor, initial beam out-of-straightness was only considered in the plane of the frame.

In Model D of both tension-only X-braced frame and chevron braced frame, nonlinear force-based beam-column elements were used for all structural members.

In these models, P-delta effects were included by adding a leaning column carrying gravity loads that was linked to the frame at every level. Elastic elements were used to model the leaning column. Gravity load was applied as two point loads on top of the braced frame columns and the leaning column.

Table B.1 shows the details of OpenSees models used for the concentrically braced frames. Nonlinear beam-column elements for braces can predict cross-section yielding and inelastic buckling, while inelastic elements for beams and columns can simulate cross-section yielding and inelastic flexural buckling; however, local buckling and lateral-torsional buckling modes cannot be considered by OpenSees.

Table B.1: Types of modelling for concentrically braced frames

Type of braced frame	Model B		Model C		Model D	
	Elastic	Inelastic	Elastic	Inelastic	Elastic	Inelastic
Tension-only	Beams, Columns	Braces	Beams	Braces, Columns	-	All members
Chevron	Beams, Columns	Braces	Columns	Braces, Beams	-	All members

In this section, the modelling of the first-storey bracing members (2L-200x200x16mm) is presented. Two strategies were examined for modelling including: (i) the braces were represented

by a single element with the properties of double angle sections; and (ii) the two angles constituting a brace were modeled as individual members connected back-to-back to each other by means of contact and gap elements to reproduce the action of a built-up member.

For the second model, the contact elements were placed between the two angles and modeled by elastic beam column elements while zero length elements were used to represent gap elements. When the two angle sections come in contact, the gap elements activate, otherwise each component can freely move away from each other. In the connection zone, the double angle sections in the second model were linked to each other by means of elastic beam column elements with high axial and flexural stiffness.

In both models, the connections of the braces to the gusset plates were represented by zero-length elements. These in turn were attached to the beams or columns by means of elastic beam column elements with high flexural and axial stiffness simulating the rigidity of the connection zones. The length of the brace members was 10223 mm while the net length of the brace, excluding the length of the brace connections, was 8307 mm. For simplicity in the preliminary investigation of the brace models, pinned connections were used at both brace ends.

The assumptions that mentioned at the beginning of this section to model double angle sections were used in this study. A yield strength of 300 MPa was assigned to the brace material. At every level in the building frame model, the two braces of the X-bracing were connected at the intersection point. For both modelling strategies, in-plane and out-of-plane lateral supports were assigned at the brace mid-length to simulate the restraint offered by the intersecting brace. Figure B.1 shows the detail of modelling of the brace and brace connection at the first level.

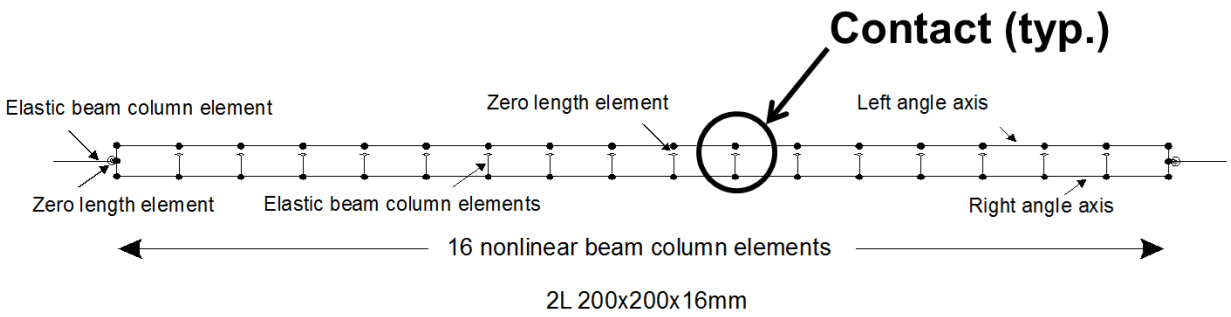

Figure B.1: Details of modelling of the brace and brace connection.

In Figure B.2.a, the hysteresis of the single element brace model is compared to that obtained with the model with two individual angle elements. For the second model, zero, one and two gap elements were considered to investigate the possible impact of the number of gap elements on the inelastic brace response. As shown, the compressive resistance is higher for the brace modelled with a single element because buckling of the individual angle members could not be represented. The study showed that in-plane buckling of the brace was the governing mode. Hence, the number of gap elements between the individual angle members had no impact on the buckling strength of the bracing member. By inspection, it was determined that in-plane buckling mode was critical for all braces in the studied 10-storey frame.

According to CSA-S16.1-M78, the maximum slenderness ratio permitted for a tension member is 300, and it equals to 200 for a compression member. To satisfy this requirement, one stitch connector was required at mid-length of all braces at the intersection of the two braces. To model the stitch connector in the second modelling strategy, an elastic beam element was used to attach the individual angle members to each other. In Figure B.2.b, the hysteretic response of a double angle member modelled with two elements with and without a stitch connector is illustrated. No gap element was used as they do not affect the brace response. As expected, the addition of a stitch at the brace mid-length had nearly no influence on the brace axial response because buckling occurs in-plane and does not induce shear in the stitch connector.

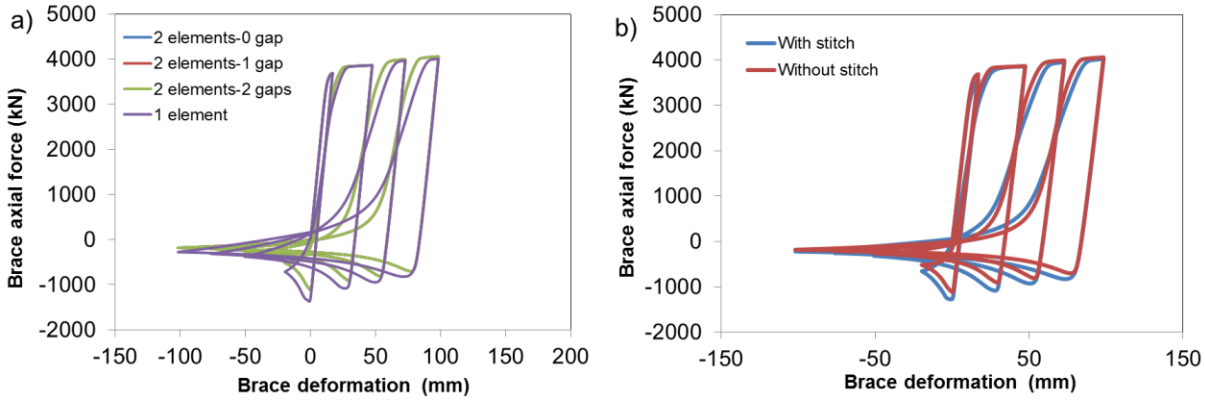

Figure B.2: Hysteretic responses of double angle bracing members: a) comparison between models with single and two individual elements; b) Influence of the stitch connector on brace axial response.

The brace buckling mode was further investigated by examining the brace response under monotonically increasing axial displacement. The section used for the braces at the 8th storey of the X-bracing (2L-125x125x8mm) was considered in this study. The brace was modelled with two individual elements. One stitch connector was assigned at mid-length of the brace. Gap elements were not introduced between the two angles. The influence of the intersecting bracing member was included in the analysis by preventing in-plane and out of plane movements at the brace mid-length. Monotonic displacement was applied in ten equal steps and in-plane and out-of-plane deformations of the two angles were recorded at each loading increment. In-plane deformations of the brace under the progressively increasing axial displacement at one end of the brace are shown in Figure B.3.a. In Figure B.3.b, the out-of-plane position of each angle is shown with respect to its longitudinal axis. In-plane deformations are much larger than out-of-plane deformations, confirming that in-plane brace buckling took place, with limited contribution of individual brace buckling.

This preliminary study showed that a single-member model is inadequate to represent the buckling response of a double angle built-up bracing member. Buckling of the braces in the frame studied is governed by in-plane deformations. In such situation, there is no contact between the two individual angles and thus the number of gap elements does not have impact on the calculated brace compressive resistance. Therefore, gap elements between the two angles were omitted in the final brace model used to analyze seismic response of the 10-storey braced frames. However, in the frames models, one stitch was located at mid-length of the brace members, as it was required to satisfy the maximum slenderness ratio of compressive and tensile members in accordance with CSA-S16.1-M78.

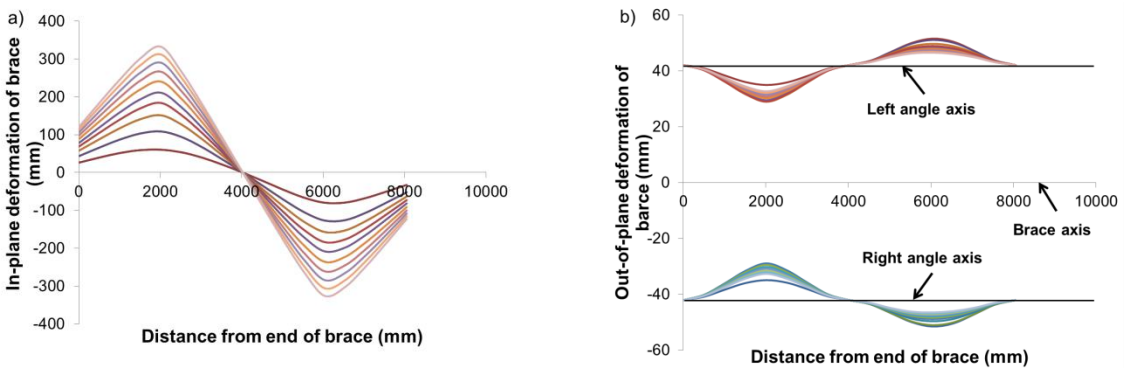

Figure B.3: a) In-plane deformation; and b) out-of-plane deformation of the brace with one stitch at the mid-length of member.

Figure B.4 shows the response of a single column using nonlinear beam-column elements to model this member. The section of the column at the first storey of the chevron braced frame was used in this study. The value of P_{CL} of this section is 8584 kN. In Figure B.4, the ratio of P_{UF}/P_{CL} is 0.97, which shows that OpenSees can predict inelastic buckling, properly.

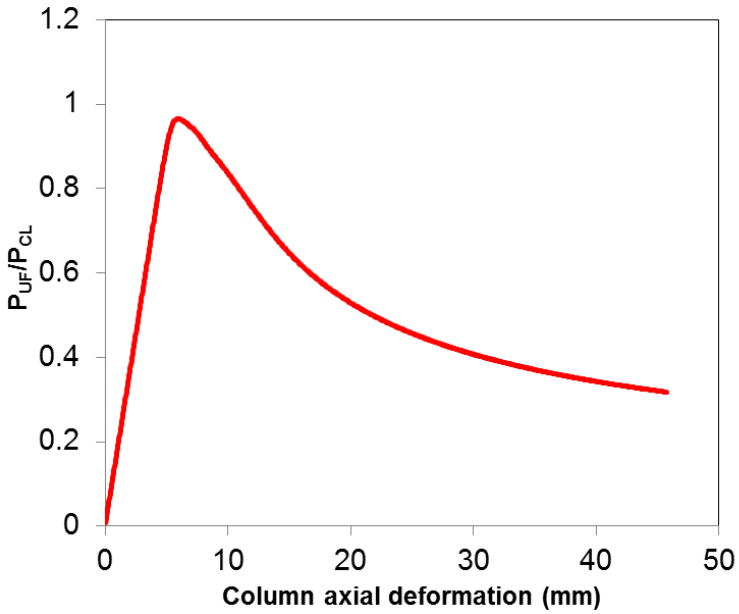

Figure B.4: Axial load-axial deformation response of the column.

In this section, beam buckling in the chevron braced was investigated by conducting incremental static (pushover) analysis of the beam located at the 1st level of the 10-storey prototype building. Five different models were considered to study in detail the beam buckling response and assess the beam compressive strength. The five models were developed by gradually including different structural components, starting from a simple beam case represented in Model 1 to a 2-storey chevron braced frame assembly in Model 5 (Figure B.5.a): Model 1 is a simple beam having half the beam length; Model 2 represents the continuous two-span beam; Model 3 includes the bracing members framing from above; Model 4 includes the gusset plate of the braces framing from below; and Model 5 includes the bracing members framing from below. In Models 3, 4 and 5, the braces were assumed to be pinned at their ends. In Models 1 and 2, axial loading was applied at one beam end. In subsequent models, beam axial load was induced by applying storey shear though the braces. Gravity loading was imposed on the beam.

In Figure B.5.b, the axial load-axial deformation responses of the compression half beam segment from the 5 different models are compared. In this figure, the beam C_n is determined with an effective length equal to half the chevron beam length. The peak C/C_n values from Models 1 to 5 are: 0.86, 0.923, 0.923, 0.964 and 0.963, respectively. The buckling strengths determined using Models 2 to 5 are higher than that obtained from Model 1. This could be expected because the additional flexural stiffness provided by the second half of the beam subjected to tension contributed to increase the buckling resistance of the compression half-beam segment. In Models 4 and 5, the presence of the gusset plate increased the beam axial and flexural stiffnesses; the latter also resulted in increased beam buckling strength. The results from the most representative Model 5 show that the C_n value from current code equations can be used to predict the beam buckling strength.

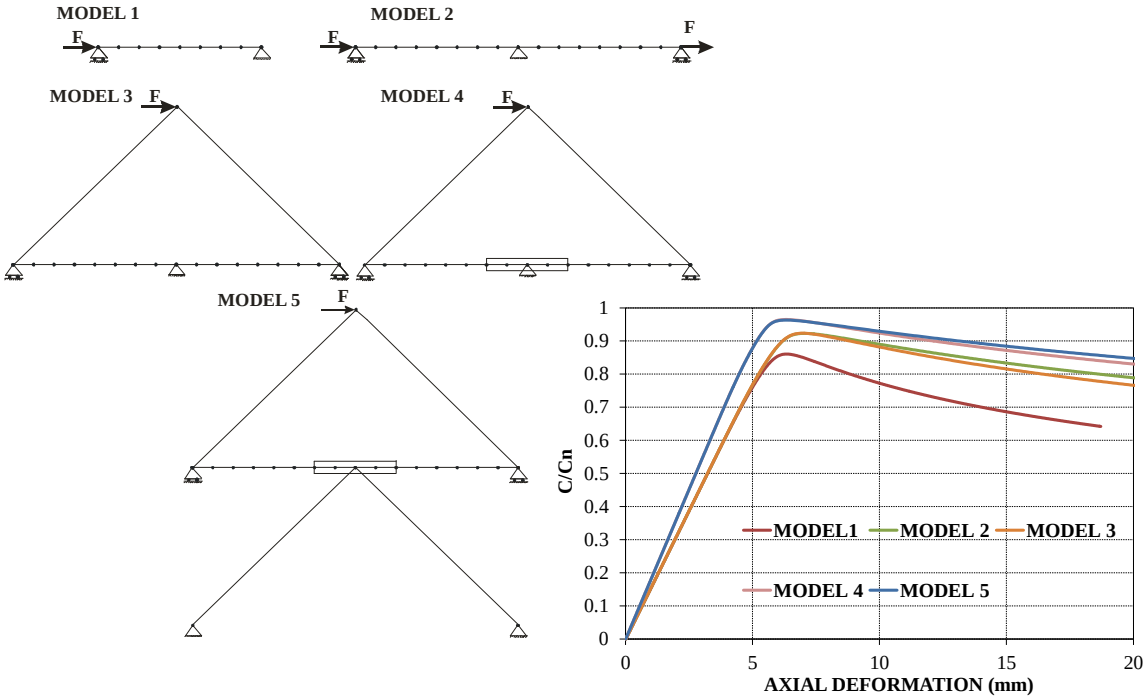

Figure B.5: a) Models used for examination of the beam buckling response at the 1st level of chevron braced frame; and b) computed beam axial load-deformation responses.

This section presents the cyclic response of a single column using Steel02 material with kinematic and isotropic hardening properties to model this member. The equations that specified for isotropic hardening parameters were used to determine the values of the a_3 and a_4 parameters. The values of a_3 and a_4 are respectively 0.2 and 26.67 at 0.04 rad, where F_y^*/F_y equals to 1.2. The boundary condition of the column was fixed-fixed, and the slenderness ratio of the member was 50. The applied axial load to the column was $0.7P_{CL}$. For the cyclic loading, the AISC loading protocol was imposed to the column.

(1) $$F_y^* = F_y\left\{1+a_3\left[\left(\varepsilon_{max}-\varepsilon_{min}\right)\Big/\left(2a_4\varepsilon_y\right)\right]^{0.8}\right\}$$

(2) $$a_3 = F_y^*\Big/F_y - 1$$

(3) $a_4 = \left(\varepsilon_{\max} - \varepsilon_{\min}\right) \Big/ \left(2\varepsilon_y\right)$

Figure B.6.a shows the moment-storey drift response of the column under cyclic loading. In this figure, the M/M_p ratio reaches 1.42. Figure B.6.b shows that the flexural demand of the column reaches M_u, which is not acceptable. In Figures B.7.a and B.7.b, the stress and strain were recorded at the left and right corners of the column cross section, which show significant values of stress and strain in the section. Regarding the results, the isotropic hardening parameters specified for Steel02 material cannot predict well the hysteric response of the member when significant numbers of cycles impose to the member.

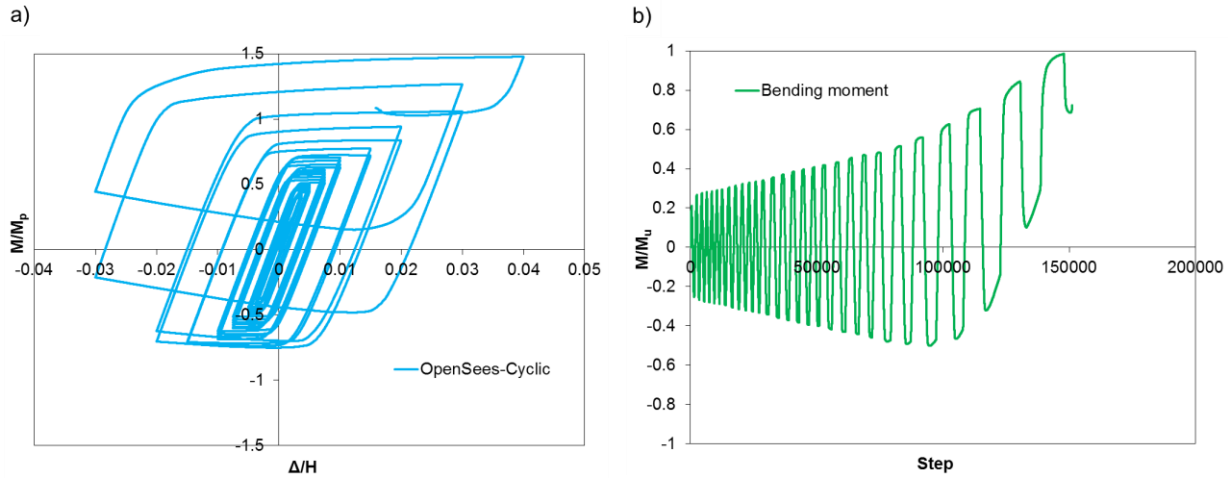

Figure B.6: a) Moment-storey drift response of the column; and b) normalized bending demand to M_u.

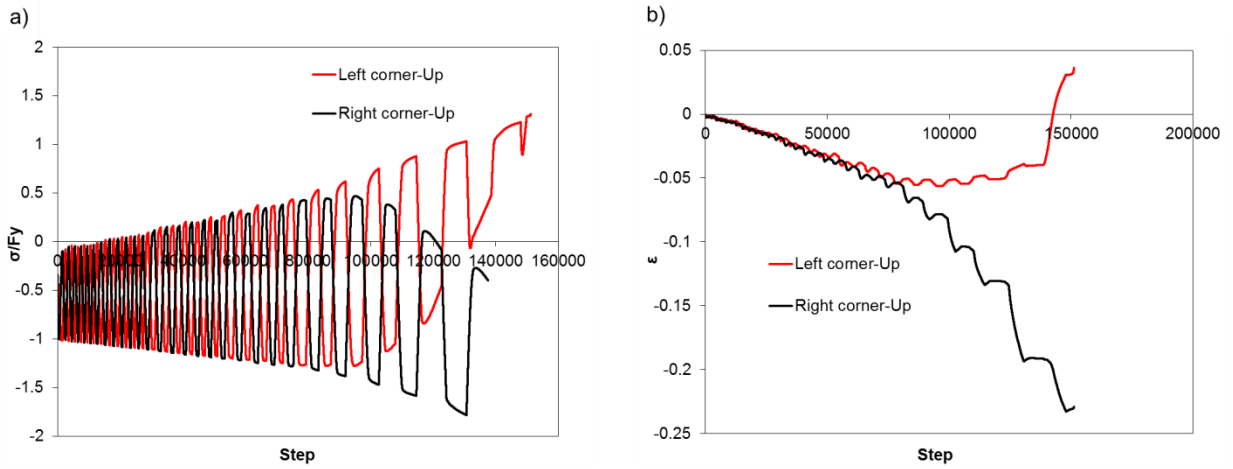

Figure B.7: a) Stress demand; and b) strain demand at the left and right corners of the column cross section.

B2. Modelling in ABAQUS

In the ABAQUS program (Dassault 2012), three dimensional models of a concentrically braced frame column and a chevron braced frame were developed using four-node shell elements with reduced integration. For each structural member, 5 integration points were used across the thickness of the component, and Simpson integration rule was considered to solve the problem. In all analyses, the direct method was selected as the equation solver, and full Newton was considered as the solution technique. Also, geometric nonlinearities (large deformations) were used for all models. The steel material property of the structural components was applied as the curve of yield stress-plastic strain, and combined hardening was used to consider cyclic hardening in the model.

To impose the residual stress, the sections of braces, beams and columns were partitioned to the strips, and the residual stress value was applied to those strips. Before applying the loads to the model, elastic buckling analysis was performed to determine the required deformed shapes. Those deformed shapes were selected and the initial imperfections were imposed to them. Then, the nonlinear static analysis was performed on the selected deformed shapes.

Figure B.8 shows the applied loads to the chevron braced frame. In this figure, the gravity load was imposed to the beam at the first level. Then, the lateral displacement time histories at mid-

span of the 1st and 2nd level beams were applied, together with the time histories of the vertical displacements at beam-to-column joints at both levels. As shown, lateral displacements were applied at gusset plate-to-beam connections. In this frame, coupling of nodes was used to constraint the nodes to the control point, and the boundary condition was applied to that point.

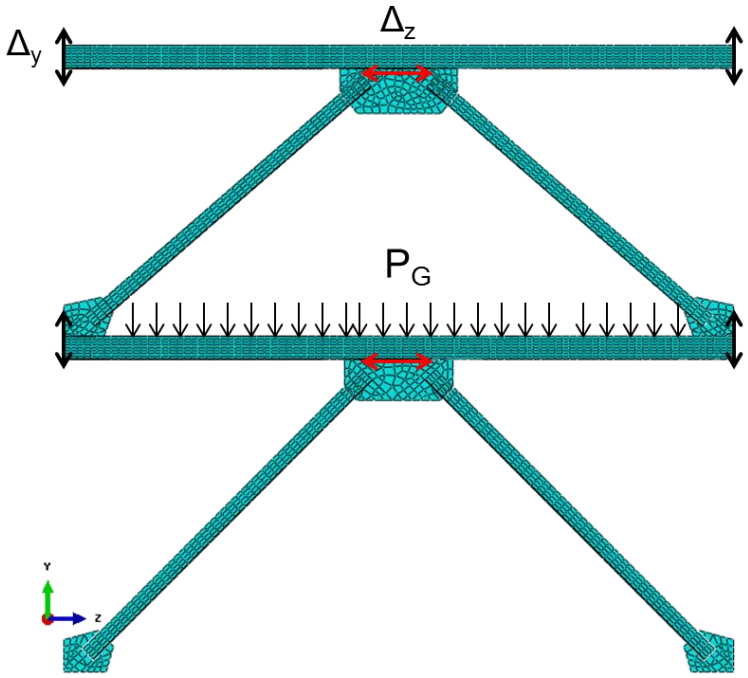

Figure B.8: Applied loads to the chevron braced frame.

B3. Braces and brace connections

In this study, the factored compressive resistance, C_r of double angle braces was determined in accordance with CSA S16-09. The double angle section was a single symmetric section; thus, the following equations were used to define elastic buckling stress, F_e. These equations were specified for a singly symmetric section with the y-axis considered as the axis of symmetry:

$$(1)\quad F_{eyz} = \frac{F_{ey} + F_{ez}}{2\Omega}\left[1 - \sqrt{1 - \frac{4F_{ey}F_{ez}\Omega}{\left(F_{ey} + F_{ez}\right)^2}}\right]$$

The values of F_{ex}, F_{ey} and F_{ez} are determined from the following equations:

(2) $$F_{ex} = \frac{\pi^2 E}{\left(\frac{K_x L_x}{r_x}\right)^2}$$

(3) $$F_{ey} = \frac{\pi^2 E}{\left(\frac{K_y L_y}{r_y}\right)^2}$$

(4) $$F_{ez} = \left(\frac{\pi^2 E C_w}{(K_z L_z)^2} + GJ\right)\frac{1}{A\bar{r}_0^2}$$

where, K_z is the effective length factor for torsional buckling.

(5) $$\bar{r}_0^2 = x_0^2 + y_0^2 + r_x^2 + r_y^2$$

(6) $$\Omega = 1 - \left[\frac{x_0^2 + y_0^2}{\bar{r}_0^2}\right]$$

In equations 5 and 6, x_0 and y_0 are principal coordinates of the shear centre with respect to the centroid of the cross-section.

Regarding CSA S16-09, flexural-torsional buckling is not a controlling limit state for equal-leg double angles connected back-to-back to a common gusset plate. Note that this is the section that was used for braces in this study.

As mentioned in Section 2.1.2, block shear failure mode was not considered in CSA S16.1-M78 (CSA 1978). In CSA S16-09, equation 7 is considered to determine the factored resistance of the connection, T_r for a potential failure.

(7) $$T_r = \phi_u\left[U_t A_n F_u + 0.6 A_{gv}\left(\frac{F_y + F_u}{2}\right)\right]$$

In this equation, A_n and A_{gv} are respectively the net area in tension and the gross area in shear for block shear failure, F_y and F_u are respectively specified minimum yield and tensile strengths and U_t is the efficiency factor. In CSA S16-09, for angles connected by one leg, U_t = 0.6 and the shear lag reduction factor is equal to 0.8 when the connection includes four or more bolts and 0.6 when fewer bolts are used. The value of ϕ_u is 0.75. Figure B.9 shows the block shear failure of a

bolted gusset plate (Singh Huns et al. 2002). In this figure, the tension plane between holes 5 and 6 has completely fractured. The shear cracks are also observed on the right shear plane.

Figure B.9: Block shear failure of a bolted gusset plate (Singh Huns et al. 2002).

APPENDIX C – UPDATE THE CROSS SECTION OF A MEMBER IN OPENSEES

There is a command in OpenSees finite element platform (McKenna and Fenves 2004) to change the specification of the cross section during the analysis. The following example explains this command.

The column at the first level of an existing 10-storey tension-only X-braced frame was modelled in OpenSees. The height of the column was 4572 mm and its cross section was W310x283 mm. The number of elements along the height of the column was ten, and nonlinear beam-column elements with 4 integration points were used along each element. The existing cross section of the column element was discretized by fibers. To reproduce the nonlinear behaviour of the existing column, the Giuffré-Menegotto-Pinto steel material with isotropic hardening (Steel02) was used. The yield strength of 300 MPa corresponding to the minimum specified yield value was assigned to the material of existing cross section, and residual stresses were assigned to the cross-section fibers. The residual stress pattern was assigned to the cross-section fibers of the existing column (Galambos and Ketter 1958). The initial out-of-straightness of the column was a half-sine deformation with maximum amplitude of 1/1000 of the unsupported member length, as described in the CSA-S16.1-M78.The initial out-of-straightness was applied both for in-plane and out-of-plane directions of the column. The column at the base was pinned.

As the existing column at the 1st level of the 10-storey braced frame required to be retrofitted, two plates of 315x44.45 mm were considered. These plates were welded to the flanges of the column. The yield strength of the plates was 345 MPa, and the plates were modeled by Steel 01 material in the model. Figure C.1 shows the details of column modelling.

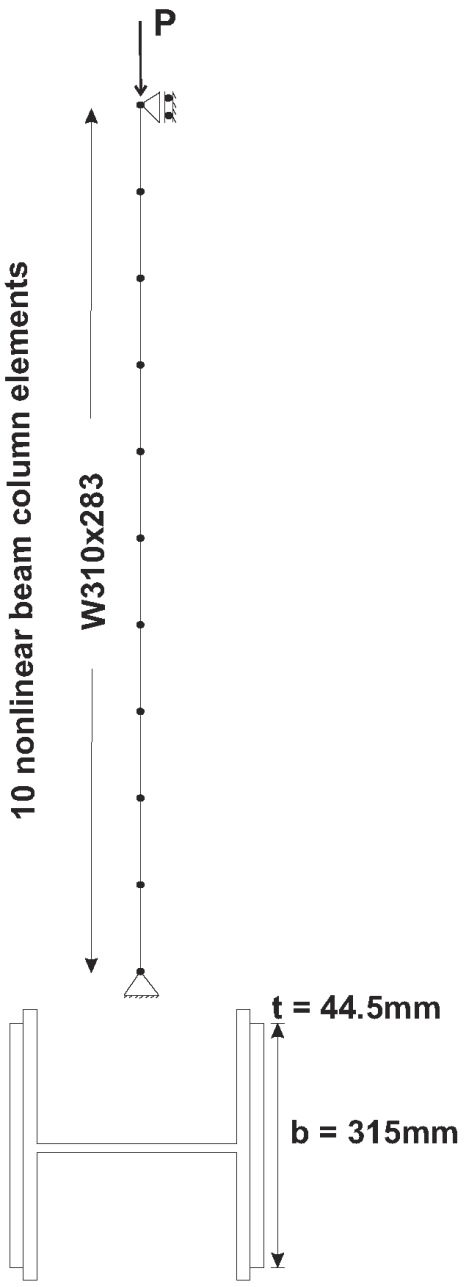

Figure C.1: Details of column modelling.

In OpenSees, the Parameter Command and the UpdateParameter Command can change the cross section of the member during the analysis. These commands can be used for sensitive parameters of the uniaxial materials; for instance, the elastic modulus, E, is one of the sensitive parameters of Steel 01 in OpenSees that can be changed during the analysis using the Parameter Command and the UpdateParameter Command. It should be noted that these commands are not available for the

Steel02 material.

In this example, the dead load was applied to the existing cross section; then, the cross section of the member was updated and the live load was employed to the retrofitted cross section. When the dead load was applied, the plates were not considered in the modelling as the value of the elastic modulus of plates was equal to zero. In the next step, the value of the elastic modulus of plates was updated to consider these elements in the modelling of columns.

In the following code, the commands of Parameter and UpdateParameter are used, where the material tag of the plate is 30001, the element tag is 111 and the parameter tag is 100001. The following code shows the updating of the column cross section:

```
wipe all;
source DisplayModel2D.tcl;
source DisplayPlane.tcl;

#Results
set dataDir Data5;          # set up name of data directory
file mkdir  $dataDir;       # create data directory

# Units = KN-mm
model BasicBuilder -ndm 3 -ndf
set Pi 3.14159265

# Number of elements and integration points
set NELEMCOL  10;   #column member
set ptoint 4
```

```
# Frame width and height
set Frame_H 4572.

# Initial out-of-straightness for Column
set f_L_1 [expr 1/1000.]

# Characteristics of the columns:
#Column properties
# Column W310x283
set Column_A 36000.
set Column_Iy  7.87E+8
set Column_Iz  2.46E+8
set Column_J  20400000.
set Column_F_b 322.
set Column_F_t 44.1
set Column_H  365.
set Column_W_t 26.9

# Retrofit of the column
# Plate 315x44.45
set Plate_b     315.
set Plate_t     44.45

# Steel material properties
```

```
set Fy  0.300

set E 200.

set nu 0.3

set G [expr $E / 2 / (1 + $nu)]


# Location of the corner nodes

node  110  0.                    0.                0.

node  1003  0. [expr $Frame_H]                0.


# Location of the Column memebrs

for {set i 111} {$i <= [expr 110 + ($NELEMCOL - 1)]}  {incr i 1} {

set Li [expr ($i - 110) * $Frame_H / $NELEMCOL];

node $i    [expr $f_L_1 * $Frame_H *   sin($Pi * $Li / $Frame_H)]    [expr (($i - 110) * ([expr $Frame_H] / $NELEMCOL))]   [expr $f_L_1 * $Frame_H *  sin($Pi * $Li / $Frame_H)] ;

}


# Boundary conditions

fix 1003  1 1 1 1 1 0

fix 110   1 0 1 1 1 0


# Vector for definitions of the member local axes

geomTransf Linear 1 0 1 0

geomTransf Linear 2 0 0 1

geomTransf Corotational 3 0 0 1

geomTransf Corotational 4 0 0 -1
```

```
geomTransf Linear 5 0 -1 0
geomTransf PDelta 6 0 0 1;   # PDelta transformation

# Column middle element
# Fiber discretization of the column member cross-section
# J of the column member (Torsion)
uniaxialMaterial Elastic 1399 [expr $G * $Column_J]
#1st story
set bc [expr $Column_F_b]
set hc [expr $Column_H]

# Assumed linearly varying stress in flanges and constant in web
# 1st story
set sigma_C [expr $Fy * -0.3]
set sigma_T [expr ($Column_F_b * $Column_F_t) / ($Column_F_b * $Column_F_t + $Column_W_t * ($Column_H - 2 * $Column_F_t)) * -$sigma_C]

# Top flange fibers
for {set i 1 } {$i <= 10 } {incr i 1} {
set sigma_r_c [expr  $sigma_C + ($i / 10. - 0.05) * ($sigma_T - $sigma_C)];
uniaxialMaterial Steel02 [expr ($i + 10)]  $Fy  $E [expr (0.1 * $Fy / 0.04) / $E]  30  0.925  0.15  0.4  22  0.4  22  $sigma_r_c ;
}
# Web fibers
```

```
uniaxialMaterial Steel02  200  $Fy  $E [expr (0.1 * $Fy / 0.04) / $E]  30  0.925  0.15  0.4  22  0.4  22  $sigma_T;


uniaxialMaterial Steel01 30001  $Fy_PL  $E [expr (0.1 * $Fy_PL / 0.04) / $E]    0.4  22  0.4  22 ;


#Retrofitted Column Section

section Fiber 1300 {

# Top flange

for {set i  1 } {$i <= 10 } {incr i 1} {

patch quad      [expr ($i + 10)]   20   1   [expr -$hc / 2.]    [expr -$bc / 2. + ($i - 1) * $bc / 20.]
        [expr -$hc / 2. + $Column_F_t]  [expr -$bc / 2. + ($i - 1) * $bc / 20.]    [expr -$hc / 2. +
$Column_F_t]  [expr -$bc / 2. + $i * $bc / 20.]  [expr -$hc / 2.]  [expr -$bc / 2. + $i * $bc / 20.]

}

for {set i  11 } {$i <= 20 } {incr i 1} {

patch quad      $i  20  1   [expr -$hc / 2. ]  [expr $bc / 2. - ($i - 10) * $bc / 20.]   [expr -$hc / 2. +
$Column_F_t ]          [expr $bc / 2. - ($i - 10) * $bc / 20.]    [expr -$hc / 2. + $Column_F_t]
        [expr $bc / 2. - ($i - 11) * $bc / 20.]  [expr -$hc / 2.]  [expr $bc / 2. - ($i - 11) * $bc / 20.]

}


# Bottom flange

for {set i  1 } {$i <= 10 } {incr i 1} {

patch quad      [expr ($i + 10)]  20  1   [expr $hc / 2. - $Column_F_t]   [expr -$bc / 2. + ($i - 1) *
$bc / 20.]   [expr $hc / 2.]   [expr -$bc / 2. + ($i - 1) * $bc / 20.]  [expr $hc / 2.]    [expr -$bc / 2. +
$i * $bc / 20.]  [expr $hc / 2. - $Column_F_t]  [expr -$bc / 2. + $i * $bc / 20.]

}

for {set i  11 } {$i <= 20 } {incr i 1} {
```

```
patch quad      $i   20   1   [expr $hc / 2. - $Column_F_t]   [expr $bc / 2. - ($i - 10) * $bc / 20.]
        [expr $hc / 2. ]          [expr $bc / 2. - ($i - 10) * $bc / 20.]    [expr $hc / 2.] [expr $bc / 2. -
($i - 11) * $bc / 20.]   [expr $hc / 2. - $Column_F_t]  [expr $bc / 2. - ($i - 11) * $bc / 20.]

}


# web

patch quad      200  1  20  [expr -$hc / 2. + $Column_F_t]  [expr -$Column_W_t / 2.]     [expr
$hc / 2. - $Column_F_t]   [expr -$Column_W_t / 2.]   [expr $hc / 2. - $Column_F_t]   [expr
$Column_W_t / 2.]  [expr -$hc / 2. + $Column_F_t]          [expr $Column_W_t / 2.]


# Left Plate

patch quad      30001  20  1  [expr -$hc/ 2. - $Plate_t ]   [expr -$Plate_b / 2.]      [expr  -$hc  /  2.]
[expr -$Plate_b / 2.]   [expr -$hc / 2.]  [expr $Plate_b / 2.]   [expr -$hc / 2. -  $Plate_t]  [expr
$Plate_b / 2.]


# Right Plate

patch quad      30001  20  1  [expr $hc/ 2. ]   [expr -$Plate_b / 2.]          [expr   $hc   /   2.   +
$Plate_t]  [expr -$Plate_b / 2. ]   [expr $hc / 2. + $Plate_t ]  [expr $Plate_b/ 2.]  [expr $hc / 2.]
[expr $Plate_b / 2.]

}

# Adding torsional stiffness to the nonlinear beam-column element

section Aggregator 1301  1399  T -section 1300


# Column middle elements

set tol 1e-6

set maxIters 100
```

```
for {set i 111} {$i <= [expr $NELEMCOL + 110 - 1 ]} {incr i 1} {
element nonlinearBeamColumn   $i   [expr $i - 1]  $i   $ptoint 1301  3  -iter $maxIters $tol;
}
element nonlinearBeamColumn   [expr $NELEMCOL + 110]   [expr $NELEMCOL + 110 - 1]  1003  $ptoint 1301  3  -iter $maxIters $tol;

# Parameter command
parameter 100001 element 111  section 1 section material 30001 E
for {set i 2} {$i <= $ptoint} {incr i} {
for {set j 111} {$j <=  $NELEMCOL + 110} {incr j 1} {
addToParameter 100001 element $j section $i section material 30001 E
}
}

updateParameter 100001  0.

# Print Elements
print nodes.out node
print elements.out element
puts "Elements OK"

# RESULTS
recorder Node -file $dataDir/Deformation_1003.out -time -node 1003  -dof 1 2 3 "disp";
recorder Node -file $dataDir/Deformation_110.out  -time -node 110   -dof 1 2 3 "disp";
```

```
#Column force

recorder Element -file $dataDir/force_Left_Column_111.out -time -ele 111 "localForce"

recorder Element -file $dataDir/force_Left_Column_120.out -time -ele 120 "localForce"


#Deformation of column

recorder Node -file $dataDir/Deformation_Left_Column_115.out -time -node 115  -dof 1 2 3 4 5 6 "disp";


# LVDT for column axial deformation

uniaxialMaterial Elastic 2000 1.; # Unit axial stiffness

element truss 5001 110 1003 [expr 0.001 * $Frame_H] 2000; # A adjusted such that axial deformation = 1000 x P (and P is small)

recorder Element -file $dataDir/Column_Deformation_3.out -time -ele 5001 localForce;  #Force values should be multiplied by 1000


# Applying Gravity Loads

# Load pattern

pattern Plain 1 "Linear" {

load 110 0.  183.9  0. 0. 0. 0.

}

# Analysis

numberer RCM

constraints Plain

system BandGeneral

test NormUnbalance 1.0e-3  1000  2
```

```
analysis Static;
set displayTag 2;
set numTimes 100;
integrator LoadControl 0.1
analyze 10

# Set time to zero and wipe analysis
loadConst -time 0.0
wipeAnalysis
updateParameter 100001  200.

# Quasi-Static Cyclic Simulation
# Include procedure for convergence
source procRC.txt

# Displacement sequence (AISC 2005 Test protocol - except that elastic cycles not repeated)
set H [expr (1 * $Frame_H)]
set IDctrlNode 110
set C1p [expr 0.10 * $H]
set C1n [expr -0.10 * $H]
set peakpts [list $C1p ]; # Displacement peaks
set NSub 500 ;          # number of substeps per displacemnt
pattern Plain 2 Linear {
load 110   0.  1.  0.  0. 0. 0.;
```

```
}
# Analysis
# Constraint Handler
 constraints  Plain
# DOF Numberer
numberer  RCM
# System of Equations
system  BandGeneral
# Convergence Test
set displayTag 2;
set numTimes 100;
test NormDispIncr      1e-6 $numTimes $displayTag
test NormUnbalance  1e-3 $numTimes $displayTag
test EnergyIncr          1.0e-3 $numTimes $displayTag

procRC $NSub $IDctrlNode 2 $peakpts
# Set time to zero and wipe analysis
loadConst -time 0.0
wipeAnalysis
```

The retrofitted column was loaded in tension and compression in Figure C.2. Figure C.2.a shows two types of cross sections for the member including existing cross section and existing cross section retrofitted with plates. In the model, the dead load was applied to the existing cross section; then, the retrofitted column was loaded in tension. In Figure C.2.a, the axial tensile demand on the retrofitted cross section is more than the existing cross section. Figure C.2.b shows four types of cross sections that have been used for the column including existing cross section, existing cross section retrofitted with plates and the application of Steel 01 for the plates, existing cross section with added plates modelled by the Steel 02 material and existing cross section with added plates that are simulated by Steel 02, while the residual stresses are assigned to the plate fibers. In all cases, the dead load was applied to the existing cross section; then, the retrofitted member was loaded in compression. It should be noted that the Parameter Command and the UpdateParameter Command are not available for the Steel 02 material; so, these commands were only applied to the plates that are modelled by the Steel 01 material.

Figure C.2.b shows that the level of axial load in compression on the existing cross section retrofitted by plates and modeled by the Steel 01 material is the same as the existing cross section with added plates that are modeled by Steel 02. The maximum level of axial compression demand on the retrofitted cross section modeled by Steel02 with the residual stresses that are assigned to the plate fibers is approximately the same demand on the cross section that is retrofitted by plates using Steel01. As mentioned earlier, the Parameter Command and the UpdateParameter Command can not be used for Steel02. Meanwhile, the effect of the residual stress of plates is negligible; thus, the plates were modeled by the Steel01 material in the analyses. Figure C.2.c shows the effect of adding the plates to the existing column cross section, as the column axial load is different in the existing and retrofitted cross sections.

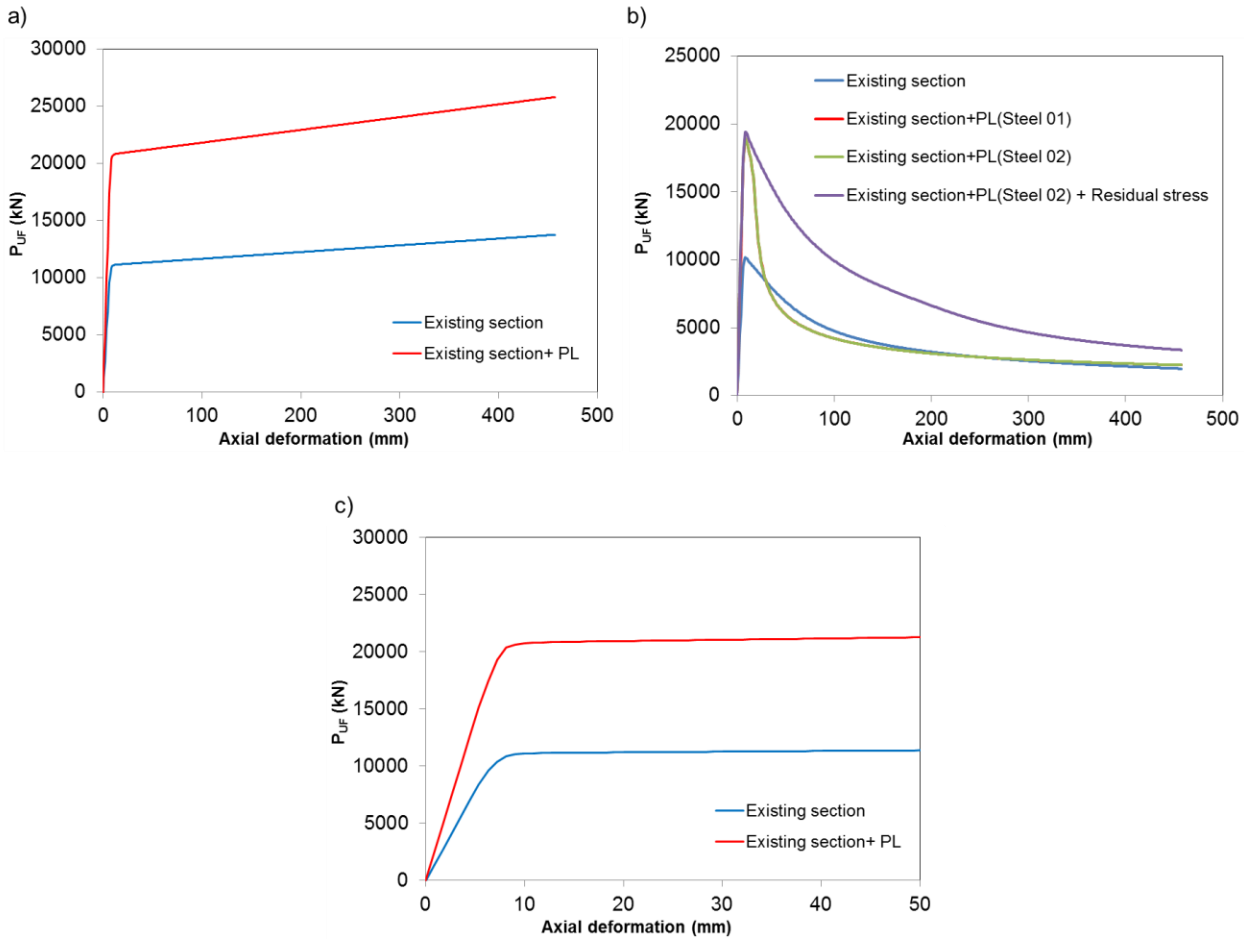

Figure C.2: Applied axial load to the existing and retrofitted column a) in tension; b) in compression; and c) Difference of column axial load using the existed and retrofitted cross sections.